Universidade de Aveiro Departamento de Química
2006

Ana Luisa dos Reis Pereira

Identificação de Radicais Livres e Produtos de Oxidação de Biomoléculas por MS

Identification of Free Radicals and Other Oxidation Products of Biomolecules by Mass Spectrometry

Universidade de Aveiro Departamento de Química
2006

Ana Luisa dos Reis Pereira

Identificação de radicais livres e produtos de oxidação de biomoléculas por MS

Identification of Free Radicals and Other Oxidation Products of Biomolecules by Mass Spectrometry

tese apresentada à Universidade de Aveiro para cumprimento dos requisitos necessários à obtenção do grau de Doutor em Bioquímica, realizada sob a orientação científica da Dra. Maria do Rosário Domingues, Professora Auxiliar do Departamento de Química da Universidade de Aveiro e do Dr. Pedro Domingues, Professor Auxiliar do Departamento de Química da Universidade de Aveiro.

Trabalho realizado com o Apoio financeiro da FCT e do FSE no âmbito do III Quadro Comunitário de Apoio (SFRH/BD/10358/2002).

o júri

presidente

Prof. Doutora Celeste de Oliveira Alves Coelho
professora catedrática do Departamento de Ambiente e Ordenamento da Universidade de Aveiro

Prof. Doutor António José Venâncio Ferrer-Correia
professor catedrático do Departamento de Química da Universidade de Aveiro

Doutor João António Nave Laranjinha
professor associado da Faculdade de Farmácia da Universidade de Coimbra

Doutor Carlos Manuel Ferreira de Sousa Borges
professor auxiliar da Faculdade de Ciências da Universidade de Lisboa

Doutor Francisco Manuel Lemos Amado
professor auxiliar do Departamento de Química da Universidade de Aveiro

Doutor Pedro Miguel Dimas Neves Domingues
professor auxiliar do Departamento de Química da Universidade de Aveiro (co-orientador)

Doutora Maria do Rosário Gonçalves dos Reis Marques Domingues
professora auxiliar do Departamento de Química da Universidade de Aveiro (orientadora)

agradecimentos

Aos meus orientadores, Rosário e Pedro Domingues, o meu sincero agradecimento pela aposta feita em mim para a realização deste trabalho, e que se prolongou ao longo destes anos não só a nível académico mas também a nível pessoal.

Ao Doutor Francisco Amado, o meu profundo reconhecimento pela prontidão e preciosas correcções e sugestões...

Aos amigos, colegas e vizinhos, Sofia e Rui, pela amizade, companheirismo e cumplicidade...

À Cristina, pelo acolhimento dado assim que cheguei ao grupo, pela amizade que foi crescendo, pela companhia nas horas de lazer e pelo apoio ao longo de 1641 dias...

Ao Zé, pela "saudável loucura" nas longas horas de análise de dados...

À Rita, Maria João e São, que sempre se mostraram amigas incondicionais e grandes colegas de trabalho...

À Helena, a minha "irmã gémea", pela cumplicidade...

...a todos vós, o meu muito obrigada. Com o vosso apoio, as "montanhas e vales" característicos de qualquer percurso tornaram-se em pequenas "lombas" na estrada.

Agradeço a todos os membros do grupo de espectrometria de massa pelo companheirismo dispensado.

À Fundação para a Ciência e Tecnologia, o apoio financeiro concedido, e ao FSE no âmbito do III Quadro Comunitário de Apoio (SFRH/BD/10358/2002).

palavras-chave

espectrometria de massa, stress oxidativo, radicais, lípidos, fosfolípidos, aductos proteína-fosfolípido.

resumo

A alteração estrutural de biomoléculas por acção de radicais livres resultantes de processos aeróbios, e mais especificamente em ácidos gordos insaturados, tem sido descrita como tendo um papel preponderante em patologias relacionadas com o envelhecimento. Esta tese tem como objectivo o uso da espectrometria de massa (MS) na identificação e caracterização estrutural de radicais livres de ácidos gordos, nomeadamente no ácido gordo ω-6, e em modelos progressivamente mais complexos, como as glicerofosfatidilcolinas (GPC) substituídas com ácidos gordos ω-9 e ω-6. Em resultado, e usando metodologia desenvolvida para a detecção de radicais livres, nomeadamente o uso de “trapas de spin”, foram identificados por MS vários radicais livres do ácido linoleico e de GPC sob a forma de aductos de spin. Estes resultaram da inserção de átomos de oxigénio na cadeia carbonada e de cisão da mesma após inserção de átomos de oxigénio. Após caracterização por espectrometria de massa tandem (MS/MS), verificou-se a presença de radicais centrados em átomos de carbono (alquilo) e de oxigénio (alcoxilo), tendo-se ainda verificado que a quebra da cadeia carbonada ocorreu preferencialmente no sentido da formação de radicais com o menor número de átomos de carbono. Em função dos radicais de GPC identificados por MS, verificou-se não existir uma relação entre a extensão da oxidação e o grau de insaturação, o que sugere um efeito retardador na reacção de peroxidação lipidica pela adição da “trapa de spin”. Esta observação parece ser corroborada pela identificação de mais de 50 produtos de oxidação não-radicalares para os 3 GPC na ausência da trapa de spin, tendo-se verificado uma relação directa entre a extensão das alterações estruturais e o grau de insaturação. De entre os produtos de oxidação não-radicalares identificados, encontram-se vários isómeros estruturais, posicionais e estruturas isobáricas que foram caracterizados por MS associada à cromatografia líquida de alta eficiência. De salientar, que as diferenças observadas para os tempos de retenção dos produtos de cadeia curta com terminal aldeído e ácido carboxílico em diferentes GPC, sugerem que este procedimento poderá ser aplicado para o fraccionamento de amostras biológicas. A formação de produtos de cadeia curta com terminal aldeído em elevada abundância relativa permitiu a identificação de aductos GPC-peptídeo, tendo sido identificadas as vias de fragmentação preferenciais por MS/MS e que se verificou serem característico de aductos GPC-peptídeo.
Em resumo, os dados obtidos mostraram ser possível a identificação por MS tanto de produtos radicalares como não-radicalares de biomoléculas contendo ácidos gordos. Mais, a predominância de produtos de oxidação de GPC modificados nos átomos de carbono mais próximos da cabeça polar, sugere um ataque preferencial dos radicais nos átomos de hidrogénio mais próximos da cabeça polar.

keywords

Mass spectrometry, oxidative stress, radical species, phospholipids, peptide-phospholipid cross-linking.

abstract

The radical peroxidation of lipids and phospholipids is an increasing topic of research due to the close association between lipid peroxidation products and age-related diseases. In this work, mass spectrometry was used for the identification and characterisation of lipid and phospholipid free radicals using the methodology developed for the detection of free radicals, namely the use of spin traps. For this, radical oxidation was performed on ω-6 unsaturated fatty acid and extended to progressive more complex structures, particularly diacyl-glycerophosphatidylcholines (GPC) containing ω-9 (oleic) and ω-6 (linoleic and arachidonic) fatty acids. Several intact and breakdown free radicals products of lipid and GPC were identified as spin adducts for the first time, and characterisation by tandem mass spectrometry (MS/MS) in association with reverse-phase chromatography (HPLC-MS/MS) allowed the assignment of such species to be carbon and oxygen centred radicals. The lipid breakdown products suggested that β-scission cleavage is selective towards the formation of the smaller alkyl radicals. Also, the intact free radicals identified for the 3 GPC suggested the occurrence of a “retarder” effect to the lipid peroxidation caused by the addition of the spin trap. The identification and characterisation by MS was extended to non-radical GPC products and the complexity of structures required previous separation method by reverse-phase chromatography prior to mass spectrometry detection (LC-MS) and tandem mass spectrometry (LC-MS/MS). More than 50 different structures were identified for only three phospholipids. Based on the LC-MS/MS data analysis, isomeric structures of long-chain products were differentiated and, short-chain products containing different terminal groups were differentiated by LC-MS data analysis according to the retention times, which was independent of the oxidised GPC. In this way, isobaric structures of short-chain products may be distinguished if present in complex mixtures.

Adducts formed by covalent interaction between GPC alkenal products and peptides established in *in vitro* conditions were characterised by MS/MS. Upon fragmentation, the peptide-GPC adducts provided information about the peptide and the lipid moiety, which is characteristic of peptide-GPC adducts due to charge retention in the polar head.

Altogether, MS is a suitable technique for the identification of both radical and non-radical products of fatty acids and phosphatidylcholines. Furthermore, the GPC peroxidation products identified in this study suggested that, during non-enzymatic phospholipid radical oxidation, bis-allylic hydrogen atoms closer to the polar head are preferably abstracted.

Índex

Abbreviations

AA- arachidonic acid
CID- collision induced dissociation
DLPC-di-lineloyl-phosphatidylcholine
DMPO- 5,5-dimethyl-1-pyrroline-N-oxide
EPR- Electron paramagnetic resonance
ESI-MS - Electrospray ionisation with mass spectrometry detection
ESR- Electron spin resonance
FAB- Fast atom bombardment ionisation
GPC- glycerophosphatidylcholine
H_2O_2- hydrogen peroxide
HNE- 4-hydroxy-2-nonenal
$HO^{\bullet}$- hydroxyl radical
LC-EPR- liquid chromatography with electron paramagnetic resonance detection
LC-MS- liquid chromatography with mass spectrometry detection
LDL- low density lipoprotein
Leu- leucine
LOOH- lipid hydroperoxide
m/z- mass to charge ratio
MALDI- matriz assisted laser desorption/ionisation
MALDI-TOF- matriz assisted laser desorption/ionisation with time-of-flight analyser
MRM- multiple reaction monitoring
MS/MS- tandem mass spectrometry
Mw- molecular mass
$OLOO^{\bullet}$- epoxy peroxyl radical
oxLDL- oxidised low density lipoprotein
PAPC- palmitoyl-arachidonoyl-phosphatidylcholine
PDPC- palmitoyl-docosahexanoyl-phosphatidylcholine
Phe- phenylalanine
PLPC- palmitoyl-lineloyl-phosphatidylcholine
POBN- α-(4-pyridyl-1-oxide)-N-tert-butylnitrone
POPC- palmitoyl-oleoyl-phosphatidylcholine
PUFA-polyunsaturated fatty acids
Q-TOF- quadrupole time-of-flight
RIC- reconstructed ion chromatogram
ROS- reactive oxygen species
SAPC- steraoyl-arachidonoyl-phosphatidylcholine
SLPC- steraoyl-lineloyl-phosphatidylcholine
SM- sphyngomyelin
SOPC- steraoyl-oleoyl-phosphatidylcholine
TIC- total ion chromatogram

List of original publications

This thesis is based on the following publications:

1. A. Reis, M.R.M. Domingues, F.M.L. Amado, A.J. Ferrer-Correia, P. Domingues "Detection and characterization by Mass Spectrometry of radical adducts produced by linoleic acid oxidation" *J. Am. Soc. Mass Spectrom.*, (2003) 14, 1250-1261.

2. A. Reis, M.R.M. Domingues, F.M.L. Amado, A.J. Ferrer-Correia, P. Domingues "Identification of linoleic acid free radicals and other breakdown products using spin trapping with reverse phase chromatography-electrospray tandem mass spectrometry", *Biomed. Chromatogr.* (2006) 20, 109-118.

3. A. Reis, P. Domingues, A.J. Ferrer-Correia, M.R.M. Domingues "Identification by Electrospray Tandem Mass Spectrometry of spin trapped free radicals from oxidized 2-oleoyl-1-palmitoyl-*sn*-glycero-3-phosphocholine" *Rapid Commun. Mass Spectrom.,* (2004) 18(10), 1047-1058.

4. A. Reis, P. Domingues, A.J. Ferrer-Correia, M.R.M. Domingues "Identification of free radicals in glycerophosphatidylcholines containing ω-6 fatty acids using spin trapping coupled with tandem mass spectrometry", submitted to *Free Rad. Res.*

5. A. Reis, P. Domingues, A.J. Ferrer-Correia, M.R.M. Domingues "Tandem mass spectrometry in the study of intact oxidation products of diacyl-phosphatidylcholines: evidence for the occurrence of the oxidation of the phosphocholine head and differentiation of isomers", *J. Mass Spectrom.* (2004) 39, 1513-1522.

6. A. Reis, M.R.M. Domingues, A.J. Ferrer-Correia, P. Domingues "Radical peroxidation of palmitoyl-lineloyl-glycero-phosphatidylcholine liposomes: identification of long-chain products by LC-MS/MS", submitted to *J. Chromatogr. B.*

7. A. Reis, P. Domingues, A.J. Ferrer-Correia, M.R.M. Domingues "Study of the fragmentation pattern of short-chain products of diacyl-phosphatidylcholines by Electrospray mass spectrometry: identification of novel short-chain products", *Rapid Commun. Mass Spectrom.* (2004) 18(23), 2849-2858.

8. A. Reis, M.R.M. Domingues, F.M.L. Amado, A.J. Ferrer-Correia, P. Domingues "Separation of peroxidation products of diacyl-phosphatidylcholines by reverse phase Liquid Chromatography-Mass Spectrometry", *Biomed. Chromatogr.* (2005) 19 (2), 129-137.

9. A. Reis, P. Domingues, A.J. Ferrer-Correia, M. R. M. Domingues "Peptide-phospholipid cross-linking reactions: Identification of Leucine enkephalin-alka(e)nal-glycerophosphatidylcholine adducts by tandem Mass Spectrometry", *J. Am. Soc. Mass Spectrom.*, (2006) 17, 657-660.

1. Introduction

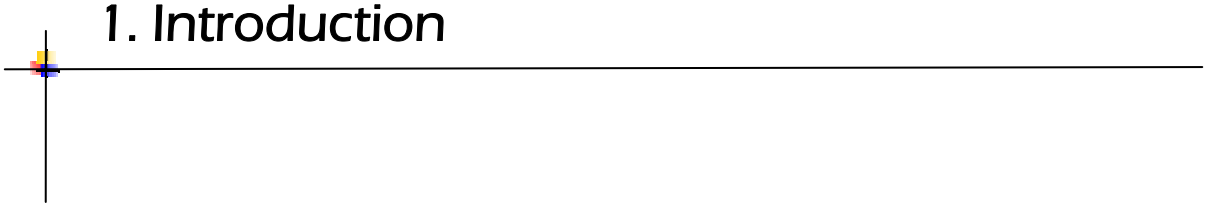

The aging process is an old question that has attracted the interest of many researchers in an attempt to understand the biochemical and physiological changes that occur with aging. Over 50 years ago, it was proposed that increased deleterious effects occurred with aging caused by free radicals and radical by-products formed within the cell, which in turn induced irreversible changes onto the structure of biomolecules. These changes were responsible for consequent loss of biochemical functions in the cell. This is currently known as the free radical theory of aging, and is supported by the increase oxidative modifications observed in biomolecules with aging, explained by the increase of the steady-state of radical species [Wong, 2001]. In view of this, a lot of research work, focused on the role of free radicals on the structure of biomolecules and on the biochemical processes in which they are involved in age-related diseases, has been carried out. However, the free radical theory is only one of many theories that have been proposed to explain the aging process, and thus the contribution of program theories (Hayflick limit theory) and error theories (free radical theory, cross-linking theory), should all be considered to understand the biochemical and physiological changes occurring throughout aging [Wong, 2001].

1.1. Free radicals in aerobic systems

Free radicals are molecules with unpaired electrons with very short lives exhibiting high reactivity towards unsaturated biological molecules, namely proteins, lipids and phospholipids, carbohydrates and DNA bases [Sergent et al., 1999; Multhaup and Masters, 1999; Sangripanti, 1999]. Free radicals comprise oxygen radical species, nitrogen radicals, sulfur radicals and others, and may be formed from exogenous sources by pollution, smoking, drug intake and ethanol intoxication, or as by-products of metabolic reactions occurring *in vivo* [De Zwart et al., 1999]. The purpose of this study will only focus on the modifications to biomolecules induced by oxygen radical species regardless of their origin.

1.1.1. Reactive oxygen species (ROS)

Oxygen plays a crucial role for proliferation of life of most living organisms on Earth and is of vital importance to mammals. In mammals during aerobic metabolism, oxygen is used as an electron acceptor in a series of one electron reduction steps (Scheme 1).

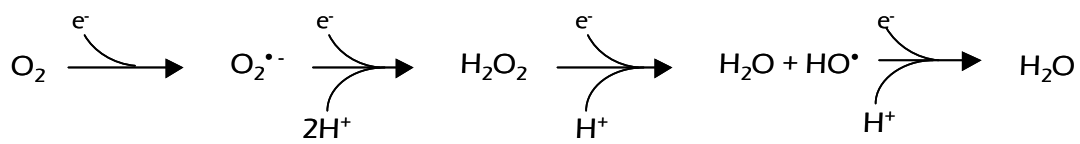

Scheme 1: Four-electron reduction of molecular oxygen to water [Rosen et al., 1999].

In the process, oxygen free radicals, such as superoxide radical ($O_2^{-\bullet}$) and hydroxyl radical ($HO^{\bullet}$) are formed, as intermediate species, during the reduction of oxygen to water with regeneration of NADH and energy synthesis (ATP) [Stryer, 1999]. The hydroxyl radical ($HO^{\bullet}$) contain unpaired electrons with high reaction rate constant and the high reduction potential of the hydroxyl radical makes the hydroxyl radical a very reactive specie with strong oxidising properties [Rosen et al., 1999]. Superoxide radical anion ($O_2^{-\bullet}$) exhibits a lower reduction potential and can reduce Fe^{3+} in ferritin to Fe^{2+} [Buettner and Jurkiewicz, 1996]. Hydrogen peroxide exhibits a lower reduction potential, when compared to the hydroxyl radical, but in the presence of transition metals results in the formation of oxygen radical species. Thus, reactive oxygen species (ROS) include oxygen radical species, such as superoxide radical anion ($O_2^{-\bullet}$) and hydroxyl radical ($HO^{\bullet}$), and also oxygen non-radical species such as hydrogen peroxide (H_2O_2). Singlet oxygen ($^1O_2$) and ozone (O_3), are powerful oxidants and may *in vivo* generate oxygen free radicals and for this reason are also considered to be reactive oxygen species.

1.1.2. Sources of ROS

As mentioned, the presence of reactive oxygen species (ROS) within the cell have their origin from exogenous sources, such as radiation exposure and xenobiotics metabolism (smoking, drugs and ethanol intoxication), or from endogenous sources, such as by-products of metabolic pathways that can either be generated by enzymatic or non-enzymatic chemical reactions. The enzymatic sources of ROS are hydrolytic enzymes present in mononuclear cells responsible for the phagocytosis (macrophages, eosinophils and neutrophils), such as NAD(P)H oxidase, xanthine-xanthine oxidase, myeloperoxidase, and others with formation of superoxide radical anion ($O_2^{-\bullet}$) and singlet oxygen ($^1O_2$) [Branchaud, 1999; Nagata, 2005]. This is also known as "respiratory burst" [Branchaud, 1999]. Also membrane proteins responsible for the transport of protons into the mitochondrial membrane may, by changes in the membrane fluidity or in the membrane potential, leak oxygen radical species [Nohl et al., 2003]. The non-enzymatic sources of oxygen radical species in *in vivo* are mainly the ones occurring between hydrogen peroxide and, transitions metals such as ferrous ions (Fe(II)) released during erythrocyte senescence [Comporti et al., 2002; Ando et al., 2003] and called the Fenton reaction (reaction 1), and superoxide anions called the Haber-Weiss reaction (reaction 2), with formation of hydroxyl radicals ($HO^{\bullet}$) [Liochev, 1999]. Due to the permeability of the cell

membrane to H_2O_2, the hydrogen peroxide may induce damage away from the site of formation.

$$Fe\ (II) + H_2O_2 \longrightarrow Fe\ (III) + HO^{\bullet} + HO^{-} \qquad \text{(reaction 1)}$$

Other reducing metal ions, such as Cu^{+} in the presence of H_2O_2 also result in the formation of oxygen radical species, however in this case they are named as Fenton-like reactions [Liochev, 1999].

$$O_2^{-\bullet} + H_2O_2 \longrightarrow O_2 + HO^{\bullet} + HO^{-} \qquad \text{(reaction 2)}$$

The hydroxyl radicals, due to their high reactivity, are usually referred to as the initiating species of the radical reactions, nevertheless, it should be mentioned that currently the (per)ferryl ion, the complex form of iron and oxygen (reaction 3 to 5), is also described as an initiator in radical reactions [Qian and Buettner, 1999].

$$Fe^{2+} + O_2 \longleftrightarrow [Fe^{2+}\text{-}O_2 \leftrightarrow Fe^{3+}\text{-}O_2^{\bullet}] \longleftrightarrow Fe^{3+} + O_2^{\bullet} \qquad \text{(reaction 3)}$$

$$Fe^{2+} + H_2O_2 \longrightarrow Fe^{2+}O + H_2O \qquad \text{(reaction 4)}$$

$$\text{or} \quad Fe^{2+} + Fe^{2+}\text{-}O_2 \longrightarrow Fe^{2+}\text{-}O_2\text{-}Fe^{2+} \longrightarrow 2\ Fe^{2+}\text{-}O \qquad \text{(reaction 5)}$$

In *in vivo*, superoxide radicals are removed by antioxidant systems, such as superoxide dismutase (SOD) (reaction 6) with formation of hydrogen peroxide (H_2O_2) [Rosen et al., 1999]. Other antioxidant systems, namely catalase (CAT) and peroxidases (GPx), are responsible for the removal of hydrogen peroxide from the cell.

$$O_2^{-\bullet} + O_2^{-\bullet} + 2H^{+} \longrightarrow H_2O_2 + O_2 \qquad \text{(reaction 6)}$$

1.1.3. Role of ROS

Reactive oxygen species (ROS), which include both radical and non-radical ones, are beneficial to the organism, being involved in a number of physiological functions including maintenance of redox homeostasis, regulation of cell adhesion, activation of transcription factor NP-κB, and many others (reviewed by Dröge, 2002). However, they are also responsible for radical oxidation reactions of unsaturated molecules and inducing

damage to biomolecules [Sergent et al., 1999; Multhaup and Masters, 1999; Sangripanti, 1999]. In *in vivo*, the concerted action of several antioxidant systems (enzymatic and non-enzymatic) keeps the naturally occurring reactive oxygen species at relatively low levels, preventing deleterious damage.

However, when an imbalance between the generation of ROS and the regeneration of antioxidants takes place, named **oxidative stress**, biomolecules may undergo structural changes resulting in loss of function and damage – **oxidative damage**. The structural changes to biomolecules induced by the oxygen radical species may either result from direct attack of the hydroxyl radical to biomolecules or from indirect attack of secondary radicals and non-radical molecules, formed during the initial attack, to biomolecules.

1.2. Oxidative damage to biomolecules

The study of radical oxidation of biomolecules is currently focused on the identification of radical oxidation of peptides and proteins [reviewed in Bertlett and Stadtman, 1997; Hawkins and Davies, 2001; Stadtman and Levine, 2003; Davies, 2005] and to a lesser extent to lipids [Spiteller, 1998] and DNA bases [Multhaup and Masters, 1999]. This may be rationalised considering that even in lipid-rich environments, such as cell membranes and low-density lipoproteins (LDL), proteins comprise the majority of the biomolecules [Davies, 2005]. By comparison of the reaction rate constants of hydroxyl radical with other macromolecules such as DNA, albumin, collagen and linoleic acid (Table 1), it is noticed that the differences vary only to small extents [Davies, 2005], which reinforces the notion that the point of radical formation determines the radical oxidation of biomolecules. Furthermore, the extent of radical damage to biomolecules will be determined by the concentration of the target, the presence of antioxidant-scavenging reactions and the presence of repair mechanisms [Davies, 2005]. The reaction rate constants exhibited by free amino acids, determined at near physiological conditions, for the $HO^{\bullet}$ (Table 1) show that some amino acids such as tyrosine, tryptophan, histidine and cysteine are more prone to ROS attack [Davies, 2005]. This suggests that the radical oxidation of amino acids in peptides and proteins is selective towards these amino acids, however radical oxidation of proteins was also observed to occur in Leu [Xu and Chance, 2005] and Phe residues [Nukuna et al., 2004].

Table 1. Rate constants for the reaction of $HO^{\bullet}$ with macromolecules, small peptides and amino acids at pH ca. 7.

Substrate	Rate constant ($M^{-1}s^{-1}$)
Linoleic acid	$9x10^{9}$
Collagen	$4x10^{11}$
Albumin	$8x10^{10}$
Glutathione (GSH)	$1.4x10^{10}$
Cysteine	$3.4x10^{10}$
Histidine	$1.3x10^{10}$
Tryptophan	$1.3x10^{10}$
Tyrosine	$1.3x10^{10}$
Leucine	$1.7x10^{9}$
Phenylalanine	$6.5x10^{9}$

Lipids, which comprise free fatty acids and other biomolecules containing fatty acids, such as triglycerides, cholesteryl esters and phospholipids [Murphy et al., 2001], also exhibit an apparent selectivity towards radical oxidation. As observed during *in vitro* fatty acid radical oxidation of LDL particles, it was suggested that the lower oxidative susceptibility of choline phospholipids and free cholesterol (FC), present in the outer layer of LDL, to radical oxidation was due to the close association observed between sphingomyelin (SM) and phosphatidylcholines (PC), with tighter acyl packing[Oborina and Yappert, 2003; Sargis and Subbaiah, 2006], when compared to the higher susceptibility of cholesteryl esters (CE), located at the inner more fluid core [Yoshida et al., 2003]. Acyl packing of unsaturated fatty acids in phosphatidylcholine liposomes was proposed to account for the similarities of oxidative stability observed between PC containing linoleic, arachidonic and docohexaenoic acids [Araseki et al., 2002]. On the other hand, the apparent selectivity of fatty acids in liposomes to radical oxidative modification may in part be attributed to the surface area of liposomes where higher surface area liposomes contain higher curvature, and facilitate higher ROS penetration, which could account for the higher susceptibility of small unilamellar vesicles (SUV) when compared with large unilamellar vesicles (LUV) [Li et al., 2000]. Also, it was reported that membranes composed with plasmenyl phospholipids were less susceptible to radical oxidation since ether bonded lipids are more resistant to radical oxidation that ester bonded phospholipids [Khaselev et al., 2000b].

The structural changes induced by hazardous oxygen radical species to biomolecules, in general, result in the insertion of oxygen atoms to the molecule or breakage of the peptide sequence, the fatty acid carbon chain or the DNA strand with formation of lower molecular weight carbonyl compounds [reviewed in Zwart et al., 1999]. The formation of radical oxidation products of biomolecules and the implication of these in the pathogenesis of age-related diseases such as atherosclerosis, neurodegenerative diseases, ischemia and reperfusion and lung and liver diseases [Pincemail, 1995] is an increasing topic of research.

1.3. Oxidative damage to lipids

Lipids comprise a wide variety of biomolecules that contain saturated and unsaturated fatty acids, namely mono, di and triglycerides, cholesteryl esters and phospholipids [Silvius, 1995], with several biochemical functions. Thus, unsaturated fatty acids, when found as free fatty acids are involved in signalling events in inflammatory processes, and also in correct insertion, folding and topology of the membrane proteins, when embedded into hydrophobic proteins, forming lipid-protein complexes providing tight integration of the protein to the membrane [Lange et al., 2001; Palsdottir and Hunte, 2004]. These interactions influence the enzymatic activity and/or transport processes across the phospholipid membrane [Hunte, 2005]. Unsaturated fatty acids when esterified to phospholipids may also exhibit supporting functions in membranes (Figure 1) or of transport when present in low density lipoproteins (LDL) particles [Yorek, 1995].

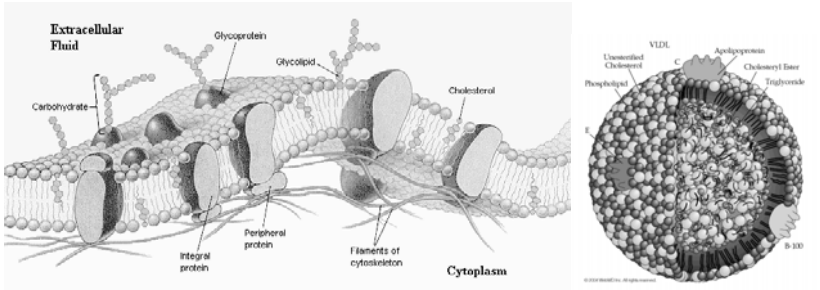

Figure 1. Phospholipids in cell membrane (www.anti-age.biz) and in low density lipoproteins (www.acpmedicine.com).

In the following section, the structural changes induced by oxygen free radicals to free unsaturated fatty acids, are described. Their presence in other biomolecules is also considered, as is the case of esterified unsaturated fatty acids in phospholipids. Also, the

experimental approaches and the techniques used for the detection and identification of fatty acid radical oxidation products are described.

1.3.1. Polyunsaturated fatty acids as targets of radical oxygen species in metal-catalysed reaction (Fenton reaction)

Allylic hydrogen atoms, present in polyunsaturated fatty acids (PUFA), and most particularly, bis-allylic hydrogen atoms exhibit low carbon-hydrogen bond energies [Schafer et al., 2000], which are readily abstracted by ROS, such as $HO^{\bullet}$, forming a lipid radical centred at the carbon atom ($L^{\bullet}$) (Scheme 2).

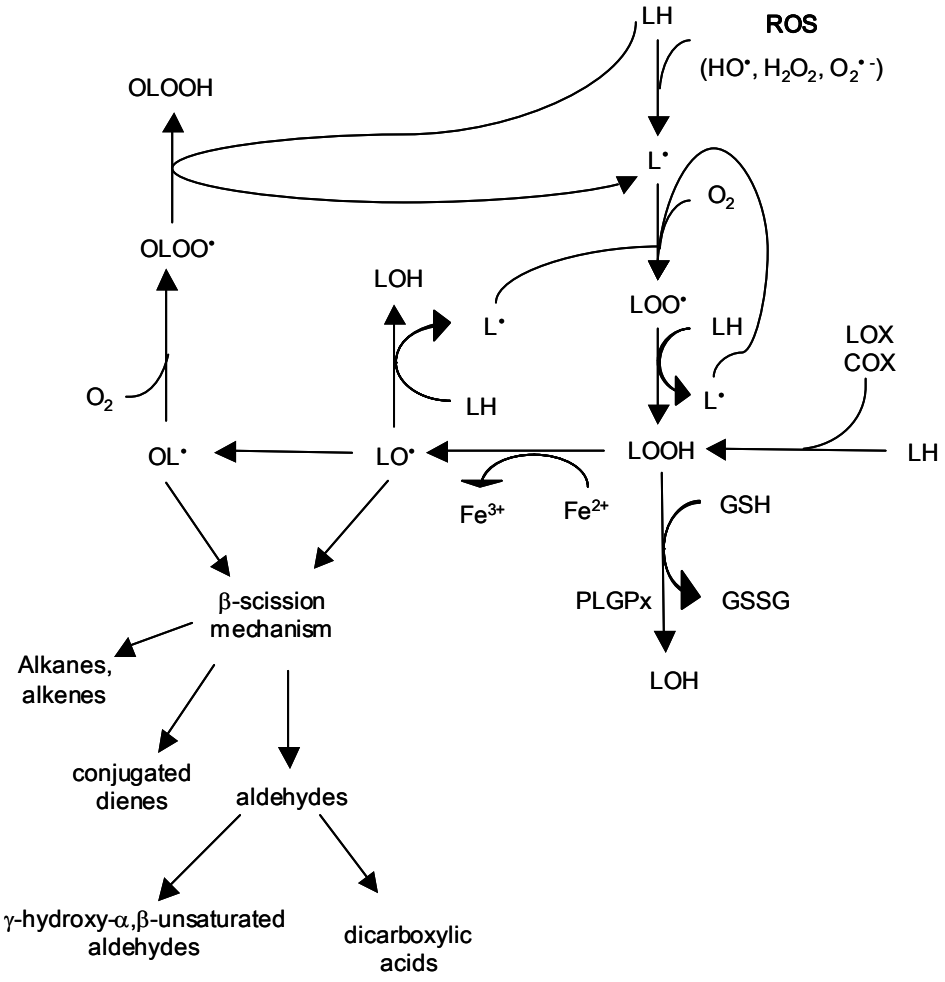

Scheme 2. Schematic representation of the lipid peroxidation reaction and the products resultant of the radical reaction (adapted from Girotti, 1998 and Schafer and Buettner, 2000).

This reaction is also referred to as radical lipid peroxidation. For this reason saturated fatty acids, also found in biological membranes (palmitoyl and stearoyl) [Silvius, 1995], are

described to be resistant to radical oxidation [Khaselev and Murphy, 2000a]. This initial abstraction step (initiation step) is limited by the concentration of ROS, thus, a number of initiating reactions are required to take place (propagation step) until the concentration of lipid radicals is high enough, after which radical-radical reactions may result in the formation of non-radical fatty acid products (termination step) [Rosen et al., 1999]. These latter products were not considered in Scheme 2.

The non-enzymatic radical lipid peroxidation is often schematised with the attack of the hydroxyl radical, however, in biological systems, the low levels of [H_2O_2] in most cells (10^{-8}-10^{-10} M) [Qian and Buettner, 1999] may limit the influence of the hydroxyl radical, formed by the Fenton reaction, in triggering the radical oxidation of fatty acids and other biomolecules. Also, the higher ratio of [O_2]/[H_2O_2] found in cells, suggests that oxidant systems, such as the perferryl (reaction 3) and the ferryl ions (reaction 4 and 5), may have more significant roles in the initiation of radical oxidation of fatty acids than the hydroxyl radical [Qian and Buettner, 1999]. Also, in cellular medium showing high concentration of iron ions, these complexes may be the initiating species for the lipid radical oxidation [Schafer and Buettner, 2000], by reaction with pre-existing fatty acid hydroperoxides (LOOH) (reaction 6), formed enzymatically by lipoxygenase (LOX) and cyclooxygenases (COX), in a reaction similar to the Fenton reaction (reaction 7). Ferric ions (Fe^{3+}) are also able to decompose fatty acid hydroperoxides (reaction 8) but the reaction is thought to undergo at a much slower rate [Sergent, 1999]. Regardless of the oxidising species responsible for initiating lipid radical peroxidation, the permeability of the cell membrane to H_2O_2 formed *in vivo* and the release of iron from its protein-bound form, hemoglobin during erythrocyte senescence [Ando et al., 2003], or transferrin, ferritin and others [Comporti et al., 2002] may turn iron available to trigger radical oxidation either by the hydroxyl radical (Fenton reaction) or by the ferryl/perferryl system [Schafer and Buettner, 2000]. In *in vitro* experiments using the Fenton reaction, the lipid peroxidation was found to be proportional to the concentration of oxidant added for a constant concentration of iron ions [Spickett et al., 1998], and also to the concentration of the iron ions added, although the lower amount of ferrous ions added reduced the latent period (initiation step) [Tang et al., 2000].

$$LOOH + Fe(II) \longrightarrow LO^{\bullet} + Fe(III) + HO^{-} \qquad \text{(reaction 7)}$$

$$LOOH + Fe\ (III) \longrightarrow Fe\ (II) + LOO^{\bullet} + H^{+} \qquad \text{(reaction 8)}$$

Once fatty acid carbon centred radicals ($L^{\bullet}$) are formed, this radical uptakes an oxygen molecule and through a number of intermediate steps leads to the formation of carbon ($L^{\bullet}$ and $OL^{\bullet}$) and oxygen centred fatty acid radicals ($LO^{\bullet}$, $LOO^{\bullet}$, $OLOO^{\bullet}$) which in turn propagate the radical reaction (Scheme 2).

Among those, the oxygen centred radicals, namely epoxy peroxyl fatty acid radicals ($OLOO^{\bullet}$), are thought to be the major contributors to the propagation of the radical reaction (Scheme 2). The intermediate fatty acid radicals such as alkyl ($L^{\bullet}$), epoxy alkyl ($OL^{\bullet}$) or hydroxy alkyl ($HOL^{\bullet}$), and alkoxyl ($LO^{\bullet}$) may, through β-scission mechanism, cause cleavage of the carbon chain with formation of smaller carbon chain compounds (carbon centred) named fatty acid small alkyl radicals and fatty acid aldehydes, alkanes and alkenes, and conjugated dienes [Spiteller, 1998]. The reactions here described are summarised in Scheme 2. The fatty acid small alkyl radicals formed are dependent on the position along the carbon chain in which the initial fatty acid radical is centred. These fatty acid small alkyl radicals may further propagate the lipid peroxidation by hydrogen abstraction and oxygen uptake. The fatty acid aldehydes, alkanes and alkenes, and conjugated dienes are also named secondary products.

As can be seen from the reactions 7 and 8, changes in the pH value also determine the lipid peroxidation, particularly the stability of the oxygen radical specie, which is pH dependent, and also the solubility of ferrous salts, which increases in acidic conditions, although at physiological pH most iron ions are in the complex form [Comporti et al., 2002]. Furthermore, the type of secondary products formed depend of the fatty acid radical species formed which in turn are determined by the oxidation state of the metal (reactions 7 and 8). This was experimentally observed during linoleic acid radical oxidation, where the authors reported higher content of hydroxy and epoxy-hydroxy derivatives in the presence of Fe^{2+} than in the presence of Fe^{3+} [Spiteller and Spiteller, 1998]. The differences observed were attributed to the presence of ascorbate, which was responsible for regeneration of Fe^{3+} back to Fe^{2+}. However, the role of ascorbate in *in vitro* oxidative experiments is problematic mainly because, depending on the concentration of metal ions, it is described to act as an antioxidant or as a pro-oxidant [Buettner and Jurkiewicz, 1996]. In *in vivo* regeneration of ferric ions to ferrous ions may take place by other reducing agents such as the superoxide radical [Liochev, 1999].

In the case of radical peroxidation of phospholipids, the products resultant from radical oxidation are very similar to the ones described for the fatty acid radical oxidation,

namely peroxidation products resulting from the insertion of oxygen atoms with formation of hydroxy and hydroperoxide fatty acids esterified to the glycerol moiety, and products resulting from cleavage of the unsaturated fatty acid chain with formation of terminal oxo and dicarboxylic groups [McIntyre et al., 1999]. In addition to these, the formation of lyso-phosphatidylcholines is also observed, not due to direct radical oxidation but probably by a saponification mechanism [McIntyre et al., 1999].

1.3.2. Detection of unsaturated fatty acid oxidation products

As described in Scheme 2, both radical and non-radical products are formed during lipid peroxidation. The identification of unsaturated fatty acid radical products, which was attempted in the early 1990 using spin traps [Iwahashi et al., 1991], an approach developed for the detection of free radicals. On the other hand, the higher chemical stability of fatty acid secondary products may explain the work that is published in the identification of fatty acid aldehydes and hydrocarbons, when compared to the fatty acid radical products. In the following section, some considerations regarding the literature published on the detection and identification of primary and secondary oxidation products of free fatty acid and of primary and secondary oxidation products esterified fatty acids to phospholipids, are described.

1.3.2.1. Experimental parameters in the detection of radical products of fatty acids

Fatty acid free radicals, like most free radicals are unstable species with very short-lives, making their detection and analysis difficult. This can be overcome by reacting the fatty acid free radical with a diamagnetic compound, named spin trap, with formation of a more stable (longer life) radical adduct, named fatty acid spin adduct. Nonetheless, some experimental parameters must be taken into consideration during spin trapping of fatty acid free radicals, such as choice of the spin trap, which in spite of similar spin trapping rate constants exhibit great variability of half-lives [Rosen et al., 1999], where the alkyl radical rate constants for spin trapping decrease with increasing chain length [Taniguchi and Madden, 1999], and the pH value which determine the formation and stability of radical species [Rosen et al., 1999]. Also, the introduction of an additional extraction step with methanol:chloroform [Folch et al., 1957] of fatty acid spin adducts prior to the detection was shown to greatly increase the lifetime of the fatty acid spin adducts [Qian et al., 2000]. The stabilisation of the fatty acid alkyl spin adducts was, according to the authors, due to prevention of radical-radical terminating steps [Qian et al. 2000]. The most widely described spin traps used for the detection of fatty acid radical species are the

nitrone spin traps, namely α-(4-pyridyl-1-oxide)-N-tert-butylnitrone (POBN) [Iwahashi et al., 1991, 2002; Iwahashi, 2000, Rota et al., 1997; Qian et al., 2000, 2002, 2003a,b], 5,5-dimethyl-1-pyrrolidine-N-oxide (DMPO) [Rota et al., 1997; Qian et al., 2000], and phenyl-tert-butyl-nitrone (PBN) [Velasco et al., 2005], although other more lipophilic spin traps such as 5-(ethoxycarbonyl)-5-methyl-1-pyrrolidine-N-oxide (EMPO) [Stolze et al., 2002], 1-(propoxycarbonyl)-5-methyl-1-pyrrolidine-N-oxide (PrMPO), 1-(butoxycarbonyl)-5-methyl-1-pyrrolidine-N-oxide (BuMPO), 1-(octyloxycarbonyl)-5-methyl-1-pyrrolidine-N-oxide (OcMPO) [Stolze et al., 2002], were also evaluated. In view of the increasing work focused on the detection and identification of spin adducts generated in lipophilic environments and in order to improve the potential of the spin trapping experiments, new spin traps are currently being developed and tested, to be further used in biological models [Hardy et al., 2005; Reybier et al., 2006; Rohr-Udilova et al., 2006].

1.3.2.2. Detection of unsaturated fatty acid radical products by EPR

The formation of spin adducts allows accumulation of fatty acid spin adducts to detectable amounts. Detection of the fatty acid spin adducts is usually performed by Electron Paramagnetic Resonance (EPR) or Electron Spin Resonance (ESR), and the identification of the fatty acid radical species present is achieved through the hyperfine coupling constants observed in the spectrum which are further inserted in a spin trapping simulation database (as an example: http://epr.niehs.nih.gov/stdb1.html) for comparison. Using the methodology developed for the detection in *in vitro* of oxygen radical species [Parker et al., 1991; Anzai et al., 2003; Qian et al., 2003; Li et al., 2004; Qian et al., 2005] and of alkyl radicals [Dikalov and Mason, 2001; Stolze et al., 2002; Guo et al., 2004; Qian et al., 2005], several studies are available in the literature reporting the identification of fatty acid alkyl spin adducts [Rota et al., 1997; Watanabe et al., 2000; Iwahashi et al., 2000, 2002; Qian et al., 2003a,b] and also of oxygen free radicals generated in *in vivo* in endothelial cells [Kaneko et al., 1995], lung [Kadiisha et al., 2004], platelet cells [Chou et al., 2005] and epithelial cells [Shi et al., 2005]. The work reporting on the identification of fatty acid spin adducts and fatty acid small alkyl spin adducts are mainly focused on the description of radical products formed enzymatically either by cytochrome [Rota et al., 1997; Iwahashi et al., 2002], lipoxygenase systems [Iwahashi et al., 1991; Iwahashi et al.; 2000; Qian et al., 2002; 2003] or manganese-dependent peroxidase [Watanabe et al., 2000], although non-enzymatic lipid peroxidation was also attempted [Stolze et al., 2002]. Based on the data obtained, the authors reported the presence of both carbon centred fatty acid alkyl and fatty acid small alkyl radicals and also of oxygen fatty acid alkyl radicals,

though, more recently some authors have drawn the attention to the similarity between the coupling constants of oxygen centred spin adducts (alkoxyl and peroxyl alkyl) in the EPR spectra [Dikalov and Mason, 2001], and of carbon centred spin adducts [Venkataraman et al., 2004], suggesting the occurrence of possible misinterpretations.

Spin trapping experiments were also attempted for the study of the radical oxidation of phospholipids, namely glycerophosphatidylcholines, although no significant conclusions were drawn [Yoshida et al., 1996; Kumamoto et al., 2005]. From the work performed, intact phospholipids spin adducts were identified by EPR analysis [Yoshida et al., 1996; Kumamoto et al., 2005], and although the phosphatidylcholines used for enzymatic oxidation [Kumamoto et al., 2005] and non-enzymatic oxidation [Yoshida et al., 1996], were expected to undergo extensive radical oxidation (PAPC (38:4) and DLPC (36:4)), the authors only reported the identification of carbon centred radicals.

More recently, another experimental approach involving the synthesis of polyclonal antibodies specific to the nitrone spin trap, named immuno-spin trapping, was developed. This methodology was initially applied to the detection of protein radicals, which, as stated by the authors, greatly increased sensitivity by detection of ESR silent species [Mason, 2004; Deterding et al., 2004; Detweiler et al., 2005].

1.3.2.3. Detection of unsaturated fatty acid radical products by mass spectrometry

The use of mass spectrometry (MS), either through Fast Atom Bombardment (FAB) [Domingues et al., 2001] or Electrospray (ES) ionisation [Iwahashi et al., 1991; 1992], in past years in the identification of spin adducts of free radicals that were EPR silent and the results achieved provided good potential for its application to radicals of other molecules. The combination of liquid chromatography coupled with EPR detection with confirmation by MS described in the study of oxygen radical spin adducts [Parker et al., 1991; Iwahashi et al., 1992] is becoming widely reported in the study of enzymatic fatty acid peroxidation and in the identification of fatty acid and fatty acid small alkyl spin adducts of ω-3 [Qian et al., 2000; 2003a] and ω-6 PUFA [Iwahashi et al., 2002; Qian et al.; 2002; 2003b] allowing to perform tandem mass spectrometry of the ions that were observed in the LC-EPR spectrum. The MS/MS data obtained provides confirmation by the presence of the product ion formed by loss of the spin trap in the product ion spectra [Qian et al., 2000; Iwahashi et al., 2002; Qian et al.; 2002; 2003a,b], although no additional information regarding the location of the substitutents or of the spin trap was drawn. In spite of this, several fatty acid spin adducts were identified comprising hydroxy and epoxy derivatives of ω-3 and ω-6 fatty acids, and once again the location of such derivatives along the unsaturated

carbon chain was not proposed. In addition to the fatty acid alkyl spin adducts, several fatty acid small alkyl spin adducts resulting from cleavage of the unsaturated fatty acid chain were identified, particularly pentyl ($^{\bullet}C_5H_{11}$) and octanoic acid ($^{\bullet}C_8H_{15}O_2$) radical for both octadecadienoic acid and eicosatetraenoic acid [Iwahashi et al.; 2000; Qian et al., 2002; 2003]. The authors noticed that in radical oxidation of the ω-6 fatty acids particular fatty acid small alkyl spin adducts were predominant, namely the pentyl radical, which was derived from the alkoxyl fatty acid attack of the ω-6 position and attributed to the specificity of the enzymatic oxidation. The authors were also able to propose the presence of other positional isomers of fatty acid alkoxyl radicals based on the fatty acid small alkyl radicals identified [Iwahashi et al., 2002; Qian et al., 2003a, b].

The use of spin trapping experiments in the identification of phospholipid free radicals and their detection by MS is, to our knowledge, limited to one single work [Kumamoto et al., 2005]. In there, the authors after enzymatic oxidation of DLPC (36:4) report the identification of the 13-alkoxyl derivative based on the presence of the pentyl (POBN/$^{\bullet}C_5H_{11}$) spin adduct [Kumamoto et al., 2005].

Still, in spite of the vast literature available reporting on the identification of lipid spin adducts and lipid small alkyl spin adducts and the results achieved by MS [Qian et al., 2002; Qian et al., 2003a,b], the use of tandem mass spectrometry for the structural characterisation of such lipid spin adducts regarding the location of the spin and of the substitutent groups along the unsaturated fatty acid chain has not been fully explored.

1.3.2.4. Detection of unsaturated fatty acid non-radical products

Briefly, and as shown in Scheme 2, non-radical products are formed from intermediate fatty acid free radicals during lipid peroxidation, namely hydroxy, keto, epoxy, hydroperoxides fatty acid derivatives, resulting from insertion of oxygen atoms and named long-chain products, and aldehydes, keto- and hydroxy-aldehydes, dicarboxylic acids, keto- and hydroxy-dicarboxylic acids, alkanes, alkenes, and conjugated dienes formed by β-scission mechanism during the propagating steps of the radical reaction and named short-chain products.

Most of the work performed on the characterisation of lipid peroxidation products by MS was achieved by two different approaches. The long-chain fatty acid products, resulting from the insertion of oxygen atoms, were analysed in the negative mode without prior derivatisation [Nakamura et al., 1997,1998; Hall et al., 1998; Dickinson et al., 2002],

although analysis by GC-MS were also found in the literature [Iwase et al., 1998; Inouye et al., 1999]. From the literature available most of the works are focused on identification, and in some cases quantification in biological fluids, of oxidation products of arachidonic acid (AA) such as isoprostanes [Li et al., 1999; Pratico et al., 2004; Ward et al., 2005], although other products such as fatty acid hydroxy, epoxy and hydroperoxide derivatives [Nakamura et al., 1997, 1998; Hall et al., 1998; Inouye et al., 1999; Dickinson et al., 2002; Ward et al., 2005].

In the case of the identification of long-chain oxidation products of phospholipids, this is performed, not directly but, by the analysis of oxidised PUFA obtained by ester hydrolysis and characterisation by tandem mass spectrometry [MacMillan et al., 1995; Nakamura et al., 1997, 1998; Hall et al., 1998; Inouye et al., 1999] and the results obtained are then extrapolated for the intact structure. Only, more recently, MS in association with liquid chromatography was applied to the study of oxidised phospholipids formed by insertion of oxygen atoms [Khaselev and Murphy, 2000a,b; Spickett et al., 1998; Jerlich et al., 2003; Adachi et al., 2004; Vitrac et al., 2004; Berry et al., 2005; Adachi et al., 2005], and it was possible to propose the presence of hydroxy [Spickett et al., 1998; Jerlich et al., 2003; Adachi et al., 2004; Vitrac et al., 2004; Berry et al., 2005; Adachi et al., 2005], keto [Adachi et al., 2004; Vitrac et al., 2004], epoxy, hydroperoxide [Spickett et al., 1998; Jerlich et al., 2003; Vitrac et al., 2004; Adachi et al., 2004, 2005], and tri-hydroxy derivatives [Adachi et al., 2004; Adachi et al., 2005]. In some cases, the LC-MS data was complemented with tandem mass spectrometry data, which based on the number of H_2O and H_2O_2 molecules lost from the precursor ion [Spickett et al., 1998; Adachi et al., 2004; Adachi et al., 2005; Berry et al., 2005] allowed corroborating the derivatives proposed for the glycerophosphatidylcholines (GPC) studied. Considering the results achieved in the identification of the hydroxy and oxo groups within the PUFA chain [Wheelan et al., 1996; Cheng and Gross, 1998] the structural characterisation of phospholipid peroxidation products by tandem mass spectrometry has not been fully explored.

Fatty acid short-chain peroxidation products resulting from the breakdown of the carbon chain, have been identified by mass spectrometry involving prior derivatisation procedures. This is carried out usually by GC-MS for the free short-chain products [Loidl-Stahlhofen and Spiteller, 1994; Mlakar and Spiteller, 1996; Inouye et al., 2000; Spiteller et al., 2001; Deng et al., 2004], and by FAB-MS or ESI-MS coupled with liquid chromatography in short-chain products esterified to phospholipids [Kayganich-Harrison et al., 1994; Harrison et al., 2000; Tokumura et al., 2000; Podrez et al., 2002]. Both

techniques were applied to the identification of oxidation products of ω-6 fatty acids, free and esterified, revealing the wide variety of carbonyl compounds formed, namely α,β-(un)saturated(hydroxy)-aldehydes, α,β-(un)saturated(hydroxy)-dicarboxylic acids, and alk(e)anes with various chain lengths. Usually, for short-chain oxidation products, the *m/z* value alone observed in the mass spectrum is indicative of the short-chain product and consequently of the structure, unlike what is observed in the mass spectrum of long-chain products, which has the difficulty of the contribution of probable structural and positional isomers in a single ion. The normal values of free aldehydes reported in blood are in μM level [O´Brien-Coker et al., 2001; Deng et al., 2004] but were described to rise in the blood of lung cancer patients [Deng et al., 2004], in atherosclerotic lesions [Watson et al., 1997; Subbanagounder et al., 2000], and although the levels of fatty acid aldehydes are very low, it is proposed that they can accumulate locally or near peroxidised membranes [Choudhary et al., 2005]. The content of short-chain aldehydic products in *in vivo* are mainly determined by the quantification of aldehydes such as hexanal and HNE, the major aldehydic products of ω-6 fatty acids, do not reflect the contribution of other free aldehydes and does not account for the bound HNE to glutathione, the main detoxification route [Völkel et al., 2005], or to proteins, predominant targets of aldehydes [Carini et al., 2004].

On the other hand, short-chain aldehydic products esterified to phospholipids are poorly studied and can be summarised to the identification of 4 compounds, namely 5-oxo-pentanoyl [Subbanagounder et al., 2000; Podrez et al., 2002], 9-oxo-nonanoyl [Itabe et al., 1996; Podrez et al., 2002; Hoff et al., 2003], 5-carboxy-pentanoyl [Subbanagounder et al., 2000; Podrez et al., 2002] and 5-hydroxy-octenoyl [Harrison et al., 2000; Khaselev and Murphy, 2000]. Based on the numerous free aldehydic products identified as fatty acid oxidation products [Loidl-Stahlhofen and Spiteller, 1994; Mlakar and Spiteler, 1996; Spiteller et al., 2001], more aldehydic and substituted aldehydic products esterified to phospholipids are expected to arise from phospholipid radical oxidation, although they were not yet described. Some of the short-chain GPC products identified in *in vitro* radical oxidation have even been reported in biological samples, namely in the blood plasma [Schlame et al., 1996; Frey et al., 2000] and in oxLDL from atherosclerotic lesions [Subbanagounder et al., 2000; Frey et al., 2000; Podrez et al., 2002; Hoff et al., 2003].

In general the presence of oxidised fatty acid chains in phospholipids increases the hydrophilic character of the membrane and was observed to induce changes in the fluidity [Borst et al., 2000; Megli and Sabatini, 2003a] and of the membrane acyl packing [Megli and Sabatini, 2003b].

1.3.3. Cytotoxicity of unsaturated fatty acid oxidation products and detoxification reactions

Much of the work devoted to the identification and quantification of short-chain fatty acid products, mainly HNE, is due to the cytotoxicity that have been shown to possess. The cytotoxicity observed in fatty acid oxidation products is attributed to the presence of terminal aldehyde group (electrophilic group) and the double bond at C-3 [Haynes et al., 2000], conferring a bifunctional electrophilic character [Lee et al., 2005; Jian et al., 2005; Blair et al., 2005]. Cytotoxicity of aldehydes is chain-length dependent, decreasing as the chain length increases until C6, and then increases for compounds with carbon chain above C6 [Haynes et al., 2000; Niknahad et al., 2003]. This behaviour may be related with the ability of such products to cross the membrane layer [Haynes et al., 2000]. The cytotoxicity of α,β-(hydroxy)-unsaturated aldehydes (alkenals) was observed in hepatocytes [Niknahad et al., 2003], in endothelial cells [Herbst et al., 1999; Jian et al., 2005] and in epithelial cells [Choudhary et al., 2005], most likely by formation of cross-linking reactions with amino groups [Miwa et al., 1997; Salomon et al., 2000; Chung et al., 2003; Ishii et al., 2003; Fenaille et al., 2003; Douki et al., 2004; Isom et al., 2004; Yocum et al., 2005; Ishii et al., 2006], where it is reported to induce apoptotic events such as DNA fragmentation and morphological changes like blistering and shrinkage [Jian et al., 2005].

At the same time, the reactivity of aldehydes towards amino and thiol groups is also responsible for the *in vivo* detoxification reactions which take place by formation of adducts with thiol groups present in glutathione [Milne et al., 2004; Völkel et al., 2005; Choudhary et al., 2005; Jian et al., 2005], or, in the presence of low levels of glutathione, with histidine-containing dipeptides such as anserine and carnosine [Aldini et al., 2002; Aldini et al., 2004].

1.3.4. Cross-linking reactions of unsaturated fatty acid oxidation products

The cytotoxicity of alkenals attributed to the reactivity of carbonyl groups towards nucleophilic groups results in the occurrence of covalent interactions by cross-linking reactions [Bertlett and Stadtman, 1997]. However, it must be considered that cross-linking reactions may result from, i) reaction of carbonyl compounds, formed from radical oxidation of lipids and/or phospholipids, with the amino acid residues (Schiff adducts), or ii) reaction of the double bond with amino acids (Michael adducts), and iii) reaction of carbonyl compounds with other amino compounds. Nonetheless, in the literature the

identification by mass spectrometry of products of cross-linking reactions are mainly focused on lipid-peptide adducts formed between 4-hydroxy-2-nonenal, which is described as the major product of ω-6 fatty acids [Lee et al., 2000; Lee et al., 2005], and peptides or proteins [reviewed in Carini et al., 2004]. Thus, minor attention has been focused on other covalent adducts that can be formed, specifically between oxidised phospholipids and peptides or proteins, named phospholipid-peptide adducts [Boullier et al., 2000; Hoff et al., 2003], which have been identified in oxLDL through the use of specific antibodies [Boullier et al., 2000; Brame et al., 2004], or between oxidised fatty acids and DNA bases [Chung et al., 2003; Douki et al., 2004].

Until recently, the identification of the peptide-lipid adducts was achieved by amino acids analysis, based on the differences of the amino acid loss observed after modification [Uchida et al., 1993; Szweda et al., 1993], but the development of soft ionisation methods (ESI and MALDI) has increased the number of studies that report the use of mass spectrometry for the identification of peptide-lipid adducts [Magni et al., 2002; Fenaille et al., 2003; Ishii et al., 2003; Shibata et al., 2003; Isom et al., 2004; Ishii et al., 2006] and characterisation of peptide-lipid adducts through tandem mass spectrometry. This has allowed researchers to notice that lipid modification, in peptides and proteins, is determined by the reactivity of the amino acids, but also by the availability of those amino acids to reaction. Amino acids like histidine [Isom et al., 2003; Fenaille et al., 2003; Ishii et al., 2003], cysteine [Shibata et al., 2003; Ishii et al., 2003], lysine [Magni et al., 2002; Fenaille et al., 2003] and the N-terminal amino acids [Magni et al., 2002; Fenaille et al., 2003] are the most reported to undergo modification. In turn, the modification of amino acids by fatty acid oxidation products, or the inter and intra molecular cross-linking reactions between the Schiff and Michael adducts [Uchida et al., 1993], occurring at the catalytic site of the enzyme [Ishii et al., 2003; Shibata et al., 2003] or at the surface of the protein [Ishii et al., 2003; Shibata et al., 2003; Yocum et al., 2005] are ultimately responsible for conformational changes and consequently loss of enzymatic activity. So far, the modification of proteins by fatty acid peroxidation products were described in glycolytic enzymes [Uchida et al., 1993; Miwa et al., 1997; Ishii et al., 2003], and in pentose-phosphate pathway enzymes [Miwa et al., 1997], although others such as cytochrome c [Isom et al., 2004] and thioredoxin involved in the transport of electrons [Shibata et al., 2003]and in β-amyloid peptides [Magni et al., 2002] and in insulin [Fenaille et al., 2003; Ishii et al., 2006], were reported.

The results achieved by MS on the identification of lipid-peptide(protein) adducts, and by MS/MS on the identification of the modified amino acids, has focused the attention

of research groups to the possible role of lipid-peptide adducts on the pathogenesis of age-related diseases [Magni et al., 2002]. On the other hand, until now it were not yet reported studies using mass spectrometry for the identification and characterisation of phospholipid-peptide(protein) adducts, which were identified in atherosclerotic plaques by sensitive immuno-detection using specific antibodies [Salomon et al., 2000; Friedman et al., 2002; Hoff et al., 2003; Brame et al., 2004]. The phospholipid-protein adducts are thought to play a significant role in the uptake of oxLDL by the macrophages receptors [Boullier et al., 2000; Friedman et al., 2002], however, the mechanism for the recognition which, according to the authors, may occur through the phospholipid or the peptide moiety, is not yet fully understood.

Other cross-linking reactions, similar to the reaction described earlier between carbonyl and nucleophilic groups, may take place between aldehydes and the amino group of phosphoethanolamines [Guichardant et al.; 1998; Bacot et al., 2003], and in this case reflect lipid-phospholipid covalent interactions. Also, polymerisation reactions between phospholipid alkenals by an aldol condensation mechanism may take place [Friedman et al., 2002], which in this case reflect the occurrence of phospholipid-phospholipid covalent interactions.

1.3.5. Biological role of unsaturated fatty acid oxidation products and others

Given the increasing number of research work that is being performed on the identification of oxidised fatty acids and phospholipids, and of other products arising from cross-linking reactions between oxidised fatty acids and other biomolecules, some work has been carried out in order to determine the possible role to the cell. In this section, not only the effects of the products that result from non-enzymatic oxidation are briefly described, but also of the ones resulting from enzymatic oxidation (LOX and COX), considering that these may in turn result in the formation of bifunctional nucleophiles (α,β-hydroxy alkenals).

In general, biological activity of oxidised phospholipids is dependent on structural requirements [Schwenk and Schröder, 1995], such as: a) the presence of phosphocholine head [Watson et al., 1999], b) the chemical bond at the *sn*-1 [Leitinger, 2003], and c) the terminal functional group present at the *sn*-2 [Kern et al., 1998; Subbanagounder et al., 2000; Podrez et al., 2002]. Thus, products arising from fatty acid oxidation are described to be involved in signalling events, such as inducing inflammatory responses including intracellular calcium increase in neutrophils [Khaselev and Murphy, 2000; Leitinger, 2003],

expression of adhesion molecules and regulation of cytokines in endothelial cells [Subbanagounder et al., 2002], and to inhibit interferon-γ in vascular smooth muscle cells in rat aorta [Tokumura et al., 2000]. Also, prostanoids compounds were reported to induce apoptosis of certain neoplastic cells and by this action inhibit tumorigenesis [Clay et al., 1999], others induced cyclooxygenase 2 in monocytes [Ponstler et al., 2002]. In the case of short-chain products esterified to phospholipids they have been described to exhibit biological activity similar to platelet aggregating factors (PAF) [McIntyre et al., 1999; Marathe et al., 2000].

In the case of lipid-peptide adducts, and particularly the alkylation of glyceraldehyde-3-phosphate dehydrogenase [Uchida et al., 1993; Ishii et al., 2003] has direct effect on ATP synthesis, of glucose-6-phosphate dehydrogenase [Szweda et al., 1993] on NADPH regeneration, and of cytochrome c [Isom et al., 2004] and of thioredoxin [Shibata et al., 2003] with implications in the electron transport chain.

1.3.6. Unsaturated fatty acid oxidation products as biomarkers of oxidative stress

As result of the chemical modifications induced to fatty acids and to fatty acid containing biomolecules by reactive oxygen species, and of the chemical modifications derived from the reaction of fatty acid oxidation products with other molecules, researchers have proposed some fatty acid oxidation products, found in the breath, blood and urine samples, as potential biomarkers of several diseases. For instance, alkanes and alkenes, have been tentatively applied as biomarkers of lung and liver diseases [Miekisch et al., 2004], short-chain products as potential biomarkers of keto-acidosis [Inouye et al., 2000] while hydroxy derivatives of unsaturated fatty acids were associated with diabetic patients [Inouye et al., 1999] and for hypertensive patients [Ward et al., 2005], and hydroperoxides for alcoholic patients [Adachi et al., 2004b], while isoprostanes and neuroprostanes were proposed as biomarkers for Alzheimer's disease [Montine et al., 2004]. Also, peptide-lipid adducts, and particularly lipid-glutathione [Völkel et al., 2005] and lipid-hemoglobin [Yocum et al., 2005] adducts were proposed as potential biomarkers of oxidative stress. However, the occurrence of elevated levels of some fatty acid oxidation products observed after extreme exercise, cigarette smoking and alcohol ingestion may result in misleading conclusions [Cracowski et al., 2002]. Also, the difficulty in determining the concentration-effects relationship in *in vivo* limits the proposal of biochemical markers [Meagher and Fitzgerald, 2000].

1.4. Aims

Following the increasing trend in the role of lipid peroxidation in the pathogenesis of oxidative stress related pathologies, and the potential of mass spectrometry coupled with other techniques for the detailed structural characterisation, the purpose of this study was primarily, and using the Fenton reaction as the generator of radical oxygen species, i) to access the use of mass spectrometry in the identification of fatty acid radicals, using the methodology developed for the detection of free radicals; ii) to determine if, and what, structural information could be drawn from the product ion spectra of the fatty acid spin adducts, and iii) finally to extend the identification of lipid free radicals to more complex structures, namely diacyl-glycerophosphatidylcholines with ω-9 and ω-6 fatty acids. In addition, iv) other products (non-radical) resulting from radical-radical terminating steps, and from reaction with secondary products, were pursued. Following this, and in order to obtain a full characterisation of the products formed upon radical oxidation, the introduction of liquid chromatography prior to mass spectrometry detection (LC-MS) is required.

1.5. Bibliography

Adachi J, Yoshioka N, Funae R, Nushida H, Asano M, Ueno Y. Determination of phosphatidylcholine monohydroperoxides using quadrupole time-of-flight mass spectrometry. *J. Chrom.* B. 2004, 806,41-46.

Adachi J, Matsushita S, Yoshioka N, Funae R, Fujita T, Higuchi S, Ueno Y. Plasma phosphatidylcholine hydroperoxide as a new marker of oxidative stress in alcoholic patients. *J. Lipid Res.* 2004, **45**, 967-971.

Adachi J, Yoshioka N, Sato M, Nakagawa K, Yamamoto Y and Ueno Y. Detection of phosphatidylcholine oxidation products in rat heart using quadrupole time-of-flight mass spectrometry. *J. Chrom. B.* 2005, **823**, 37-43.

Aldini G, Granata P, Carini M. Detoxification of cytotoxic α,β-unsaturated aldehydes by carnosine: characterization of conjugated adducts by electrospray ionization tandem mass spectrometry and detection by liquid chromatography/mass spectrometry in rat skeletal muscle. *J. Mass Spectrom.* 2002, 37, 1219-1228.

Aldini G, Orioli M, Carini M, Facino RM. Profiling histidine-containing dipeptides in rat tissues by liquid chromatography/electrospray ionization tandem mass spectrometry. *J. Mass Spectrom.* 2004, **39**, 1417-1428.

Ando K, Ogawa K, Misaki S, Kikugawa K. Increased release of free Fe ions in human erythrocytes during aging in the circulation. *Free Rad. Res.* 2002, **36**, 1079-1084.

Anzai K, Aikawa T, Furukawa Y, Matsushima Y, Urano S, Ozawa T. ESR measurement of rapid penetration of DMPO and DEPMPO spin traps through lipid bilayer membranes. *Arch. Biochem. Biophys.* 2003, **415**, 251-256.

Araseki M, Yamamoto K, Miyashita K. Oxidative stability of polyunsaturated fatty acid in phosphatidylcholine liposomes. *Biosci. Biotechnol. Biochem.* 2002, 66, 2573-2577.

Bacot S, Bernoud-Hubac N, Baddas N, Chantegrel B, Deshayes C, Doutheau A, Lagarde M, Guichardant M. Covalent binding of hydroxy-alkenals 4-HDDE, 4-HHE and 4-HNE to ethanolamine phospholipid subclasses. *J. Lipid Res.* 2003, **44**, 917-926.

Berry KAZ and Murphy RC. Free radical oxidation of plasmalogen glycerophosphocholine containing esterified docosahexaenoic acid: structure determination by mass spectrometry. *Antioxid. Redox Signal.* 2005, **7**, 157-169.

Bertlett BS and Stadtman ER. Protein oxidation in aging, disease and oxidative stress. *J. Biol. Chem.* 1997, **272**, 20313-20316.

Borst JW, Visser NV, Kouptsova O, Visser AJWG. Oxidation of unsaturated phospholipids in membrane bilayer mixtures is accompanied by membrane fluidity changes. *Biochim. Biophys. Acta.* 2000, **1487**, 61-73.

Boullier A, Gillote KL, Hörkkö S, Green SR, Friedman P, Dennis EA, Witztum JL, Steinberg D, Quehenberger O. The binding of oxidized low density lipoprotein to mouse CD36 is mediated in part by oxidized phospholipids that are associated with both the lipid and protein moieties of the lipoprotein. *J. Biol. Chem.* 2000, **275**, 9163-9169.

Buettner GR and Jurkiewicz BA. Catalytic metals, ascorbate and free radicals: combinations to avoid. *Radiat. Res*. 1996, **145**, 532-541.

Carini M, Aldini G, Facino RM. Mass spectrometry for detection of 4-hydroxy-trans-2-nonenal (HNE) adducts with peptides and proteins. *Mass Spectrom. Rev.* 2004, **23**, 281-305.

Cheng C, Gross ML. Fragmentation mechanisms of oxofatty acids via high-energy collisional activation. *J. Am. Soc. Mass Spectrom*. 1998; **9**: 620-627.

Choudhary S, Xiao T, Srivastava S, Zhang W, Chan LL, Vergara LA, van Kuijk FJGM, Ansari NH. Toxicity and detoxification of lipid-derived aldehydes in cultured retinal pigmented epithelial cells. *Toxicol. Applied Pharmacol*. 2005, **204**, 122-134.

Chou D-S, Hsiao G, Shen M-Y, Tsai Y-J, Chen T-F, Sheu J-R. ESR spin trapping of a carbon centered free radical from agonist-stimulated human platelets. *Free Rad. Biol.& Med*. 2005, **39**, 237.

Chung F-L, Pan J, Choudhury S, Roy R, Hu W, Tang M. Formation of trans-4-hydroxy-2-nonenal and other enal-derived cyclic DNA adducts from ω-3 and ω-6 polyunsaturated fatty acids and their roles in DNA repair and human p53 gene mutation. *Mutat. Res*. 2003, **531**, 25-36.

Comporti M, Signorini C, Buonocore G, Ciccoli L. Iron release, oxidative stress and erythrocyte ageing. *Free Rad. Biol. & Med*. 2002, **32**, 568-576.

Cracowski J-L, Durand T, Bessard G. Isoprostanes as a biomarker of lipid peroxidation in humans: physiology, pharmacology and clinical implications. *Trends Pharmacol. Sci.* 2002, **23**, 360.

Davies MJ. The oxidative environment and protein damage. *Biochim. Biophys. Acta*. 2005, **1703**, 93-109.

De Zwart LL, Meerman JHN, Commandeur JNM and Vermeulen NPE. Biomarkers of free radical damage applications in experimental animals and in humans. *Free Rad. Biol. & Med.* 1999, **26**, 202-226.

Deng C, Zhang X. A simple, rapid and sensitive method for determination of aldehydes in human blood by gas chromatography/mass spectrometry and solid-phase microextraction with on-fiber derivatization. *Rapid Commun. Mass Spectrom*. 2004, **18**, 1715-1720.

Detweiler CD, Lardinois OM, Deterding LJ, Ortiz de Montellano PR, Tomer KB, Mason RP. Identification of the myoglobin tyrosyl radical by immuno-spin trapping and its dimerization. *Free Rad. Biol. & Med*. 2005, **38**, 969-976.

Dikalov SI and Mason RP. Spin trapping of polyunsaturated fatty acid-derived alkyl peroxyl radicals: reassignment to alkoxyl radical adducts. *Free Rad. Biol.* & *Med*. 2001, **30**, 187-197.

Domingues P, Domingues MRM, Amado FML, Ferrer-Correia AJ. Detection and characterisation of hydroxyl radical adducts by mass spectrometry. *J. Am. Soc. Mass Spectrom*. 2001, **12**,1214-1219.

Douki T, Odin F, Caillat S, Favier A, Cadet J. Predominance of the 1,N^2-propano 2'-deoxyguanosine adduct among 4-hydroxy-2-nonenal-induced DNA lesions. *Free Rad. Biol. & Med*. 2004, **37**, 62-70.

Dröge W. Free radicals in the physiological control of cell function. *Physiol. Rev.* 2002, **82**, 47.

Fenaille F, Guy PA, Tabet J-C. Study of protein modification by 4-hydroxy-2-nonenal and other short chain aldehydes analysed by electrospray tandem mass spectrometry. *J. Am. Soc. Mass Spectrom*. 2003, **14**, 215-226.

Folch J, Lees M, Stanley GHS. A simple method for the isolation and purification of total lipids from animal tissues. *J. Biol. Chem*. 1957; **226**: 497.

Frey B. Haupt R. Alms S, Holzmann G, König T, Kern H, Kox W, Rüstow B, Schlame M. Increase in fragmented phosphatidylcholine in blood plasma by oxidative stress. *J. Lipid Res*. 2000, **41**, 1145.

Guichardant M, Taibi-Tronche P, Fay LB, Lagarde M. Covalent modification of aminophospholipids by 4-hydroxy-2-nonenal. *Free Rad. Biol. & Med*. 1998, **25**, 1049-1056.

Guo Q, Qian SY, Mason RP. Separation and identification of DMPO adducts of oxygen-centred radicals formed from organic hydroperoxides by HPLC-ESR, ESI-MS and MS/MS. *J. Am. Soc. Mass Spectrom*. 2004, **14**, 862-871.

Hall LM and Murphy RC. Electrospray mass spectrometric analysis of 5-hydroperoxy and 5-hydroxy eicosatetraenoic acids generated by lipid peroxidation of red blood cell ghost phospholipids. *J. Am. Soc. Mass Spectrom*. 1998, **9**, 527-532.

Hardy M, Ouari O, Charles L, Finet J-P, Iacazio G, Monnier V, Rockenbauer A, Tordo P. Synthesis and spin-trapping behaviour of 5-ChEPMPO, a cholesteryl ester analogue of the spin trap DEPMPO. *J. Org. Chem.* 2005, **70**, 10426-10433.

Harrison KA, Davies SS, Marathe GK, McIntyre T, Prescott S, Reddy KM, Falck JR, Murphy RC. Analysis of oxidised glycerophosphocholine lipids using electrospray ionisation mass spectrometry and microderivatization techniques. *J. Mass Spectrom*. 2000, **35**, 224-236.

Hawkins CL and Davies MJ. Generation and propagation of radical reactions on proteins. *Biochim. Biophys. Acta*. 2001, **1504**, 196-219.

Haynes RL, Szweda L, Pickin K, Welker ME, Townsend AJ. Structure-activity relationship for growth inhibition and induction of apoptosis by 4-hydroxy-2-nonenal in raw 264.7 cells. *Mol. Pharmacol*. 2000, **58**, 788-794.

Herbst U, Toborek M, Kaiser S, Mattson MP, Henning B. 4-hydroxy-nonenal induces dysfunction and apoptosis of cultured endothelial cells. *J. Cell. Physiol*. 1999, **181**, 295-303.

Hoff HF, O'Neill J, Wu S, Hoppe G, Salomon R. Phospholipid hydroxyalkenals. Biological and chemical properties of specific oxidized lipids present in atherosclerotic lesions. *Arterioscler. Thromb. Vasc. Biol*. 2003, **23**, 275-282.

Hunte C. Specific protein-lipid interactions in membrane proteins. *Biochem. Soc. Trans*. 2005, **33**, 938-942.

Inouye M, Mio T, Sumino K. Dicarboxylic acids as markers of fatty acid peroxidation in diabetes. *Atheroscler*. 2000, **148**, 197-202.

Inouye M, Mio T, Sumino K. Formation of 9-hydroxy linoleic acid as a product of phospholipid peroxidation in diabetic erythrocyte membranes. *Biochim. Biophys. Acta*. 1999, **1438**, 204-212.

Ishii T, Tatsuda E, Kumazawa S, Nakayama T, Uchida K.Molecular basis of enzyme inactivation by an endogenous electrophile 4-hydroxy-2-nonenal: identification of modification sites in glyceraldehyde-3-phosphate dehydrogenase. *Biochem*. 2003, **42**, 3474-3480.

Ishii T, Kumazawa S, Sakurai T, Nakayama T, Uchida K. Mass spectroscopic characterization of protein modification by malonaldehyde. *Chem. Res. Toxicol.* 2006, **19**, 122-129.

Isom AL, Barnes S, Wilson L, Kirk M, Coward L, Darley-Usmar V. Modification of cytochrome c by 4-hydroxy-2-nonenal: evidence for histidine, lysine and arginine-aldehyde adducts. *J. Am. Soc. Mass Spectrom.* 2004, **15**, 1136-1147.

Itabe H, Yamamoto H, Suzuki M, Kawai Y, Nakagwa Y, Suzuki A, Imanaka T, Takano T. Oxidized phosphatidylcholines that modify proteins: analysis by monoclonal antibody against oxidized low density lipoprotein. *J. Biol. Chem*. 1996, **271**, 33208-33217.

Iwahashi H, Parker CE, Mason RP, Tomer KB. Combined liquid chromatography/electron paramagnetic resonance spectrometry/Electrospray ionization mass spectrometry for radical identification. *Anal. Chem*. 1992, **64**, 2244-2252.

Iwahashi H, Nishizaki K, Takagi I. Cytochrome c catalyses the formation of pentyl radical and octanoic acid radical from linoleic acid hydroperoxide. *Biochem. J.* 2002, **361**, 57-66.

Iwase H, Takatori T, Nagao M, Nijima H, Iwadate K, Matsuda Y, Kobayashi M. Formation of keto and hydroxy compounds of linoleic acid in submitochondrial particles of bovine heart. *Free Rad. Biol. & Med.* 1998, **24**, 1492-1503.

Jerlich A, Schaur RJ, Pitt AR, Spickett CM. The formation of phosphatidylcholine oxidation products by stimulated phagocytes. *Free Rad. Res*. 2003, **37**, 645-653.

Jian W, Arora JS, Oe T, Shuvaev VV, Blair IA. Induction of endothelial cell apoptosis by lipid hydroperoxide-derived bifunctional electrophiles. *Free Rad. Biol. & Med*. 2005, **39**, 1162-1176.

Kadiiska MB, Ghio AJ, Mason RP. ESR investigation of the oxidative damage in lungs caused by asbestos and air pollution particles. *Spectrochim. Acta A* 2004, **60**, 1371-1377.

Kaneko M, Kodama M, Inoue F. The localization of DMPO spin adducts of OH in endothelial cells exposed to hydrogen peroxide. *Toxicol. Lett*. 1995, **81**, 73-78.

Kayganich-Harrison KA and Murphy RC. Characterization of chain-shortened oxidized glycerophosphocholines lipids using fast atom bombardment and tandem mass spectrometry. *Anal. Biochem*. 1994; **221**, 16.

Kern H, Volk T, Knauer-Schiefer S, Mieth T, Rüstow B, Kox WJ, Schlame M. Stimulation of monocytes and platelets by short-chain phosphatidylcholines with and without terminal carboxyl group. *Biochim. Biophys. Acta*. 1998, **1394**, 33-42.

Khaselev N and Murphy RC. Peroxidation of arachidonate containing plasmenyl glycerophosphocholines: facile oxidation of esterified arachidonate at carbon-5. *Free Rad. Biol. & Med*. 2000a, **29**, 620-632.

Khaselev N, Murphy RC. Structural characterization of oxidized phospholipid products derived from arachidonate-containing plasmenyl glycerophosphocholine. *J. Lipid Res*. 2000b, **41**, 564-572.

Kumamoto K, Hirai T, Kishioka S, Iwahashi H. Identification of a radical formed in the reaction mixtures of oxidised phosphatidylcholines with ferrous ions using HPLC-ESR and HPLC-ESR-MS. *Free Rad. Res*. 2005, **39**, 987-993.

Lange C, Nett JH, Trumpower BL, Hunte C. Specific roles of protein-phospholipid interactions in the yeast cytochrome bc1 complex structure. *Eur. Mol. Biol. Org*. 2001, **20**, 6591-6600.

Lee SH, Oe T, Arora JS, Blair IA. Analysis of Fe(II)-mediated decomposition of a linoleic acid-derived lipid hydroperoxide by liquid chromatography/mass spectrometry. *J. Mass Spectrom*. 2005, **40**, 661-668.

Leitinger N. Oxidized phospholipids as modulators of inflammation in atherosclerosis. *Curr. Opin. Lipidol.* 2003, **14**, 421-430.

Li H, Lawson JA, Reilly M, Adiyaman M, Hwang S-W, Rokach J, Fitzgerald GA. Quantitative high performance liquid chromatography/tandem mass spectrometric analysis of the four classes of F2-isoprostanes in human urine. *PNAS USA*1999, **96**, 13381-13386.

Li Q-T, Yeo MH, Tan BK. Lipid peroxidation in small and large phospholipid unilamelar vesicles induced by water-soluble free radical sources. *Biochem. Biophys. Res. Commun*. 2000, **273**, 72-76.

Liochev SI. The mechanism of "Fenton-like" reactions and their importance for biological systems. A biologist's view. *In* Metal Ions in Biological Systems, ed. Sigel, A. and Sigel H, Vol 36, Marcel Dekker, INC. New York, 1999, pp 1-39.

Loidl-Stahlhofen A and Spiteller G. α-hydroxyaldehydes, products of lipid peroxidation. *Biochim. Biophys. Acta.* 1994; **1211**: 156.

Magni F, Galbusera C, Tremolada L, Ferrarese C, Kienle MG. Characterisation of adducts of the lipid peroxidation product 4-hydroxy-2-nonenal and amyloid β-peptides by liquid chromatography/electrospray ionisation mass spectrometry. *Rapid Commun. Mass Spectrom*. 2002, **16**, 1485-1493.

Mason RP. Using anti-5,5-dimethyl-1-pyrrolidine N-oxide (anti-DMPO) to detect protein radicals in time and space with immuno-spin trapping. *Free Rad. Biol. & Med*. 2004, **36**, 1214-1223.

McIntyre TM, Zimmerman GA, Prescott SM. Biologically active oxidized phospholipids. *J. Biol. Chem*. 1999, **274**, 25189-25192.

Meagher EA and Fitzgerald GA. Indices of lipid peroxidation in vivo: strengths and limitations. *Free Rad. Biol. & Med*. 2000, **28**, 1745-1750.

Megli FM and Sabatini K. EPR studies of phospholipid bilayers after lipoperoxidation. 1. Inner molecular order and fluidity gradient. *Chem. Phys. Lipids*. 2003, **125**, 161-172.

Megli FM and Sabatini K. Respiration state IV-generated ROS destroy mitochondrial bilayer packing order in vitro. An EPR study. *FEBS Lett*. 2003, **550**, 185-189.

Megli FM and Sabatini K. Mitochondrial phospholipid bilayer structure is ruined after liver oxidative injury in vivo. *FEBS Lett*. 2004, **573**, 68-72.

Milne GL, Zanoni G, Porta A, Sasi S, Vidari G, Musiek ES, Freeman ML, Morrow JD. The cyclopentenone product of lipid peroxidation, 15-A_{2t}-isoprostane, is efficiently metabolised by HepG2 cells via conjugation with glutathione. *Chem. Res. Toxicol*. 2004, **17**, 17-25.

Miwa I, Adachi K, Murase S, Hamada Y, Sugiura M. 4-Hydroxy-2-nonenal hardly affects glycolysis. *Free Rad. Biol. & Med*. 1997, **23**, 610-615.

Mlakar A and Spiteller G. Previously unknown aldehydic lipid peroxidation compounds of arachidonic acid. *Chem. Phys. Lipids*. 1996; **79**, 47.

Montine KS, Quinn JF, Zhang J, Fessel JP, Roberts II LJ, Morrow JD, Montine TJ. Isoprostanes and related products of lipid peroxidation in neurodegenerative diseases. *Chem. Phys. Lipids*. 2004, **128**, 117-124.

Multhaup G and Masters CL. Metal binding and radical generation of proteins in human neurological diseases and aging. *In* Metal Ions in Biological Systems, ed. Sigel, A. and Sigel H, Vol 36, Marcel Dekker, INC. New York, 1999, pp 365-387.

Murphy RC. Free-radical induced oxidation of arachidonoyl plasmalogen phospholipids: antioxidant mechanism and precursor pathway for bioactive eicosanoids. *Chem. Res. Toxicol.* 2001, **14**, 463-472.

Nagata M. Inflammatory cells and oxygen radicals. *Current Drug Targets*. 2005, **4**, 503-504.

Nakamura T, Bratton DL, Murphy RC. Analysis of epoxyeicosatetraenoic and monohydroxyeicosatetraenoic acids esterified to phospholipids in human red blood cells by electrospray tandem mass spectrometry. *J. Mass Spectrom*. 1997, **32**, 888-896.

Nakamura T, Henson PM, Murphy RC. Occurrence of oxidized metabolites of arachidonic acid esterified to phospholipids in murine lung tissue. *Anal. Biochem*. 1998, **262**, 23-32.

Niki E, Yoshida Y, Saito Y, Nguchi N. Lipid peroxidation: mechanisms, inhibition, and biological effects. *Biochem. Biophys. Res. Commun*. 2005, **338**, 668-676.

Niknahad H, Siraki AG, Shuhendler A, Khan S, Teng S, Galati G, Easson E, Poon R, O'Brien PJ. Modulating carbonyl cytotoxicity in intact rat hepatocytes by inhibiting carbonyl-metabolizing enzymes. I. Aliphatic alkenals. *Chem. Biol. Interact*. 2003, **143-144**, 107-117.

Nohl H, Gille L, Koxlov A, Staniek K. Are mitochondria a spontaneous and permanent source of reactive oxygen species? *Redox Report*, 2003, **8**, 135-141.

Nukuna BN, Sun G, Anderson VE. Hydroxyl radical oxidation of cytochrome c by aerobic radiolysis. Free Rad. Biol. Med. 2004, **37**, 1203-1213.

O'Brien-Coker IC, Perkins G, Mallet AI. Aldehyde analysis by high performance liquid chromatography/tandem mass spectrometry. *Rapid Commun. Mass Spectrom*. 2001, **15**, 920-928.

Oborina EM and Yappert MC. Effect of sphingomyelin versus dipalmitoylphosphatidylcholine on the extent of lipid oxidation. *Chem. Phys. Lipids*. 2003, **123**, 223-232.

Orioli M, Aldini G, Beretta G, Facino RM, Carini M. LC-ESI-MS/MS determination of 4-hydroxy-*trans*-2-nonenal Michael adducts with cysteine and histidine-containing peptides as early markers of oxidative stress in excitable tissues. *J. Chrom. B.* 2005, **827**, 109-118.

Palsdottir H and Hunte C. Lipids in membrane protein structures. *Biochim. Biophys. Acta*. 2004, **1666**, 2-18.

Podrez EA, Poliakov E, Shen Z, Zhang R, Deng Y, Sun M, Finton PJ, Shan L, Gugiu B, Fox PL, Hoff HF, Salomon RG, Hazen SL. Identification of a novel family of oxidised phospholipids that serve as ligands for the macrophage scavenger receptor CD36. *J. Biol. Chem*. 2002, **277**, 38503-38516.

Qian SY and Buettner GR. Iron and dioxygen chemistry is and important route to initiation of biological free radical oxidations: an electron paramagnetic resonance spin trapping study. *Free Rad. Biol. & Med*. 1999, **26**, 1447-1456.

Qian SY, Wang HP, Schafer FQ and Buettner GR. EPR detection of lipid-derived free radicals from PUFA, LDL, and cell oxidations. *Free Rad. Biol. & Med*. 2000, **29**, 568-579.

Qian SY, Tomer KB, Yue G, Guo Q, Kadiisha MB, Mason RP. Characterization of the initial carbon-centered pentadienyl radical and subsequent radicals in lipid peroxidation: identification via on-line high performance liquid chromatography/electron spin resonance and mass spectrometry. *Free Rad. Biol. & Med.* 2002, 33, 998-1009.

Qian SY, Guo Q, Mason RP. Identification of spin trapped carbon-centered radicals in soybean lipoxygenase-dependent peroxidation of ω-3 polyunsaturated fatty acids by LC/ESR, LC/MS and tandem MS. *Free Rad. Biol. & Med*. 2003a, **35**, 33-44.

Qian SY, Yue G, Tomer KB, Mason RP. Identification of all classes of spin-trapped carbon-centered radicals in soybean lipoxygenase-dependent lipid peroxidation of ω-6 polyunsaturated fatty acids via LC/ESR, LC/MS and tandem MS. *Free Rad. Biol. & Med*. 2003b, **34**, 1017-1028.

Reybier K, Boyer J, Farines V, Camus F, Souchard J-P, Monje M-C, Bernardes-Genisson V, Goldstein S, Nepveu F. Radical trapping properties of imidazol nitrones. *Free Rad. Res*. 2006, **40**, 11.

Rohr-Udilova N, Stolze K, Marian B, Nohl H. Cytotoxicity of novel derivatives of the spin trap EMPO. *Bioorg. Med. Chem. Lett*. 2006, **16**, 541-546.

Rosen, G.M.; Britigam, B.E.; Halpern, H.J.; Pou, S., Eds.; The oxygen paradox. In *Free Radicals, Biology and Detection by Spin Trapping*; Oxford University Press: N.Y. 1999; pp 10-82.

Rosen, G.M.; Britigam, B.E.; Halpern, H.J.; Pou, S., Eds.; kinetics of spin trapping free radicals. In *Free Radicals, Biology and Detection by Spin Trapping*; Oxford University Press: N.Y. 1999; pp 321-353.

Rota C, Barr DP, Martin MV, Guengerich FP, Tomasi A, Mason RP. Detection of free radicals produced from the reaction of cytochrome P-450 with linoleic acid hydroperoxide. *Biochem J.* 1997, **328**, 565-571.

Salomon RG, Kaur K, Podrez E, Hoff HF, Krushinsky AV, Sayre LM. HNE-derived 2-pentylpyrroles are generated during oxidation of LDL, are more prevalent in blood plasma from patients with renal disease or atherosclerosis and are present in atherosclerotic plaques. *Chem. Res. Toxicol*. 2000, **13**, 557-564.

Sampson MJ, Gopaul N, Davies IR, Hughes DA, Carrier MJ. Plasma F2 isoprostanes. *Diabetes Care* 2002, **25**, 537-541.

Sangripanti J-L. DNA damage mediated by metal ions with special reference to copper and iron. *In* Metal Ions in Biological Systems, ed. Sigel, A. and Sigel H, Vol 36, Marcel Dekker, INC. New York, 1999, pp 179-210.

Sargis RM, Subbaiah PV. Protection of membrane cholesterol by sphingomyelin against free radical-mediated oxidation. *Free Rad. Biol. & Med*. 2006, in press.

Schafer FQ and Buettner GR. Acidic pH amplifies iron-mediated lipid peroxidation in cells. *Free Rad. Biol. & Med*. 2000, **28**, 1175-1181.

Schafer FQ, Qian SY, Buettner GR. Iron and free radical oxidations in cell membranes. *Cell Mol. Biol*. 2000, **46**, 657-662.

Schlame M, Haupt R, Wiswedel I, Kox WJ, Rüstow B. Identification of short-chain oxidized phosphatidylcholine in human plasma. *J. Lipid Res*. 1996, **37**, 2608-2615.

Schwenk U and Schröder J-M. 5-oxo-eicosanoids are potent eosinophil chemotactic factors. *J. Biol. Chem.* 1995, **270**,15029-15036.

Sergent O, Morel I, Cillard J. "Involvement of metal ions in lipid peroxidation: biological implications" *In* Metal Ions in Biological Systems, ed. Sigel, A. and Sigel H, Vol 36, Marcel Dekker, INC. New York, 1999, pp 251-262.

Shi H, Timmins G, Monske M, Burdick A, Kalyanaraman B, Liu Y, Clément J-L, Burchiel S, Liu KJ. Evaluation of spin trapping agents and trapping conditions for detection of cell-generated reactive oxygen species. *Arch. Biochem. Biophys*. 2005, **437**, 59-68.

Shibata T, Yamada T, Ishii T, Kumazawa S, Nakamura H, Masutani H, Yodoi J, Uchida K. Thioredoxin as a molecular target of cyclopentenone prostaglandins. *J. Biol. Chem*. 2003, **278**, 26046-26054.

Spickett CM, Pitt AR, Brown AJ. Direct observation of lipid hydroperoxides in phospholipid vesicles by electrospray mass spectrometry. *Free Rad. Biol. & Med*. 1998, **25**, 613-620.

Spickett CM, Rennie N, Winter H, Zambonin L, Landi L, Jerlich A, Schaur RJ, Pitt AR. Detection of phospholipid oxidation in oxidatively stressed cells by reverse-phase HPLC coupled with positive-ionization electroscopy MS. *Biochem. J*. 2001, **355**, 449-457.

Spiteller G. Linoleic acid peroxidation- the dominant lipid peroxidation process in low density lipoprotein and its relationship to chronic diseases. *Chem. Phys. Lipids* 1998, **95**, 105-162.

Spiteller P and Spiteller G. Strong dependence of the lipid peroxidation product spectrum whether Fe^{2+}/O_2 or Fe^{3+}/O_2 is used as oxidant. *Biochim. Biophys. Acta*. 1998, **1392**, 23-40.

Spiteller P, Kern W, Reiner J and Spiteller G. Aldehydic lipid peroxidation products derived from linoleic acid. *Biochim. Biophys. Acta*. 2001; **1531**: 188-208.

Stadtman ER and Levine RL. Free radical mediated oxidation of free amino acids and aminoacid residues in proteins. *Aminoacids* 2003, **25**, 207-218.

Stolze K, Udilova N, Nohl H. Spin adducts of superoxide, alkoxyl and lipid-derived radicals with EMPO and its derivatives. *Biol. Chem*. 2002, **383**, 813-820.

Stryer L. Biochemistry, 4th Ed. 1999 NY, WH Freeman.

Subbanagounder G, Leitinger N, Schwenke DC, Wong JW, Lee H, Rizza C, Watson AD, Faull KF, Fogelman AM, Berliner JA. Determinants of bioactivity of oxidised phospholipids: specific oxidised fatty acyl groups at the sn-2 position. *Arterioscler. Thromb. Vasc. Biol*. 2000, **20**, 2248-2254.

Subbanagounder G, Deng Y, Borromeo C, Dooley AN, Berliner JA, Salomon RG. Hydroxy alkenal phospholipids regulate inflammatory functions of endothelial cells. *Vasc. Pharmacol*. 2002, **38**, 201-209.

Szweda LI, Uchida K, Tsai L, Stadtman ER. Inactivation of glucose-6-phosphate dehydrogenase by 4-hydroxy-2-nonenal. *J. Biol. Chem*. 1993 **268**, 3342-3347.

Tang L, Zhang Y, Qian Z, Shen X. The mechanism of Fe2+-initiated lipid peroxidation in liposomes: the dual function of ferrous ions, the roles of the pre-existing lipid peroxides and the lipid peroxyl radical. *Biochem. J.* 2000, **352**, 27-36.

Taniguchi H and Madden KP. An *in situ* time-resolved ESR study of the kinetics of spin trapping by 5,5-dimethyl-1-pyrroline-N-oxide. *J. Am. Chem. Soc.* 1999, **121**, 11875-11879.

Uchida K and Stadtman ER. Covalent attachment of 4-hydroxynonenal to glyceraldehydes-3-phosphate dehydrogenase. *J. Biol. Chem*. 1993, **268**, 6388-6393.

Venkataraman S, Schafer FQ, Buettner GR. Detection of lipid radicals using EPR. *Antioxid. Redox Signal*. 2004, **6**, 631-638.

Velasco J, Andersen ML, Skibsted LH. Electron spin resonance spin trapping for analysis of lipid oxidation in oils: inhibiting effect of the spin trap phenyl-N-tert-butylnitrone on lipid oxidation. *J. Agric. Food Chem*. 2005, **53**, 1328-1336.

Vitrac H, Courrègelongue M, Couturier M, Collin F, Thérond P, Rémita S, Peretti P, Dore D, Gardès-Albert M. Radiation-induced peroxidation of small unilamellar vesicles of phosphatidylcholine generated by sonication. *Can. J. Physiol. Pharmacol*. 2004, **82**, 153-160.

Völkel W, Alvarez-Sanchez R, Weick I, Mally A, Dekant W, Pähler A. Glutathione conjugates of 4-hydroxy-2(E)-nonenal as biomarkers of hepatic oxidative stress-induced lipid peroxidation in rats. *Free Rad. Biol. & Med*. 2005, **38**, 1526-1536.

Ward NC, Ouddey IB, Hodgson JM, Beilin LJ, Croft KD. Urinary 20-hydroxyeicosatetraenic acid excretion is associated with oxidative stress in hypertensive subjects. *Free Rad. Biol. & Med*. 2005, **38**, 1032-1036.

Watanabe T, Katayame S, Enoki M, Honda Y, Kuwahara M. Formation of acyl radical in lipid peroxidation of linoleic acid by manganese-dependent peroxidase from *Ceriporiopsis subvermispora* and *Bjerkandera adusta*. *Eur. J. Biochem*. 2000, **267**, 4222-4231.

Watson AD, Leitinger N, Navab M, Faull KF, Hörkö S, Witztum JL, Palinski W, Schwenke D, Salomon RG, Sha W, Subbanagounder G, Fogelman AM and Berliner JA. Structural identification by mass spectrometry of oxidized phospholipids in minimally oxidized low density lipoprotein that induce monocyte/endothelial interactions and evidence for their presence in vivo. *J. Biol. Chem*. 1997; **272**: 13597.

Watson AD, Subbanagounder G, Welsbie DS, Faull KF, Navab M, Jung ME, Fogelman AM, Berliner JA. Structural identification by mass spectrometry of oxidized phospholipids in minimally oxidized low density lipoprotein that induce monocyte/endothelial interactions and evidence for their presence in vivo. *J. Biol. Chem*. 1999, **274**, 24787-24798.

Wheelan P, Zirrolli JA, Murphy RC. Electrospray ionisation and low energy tandem mass spectrometry of polyhydroxy unsaturated fatty acids. *J. Am. Soc. Mass Spectrom*. 1996, **7**, 140-149.

Wong TP. An old question revisited: Current understanding of aging theories. *McGill J. Med*. 2001, **6**, 41-47.

Xu G and Chance M. Radiolytic modification of aminoacid residues serving as structural probes for protein footprinting. *Anal. Chem*. 2005, **77**, 4549-4555.

Yocum AK, Oe T, Yergey AL, Blair IA. Novel lipid hydroperoxide-derived hemoglobin histidine adducts as biomarkers of oxidative stress. J*. Mass Spectrom*. 2005, **40**, 754-764.

Yorek MA. Biological distribution. In Phospholipids handbook. Ed. Gregor Cevc, 1995, p. 745.

Yoshida T, Otake H, Aramaki Y, Hara T, Tsuchiya S, Hamada A, Utsumi H. Free radicals from 1-palmitoyl-2-arachidonoyl-phosphatidylcholine liposomes in Fe^{2+}/ascorbic acid solution. *Biol. Pharm. Bull*. 1996, **19**, 779-782.

Yoshida Y, Ito N, Shimakawa S, Niki E. Susceptibility of plasma lipids to peroxidation. *Biochem. Biophys. Res. Commun*. 2003, **305**, 747-753.

2. Unsaturated fatty acid radical products

Manuscript I: *Detection and characterization by mass spectrometry of radical adducts produced by linoleic acid oxidation*

Manuscript II: *Identification of linoleic acid free radical and other breakdown products using spin-trapping with liquid chromatography-electrospray tandem mass spectrometry*

Detection and Characterization by Mass Spectrometry of Radical Adducts Produced by Linoleic Acid Oxidation

Ana Reis, M. Rosário M. Domingues, Francisco M. L. Amado, A.J.V. Ferrer-Correia, and Pedro Domingues
Department of Chemistry, University of Aveiro, Aveiro, Portugal

The formation of linoleic acid radical species under the oxidative conditions of the Fenton reaction (using hydrogen peroxide and Fe (II)) was monitored by FAB-MS and ES-MS using the spin trap 5,5-dimethyl-1-pyrrolidine-N-oxide, DMPO. Both the FAB and ES mass spectra were very similar and showed the presence of ions corresponding to carbon- and oxygen centered spin adducts (DMPO/L$^{\cdot}$, DMPO/LO$^{\cdot}$, and DMPO/LOO$^{\cdot}$). Cyclic structures, formed between the DMPO oxygen and the neighboring carbon of the fatty acid, were also observed. Electrospray tandem mass spectrometry of these ions was performed to confirm the proposed structure of these adducts. All MS/MS spectra showed an ion at *m/z* 114, correspondent to the $[DMPO + H]^+$, and a fragment ion due to loss of DMPO (loss of 113 Da), confirming that they are DMPO adducts. ES-MS/MS spectra of alkoxyl radical adducts (DMPO/LO$^{\cdot}$) showed an additional ion at *m/z* 130 $[DMPO^{\cdot} - O + H]^+$, while ES MS/MS of peroxyl radical adducts (DMPO/LOO$^{\cdot}$) showed a fragment ion at *m/z* 146 $[DMPO - OO + H]^+$, confirming both structures. Other fragment ions were observed, such as alkyl acylium radical ions, formed by cleavage of the alkyl chain after loss of water and the DMPO molecule. The identification of fragment ions observed in the MS/MS spectra of the different DMPO adducts suggests the occurrence of structural isomers containing the DMPO moiety both at C_9 and C_{13}. The use of ES tandem mass spectrometry, associated with spin trapping experiments, has beee shown to be a valuable tool for the structural characterization of carbon and oxygen-centered spin adducts of lipid radicals. (J Am Soc Mass Spectrom 2003, 14, 1250–1261) © 2003 American Society for Mass Spectrometry

Polyunsaturated fatty acids, such as linoleic acid, are the main components found in cell membranes of biological tissues. During cell metabolism, aerobic processes taking place at the mitochondria promote the formation of oxygen radicals known as reactive oxygen species (ROS). These ROS are cytotoxic and are removed by antioxidant systems occurring in living systems [1]. The ROS species such as hydroxyl ($^{\cdot}$OH) radicals, because of the unpaired electron in the oxygen atom, are very unstable and react readily with conjugated double bonds found in cell constituents such as lipids, proteins, and DNA bases, modifying the structures and damaging the tissues [2]. Oxidative damage is thought to cause a decrease in fluidity and disruption of the cell membrane, and to affect mitochondrial functions [3]. This has been connected to several age related diseases such as the case of Alzheimer's disease, Parkinson's disease, multiple sclerosis, and cataracts [2].

The lipid peroxidation reaction involves a number of intermediate steps in a chain reaction forming lipid radicals (L$^{\cdot}$, LO$^{\cdot}$, LOO$^{\cdot}$), which in turn trigger the propagation of peroxidation reaction [4]. The extent of lipid peroxidation is used to estimate the extent of biological tissue damage. In in vitro assays, oxidative conditions may be induced by the addition of hydrogen peroxide to lipids in the presence of Fe^{2+} ions. This reaction, known as the Fenton reaction, leads to the formation of hydroxyl radicals, which then react, by a hydrogen abstraction mechanism, with unsaturated compounds such as lipids, forming radicals [5]. The radical species formed are very unstable, but the addition of nitroso compounds radicals, known as "spin traps", react with the lipid radicals leading to the formation of much more stable radical adducts. The radical adducts are usually examined by ESR spectroscopy [6–12].

Electron spin-trapping experiments are the most widely used approach for the identification of carbon-centered lipid radicals formed during lipid peroxidation (after trapping with POBN [9–13]), or for the identification of oxygen-centered lipid radicals (after trapping with DMPO [7, 8, 14]).

Studies have demonstrated the applicability of mass

Published online August 26, 2003
Address reprint requests to Dr. P. Domingues, Department of Chemistry, University of Aveiro, 3810-193 Aveiro, Portugal. E-mail: pedrom@dq.ua.pt

1044-0305/03/$30.00
doi:10.1016/S1044-0305(03)00538-5

Received March 24, 2003
Revised July 15, 2003
Accepted July 15, 2003

spectrometry to the identification of carbon-centered radical adducts derived from lipids using the spin trap POBN [9, 11–13]. Other applications of mass spectrometry to the detection of spin adducts include the identification of alkyl radicals, namely POBN radical adducts of pentadienyl, by electrospray ionization ES-MS [15], and the detection and characterisation of hydroxyl-DMPO radical adducts by FAB-MS [16] and ES-MS [17, 18]. ES-MS has shown to be a valuable tool for the detection and characterization of oxidation radical products, mainly due to its high sensitivity, accuracy, simple sample preparation and the structural information obtained.

Both carbon- and oxygen-centered radicals occur during lipid oxidation, according to ESR results obtained during the investigation of reaction of linoleic acid with cytochrome [7, 13], or with soybean lipoxygenase [11]. The identification by ES-MS and tandem mass spectrometry of oxygen-centered lipid radicals using the DMPO spin trap has, to our knowledge, not yet been reported. In this work we will present the results of a study of the adducts of DMPO with the linoleic acid radical species produced under Fenton reaction conditions. The formation of the stable DMPO radical adducts was monitored by FAB-MS, ES-MS, and ES-MS/MS using our previously developed methodology [16].

Experimental

Chemicals

Linoleic acid and DMPO were obtained from Sigma (St. Louis, MO) and used without further purification. Nitrobenzyl alcohol (NBA) matrix was purchased from Merck (Darmstadt, Germany). Iron (II) chloride ($FeCl_2$) and hydrogen peroxide (H_2O_2) used for the peroxidation reactions were purchased from Merck.

Oxidation of Linoleic Acid by Fenton Reaction

Spin trapping experiments for subsequent analysis by FAB-MS were done in the following manner. Approximately 100 ng of linoleic acid in a chloroform solution (1 μL), approximately 6 μmol of hydrogen peroxide and 0.6 μmol of $FeCl_2$ were left to react for different periods of time. Then, 5 μl of DMPO and one drop of NBA matrix were added and the sample was analyzed by FAB-MS. Spin trapping experiments for subsequent ES-MS and ES-MS/MS were performed by adding to 100 ng of linoleic acid, 5 mmol $FeCl_2$ solution and 50 mmol of hydrogen peroxide (H_2O_2) in 0.5 ml of ammonium bicarbonate buffer solution (pH 7.4). This mixture was left to react for different periods of time with occasional sonication, after which 1 μL (9 mmol) of DMPO was added. The lipid oxidation products and spin adducts were extracted using a modified Folch method with chloroform:methanol (2:1, vol/vol) [19].

FAB Mass Spectrometry

Positive ion FAB mass spectra were acquired with a VG AutoSpecQ (VG Analytical Manchester, UK). The instrument is of EBE geometry and is equipped with a cesium gun. The applied accelerating voltage was 8 kV and the cesium ion beam intensity was 3 μA at 20 kV. In MS experiments, the EBE resolution was set to approximately 1500.

ES Mass Spectrometry

Positive ion ES mass spectra and tandem mass spectra were acquired in a Q-TOF 2 instrument (Micromass, Manchester, UK) using a MassLynx software system (version 3.5). The samples for electrospray analysis were prepared by diluting 1 μL of the sample with 200 μL of chloroform:methanol solution (1:1, vol/vol) containing 0.5% (vol/vol) of acetic acid. Samples were introduced into the mass spectrometer using a flow rate of 10 μL /min, setting the needle voltage at 3000 V with the ion source at 80 °C and cone voltage at 35 V. Tandem mass spectra (MS/MS) of the protonated molecules were obtained by collision-induced dissociation (CID), using argon as the collision gas (Penning gauge pressure $\sim 6 \times 10^{-6}$ mBar) and varying collision energy between 20–35 eV. In MS and MS/MS experiments TOF resolution was set to approximately 9000.

Results and Discussion

Mass Spectrometry Analysis of DMPO Adducts

The positive ion FAB mass spectrum of linoleic acid with H_2O_2 in the presence of Fe^{2+} and DMPO is shown in Figure 1a. For comparison, the mass spectrum of linoleic acid obtained under the same conditions but without the addition of H_2O_2 is shown in Figure 1b. Significant differences can be observed.

Comparing both spectra, new ions were observed in the presence of H_2O_2 and DMPO, namely the ions at *m/z* 392–394, at *m/z* 408–410 and at *m/z* 424–426. These ions correspond to spin adducts of DMPO with radical species formed by the oxidation of linoleic acid under Fenton reaction conditions. They were not assigned as isolated oxidized species of the linoleic acid because they were not detected in the FAB mass spectrum of linoleic acid with H_2O_2 (spectra not shown). The ions of *m/z* 394, 416, and 438 observed in Figure 1b correspond to, respectively, the proton bound adduct of DMPO with the fatty acid, the sodium bound adduct of DMPO with the fatty acid and the sodium bound adducts of DMPO with the sodiated fatty acid.

The most abundant ions corresponding to DMPO adducts of linoleic acid radical species observed in Figure 1, are the ions at *m/z* 392, 393, and 394, which were attributed to the carbon-centered radical adducts represented in Scheme **1a, b, c**, respectively. Although DMPO is usually considered a spin trap more specific

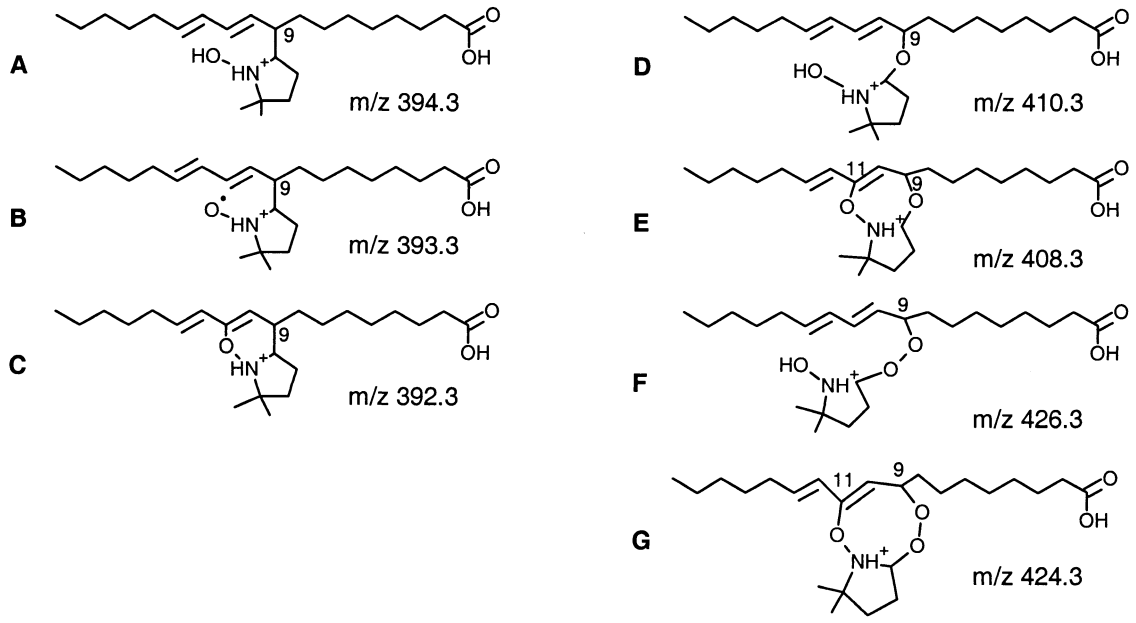

Scheme 1. Schematic structures of the DMPO spin radical adducts of the linoleic acid. The number on structures shows the carbon number.

for oxygen radicals, DMPO carbon-centered radicals have previously been observed during tryptophan oxidation [18].

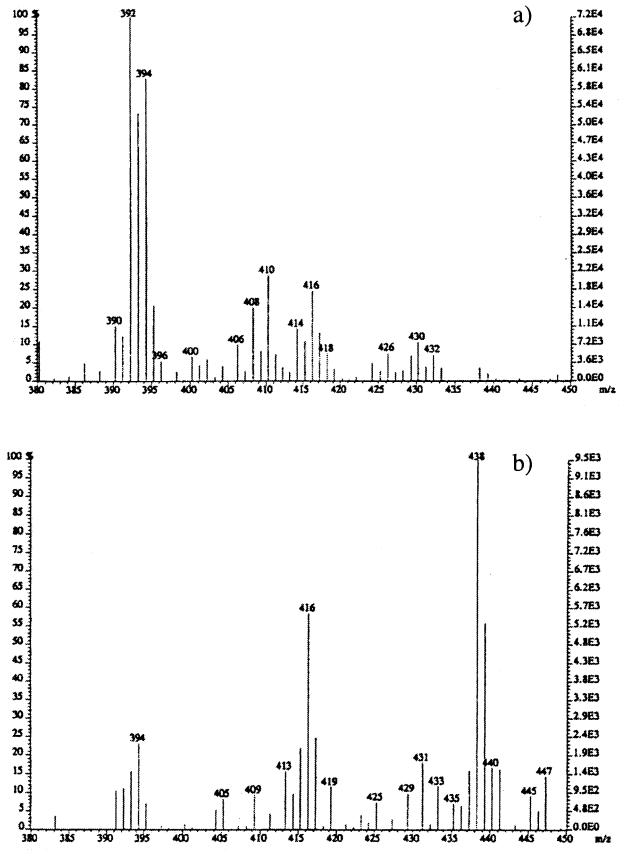

Figure 1. FAB-MS spectra of linoleic acid in presence of DMPO, (**a**) under oxidative conditions induced by Fenton reaction, and (**b**) under non-oxidative conditions.-

Additional ions at *m/z* 408–410, 16 Da above the ions at *m/z* 392–394, were attributed to alkoxyl (or hydroxyalkyl) radical adducts (DMPO/LO$^{\cdot}$). The proposed structures for the ions at *m/z* 410 and 408 are presented in Scheme **1d, e**. On another group of ions at *m/z* 424–426, a further 16 Da increase were assigned as peroxyl alkyl radical adducts (DMPO/LOO$^{\cdot}$) of linoleic acid (Scheme **1g** and **f**). The structures proposed for these spin adducts presume the formation of an oxygen-centered radical, with the DMPO linked to the peroxyl alkyl radical. All the structures shown in Scheme **1** consider the radical adduct to be at the position C_9, but it can also be placed at C_{13} [20].

The ions in each envelope correspond to different species of adducts, and have some structural differences. The ions at *m/z* 392, 408, and 424 were attributed to cyclic radical adducts (Scheme **1b, e, g**).The other adducts (at *m/z* 393, 409, and 425) are considered as open structure adducts although some are odd ions with an unpaired electron at the DMPO oxygen atom, as is represented in Scheme **1** for the adduct at *m/z* 393. The other adducts (at *m/z* 394, 410 and 426) are even-electron species (Scheme **1a, d, f**). The unpaired electron will not be stable in solution and thus unlikely to occur significantly, which might explain the low relative abundance of these odd *m/z* ions, when compared to the adjacent ions. Therefore, these odd mass ions will not be discussed further in this paper. The mass spectrum obtained after reaction with H_2O_2 (Figure 1a) also showed the presence of each of these clusters with an increase of 22 Da, which were attributed to the sodiated molecules of the DMPO adducts.

It is known that in the presence of reactive oxygen species (ROS) such as the hydroxyl radical formed by

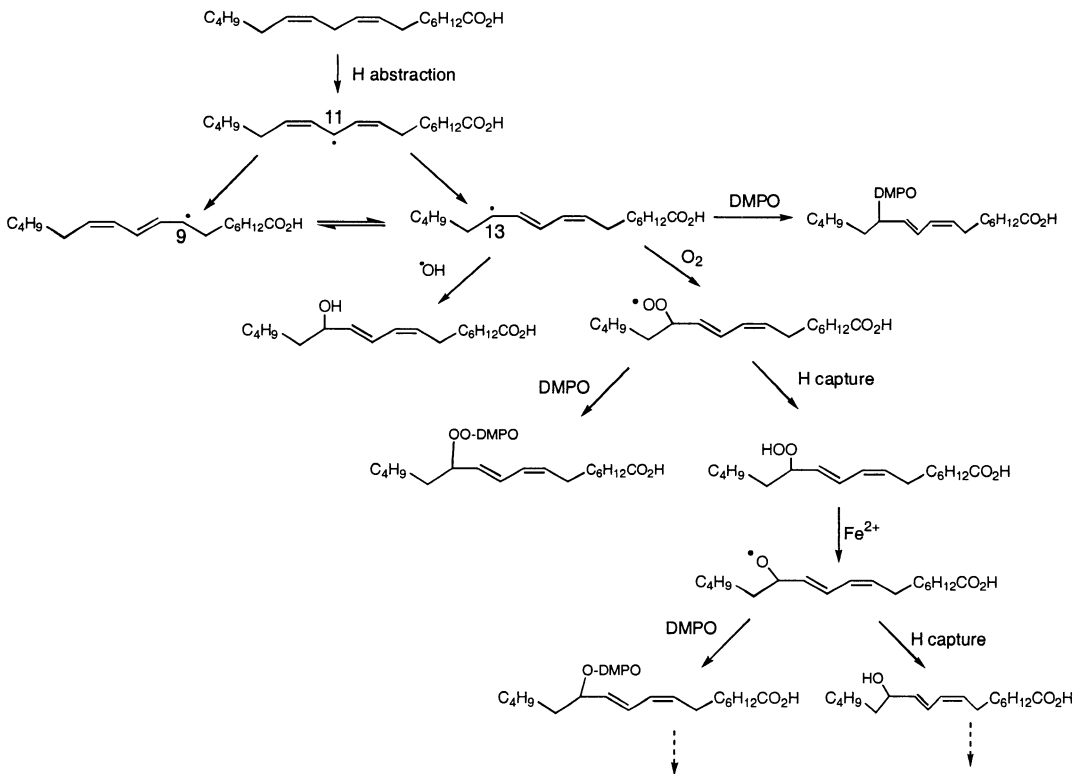

Scheme 2. Schematic representation of the pathways for the formation of the carbon and oxygen-centered DMPO adducts of linoleic acid oxidation (adapted from references [11] and [14]).

the Fenton reaction, linoleic acid undergoes the removal of the bis-allylic hydrogen at carbon 11, leaving an unpaired electron and generating a carbon-centered radical (Scheme **2**). This radical may be shifted, generating two stable resonant structures, with the radical either on C_9 or C_{13} [20]. The radical can also be located in other places due to double bond migration, although their contribution should be minimal. Both carbon radical species (Scheme **2**) may capture the spin trap, forming the carbon-centered adducts at *m/z* 392–394 or they can take up an oxygen molecule, thus forming an alkyl peroxyl radical. The alkyl peroxyl radical may react with DMPO forming adducts at *m/z* 424–426, or may capture a hydrogen by abstraction from another

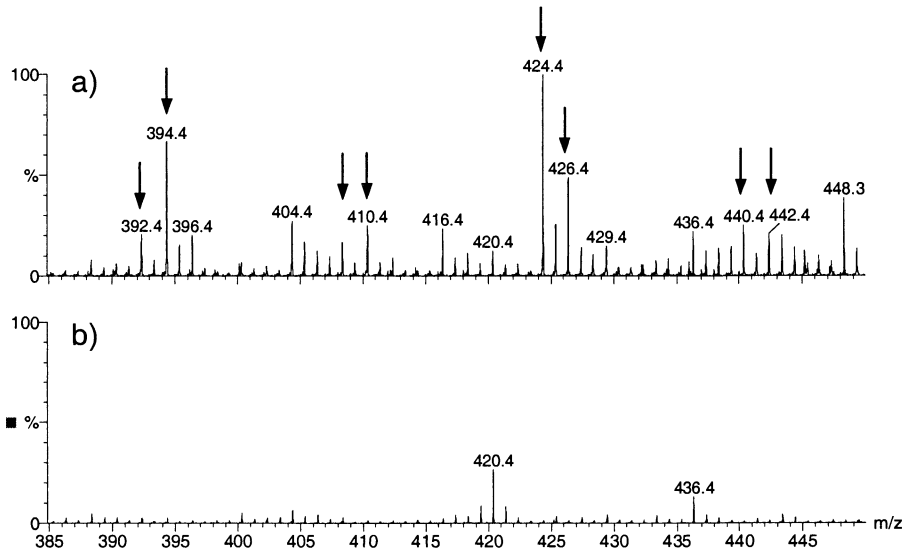

Figure 2. ES-MS mass spectra of linoleic acid in presence of DMPO (**a**) under oxidative conditions induced by Fenton reaction, and (**b**) under non-oxidative conditions. Arrows indicate new ions formed under oxidative conditions.

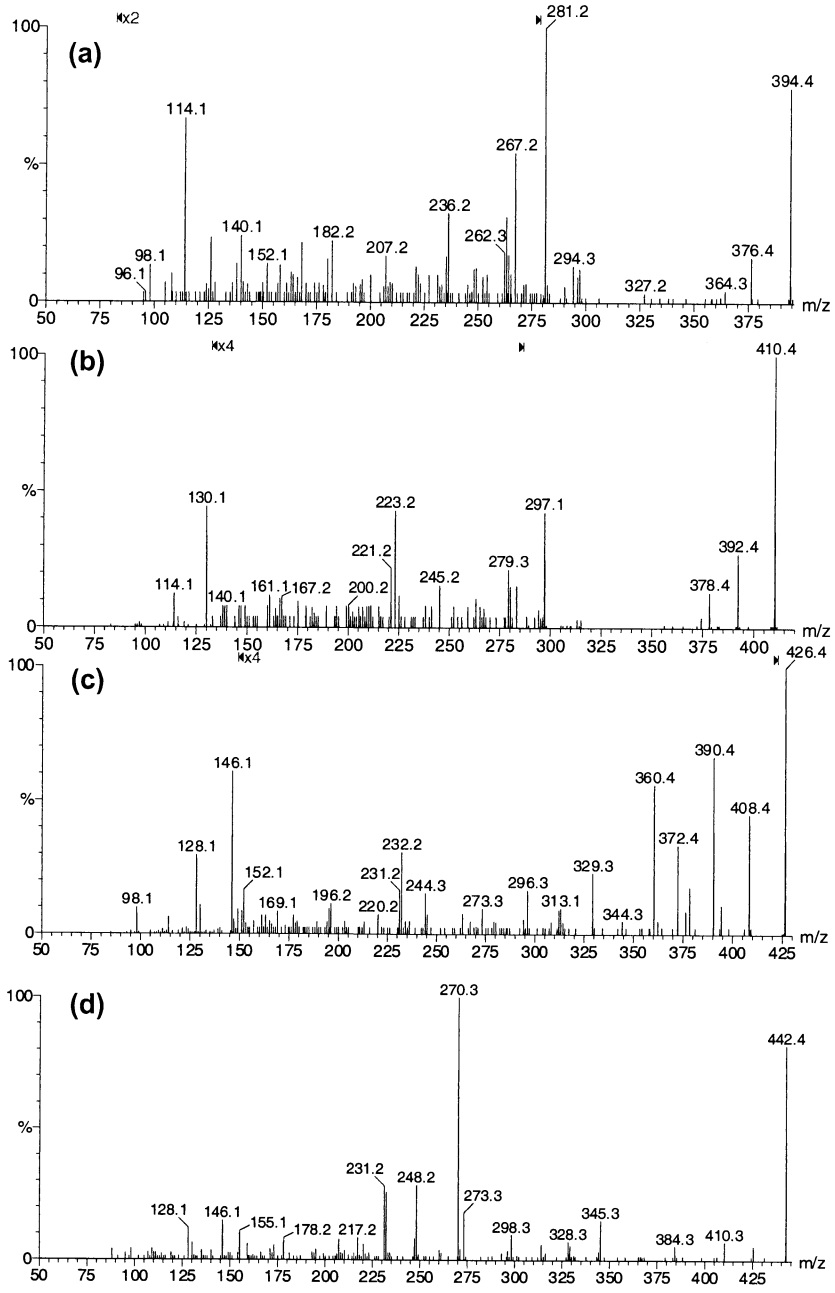

Figure 3. ES-MS/MS spectra of the carbon and oxygen-centered radical adducts of linoleic acid at (**a**) *m/z* 394 and (**b**) *m/z* 410, (**c**) *m/z* 426, and (**d**) *m/z* 442.

linoleic acid molecule generating a hydroperoxide. However, this specie is not stable in solution and decomposes in the presence of metal ions to an alkoxyl radical, which in turn may either be stabilized by hydrogen abstraction forming a hydroxy group or by capture of a DMPO molecule to form the alkoxyl DMPO adducts at *m/z* 408–410. The formation pathway and the structures of the carbon- and oxygen-centered adducts are shown in Scheme **2**.

The reaction of linoleic acid with DMPO in the presence and absence of hydrogen peroxide (under conditions similar to those reported above) was also monitored by ES-MS (Figure 2a and b). The ES-MS spectrum of linoleic acid in the presence H_2O_2 and DMPO shows high abundance ions at *m/z* 392, 394, 408,

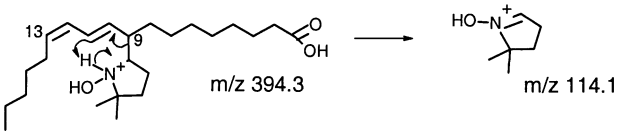

Scheme 3. Proposed mechanism for the formation of the protonated molecule of DMPO, at *m/z* 114 from the ion at *m/z* 394.

Table 1. Fragment ions observed in the MS/MS spectra of open structures of DMPO spin adducts of linoleic acid radicals (% of relative abundance normalised to base peak

Fragments	*m/z* 394	*m/z* 410	*m/z* 426	*m/z* 442
$[DMPO+H]^+$	114 (35)	114 (30)	114 (10)	114 (<5)
$[DMPO-O+H]^+$	—	130 (100)	130 (20)	130 (<5)
$[DMPO-OO+H]^+$	—	—	146 (100)	146 (15)
$-H_2O$	376 (20)	392 (60)	408 (20)	424 (10)
$-2H_2O$	—	374 (10)	390 (30)	
−97 Da (C_{11}-C_{12} cleavage isomer C_9)	297 (15)	313 (10)	329 (25)	345 (20)
−113 (loss of DMPO)	281 (100)	297 (80)	313 (15)	329 (10)
$-113-H_2O$	263 (30)	279 (10)		311 (<5)

410, 424, and 426. This is in agreement with the results obtained by FAB-MS. The ES-MS spectrum showed additional ions at *m/z* 440 and 442, 16 Da above *m/z* 424 and 426 ions mentioned above, which could be attributed to alkyl peroxyl radical adducts containing a hydroxy group. The hydroxy group could be located at either at C_8 or C_{14}. These ions can also be attributed to an alkyl epoxyperoxyl spin adduct. Besides the formation of an additional hydroxy group, the epoxy formation from alkoxyl radicals has already been reported in lipid peroxidation, during a study of linoleic carbon-centered radicals using the spin trap POBN [11, 21].

Ions at *m/z* 130, 146, 158, 211, 227, and 354 (data not shown) were identified as DMPO radicals resulting from the oxidative conditions in solution, and were previously detected by FAB-MS [16] and ES-MS [17].

In order to elucidate the structure of the ions identified as DMPO radical adducts of the linoleic acid oxidation reaction, collision induced decomposition of the ES produced ions was performed. ES-MS/MS spectra of the ions were analyzed, rather than the FAB-MS/MS, because of the higher sensitivity and resolution achieved with the QTOF 2 instrument. As referred to previously, several isomers of DMPO adducts can be formed although the most probable location of the spin bond is on C_9 or C_{13}. In the MS-MS experiments, since there was no previous separation, all the isomers were selected, so different fragmentation pathways derived from different isomers are overlapped. Some evidence of this will be shown in the discussion.

MS/MS Spectra of Open Structures of DMPO Radical Adducts

The ES-MS/MS mass spectra obtained for the ions at *m/z* 394, 410, 426, and 442, corresponding to open structures of carbon and oxygen-centered DMPO adducts of the linoleic acid radical formed by oxidation, are shown in Figure 3a, b, c, d. In the MS/MS spectra of all adducts, an abundant fragment ion at *m/z* 114 is observed, corresponding to the protonated molecule of DMPO, $[DMPO + H]^+$, thus confirming that all these ions are DMPO adducts. A proposed mechanism for the formation of the ion at *m/z* 114 is presented in Scheme **3**. In the MS/MS spectrum of the alkoxyl adduct, *m/z* 410, it is possible to observe the ion at *m/z* 130, corresponding to the protonated molecule of the DMPO hydroxy adduct (DMPO − OH) [16, 17], thus confirming that this adduct is an alkoxyl radical adduct. In the MS/MS spectra of the adducts at *m/z* 426 and 442, a fragment at *m/z* 146 corresponding to the protonated molecule of the DMPO peroxyl adduct (DMPO − OOH) was observed, thus confirming the presence of the linoleic peroxyl radical adducts. Common fragment ions observed in the MS/MS spectra are summarized in Table 1.

Other common fragmentations observed in all spectra were the loss of water (Table 1), and combined loss of two water molecules. Loss of one water molecule can occur either from the carboxylic acid group (due to the acidity of the α hydrogen adjacent to the carbonyl group) forming an unsaturated terminal carbonyl group (Scheme **4**), and/or from the DMPO moiety.

The major fragment ion of the carbon-centered adduct at *m/z* 394 corresponds to the loss of 113 Da. This fragmentation is probably due to loss of the DMPO moiety. This fragmentation pathway is observed in all of the spectra, although with variable relative abundances. Another common fragmentation pathway corresponds to the combined loss of water and loss of 113 Da, which suggests the loss of water from the carboxylic moiety with the charge being retained on the carbonylic group formed, resulting in the acylium ion, $RC{=}O^+$. Loss of 113 Da can also be due to the combined loss of

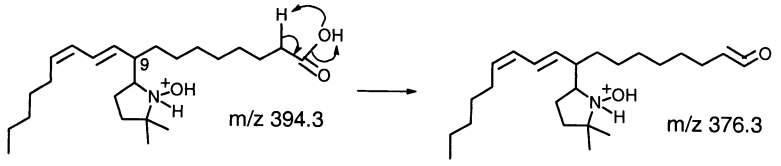

Scheme 4. Loss of water from the carboxylic acid group, showed for the ion at *m/z* 394.

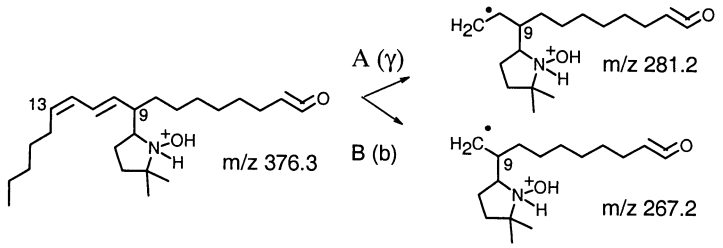

Scheme 5. Fragment ions formed from the combined loss of water and homolytic cleavage of (**a**) the bond between C_{11}–C_{12} and (**b**) the bond between C_{10}–C_{11} of the isomer C_9 at *m/z* 394.

one water molecule and the homolytic scission between C_{11}–C_{12} of the spin adduct containing the DMPO linked to the C_9 with the charge being retained at the DMPO. This mechanism presupposes double bond migration, as represented in Scheme **5a**, for the adduct at *m/z* 394. The same fragmentation could occur for the other radical adducts. In all of the MS/MS spectra, fragment ions from the combined loss of water and homolytic cleavage between C_{10}–C_{11} of the isomer C_9 (Scheme **5b**) were observed.

The cleavage of C–C bond by homolytic scission, between C_{11}–C_{12}, can also occur without loss of water, generating the fragment ion at *m/z* 297 for the spin adduct at *m/z* 394, as represented in Scheme **6**. The spin adduct at *m/z* 410, 426, and 442 generates the fragment ions at *m/z* 313, 329, and 345 respectively. These fragmentation pathways provide evidence for the presence of the spin trap at C_9.

A common fragmentation pathway corresponding to 1,4-elimination involving the cleavage of the C_7–C_8 bond, occurring either for isomer C_9 or isomer C_{13}, leads to the fragment ion at *m/z* 264 (adduct at *m/z* 394), 280 (adduct at *m/z* 410), and 296 (adduct at *m/z* 426). The mechanism for this fragmentation is represented in Scheme **7** for the adduct at *m/z* 394.

Scission of the C_{10}–C_{11} bond with the DMPO molecule located at C_{13} occurs in almost all adducts. For some adducts it occurs combined with loss of water from the DMPO moiety. This is evidence for the presence of DMPO linked to the C_{13}. This fragmentation combined with loss of water occurs for the adducts at *m/z* 394 and 410, forming the ions at *m/z* 207 and 223 respectively. This fragmentation pathway, without loss of water, occurs for ion at *m/z* 442 forming the ion at *m/z* 273.

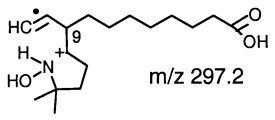

Scheme 6. Proposed structure for the fragment ion formed by to C–C bond homolytic scission, between C_{11}–C_{12}, of isomer C_9 (*m/z* 394).

MS/MS Spectra of the Carbon-Centered Adduct at m/z 394

The MS/MS spectra of the carbon-centered adduct at *m/z* 394 (Figure 3a) shows, low-mass ions that seem to be due to charge remote fragmentation. Charge-remote fragmentation occurs probably after loss of water and DMPO molecule, originating alkyl acylium ions. Charge-remote fragmentation has already been observed in MS/MS spectra of anilide derivatives of fatty acids, obtained with a Q-TOF2 instrument [22]. In the adducts from the other clusters (*m/z* 410, 426, and 442), charge-remote fragmentation also seems to occur with formation of alkyl acylium ions, but is less extensive, presumably because of the presence of an oxygen atom on the alkyl chain after loss of DMPO. A group of low-mass ions at *m/z* 126, 140, 152, 168, 180, and 182, attributable to alkyl acylium radical ions, is represented in Scheme **8**. They are probably formed by combined loss of one water molecule and loss of DMPO moiety, the charge being retained in the acylium ion, with cleavage in the vicinity of the double bonds ions. Interestingly, homolytic cleavages occurred predominantly between the C_{12}–C_{13} and C_9–C_8 bond, thus giving an indication of the location of the double bonds, namely at C_{13} and C_9. The fragment ions at *m/z* 364 can be due to 1,4-hydrogen rearrangement mechanism, with loss of C_2H_2 and H_2.

MS/MS Spectra of the Alkoxy Adduct at m/z 410

The MS/MS spectrum obtained for the ion at *m/z* 410, attributed to the alkoxyl DMPO adduct of linoleic acid (shown in Figure 3b), showed a fragment ion at *m/z* 263 formed because of the combined loss of DMPO − O (loss of 129 Da) and water from the precursor ion. The lower-mass fragment ions observed at *m/z* 140 ($C_8H_{16}CO^{+\cdot}$), 167 ($C_{10}H_{19}CO^{+}$) and 194 (OH-$C_{11}H_{17}CO^{+\cdot}$), correspond to alkyl acylium radical ions.

MS/MS Spectra of the Peroxyl Adduct at m/z 426

The MS/MS spectrum obtained for the ion at *m/z* 426 (Figure 3c), previously ascribed to the alkyl peroxyl spin adduct (Scheme **1f**), showed abundant fragment ions at *m/z* 408, 390, and 372 that can be attributed to the

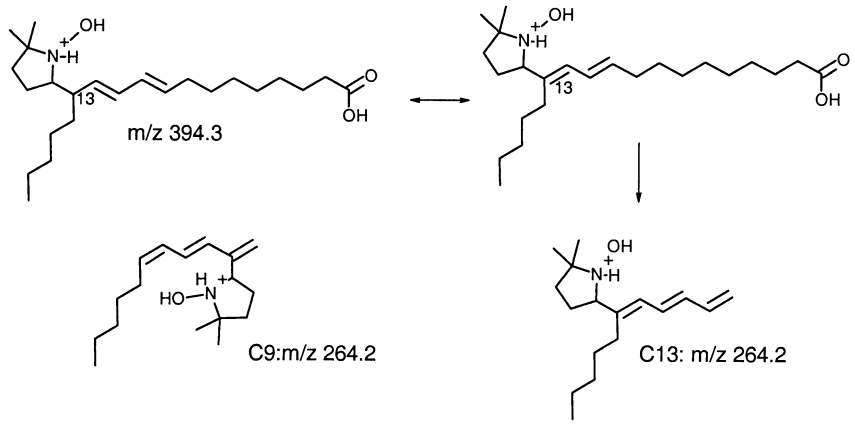

Scheme 7. 1,4-elimination involving the cleavage of the linkage of C_7–C_8 occurring either in isomer C_9 or isomer C_{13}.

loss of one, two and three water molecules. The combined loss of three water molecules could indicate the presence of an alkoxy radical adduct, with a hydroxy group in the alkyl chain. The presence of a fragment ion at *m/z* 130 seems to justify the presence of this isomer of the peroxyl radical adduct. The fragment ions at *m/z* 146 and 263, attributed to combined loss of water and (DMPO + OO), confirms that it is a alkyl peroxyl spin adduct. The ion at *m/z* 128 can occur by the loss of water from the peroxyl-DMPO adduct (*m/z* 146).

The fragment ion at *m/z* 296 formed by 1,4-hydrogen rearrangement with cleavage of the C_7–C_8 bond adjacent to the hydroxy group, suggests the contribution of an alkoxyl spin adduct placed at C_{13} containing a hydroxy group at C_8. The fragment ion at *m/z* 378 could be formed by 1,4-hydrogen rearrangement, corresponding to the loss of C_3H_6 plus H_2, and the fragment ion at *m/z* 360 due to further loss of water.

Low mass fragment ions at *m/z* 152 ($C_9H_{16}CO^{+\cdot}$), 169 (OH-$C_9H_{16}CO^{+\cdot}$), and 196 (OH-$C_{11}H_{19}CO^{+\cdot}$), were attributed to alkyl acylium radical ions formed by homolytic cleavage of the C–C bond in the vicinity of the spin trap, after combined loss of the DMPO moiety and a water molecule.

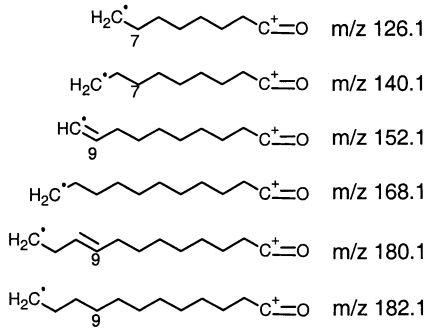

Scheme 8. Proposed structures for the alkyl acylium radical ions observed in the MS/MS spectrum of the ion at *m/z* 394.

MS/MS Spectra of the DMPO Adduct at m/z 442

The ion at *m/z* 442 (Figure 3d), showing a difference of 16 Da relative to the ion at *m/z* 426, can be attributed either to a monohydroxy alkylperoxyl spin adduct and/or to an epoxyalkyl peroxyl spin adduct. The presence of ions at *m/z* 146 and 128 confirms that it is a peroxyl adduct of DMPO.

The MS/MS spectrum of this adduct (Figure 3d) shows an abundant fragment ion at *m/z* 270. This fragment ion, not observed in the MS/MS spectra at *m/z* 426 ion, can be due to heterolytic cleavage of the C_9–C_{10}, by rearrangement of the epoxide, from isomer C_{13} (Scheme **9**).

The fragment ion at *m/z* 384 is originated from hydrogen rearrangement involving the hydroxy group, with cleavage of the C_{14}–C_{15} bond (Scheme **10**). This fragment ion indicates that the ion at *m/z* 442 is also a monohydroxy alkyl peroxyl radical adduct.

MS/MS Spectra of Cyclic Structure Radical Adducts

The ES-MS spectrum (Figure 2) contained ions at *m/z* 392, 408, 424, and 440 which are 2 Da lower than the previously described open structures. These ions were attributed to cyclic structures of carbon-centered and oxygen-centered spin adducts (Scheme **1c, e, g**). The MS/MS spectra of these ions are shown in Figure 4a, b, c, d. As can be seen from the MS/MS spectra, these ions show different fragmentation pathways than the open structures, although some fragment ions are common to both.

Under the oxidative conditions present in solution, the DMPO molecule can be oxidized to 5,5-dimethyl-1-pyrroline-3-ene-N-oxide (*m/z* 112), which can, in turn, form an adduct with the linoleic acid alkyl radical, resulting in the formation of these ions with a 2 mass units decrease when compared with the initial ions at *m/z* 392, 408, 424, and 440. The presence of an abundant

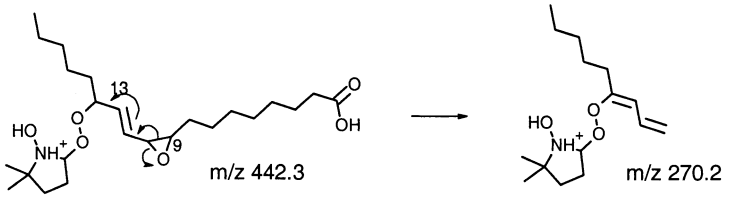

Scheme 9. Fragmentation pathway of the DMPO adduct at *m/z* 442.

fragment ion at *m/z* 114 in the MS/MS spectra (Figure 4) along with the absence of a fragment ion at *m/z* 112, suggests that these ions correspond to the cyclic adduct of the carbon and oxygen-centered spin adducts and not to the open structure containing the oxidised DMPO molecule linked to the linoleic acid radicals. Moreover, the fragment ion at *m/z* 114 in all the MS/MS spectra confirms the presence of the DMPO spin adducts. The mechanism proposed for the formation of the ion at *m/z* 114 from the cyclic adduct at *m/z* 392 is shown in Scheme **11**.

Fragment ions at *m/z* 130 and 146 observed in the MS/MS spectra of ions at *m/z* 408 and 424 respectively (Figure 4b and c), confirm the presence of the hydroxyl and peroxyl radical adducts, as was observed for the open structures (Table 1). Other common fragmentations are observed such as the loss of one and two molecules of water, the loss of DMPO molecule combined with loss of water, and cleavage of C_{11}–C_{12} bond of isomer C_9 (Table 2).

A common fragment ion at *m/z* 360, observed in the Figure 4 a, b, c, formed due to loss of 32, 48, and 64 Da, respectively, are attributable to loss of two, three, and four oxygen atoms, respectively. For the hydroxyl and peroxyl spin adducts, respectively, losses of O and O_2 were observed. The loss of O_2 in the case of the carbon-centered adduct at *m/z* 392 can only be explained if the DMPO is linked to the carboxylic group as is shown in Scheme **12**. An intramolecular ring has already been suggested to occur in the bis DMPO adducts [16].

MS/MS Spectra of the Cyclic Carbon-Centered Adduct at m/z 392

The MS/MS spectrum of this adduct (Figure 4a) shows a series of ions that can be attributed to charge remote

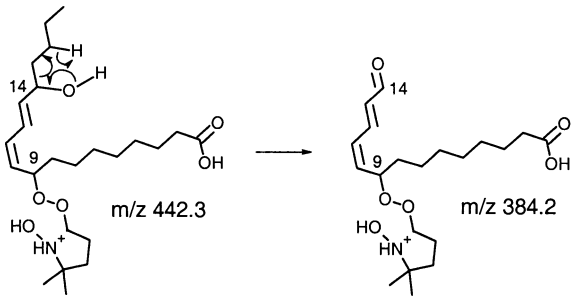

Scheme 10. Mechanism proposed for the cleavage of the C_{14}–C_{15} bond of isomer C_9 (*m/z* 442).

fragmentation of the ion formed after loss of DMPO and also after the combined loss of DMPO and water. These two series of charge remote formed ions overlap in the mass spectrum. In the other closed-ring adducts (*m/z* 408, 424, and 440) charge remote fragmentation also seems to occur with formation of alkyl acylium ions, but less extensively. The series of low mass fragment ions at *m/z* 126 ($C_7H_{14}CO^{+\cdot}$), 138 ($C_8H_{14}CO^{+\cdot}$), 140 ($C_8H_{16}CO^{+\cdot}$), 154 ($C_9H_{18}CO^{+\cdot}$), 166 ($C_{10}H_{18}CO^{+\cdot}$), 180 ($C_{11}H_{20}CO^{+\cdot}$), 182 ($C_{11}H_{22}CO^{+\cdot}$), 194 ($C_{12}H_{22}CO^{+\cdot}$), 208 ($C_{13}H_{24}CO^{+\cdot}$), 210 ($C_{13}H_{26}CO^{+\cdot}$) are attributed to homolytic cleavages of the unsaturated chain, forming alkyl acylium radical cations. Fragment ion at *m/z* 249 can result from homolytic cleavage between C_8–C_9 involving the spin trap located at the C_9.

MS/MS Spectra of the Alkoxyl Adduct at m/z 408

The presence, in the MS/MS spectrum of the ion at *m/z* 408 (Figure 4b) and of a fragment ion at *m/z* 130, identified as $[(DMPO +O) + H]^+$, is evidence for the presence of a hydroxyl spin adduct. Ions at *m/z* 263 and 249 correspond to the cleavage of the C_7–C_8 and the C_8–C_9 bonds, respectively, with the DMPO bond located at C9. These fragmentations suggest the presence of a carbon-centered radical adduct of hydroxy linoleic acid. Other fragment ions observed in the low mass region at *m/z* 149 ($C_9H_{13}CO^+$), 151 ($C_9H_{15}CO^+$), 165 ($C_{10}H_{17}CO^+$), 182 ($C_{11}H_{22}CO^{+\cdot}$), 194 ($C_{12}H_{22}CO^{+\cdot}$), 196 (OH-$C_{11}H_{19}CO^{+\cdot}$), and 212 (OH_2-$C_{11}H_{18}CO^+$) or (OH-$C_{12}H_{23}CO^+$), can be assigned to alkyl radical ions attributable to homolytic cleavage of the bonds near the location of the DMPO bond.

MS/MS Spectra of the Cyclic Alkyl Peroxyl Adduct at m/z 424

The MS/MS spectrum of the ion at *m/z* 424 (Figure 4c) exhibited an abundant fragment ion at *m/z* 146 corresponding to $[(DMPO + OO) + H]^+$, thus confirming that is an alkyl peroxyl spin adduct. The fragment ion at *m/z* 279 may be attributed to the loss of an oxidized DMPO molecule (DMPO − OO), and the ion at *m/z* 261 is due to combined loss of DMPO − OO and water.

The fragment ion at *m/z* 294, resulting from the 1,4-hydrogen rearrangement in isomer C_{13}, involving the hydroxy group placed at the C_8 and cleavage of C_8-C_7 bond, suggests the contribution of a alkoxyl adduct with an hydroxy group in the chain as an isomer of the alkyl peroxyl adduct. This mono-hydroxy alkoxyl

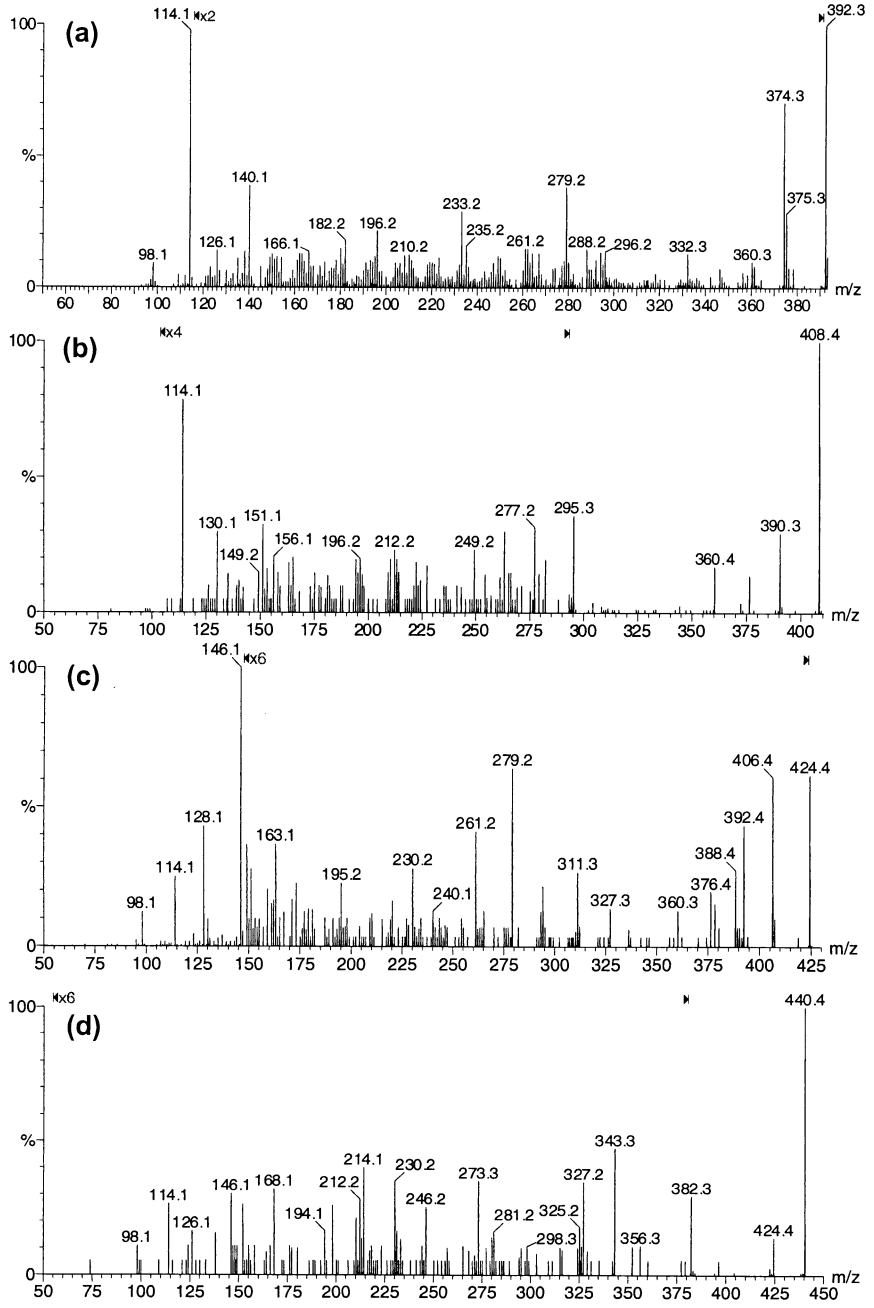

Figure 4. ES-MS/MS spectra of the carbon and oxygen-centered radical adducts of linoleic acid of (**a**) *m/z* 392, (**b**) *m/z* 408, (**c**) *m/z* 424, and (**d**) *m/z* 440.

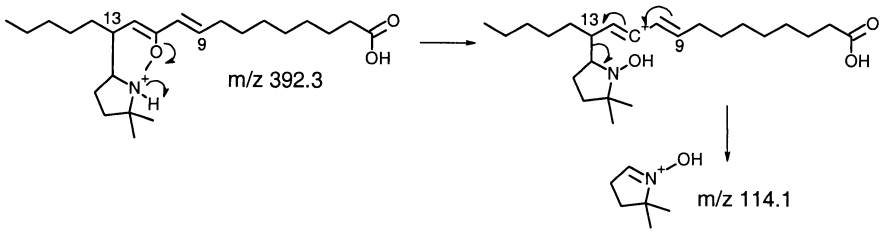

Scheme 11. Proposed mechanism for the formation of the ion at *m/z* 114 from the cyclic adduct at *m/z* 392.

Table 2. Fragment ions observed in the MS/MS spectra of cyclic structures of DMPO spin adducts of linoleic acid (% of relative abundance normalized to base peak)

Fragments	*m/z* 394	*m/z* 410	*m/z* 426	*m/z* 442
$[DMPO+H]^+$	114 (100)	114 (55)	114 (25)	114 (20)
$[DMPO-O+H]^+$		130 (20)	130 (10)	
$[DMPO-OO+H]^+$			146 (100)	146 (20)
$-H_2O$	374 (35)	390 (80)	406 (10)	442 (<5)
$-2H_2O$		372 (10)	388 (5)	
−97 (C_{11}-C_{12} cleavage isomer C_9)	295 (10)	311 (5)	327 (5)	343 (30)
−113	279 (20)	295 (100)	311 (5)	327 (20)
$-113\text{-}H_2O$	261 (10)	277 (10)	293 (<5)	

adduct was also suspected to occur in the open adduct. The mechanism for its origin is similar with the one presented in Scheme **10**, involving the hydroxy group similar to the adduct at *m/z* 442. The fragment ion at *m/z* 230 may result from cleavage of the C_{13}–C_{12} bond adjacent to the spin trap in isomer C_{13} with loss of $C_{11}H_{22}CO_2H$. The fragment ions at *m/z* 149 ($C_9H_{13}CO^+$), 151 ($C_9H_{15}CO^+$), 163 ($C_{10}H_{15}CO^+$), 181 (OH-$C_{10}H_{16}CO^+$), 195 (OH-$C_{11}H_{18}CO^+$), and 209 (OH-$C_{12}H_{20}CO^+$), correspond to alkyl acylium radical fragment ions.

MS/MS Spectra of the DMPO Adduct at m/z 440

The MS/MS spectrum of the ion at *m/z* 440 (Figure 4d), unlike all the other MS/MS spectra, showed fragment ions with very low relative abundance. It was possible to observe the presence of fragment ions at *m/z* 114 and 146, confirming the presence of an alkyl peroxyl spin adduct containing an hydroxy group. Fragment ion at *m/z* 327 is due to loss of DMPO moiety. The presence of a fragment ion at *m/z* 424 results from the loss of O. The formation of the fragment ion at *m/z* 382 is originated by a mechanism similar to that presented for the formation of the fragment ion at *m/z* 384 from the adduct at *m/z* 442 (Scheme **10**). The fragments observed in the low mass region were attributed to unsaturated alkyl acylium radical ions (126 ($C_7H_{14}CO^{+\cdot}$), 138 ($C_8H_{14}CO^{+\cdot}$), 152 ($C_9H_{16}CO^{+\cdot}$), 168 (OH-$C_9H_{15}CO^{+\cdot}$), 194(OH-$C_{11}H_{17}CO^{+\cdot}$), 198(OH-$C_{11}H_{21}CO^{+\cdot}$), 212 (OH_2-$C_{11}H_{18}CO^+$) or (OH-$C_{12}H_{23}CO^+$).

Conclusions

FAB-MS, ES-MS, and MS/MS have proven to be useful for the identification and characterisation of DMPO spin adducts of linoleic acid, namely alkyl, alkoxyl and alkyl peroxyl spin adducts. Both FAB-MS and ES-MS spectra gave similar results, allowing the identification of linoleic acid peroxidation products, but due to the higher sensitivity of ES-MS, it was possible to observe characteristic new adducts in the ES-MS spectrum. Both carbon-centered and oxygen-centered adducts of DMPO were found to occur, namely alkoxyl, peroxyl, hydroxyalkoxyl, and hydroxyperoxyl radical adducts. Epoxy adducts were also identified.

Characteristic fragment ions, such as the fragment ion at *m/z* 114 and the loss of 113 Da were observed in the MS/MS spectra of all adducts, thus confirming that they are DMPO adducts. In the alkoxyl radical adducts, a fragment ion at *m/z* 130 confirmed the presence of the alkoxyl radical, and the fragment ion at *m/z* 146 and loss of 145 Da confirmed the presence of the alkyl peroxyl adduct. Alkoxyl radical adducts with hydroxyl group in the alkyl chain, an isomer of the peroxyl adduct, were also found. Alkyl peroxyl DMPO adducts containing an hydroxyl group were also observed in the MS spectra, and the corresponding MS/MS spectra showed the characteristic fragment ions at *m/z* 114 and 146, and loss of 113 and 145 Da. Although the experimental approach used in this work does not allow identifying unambiguously the different isomers that are present, fragmentation observed in the vicinity of the DMPO linkage suggested the occurrence of structural isomers containing the DMPO moiety both at C_9 and C_{13}.

Adducts with the DMPO linked to the carboxylic acid group forming an intramolecular ring were also found. Additional fragmentation involved loss of one and two molecules of oxygen, or loss of one molecule of oxygen and an oxygen atom, for the alkyl, alkoxyl, and peroxyl adducts, respectively.

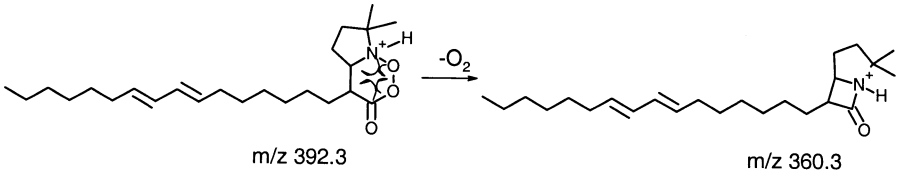

Scheme 12. Loss of O_2 from the adduct at *m/z* 392 forming the fragment ion at *m/z* 360.

Acknowledgments

The authors gratefully acknowledge to Foundation for Science and Technology (FCT) for the financial support provided by the project POCTI 33279/99 and PhD. Grant to Ana Reis (SFRH/BD/10358/2002). The authors also acknowledge the Research Unit 62/94 Química Orgânica, Produtos Naturais e Agro-alimentares.

References

1. Jackson, M. J. Free Radical in the Pathogeneses of Tissue Damage in Calcium, Oxygen Radical and Cellular Damage; (Society for Experimental Biology Seminar Series, 46); Duncan, C. J., Ed., Cambridge University Press: Cambridge, 1991; pp 11–16.
2. Pincemail, J. Free Radicals and Antioxidants in Human Diseases. In *Analysis of Free Radicals in Biological Systems*; Favier, A. E.; Cadet, J.; Kalyanaraman, B.; Fontecave, M.; Pierre, J. L.; Birkhäuser Verlag: Berlin, 1995; pp. 83–98.
3. Shigenaga, M. K.; Hagen, T. M.; Ames, B. N. Oxidative Damage and Mithocondrial Decay in Aging. *Proc. Natl. Acad. Sci.* **1994,** *91,* 10771–10778.
4. Wills, E. Evaluation of Lipid Peroxidation in Lipids and Biological Membranes. *Biochemical Toxicology: A Practical Approach;* In: Snell, K.; Mullock, B., Eds.; IRL Press: Oxford, 1987; 127–152.
5. (a) Liochev, S. I. The Mechanism of Fenton-Like Reactions and Their Importance for Biological Systems. A Biologist's View. *In Metal Ions in Biological Systems,* Sigel, A.; Sigel, H., Eds., Vol. XXXVI; Marcel Dekker, Inc: New York, NY, 1999; pp 1–40. (b) Sergent, O.; Morel, I.; Cillard, J. Involvent of Metal Ions in Lipid Peroxidation. *Biological Implications in Metal Ions in Biological Systems,* Sigel, A.; Sigel, H., Eds., Vol XXXVI; Marcel Dekker, Inc: New York, NY, 1999; pp 251–262.
6. Knecht, K. T.; Mason, R. P. In vivo Spin Trapping of Xenobiotics Free Radical Metabolites. *Arch. Biochem. Biophys.* **1993,** *303,* 185–194.
7. Rota, C.; Barr, D. P.; Martin, M. V.; Guengerich, F. P.; Tomasi, A.; Mason, R. P. Detection of Free Radicals Produced from the Reaction of Cytochrome. P-450 with Linoleic Acid Hydroperoxide. *Biochem. J.* **1997,** *328,* 565–571.
8. Qian, S. Y.; Wang, H. P.; Schafer, F. Q.; Buettner, G. R. EPR Detection of Lipid-Derived Free Radicals from PUFA, LDL, and Cell Oxidations. *Free Rad. Cell Med.* **2000,** *29,* 568–579.
9. Iwahashi, H.; Albro, P. W.; McGrown, S. R.; Tomer, K. B.; Mason, R. P. Isolation and Identification of α-(4-Pyridyl-1-Cxide)-N-Tert-Butylnitrone Radical Adducts Formed by the Decomposition of Hydroperoxides of the Linoleic Acid by Soybean Lipoxygenase. *Arch. Biochem. Biophys.* **1991,** *285,* 172–180.
10. Iwahashi, H. High-Performance Liquid Chromatographic Determination of Linoleic Acid Peroxide-Derived Radicals Using Electrochemical Detection. *J. Chromatogr. A.* **2000,** *904,* 197–202.
11. Qian, S. Y.; Tomer, K. B.; Yue, G. Guo, Q;; Kadiisha, M. B.; Mason, R. P. Characterization of the Initial Carbon-Centered Pentadienyl Radical and Subsequent Radicals in Lipid Peroxidation: Identification via On-Line High Performance Liquid Chromatography/Electron Spin Resonance and Mass Spectrometry. *Free Rad. Biol. Med.* **2002,** *33,* 998–1009.
12. Iwahashi, H.; Parker, C. E.; Mason, R. P.; Tomer, K. B. Combined Liquid Chromatography/Electron Paramagnetic Resonance Spectrometry/Electrospray Ionization Mass Spectrometry for Radical Identification. *Anal Chem.* **1992,** *64,* 2244–2252.
13. Iwahashi, H.; Nishizaki, K.; Takagi, I. Cytochrome *c* catalyzes the Formation of Pentyl Radical and Octanoic Acid Radical from Linoleic Acid Hydroperoxide. *Biochem. J.* **2002,** *361,* 57–66.
14. Dikalov, S. I.; Mason, R. P. Spin Trapping of Polyunsaturated Fatty Acid-Derived Alkyl Peroxyl Radicals: Reassignment to Alkoxyl Radical Adducts. *Free Rad. Biol. Med.* **2001,** *30,* 187–197.
15. Parker, C. E.; Iwahashi, H.; Tomer, K. B. Spin-Trapped Radicals: Determination by LC-TSP-MS. *J. Am. Soc. Mass Spectrom.* **1991,** *2,* 413–418.
16. Domingues, P.; Domingues, M. R. M.; Amado, F. M. L.; Ferrer-Correia, A. J. Detection and Characterization of Hydroxyl Radical Adducts by Mass Spectrometry. *J. Am. Soc. Mass Spectrom.* **2001,** *12,* 1219–1241.
17. Jurva, U.; Wikström, H. V.; Bruins, A. P. Electrochemically Assisted Fenton Reaction: Reaction of Hydroxyl Radicals with Xenobiotics Followed by On-Line Analysis with High-Performance Liquid Chromatography/Tandem Mass Spectrometry. *Rapid Commun. Mass Spectrom.* **2002,** *16,* 1934–1940.
18. Domingues, M. R. M.; Domingues, P.; Reis, A.; Fonseca, C.; Amado, F. M. L.; Ferrer-Correia, A. J. V. Identification of Oxidation Products and Free Radicals of Tryptophan by Mass Spectrometry. *J. Am. Soc. Mass Spectrom.* **2003,** *14,* 406–416.
19. Folch, J.; Lees, M.; Stanley, G. H. S. A Simple Method for the Isolation and Purification of Total Lipids from Animal Tissues. *J. Biol. Chem.* **1957,** *226,* 497–509.
20. Spiteller, P.; Kern, W.; Reiner, J.; Spiteller, G. Aldehydic Lipid Peroxidation Products Derived from Linoleic Acid. *Biochim. Biophys. Acta.* **2001,** *1531,* 188–208.
21. Marnett, L. J.; Wilcox, A. L. Polyunsaturated Fatty Acid Alkoxyl Radicals Exist as Carbon-Centered Epoxyallylic Radicals: A Key Step in Hydroperoxide-Amplified Lipid Peroxidation. *Chem. Res. Toxicol.* **1993,** *6,* 413–416.
22. Crow, F. W.; Cragun, J. D.; Johnson, K. L.; Ruiz, M. V. de la; Paz, M. P.; Naylor, S. On-Line HPLC-UV-Mass Spectrometry and Tandem Mass Spectrometry for the Rapid Delineation and Characterization of Differences in Complex Mixtures: A Case Study Using Toxic Oil Variants. *Biomed. Chromatogr.* **2002,** *16,* 311–318.

BIOMEDICAL CHROMATOGRAPHY
Biomed. Chromatogr. **20**: 109–118 (2006)
Published online in Wiley InterScience (www.interscience.wiley.com).
DOI: 10.1002/bmc.536

ORIGINAL RESEARCH

Identification of linoleic acid free radicals and other breakdown products using spin trapping with liquid chromatography-electrospray tandem mass spectrometry

A. Reis, M. R. M. Domingues, F. M. L. Amado, A. J. V. Ferrer-Correia and P. Domingues*

Department of Chemistry, University of Aveiro, 3810-193 Aveiro, Portugal

Received 14 March 2005; revised 29 April 2005; accepted 3 May 2005

ABSTRACT: Linoleic acid radical products formed by radical reaction (Fenton conditions) were trapped using 5,5-dimethyl-1-pyrrolidine-*N*-oxide (DMPO) and analysed by reversed-phase liquid chromatography coupled to electrospray mass spectrometry (LC-MS). The linoleic acid radical species detected as DMPO spin adducts comprised oxidized linoleic acid and short-chain radical species that resulted from the breakdown of carbon and oxygen centred radicals. Based on the m/z values, the short-chain products were identified as alkyl and carboxylic acid DMPO radical adducts that exhibited different elution times. The ions identified as DMPO radical adducts were studied by liquid chromatography–tandem mass spectrometry (LC-MS/MS). The LC-MS/MS spectra of linoleic acid DMPO radical adducts exhibited the fragment ion at m/z 114 and/or the loss of neutral molecule of 113 Da (DMPO) or 131Da (DMPO + H_2O), indicated to be DMPO adducts. The short-chain products identified allowed inference of the radical oxidation along the linoleic acid chain by abstraction of hydrogen atoms in carbon atoms ranging from C-8 to C-14. Other ions containing the fragment ion at m/z 114 in the LC-MS/MS spectra were attributed to DMPO adducts of unsaturated aldehydes, hydroxy-aldehydes and oxocarboxylic acids. The identification of aldehydic products formed by radical oxidation of linoleic acid peroxidation products, as short-chain product DMPO adducts, is a means of identifying lipid peroxidation products.

KEYWORDS: linoleic acid; Fenton reaction; DMPO adducts; free radicals; LC-MS/MS

INTRODUCTION

Free radicals formed under physiological conditions as by-products of aerobic processes such as respiration react with proteins, DNA bases and lipids that are found in the intracellular medium (Cadet *et al.*, 1995). In consequence, the structures of these compounds are altered as well as their function within the cells. For this reason, free radicals have been thought to play an active role in several diseases such as lung and liver cancer, cataract formation, atherosclerotic lesions and in aging processes (Pincemail, 1995).

*Correspondence to: P. Domingues, Department of Chemistry, University of Aveiro, 3810-193 Aveiro, Portugal.
E-mail: pedrom@dq.ua.pt

Abbreviations used: DMPO, 5,5-dimethyl-1-pyrrolidine-*N*-oxide; ESI, electrospray ionization; ESR, electron spin resonance; GC-MS, gas chromatography coupled with mass spectrometry; HPLC, high performance liquid chromatography; LC-MS, liquid chromatography coupled with mass spectrometry; LC-MS/MS, liquid chromatography coupled with tandem mass spectrometry; MS, mass spectrometry; MS/MS, tandem mass spectrometry; POBN, α-(4-pyridil-1-oxide)-N-tert-butylnitrone; PUFA, polyunsaturated fatty acids; RIC, reconstructed ion chromatogram; ROS, reactive oxygen species; rt, retention time; UV, ultraviolet detection.

Contract/grant sponsor: Foundation for Science and Technology and FSE; Contract/grant number: SFRH/BD/10358/2002.

Published online 24 June 2005

In biological systems, free radicals resulting from aerobic processes are also known as reactive oxygen species (ROS). One of the most reactive species is the hydroxyl radical ($^{\bullet}OH$), which, under physiological conditions, is formed by a Fenton-like reaction (Liochev, 1999). The hydroxyl radical reacts readily with polyunsaturated fatty acids (PUFA), through the abstraction of allylic hydrogen atoms, resulting in a non-selective reaction. The ω-6 PUFA, such as linoleic and arachidonic acids, found in membrane phospholipids, in triglycerides and in low-density lipoprotein, are a major source of ROS attack (Rosen *et al.*, 1999). Lipid radicals ($L^{\bullet}$), formed by abstraction of allylic hydrogen atoms by the hydroxyl radical, react with molecular oxygen, leading to the formation of lipid hydroperoxides (LOOH) and, through a radical cascade reaction, may originate lipid alkoxyl radicals ($LO^{\bullet}$). These lipid alkoxyl radicals may break down to short chain products that can either be neutral products (aldehydes) or free radicals (Sergent *et al.*, 1999). Aldehydic products formed during lipid peroxidation can react with amino acids and proteins (Fruebis *et al.*, 1992) and affect enzymes involved in the glycolytic and the pentose phosphate pathways (Novotny *et al.*, 1994; Tavazzi *et al.*, 2000), causing cytotoxicity (Spiteller, 1998; Niknahad *et al.*, 2003).

Radicals are very unstable species and through the addition of nitroso compound radicals, known as 'spin traps', form much more stable 'radical adducts'. The most common approach used in the study of lipid radicals is trapping experiments with either POBN [α-(4-pyridil-1-oxide)-*N*-tert-butylnitrone] or DMPO (5,5-dimethyl-1-pyrrolidine-*N*-oxide); the trapped radicals can be further detected and identified by electron spin resonance (ESR; Rota *et al.*, 1997; Qian *et al.*, 2000, 2002; Iwahashi, 2000; Dikalov and Mason, 2001). This approach has allowed the identification of carbon-centred lipid radicals formed by enzymatic reactions with lipoxygenase (Iwahashi *et al.*, 1991, 2002; Rota *et al.*, 1997; Iwahashi, 2000; Qian *et al.*, 2003a,b). However, recently some authors have shown the similarity of ESR spectra peroxyl to alkoxyl lipid radicals when in aqueous and non-aqueous solvents, owing to the similarity of the hyperfine coupling constants of these species, suggesting the problem of ESR data misinterpretation (Dikalov *et al.*, 2001). Mass spectrometry (MS), coupled with spin trapping experiments, is increasingly being used in the identification of lipid radicals and has led to interesting results (Iwahashi *et al.*, 2002; Qian *et al.*, 2003a,b; Reis *et al.*, 2003). The data obtained allowed the identification of oxidized intact fatty acids that contained the radical centred in carbon atoms (Qian *et al.*, 2003a,b; Reis *et al.*, 2003) as well as in oxygen atoms (oxygen-centred radicals; Reis *et al.*, 2003). Other breakdown products such as short-chain lipid radicals have also been identified as POBN adducts by MS (Iwahashi, 2000; Iwahashi *et al.*, 2002; Qian *et al.*, 2003a,b). The detection of short-chain lipid spin adducts by MS in extracts purified by high-performance liquid chromatography (HPLC) has, so far, mainly focused on the identification of pentyl ($POBN/C_5H_{11}$) and octanoic acid radical adducts ($POBN/C_8H_{15}O_2$) as products of linoleic acid oxidation (Iwahashi, 2000; Iwahashi *et al.*, 2002; Qian *et al.*, 2003a), and on the identification of pentyl ($POBN/C_5H_{11}$), 6-octenyl ($POBN/C_8H_{15}$), butanoic acid ($POBN/C_4H_7O_2$), 5-heptenoic acid ($POBN/C_7H_{11}O_2$) and others, as radical products of arachidonic acid oxidation (Qian *et al.*, 2003a). All the short-chain lipid radicals identified were carbon-centred radicals and the identification of the pentyl radical in both linoleic and arachidonic acids provided evidence for the oxidation of the C-13 carbon (ω-6 position in linoleic acid) and C-15 (ω-6 position in arachidonic acid; Qian *et al.*, 2003a,b). So far, to our knowledge, there are no surveys on LC-MS of the radical adducts and other breakdown radical products formed by non-selective reaction of the linoleic acid.

In this work, we present and discuss the results obtained by oxidation of linoleic acid through the Fenton reaction in the presence of DMPO. The spin adducts formed were analysed by LC-MS and characterized by LC-MS/MS.

EXPERIMENTAL

Chemicals. Linoleic acid and DMPO were obtained from Sigma (St Louis, MO, USA) and used without further purification. Iron (II) chloride ($FeCl_2$) and hydrogen peroxide (H_2O_2), used for the peroxidation reaction, were purchased from Merck (Darmstadt, Germany).

Oxidation of linoleic acid by Fenton reaction. Spin trapping experiments were performed by adding to 1 mg of linoleic acid in 50 µL bicarbonate buffer solution (pH 7.4), 5 mmol $FeCl_2$ solution and 50 mmol H_2O_2. This mixture was left to react in the dark for different periods of time with occasional sonication, after which 1 µL (9 mmol) of DMPO was added. The control was performed by replacing H_2O_2 with water. The lipid DMPO adducts were extracted using a modification of the Folch method with chloroform–methanol (2:1, v/v; Folch *et al.*, 1957). The reaction was monitored using ESI-MS.

HPLC and mass spectrometry conditions (LC-MS/MS). The linoleic acid DMPO adducts were separated on an HPLC system (Waters Aliance 2690) equipped with a UV detector (Knauer K-2500) set at λ = 233 nm. The reaction mixture (25 µL) was introduced into a Spherisorb C_{18} ODS-2 HPLC column (150 × 1 mm i.d., 5.0 µm, Waters) kept at room temperature. The mobile phase consisted of 0.1% TFA in acetonitrile (eluent A) and water (eluent B). The elution gradient was 10% A to 80% A in a linear gradient for 60 min and a flow rate of 1 mL/min. After the UV detector the flow was redirected into the MS interface with a 1:20 home-made split. Mass spectrometry (MS) and tandem mass spectrometry (MS/MS) analyses using electrospray ionisation (ESI) in the positive mode, were obtained with a Q-TOF 2 instrument (Micromass, Manchester, UK) using a MassLynx software system (version 4.0). The mass spectrometer was operated with a capillary voltage of 3000 V, a cone voltage of 35 V, the source block temperature set to 100°C and the desolvation temperature set to 180°C. Mass spectra (LC-MS) were obtained over a mass to charge ratio (m/z) of 50–1000 at a resolution of 10,000 (50% valley). LC-MS/MS experiments were carried out by selecting the precursor ion of interest using Q1 and collision-induced fragmentation in a hexapole collision cell using argon as a collision gas, and the collision energy was varied according to the ion of interest (typically 20–30 eV).

RESULTS AND DISCUSSION

The extract containing the linoleic acid DMPO adducts was injected into the HPLC system and the UV and the MS chromatograms obtained (data not shown) revealed the presence of peaks that were absent during the elution of linoleic acid blank runs, suggesting the formation of new products formed by reaction of the linoleic acid with the hydroxyl radical. During the previous identification of linoleic acid DMPO adducts by ESI-MS (Reis *et al.*, 2003), several oxidized species were

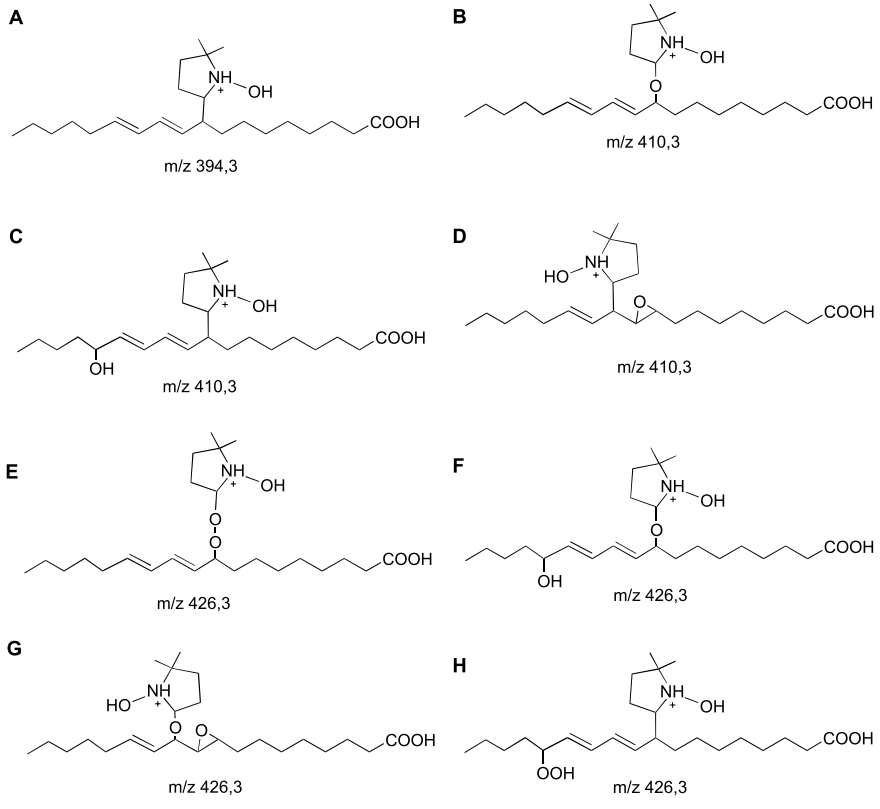

Scheme 1. Structures of the long-chain linoleic acid DMPO radical adducts for the ions at *m*/*z* 394, 410 and 426.

identified and characterized as alkyl spin adducts (*m*/*z* 394; A in Scheme 1), as alkoxyl spin adducts (*m*/*z* 410; B in Scheme 1) and hydroxy-alkyl spin adducts (*m*/*z* 410; C in Scheme 1) or epoxy-alkyl spin adducts (*m*/*z* 410; D in Scheme 1), and as peroxyl spin adducts (*m*/*z* 426; E in Scheme 1), hydroxy-alkoxyl spin adducts (*m*/*z* 426; F in Scheme 1) or epoxy alkoxyl spin adducts (*m*/*z* 426; G in Scheme 1) and hydroperoxide-alkyl spin adducts (*m*/*z* 426; H in Scheme 1). The fragmentation pattern obtained for each ion suggested the occurrence of both structural and positional isomers of each of the spin adducts (Reis *et al.*, 2003). In this work, by plotting the reconstructed ion chromatogram (RIC) of each ion observed at *m*/*z* 394, 410 and 426 (Fig. 1), it was possible to propose the elution of the alkyl adduct (*m*/*z* 394) with a retention time (rt) of 43 min, the alkoxyl adduct (*m*/*z* 410) with an rt of 33.3 min, and the peroxyl adduct (*m*/*z* 426) with an rt of 31.8 min. The ion at *m*/*z* 426 also shows a minor peak eluting at 42.4 min, which is similar to the retention time of the alkyl adduct (*m*/*z* 394). This may indicate the contribution of the carbon-centred adduct (hydroperoxide-alkyl) to the ion at *m*/*z* 426. On the other hand, the absence of chromatographic peaks for each of the different oxidized linoleic acid adducts suggested that separation between expected positional isomers (placed at C-9 and C-13) was not achieved under the chromatographic conditions used. The LC-MS/MS spectra (data not shown) obtained for the ion at *m*/*z* 394 (rt 43 min) exhibited the fragment ion at *m*/z 114, confirming that it is indeed the DMPO adduct (Domingues *et al.*, 2001; Reis *et al.*, 2003). The LC-MS/MS spectrum of the ion at *m*/*z* 410 (rt 33.3 min) exhibited the fragment ion at *m*/*z* 114 as well as the fragments due to loss of 113 Da (–DMPO), 131 Da (DMPO+H_2O), 129 Da (–DMPO–OH) and loss of

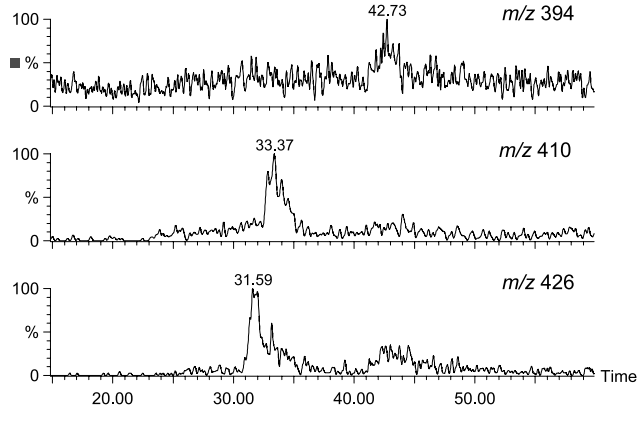

Figure 1. RIC chromatograms of long-chain linoleic acid DMPO adducts observed at: (a) *m*/*z* 394, (b) *m*/*z* 410 and (c) *m*/*z* 426.

Table 1. DMPO spin adducts of ions observed in the MS spectrum resulting from β-scission of carbon- and oxygen-centred radicals. The fragment ions identified in the LC-MS/MS spectra, the retention times observed, the compound and the probable site of oxidation are also indicated

m/z value $[M+H]^+$	RT (min)	Fragments in the LC-MS/MS spectrum (% RA)	DMPO adduct	Site of oxidation
Long-chain				
394	43.0	114 (5), 263 (20), 279[a] (5), 335 (50), 353 (100), 376 (10)	Alkyl octadecadienoic acid	
410	33.3	114 (5), 184 (20), 199 (25), 239 (30), 257 (25), 263 (20), 265 (20), 283 (25), 297[a] (20), 333 (30), 351 (100), 392 (45)	Hydroxy-alkyl octadecadienoic acid	
426	31.8	114 (35), 187 (20), 236 (25), 277 (30), 297 (100), 308 (40), 334 (35), 351 (20), 385 (55), 408 (60)	Hydroxy-alkoxyl octadecadienoic acid	
426	42.4	114 (25), 251[a] (10), 279 (100), 297 (15), 334 (45), 367 (30), 385 (70), 408 (80)	Hydroperoxide-alkyl octadecadienoic acid	
Short-chain				
158	41.3	114 (20), 129[a] (30), 140 (20), 143 (100)	Propyl	C-14
186	42.7	114 (25), 129[a] (40), 143 (100), 168 (50)	Pentyl	C-13
198	42.9	114 (10), 139 (40), 157[a] (100), 180 (20)	Hexenyl	C-12
212	43.2	99 (10), 114 (10), 153 (50), 171[a] (100), 194 (25)	Heptenyl	C-11
244	31.4	114 (10), 157 (40), 185 (40), 208 (50), 226 (100)	Heptanoic acid	C-9
258	31.6	114 (10), 129[a] (100), 145 (15), 157 (40), 185 (45), 199 (50), 240 (20)	Octanoic acid	C-9
270	31.5	114 (10), 155 (20), 182 (15), 197 (10), 211 (40), 229[a] (100), 252 (20)	8-Nonenoic acid	C-9
284	31.5	114 (15), 171 (100), 243[a] (50), 266 (20)	9-Decenoic acid	C-11

(%RA) indicates the percentage of relative abundance normalized to base peak.
[a] Fragments formed by homolytic cleavage of α-bond relative to the spin trap.

147 Da (DMPO–$OH+H_2O$) from the precursor ion (Table 1). The LC-MS/MS spectrum of the ion at *m/z* 426 (rt 42.4 min) showed a fragment ion at *m/z* 114, suggesting that the ion at *m/z* 426 corresponded to the hydroperoxide-alkyl adduct. The absence of the fragment ion *m/z* 146 and the presence of the fragment ion at *m/z* 279 (loss of DMPO–$OH+H_2O$), in the LC-MS/MS spectrum of the ion at *m/z* 426 (31.8 min), suggested the presence of the hydroxy-alkoxyl adduct and not the peroxyl adduct. The fragments observed in the LC-MS/MS spectra of the oxidized long-chain radicals are summarized in Table 1. The fragments observed in the LC-MS/MS spectra have odd and even *m/z* values, indicating the mechanisms involved in their formation either by homolytic cleavage or loss of neutral molecules, respectively. The fragments resulting from homolytic cleavage occurring in the α-bond, close to the spin trap (marked with an asterisk in Table 1), allowed proposal of the location of the spin along the unsaturated carbon chain. Other fragments resulting from cleavages involving the hydroxy group, and the cleavage of the β- and/or γ-bond relative to the spin trap occurring in the $[M+H]^+$ ion or the in the acylium ion (RCO^+) were also observed, giving structural information. As an example, the fragment at *m/z* 279 for the alkyl adducts may be attributed to the cleavage of the α-bond in the acylium ion considering the radical at C-11. Similar considerations can be drawn using the fragments at *m/z* 297 for the hydroxy-alkyl adduct, suggesting the 14-hydroxy derivative with the spin at the C-11, and the fragment at *m/z* 251 attributed to the cleavage of the α-bond combined with loss of O_2 for the ion at *m/z* 426 (rt 42.4 min), suggesting the location of the spin at C-9. Fragments formed by the cleavage of the β-bond relative to the carboxy group were also identified, although these fragments did not provide structural information regarding the location of the spin trap. The fragmentation of epoxy derivatives takes place through loss of water, cleavages of the α- or β-bond and with cleavage in the ring (Nakamura *et al.*, 1997), yielding fragments with the same *m/z* value as the hydroxy derivatives, which makes the unambiguous identification of these structures difficult. Therefore, the contribution of epoxy linoleic acid adducts should also be considered. The results reported here were obtained from the reaction mixtures, which were 1–5 days old, showing the high stability of DMPO spin adducts. This was also observed during EPR measurements in lipid radical POBN adducts and attributed to the Folch extraction step that stopped the oxidation reaction (Qian *et al.*, 2000).

Identification of spin adducts formed by β-scission of carbon-centred radicals

The positional isomers of the oxidized linoleic acid radicals at either the C-9 or the C-13 position were expected, although they have not been fully isolated under the elution conditions used in this study. Still, the alkoxyl radicals, when placed at either the C-9 or the C-13, may undergo β-scission with cleavage of the carbon chain leading to several short-chain peroxidation products (Spiteller, 1998). These short-chain products may be neutral molecules (alkanes, alkenes or

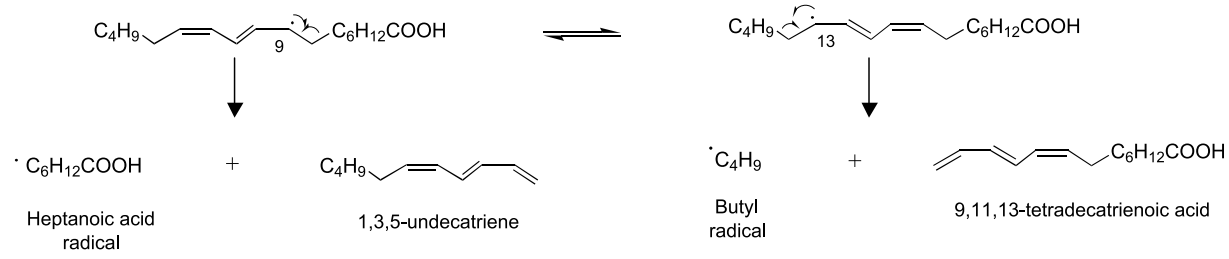

Scheme 2. Proposed formation of short-chain radicals by b-scission mechanism of intact linoleic acid carbon-centred radicals placed at C-9 and C-13.

carboxylic acids) or free radicals (carbon-centred), and the identification of such products may provide information about the presence or absence of the positional isomers formed under radical peroxidation reaction. The short-chain DMPO adducts formed by the β-scission mechanism of carbon- and oxygen-centred radicals of the linoleic acid were at very low levels, therefore the presence of the calculated mass of the protonated molecule (±0.1 Da) for the predicted structures was investigated by plotting the RIC of each of this ions. The carbon-centred (alkyl) radicals placed at C-9 and C-13 can lead, by β-scission cleavage, to the formation of short-chain neutral molecules and also to short-chain carbon-centred radicals (Scheme 2). These radical species may form carbon-centred DMPO adducts. The alkyl radical at C-9 yields the radical heptanoic acid radical and the 1,3,5-undecatriene, and the isomer in C-13 the butyl radical and the 9,11,13-tetradecatrienoic acid (as shown in Scheme 2). These short-chain DMPO adducts, if present, are expected at m/z 244 (heptanoic acid DMPO adduct), resulting from the isomer at C-9, and at m/z 172 (butyl DMPO adduct), resulting from the isomer at C-13. The RIC for the ions observed at m/z 172 and at m/z 244 are shown in Fig. 2. As can be seen, only the ion at m/z 244 showed a maximum, eluting at 27.9 min, and no peak was observed for the ion at m/z 172. The absence of an ion at m/z 172 (β-scission of isomer C-13) may suggest the absence of carbon-centred isomer at C-13 and/or the predominance of the C-9 carbon-centred isomer, indicating the carbon-centred isomer placed at C-9 to be more stable or its formation more favourable. The LC-MS/MS spectra obtained for the ion at m/z 244 (Table 1) gave a fragment ion at m/z 114 ($[DMPO+H]^+$) and the fragments due to loss of 113 Da (–DMPO) and loss of 131 Da (–DMPO–H_2O), which were used for the confirmation of the DMPO adducts. The fragment ions observed at m/z 157 and 185 (Table 1), formed by cleavage of the carbon bonds of the γ-bond relative to the spin trap and the β-bond relative to the carboxylic acid group, respectively, suggest the presence of the heptanoic acid DMPO radical adduct.

Abstraction of allylic hydrogen atoms, namely the ones at the C-8 and C-14 positions of the linoleic acid carbon chain, could also be considered to occur, and if present, may lead to short-chain radicals (carbon-centred) at m/z 158 (propyl adduct) from β-scission of alkyl radical at C-14, and at m/z 230 (hexanoic acid adduct) from β-scission of the alkyl radical at C-8. However, the RIC obtained (Fig. 3) only shows elution peak for the ion at m/z 158, suggesting that formation of the radical placed at C-14 may be residual. On the other hand, an ion with m/z 198 (hexenyl adduct), which may derive from β-scission cleavage of the

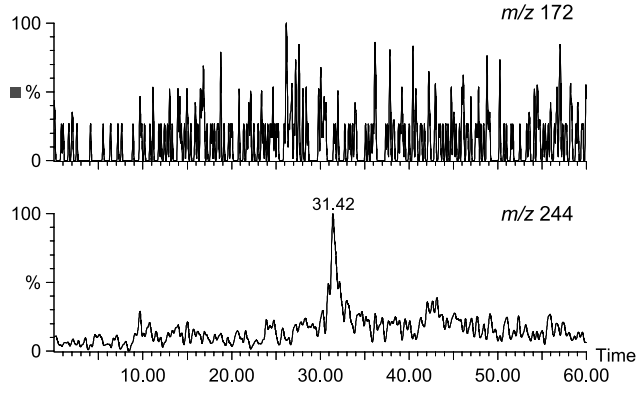

Figure 2. RIC chromatograms of short-chain products spin adducts resulting from cleavage of carbon-centred radicals of linoleic acid observed at: (a) m/z 172 and (b) m/z 244.

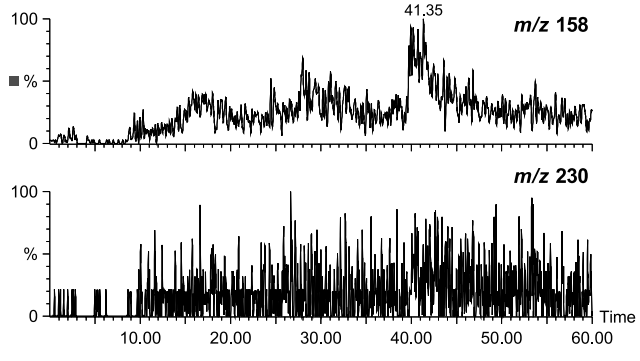

Figure 3. RIC chromatograms of short-chain products spin adducts resulting from cleavage of carbon-centred radicals of linoleic acid observed at: (a) m/z 158 and (b) m/z 230.

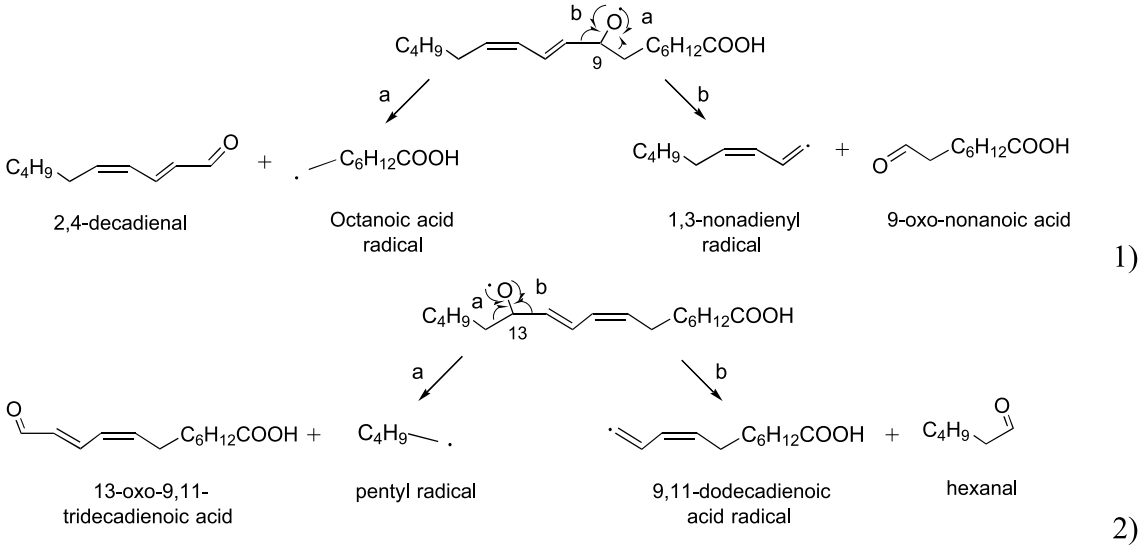

Scheme 3. Proposed formation of short-chain radicals by b-scission mechanism of intact linoleic acid oxygen-centred radicals placed at C-9 (1) and C-13 (2).

radical at C-12, was observed with an rt of 42.8 min, with the LC-MS/MS spectrum (Table 1) exhibiting the fragment ions at *m/z* 157 (homolytic α-cleavage) and *m/z* 139. These fragment ions can only be rationalized considering the occurrence of double bond migration with formation of the more stable alkenyl radical and not the vinyl radical.

Identification of spin adducts formed by β-scission of oxygen-centred radicals

The oxygen-centred radical positions at C-9 and C-13 may undergo decomposition by the β-scission mechanism, similar to carbon-centred radicals, yielding a short-chain radical species (carbon-centred) and a neutral molecule (aldehyde, carboxylic acid or oxo-acid), as shown in Scheme 3. However, in oxygen-centred radicals the β-scission mechanism can take place by two similar pathways towards different directions (a and/or b; Scheme 3), giving different breakdown products. Thus, the β-scission through pathway a of the alkoxyl radical at C-9 can lead to the octanoic acid radical and, if present, its DMPO adduct can be expected at *m/z* 258 (octanoic acid adduct), while the β-scission of the alkoxyl radical placed at C-13 can lead to the pentyl radical and its DMPO adduct at *m/z* 186 (pentyl adduct). The RIC of the ions at *m/z* 258 and 186, shown in Fig. 4, exhibit different retention times and were observed at 31.6 and 42.6 min, respectively. The fragment ions observed in the LC-MS/MS spectrum of ion at *m/z* 258 (Table 1) corresponded to fragments formed by homolytic cleavages occurring along the saturated chain (*m/z* 129, 157, 185 and 199) as well as the fragment ion at *m/z* 114 $[DMPO+H]^+$, allowing corroboration of the proposed structure (Scheme 4). The LC-MS/MS spectrum of ion at *m/z* 186 (Table 1) exhibits the fragment ion at *m/z* 114 and 168 ($-H_2O$), and the fragment ions at *m/z* 129 and 143, allowing the proposal of the pentyl DMPO adduct. Both these adducts have previously been identified by ESR as POBN adducts during enzymatic oxidation of linoleic acid (Iwahashi, 2000; Qian *et al.*, 2003a). The occurrence of the β-scission cleavage through pathway b in the

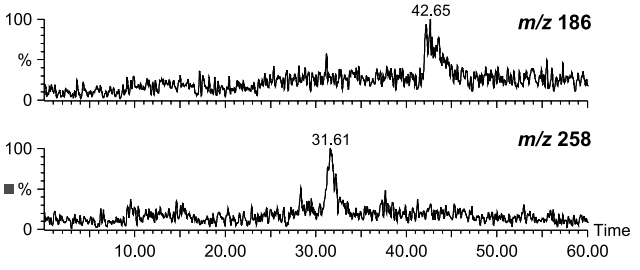

Figure 4. RIC chromatograms of short-chain products spin adducts resulting from cleavage of carbon-centred radicals of linoleic acid observed at: (a) *m/z* 186 and (b) *m/z* 258.

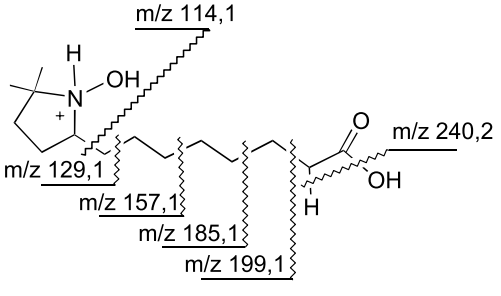

Scheme 4. Proposed fragmentation for the ion at *m/z* 258 (octanoic acid DMPO adduct).

Table 2. DMPO adducts of ions observed in the MS spectrum resulting from oxidation of unsaturated short-chain aldehydic products formed by β-scission of carbon- and oxygen-centred radicals. The fragment ions identified in the LC-MS/MS spectra, the retention times observed, the compound and the probable site of oxidation are also indicated

m/z value $[M+H]^+$	RT (min)	Fragments in the MS/MS spectrum (% RA)	DMPO adduct	Site of oxidation
256	30.4	114 (90), 143[a] (40), 170 (100), 226 (60), 238 (35)	4-Hydroxy-2-octenal	C-11
264	42.7	114 (5), 133 (20), 148 (25), 161 (15), 164 (20), 169 (20), 190 (15), 207[a] (15), 220 (5), 246 (100)	1,3,5-Undecatriene	C-9
282	31.8	114 (10), 134 (25), 164 (40), 176 (40), 185[a] (20), 211 (30), 222 (30), 246 (50), 264 (100)	2,4-Decenoic acid	C-9
298	33.1	114 (10), 130 (10), 169 (40), 187 (40), 225 (15), 239 (40), 257[a] (30), 280 (100)	10-Oxo-8-decenoic acid	C-10
324	31.7	98 (10), 114 (10), 126 (10), 138 (5), 152 (15), 166 (15), 182 (40), 193 (10), 194 (75), 199 (25), 209[a] (98), 210 (80), 211 (25), 227 (90), 250 (20), 265 (20), 267 (100), 288 (20), 306 (75)	12-Oxo-8,10-dodecenoic acid	C-12
336	31.4	114 (5), 211 (100), 239[a] (10), 248 (10), 257 (10), 318 (15)	9,11,13-Tetradecatrienoic acid	C-13
338	32.9	114 (8), 154 (15), 173 (12), 209[a] (10), 243 (5), 257 (20), 279 (15), 283 (10), 296 (100), 320 (10)	13-Oxo-9,11-tridecadienoic acid	C-13
340	33.0	114 (35), 167 (25), 201 (30), 209 (100), 243[a] (30), 251 (15), 269 (15), 280 (25), 322 (20)	12-Carboxy-2,4-dodecenoic acid	C-12

(% RA) indicates the percentage of relative abundance normalized to base peak.
[a] Fragments formed by cleavage of α-bond relative to the spin trap.

alkoxyl radicals at C-9 and C-13 (Scheme 3) can form DMPO adducts that, if present, are expected at *m/z* 238 (1,3-nonadienyl adduct) and 310 (9,11-dodecadienoic acid adduct), respectively. The RIC chromatograms obtained for each ion (data not shown) did not show the presence of ions with these *m/z* values.

The presence of the alkoxyl radical placed at C-11 is also possible to deduce by the presence of the heptenyl adduct (*m/z* 212) and of the 9-decenoic acid adduct (*m/z* 284). The RIC obtained for both ions (data not shown) showed an rt of 31.5 min for the ion at *m/z* 284, while for the ion at *m/z* 212 two chromatographic peaks were observed, with rts of 16.7 and 42.9 min. The LC-MS/MS spectrum obtained for the ion at *m/z* 212 at an rt of 42.9 min (Table 2) gave a fragment ion at *m/z* 114, confirming that it is a DMPO adduct and, in particular, the fragment ions at *m/z* 171 (cleavage of the α-bond) and 153, support the location of the spin trap. Furthermore, the fragment ion at *m/z* 171 in the LC-MS/MS of the precursor ion at *m/z* 212, formed by homolytic cleavage of the α-bond, suggests that vinylic radicals undergo bond migration, with formation of the more stable alkenyl radicals. The same behaviour was proposed based on the fragment ions observed in the LC-MS/MS spectrum of the ion at *m/z* 198. The ion at *m/z* 212 observed at 16.7 min corresponded to the elution of the DMPO adduct formed with the buffer solution (bicarbonate radical; Zhang *et al.*, 2000), as confirmed by the respective LC-MS/MS (data not shown). The LC-MS/MS spectrum obtained for the ion at *m/z* 284 (Table 1) gave fragment ions at *m/z* 114 ($[DMPO+H]^+$), 171 (–DMPO), 243 (cleavage of the α-bond) and 266 ($-H_2O$), and showed the presence of the 9-decenoic acid adduct.

Most of the lipid spin adducts described here are reported for the first time, since the study of linoleic acid radicals has mainly focused on the detection and identification of the pentyl and octanoic acid radicals (Rota *et al.*, 1997; Iwahashi, 2000; Qian *et al.*, 2003a). Furthermore, the identification of these short chain adducts suggests that β-scission of alkoxyl radicals proceeded through pathway a (Scheme 3), towards the formation of spin radicals of smaller carbon chain.

Identification of other spin adducts formed by β-scission

Aldehydic short-chain products, formed as neutral molecules of the β-scission mechanism of carbon-centred (Scheme 2) and oxygen-centred radicals (Scheme 3), and particularly the unsaturated ones, contain allylic hydrogen atoms and can undergo further radical oxidation by hydrogen abstraction. The radical species thus formed can, in turn, react with the DMPO spin trap, allowing their detection as carbon-centred DMPO adducts. This may explain the identification in the MS chromatogram of other ions of low molecular mass, which upon fragmentation yielded the fragment ion at *m/z* 114. Some of the DMPO adducts that can occur, formed by this mechanism, are expected at *m/z* 264 (1,3,5-undecatriene adduct) from β-scission of alkyl radical at C-9 (Scheme 2), at *m/z* 336 (9,11,13-tetradecatrienoic acid adduct) from alkyl radical at C-13, at *m/z* 266 (2,4-decadienal adduct) from alkoxyl at C-9, at *m/z* 240 (2-octenal adduct) and 312 (11-oxo-9-undecenoic acid adduct) from alkoxyl at C-11, and at *m/z* 338 (13-oxo-9,11-tridecadienoic acid adduct) from alkoxyl at C-13. The mono-allylic hydrogen atoms

placed at C-8 and C-14 can also be abstracted, and as a site of oxidation, other short-chain products can be formed and detected as DMPO adducts.

By plotting the RIC for the ions resulting from alkyl and alkoxyl radicals (data not shown), elution at different retention times was observed for the ions at *m/z* 264, 336 and 338 (Table 2), although the ions at *m/z* 266 (2,4-decadienal adduct), 240 (2-octenal adduct) and 312 (11-oxo-9-undecenoic acid adduct) were not observed. The LC-MS/MS mass spectra obtained for each of the observed ions (Table 2) exhibited the fragment ion at *m/z* 114, supporting the hypothesis that they were indeed DMPO adducts. The loss of the DMPO as a neutral molecule (–113 Da) was used to further confirm the proposed structure. Fragment ions observed in the LC-MS/MS spectra resulting from homolytic cleavages of the carbon chain in the vicinity of the spin trap (marked with an asterisk in Table 2), allow the spin to be pinpointed along the carbon chain. Charge-remote fragmentations resulting from homolytic cleavages in the vicinity of the functional group were also identified. These occurred in the β-bond relative to the carboxylic group (fragment with *m/z* 351 for hydroxy-alkyl octadecadienoic acid, fragment with *m/z* 199 for octanoic acid and fragment with *m/z* 269 for 12-carboxy-2,4-dodecenoic acid). Heterolytic cleavage of the β-bond relative to the oxo group (fragment with *m/z* 296 for 13-oxo-9,11-tridecadienoic acid) was observed, which allowed the functional group of the short-chain product to be ascertained. Also, fragments resulting from hydrogen elimination occurring in the saturated moiety of the short-chain product (as an example, the fragment with *m/z* 248 for the 9,11,13-tetradecatrienoic acid) were identified. The fragmentations described here also occurred for the acylium ions of short-chain products of linoleic acid. The fragments observed in the LC-MS/MS spectra of the different ions identified are described in Table 2.

As an example, the LC-MS/MS of the ion observed at *m/z* 256 is shown in Fig. 5(a). The LC-MS/MS spectrum gave a fragment ion at *m/z* 114 which is consistent with a DMPO adduct. The ion at *m/z* 256 can be attributed to the DMPO adduct of the product formed by β-scission of the alkoxyl radical (oxygen-centred) at C-10 (10-alkoxyl-14-hydroxy-11-oxo-8,12-octadecadienoic acid). This compound may result from the presence of the 11-hydroperoxide-9,12-octadecadienoic acid, and after double bond rearrangement and by β-scission leads to the C_8 acyl radical (structure A, Scheme 5) and to 10-oxo-8-decenoic acid. The same ion could also result from secondary pathways, such as the oxidation of 2-octenal to 4-hydroxy-2-octenal or 4-alkoxyl-2-octenal (structure B, Scheme 5), which is a by-product of the 11-alkoxyl-9,12-octadecadienoic acid. However, the 2-octenal was not detected during this study. This ion at *m/z* 256 eluted at 30.4 min (Table 2) and the fragment

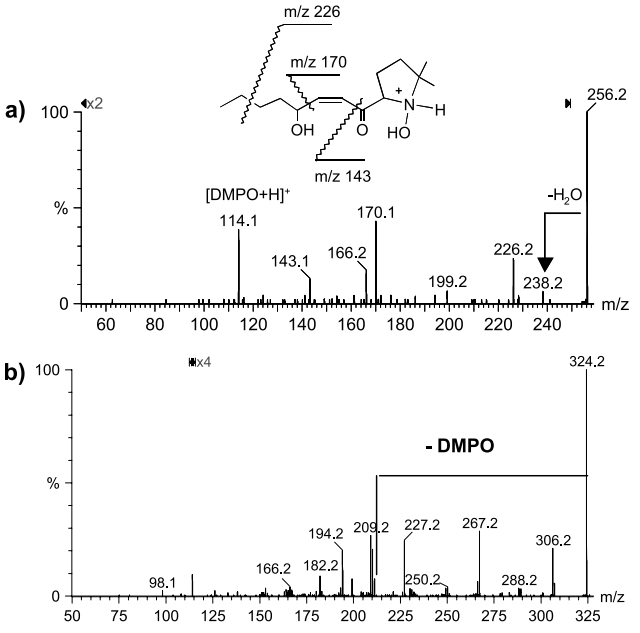

Figure 5. LC-MS/MS mass spectra of precursor ions with (a) *m/z* 256 and (b) *m/z* 324.

ions at *m/z* 143, 170, 226 and 238 suggest the presence of an acyl DMPO adduct (structure A, Scheme 5). The absence of an ion at *m/z* 130 $[DMPO–OH+H]^+$ in the LC-MS/MS mass spectrum, and the absence of a loss of DMPO–OH (–129 Da) and DMPO–OH+H_2O (–147 Da), provided evidence for the absence of the oxygen-centred adduct (structure B, Scheme 5). The identification of acyl radical species has been described by other authors using ESR measurements, during enzymatic oxidation of a 13-hydroperoxide derivative of linoleic acid (Watanabe *et al.*, 2000). The LC-MS/MS mass spectra of the ion at *m/z* 324 (12-oxo-8,10-dodecadienoic acid adduct), shown in Fig. 5(b), showed the fragment ion with *m/z* 114 $[DMPO+H]^+$ and with *m/z* 211 (loss of DMPO), as well as the fragment ions with *m/z* 209 (cleavage of the α-bond), *m/z* 250 (cleavage of the β-bond in the saturated moiety), *m/z* 265 (cleavage of β-bond relative to the carboxy function) and *m/z* 288 (loss of $2H_2O$ from the carboxylic group and from the DMPO molecule). The

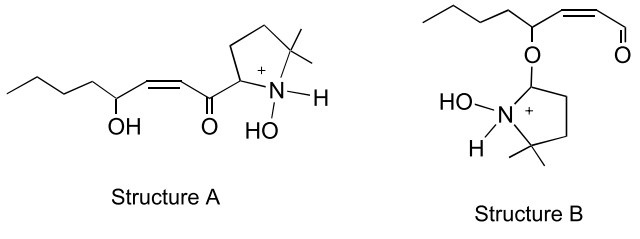

Scheme 5. Proposed structures for the DMPO adduct observed at *m/z* 256: (A) 4-hydroxy-2-octenal and (B) 4-alkoxyl-2-octenal.

fragment ions with m/z 126 ($C_8H_{14}O^{\bullet+}$), 138 ($C_9H_{14}O^{\bullet+}$), 152 ($C_{10}H_{16}O^{\bullet+}$) and 166 ($C_{11}H_{16}O^{\bullet+}$) are relative to cleavages in the unsaturated alkyl moiety and corroborate the presence of the oxo-acid DMPO adduct.

The detection of unsaturated short-chain products, namely hydroxy-aldehydes (m/z 256 and 296) and oxo-acids (m/z 298, 324 and 338) as DMPO adducts is novel, although the detection of such products as products of lipid peroxidation is not new (Spiteller, 1998; Kim *et al.*, 1999). Most of the aldehydic products identified here as DMPO adducts are described as lipid peroxidation products in rat and human urine (Kim *et al.*, 1999), and according to the literature available, alkenals are currently recognized to possess cytotoxicity towards humans (De Zwart *et al.*, 1999), which is proportional to the increase in carbon chain length (Niknahad *et al.*, 2003). The cytotoxicity is mainly due to the fact that they have been found to be potent inhibitors of enzymes in several metabolic pathways, namely of glycolytic enzymes (Novotny *et al.*, 1994), although the subject has not reached a consensus (Miwa *et al.*, 1997). Other short-chain products such as dicarboxylic acids have also been detected and identified using GC-MS (Inouye *et al.*, 2000) and were proposed as reliable biomarkers of keto acidosis (Inouye *et al.*, 2000).

CONCLUDING REMARKS

Liquid chromatography–electrospray mass spectrometry, coupled with spin trap experiments, was applied for the separation and identification of linoleic acid peroxidation products. The data obtained show that long-chain DMPO adducts, namely alkyl and alkoxyl adducts, were separated. Although the expected positional isomers from these DMPO adducts were not separated and identified under the elution conditions used, their presence could be established by the identification of alkyl (carbon-centred radicals) and alkoxyl (oxygen centred radicals) degradation products. The degradation products named short-chain products formed by β-scission mechanism of both carbon and oxygen-centred radicals were identified as short-chain DMPO adducts. Most of the short-chain products identified here (Table 2) are reported for the first time as radical products of the linoleic acid radical oxidation, and allowed deduction of the occurrence of radical attack at the carbon positions ranging from C-8 to C-14, which provided evidence for random attack by the hydroxyl radical. Other products identified were attributed to DMPO adducts of aldehydic products. The detection and identification of unsaturated aldehydic products such as DMPO adducts is novel, and is a simple approach for the detection and identification of this class of lipid peroxidation products.

The use of LC-MS/MS for the characterization of oxidized linoleic acid DMPO adducts was very helpful in the interpretation of LC-MS data, owing to the presence of DMPO adducts with the same m/z value.

Acknowledgements

The authors gratefully acknowledge the PhD grant to Ana Reis (SFRH/BD/10358/2002) provided by Foundation for Science and Technology (FCT) and FSE (III Quadro Comunitário de Apoio).

REFERENCES

Cadet J, Berger M, Morin B, Raoul S and Wagner JR. Oxidative damage to DNA. In *Analysis of Free Radicals in Biological Systems*, Favier AE, Cadet J, Kalyanaraman B, Fontecave M and Pierre JL (eds). Springer: Berlin, 1995; 51–64.

De Zwart LL, Meerman JHN, Commandeur JNM and Vermeulen NPE. Biomarakers of free radical damage applications in experimental animals and in humans. *Free Radical Biology and Medicine* 1999; **26**: 202.

Dikalov SI and Mason RP. Spin trapping of polyunsaturated fatty acid-derived alkyl peroxyl radicals: reassignment to alkoxyl radical adducts. *Free Radical Biological Medicine* 2001; **30**: 187.

Domingues P, Domingues MRM, Amado FML and Ferrer-Correia AJV. Detection and characterization of hydroxyl radical adducts by Mass Spectrometry. *Journal of the American Society of Mass Spectrometry* 2001; **12**: 1214.

Folch J, Lees M and Sloane-Staley GH. A simple method for the isolation and purification of total lipids from animal tissues. *Journal of Biological Chemistry* 1957; **23**: 497.

Fruebis J, Parthasarathy S and Steinberg D. Evidence for a concerted reaction between lipid hydroperoxides and polypeptides. *Proceedings of the National Academy of Science USA*. 1992; **89**: 10588.

Inouye M, Mio T and Sumino K. Dicarboxylic acids as markers of fatty acid peroxidation in diabetes. *Atherosclerosis* 2000; **148**: 197.

Iwahashi H. High-performance liquid chromatographic determination of linoleic acid peroxide-derived radicals using electrochemical detection. *Journal of Chromatography A* 2000; **904**: 197.

Iwahashi H, Albro PW, McGown SR, Tomer KB and Mason RP. Isolation and identification of α-(4-pyridil-1-oxide)-*N*-tert-butylnitrone radical adducts formed by the decomposition of the hydroperoxides of linoleic acid, linolenic acid and arachidonic acid by soybean lipoxygenase. *Archives of Biochemistry and Biophysics* 1991; **285**: 172.

Iwahashi H, Nishizaki K and Takagi I. Cytochrome c catalyses the formation of pentyl radical and octanoic acid radical from linoleic acid hydroperoxide. *Biochemistry Journal* 2002; **361**: 57.

Kim SS, Gallaher DD and Csallany AS. Lipophilic aldehydes and related carbonyl compounds in rat and human urine. *Lipids* 1999; **34**: 489.

Liochev SI. The mechanism of 'Fenton-like' reactions and their importance for biological systems. A biologist's view. In *Metal Ions in Biological Systems*, Sigel A and Sigel H (eds), Vol. 36. Marcel Dekker: New York, 1999; 1–40.

Miwa I, Adachi K, Murase S, Hamada Y and Sugiura M. 4-Hydroxy-2-nonenal hardly affects glycolysis. *Free Radical Biology and Medicine* 1997; **23**: 610.

Nakamura T, Bratton DL and Murphy RC. Analysis of epoxyeicosatetraenoic and monohydroxyeicosatetraenoic acids esterified to phospholipids in human red blood cells by electrospray tandem mass spectrometry. *Journal of Mass Spectrometry* 1997; **32**: 888.

Niknahad H, Siraki AG, Shuhendler A, Khan S, Teng S, Galati G, Easson E, Poon R and O'Brien PJ. Modulating carbonyl cytotoxicity in intact rat hepatocytes by inhibiting

carbonylmetabolizing enzymes. I. Aliphatic alkenals. *Chemical and Biological Interactions* 2003; **143–144**: 107.

Novotny MV, Yancey MF, Stuart R, Wiesler D and Peterson RG. Inhibition of glycolytic enzymes by endogenous aldehydes: a possible relation to diabetic neuropathies. *Biochimica Biophysica Acta* 1994; **1226**: 145.

Pincemail J. Free radicals and antioxidants in human diseases. In *Analysis of Free Radicals in Biological Systems*, Favier AE, Cadet J, Kalyanaraman B, Fontecave M and Pierre JL (eds). Springer: Berlin, 1995; 83–98.

Qian SY, Wang HP, Schafer FQ and Buettner GR. EPR detection of lipid-derived free radicals from PUFA, LDL, and cell oxidations. *Free Radical Biology and Medicine* 2000; **29**: 568.

Qian SY, Tomer KB, Yue G, Guo Q, Kadiiska MB and Mason RP. Characterization of the initial carbon-centred pentadienyl radical and subsequent radicals in lipid peroxidation: identification via on-line high performance liquid chromatography/electron spin resonance and mass spectrometry. *Free Radical Biology and Medicine* 2002; **33**: 998.

Qian SY, Guo Q and Mason RP. Identification of spin trapped carbon-centred radicals in soybean lipoxygenase-dependent peroxidations of ω-3 polyunsaturated fatty acids by LC/ESR, LC/MS and tandem MS. *Free Radical Biology and Medicine* 2003a; **35**: 33.

Qian SY, Yue G-H, Tomer KB and Mason RP. Identification of all classes of spin-trapped carbon-centred radicals in soybean lipoxygenase-dependent lipid peroxidations of ω-6 polyunsaturated fattu acids via LC/ESR, LC/MS and tandem MS. *Free Radical Biology and Medicine* 2003b; **34**: 1017.

Reis A, Domingues MRM, Amado FML, Ferrer-Correia AJV and Domingues P. Detection and Characterisation by mass spectrometry of radicals adducts produced by Linoleic acid oxidation. *Journal of the American Society of Mass Spectrometry* 2003; **14**: 1250.

Rosen GM, Britigan BE, Halpern H and Pou S. *Free Radicals: Biology and Detection by Spin Trapping*. Oxford University Press: New York, 1999; 35–41.

Rota C, Barr DP, Martin MV, Guengerich FP, Tomasi A and Mason RP. Detection of free radicals produced from the reaction of cytochrome P-450 with linoleic acid hydroperoxide. *Biochemistry Journal* 1997; **328**: 565.

Sergent O, Morel I and Cillard J. Involvement of metal ions in lipid peroxidation: biological implications. In *Metal Ions in Biological Systems*, Sigel A and Sigel H (eds), Vol. 36. Marcel Dekker: New York, 1999; 251–262.

Spiteller G. Linoleic acid peroxidation- the dominant lipid peroxidation process in low density lipoprotein- and its relationship to chronic diseases. *Chemistry and Physics of Lipids* 1998; **95**: 105.

Tavazzi B, Di Pierro D, Amorini AM, Fazzina G, Tuttobene M, Giardina B and Lazzarino G. Energy metabolism and lipid peroxidation of human erythrocytes as a function of increased oxidative stress. *European Journal of Biochemistry* 2000; **267**: 684.

Watanabe T, Katayame S, Enoki M, Honda Y and Kuwahara M. Formation of acyl radical in lipid peroxidation of linoleic acid by manganese-dependent peroxidase from *Ceriporiopsis subvermispora* and *Bjerkandera adusta*. *European Journal of Biochemistry* 2000; **267**: 4222.

Zhang H, Joseph J, Felix C and Kalyanaraman B. Bicarbonate enhances the hydroxylation, nitration, and peroxidation reactions catalysed by copper, zinc superoxide dismutase. *Journal of Biological Chemistry* 2000; **275**: 14045.

3. Phosphatidylcholine radical products

Manuscript III: Identification by electrospray tandem mass spectrometry of spin-trapped free radicals from oxidized 2-oleoyl-1-palmitoyl-*sn*-glycero-3-phosphocholine

Manuscript IV: Identification of free radicals of glycerophosphatidylcholines containing ω-6 fatty acids using spin-trapping coupled with tandem mass spectrometry

RAPID COMMUNICATIONS IN MASS SPECTROMETRY
Rapid Commun. Mass Spectrom. 2004; **18**: 1047–1058
Published online in Wiley InterScience (www.interscience.wiley.com). DOI: 10.1002/rcm.1444

RCM

Identification by electrospray tandem mass spectrometry of spin-trapped free radicals from oxidized 2-oleoyl-1-palmitoyl-*sn*-glycero-3-phosphocholine

A. Reis, P. Domingues, A. J. V. Ferrer-Correia and M. R. M. Domingues*
Chemistry Department, University of Aveiro, 3810-193 Aveiro, Portugal

Received 22 January 2004; Revised 5 March 2004; Accepted 5 March 2004

GPC radical species formed during oxidation of a glycerophosphocholine (16:0/18:1) under the Fenton reaction conditions were detected using a spin trap, 5,5-dimethyl-1-pyrrolidine *N*-oxide (DMPO). The stable spin-trapped radical adducts were identified by mass spectrometry (MS) using electrospray (ES) as ionization method and characterized by tandem mass spectrometry (MS/MS). Radical adducts of oxidized free *sn*-2 fatty acid and of oxidized intact GPC, containing one, two and three additional oxygen atoms, were assigned. DMPO adducts of oxidized intact GPC were observed as singly and doubly charged ions in ES-MS, while adducts of oxidized free fatty acids were observed as singly charged ions. Oxidized free *sn*-2 fatty acids and intact GPC-DMPO adducts correspond to carbon- and oxygen-centered radicals that were identified by MS/MS as alkyl, hydroxy-alkyl, alkoxyl, hydroxy-alkoxyl, peroxyl and hydroperoxide-alkoxyl spin adducts. The DMPO molecule was attached predominantly at C_9 of the oleic chain. The fragmentation pathway of spin adducts with two DMPO molecules strongly suggests the presence of species that were simultaneously carbon- and oxygen-centered radicals. Several fragments identified are consistent with the presence of isomeric structures contributing to the same ions. Copyright © 2004 John Wiley & Sons, Ltd.

Phospholipids, such as glycerophosphotidylcholines (GPC), which are composed of a polar head and a glycerol moiety substituted by two fatty acid chains at the *sn*-1 and *sn*-2 positions, are major components of the cellular membrane bilayer.[1] In mammals the fatty acids often encountered as substituents are linoleic and arachidonic acids.[1] The unsaturated fatty acids present are prone to react with reactive oxygen species (ROS) formed as a consequence of aerobic metabolism occurring in the cell, the hydroxyl radical ($OH^{\cdot}$) being the most reactive ROS.[2] The oxidation reactions induced by $OH^{\cdot}$ alter the chemical properties of the phospholipids and their role within the cell membranes. This is thought to be the cause of several pathological conditions such as atherosclerosis, Alzheimer's disease, Parkinson's disease, cataracts, diabetes, and other age-related diseases.[2–4] On the other hand, some of the oxidized phosphatidylcholines have been found to possess biological activity similar to platelet-activating factor (PAF).[4,5]

The oxidation reaction of the unsaturated chains of a fatty acid of GPC phospholipids is a process initiated by radicals, mainly $OH^{\cdot}$, initiating a radical cascade reaction that, due to the production of consecutive radical species, propagates the peroxidation reaction. So far it is known that, during the GPC peroxidation reaction, several products can be formed such as: (a) oxidized intact GPC, by the insertion of oxygen atoms,[6–9] (b) oxidized short-chain GPC products formed through a β-cleavage mechanism,[10–12] (c) ester hydrolysis releasing the free fatty acids that were originally at the *sn*-1 or *sn*-2 positions of the phospholipids,[13,14] and (d) intermediate free radicals that in turn will be responsible for the propagation step.[15]

Radicals are unstable species with very short lifetimes, and are difficult to detect and identify. Addition of a spin trap confers chemical stability due to the formation of stable radical spin adducts, allowing identification and characterization of the radical. The radical adducts of lipids are usually examined by electron spin resonance (ESR) spectroscopy; however, the ESR spectra give little structural information[16–20] and only one publication has reported the identification of spin-trap adducts of intact phospholipids using ESR spectroscopy.[21] More recently, mass spectrometry has been used for the identification of spin-trap adducts of oxidation products of radical-derived reactions,[20,22] and in particular was applied to the characterization of the spin-trap adducts of α-[4-pyridyl 1-oxide]-N-*tert*-butyl nitrone (POBN)[20,23–25] and 5,5-dimethyl-1-pyrrolidine-*N*-oxide (DMPO)[26] with radicals formed during oxidation of unsaturated fatty acids. This approach allowed the identification of alkoxyl, peroxyl and epoxy radical species, enabling proposals of probable locations for the radical site along the fatty chain.[26] However, to our knowledge, identification of glycerophospholipid radicals using spin trapping and analysis by mass spectrometry have not yet been performed.

*Correspondence to: M. R. M. Domingues, Department of Chemistry, University of Aveiro, 3810-193 Aveiro, Portugal.
E-mail: mrd@dq.ua.pt
Contract/grant sponsor: Foundation for Science and Technology; contract/grant number: POCTI 33279/99.
Contract/grant sponsor: III Quadro Comunitário de Apoio; contract/grant number: SFRH/BD/10358/2002.

RCM

In this study we will present and discuss the results obtained from oxidation of glycerophospholipid (16:0/18:1) by the Fenton reaction in the presence of DMPO, monitored by ES-MS. The use of the spin-trap DMPO allowed the identification of radical products. Electrospray ionization with tandem mass spectrometry (ES-MS/MS) was used for the characterization of glycerophospholipid radical spin-trap adducts.

EXPERIMENTAL

Chemicals

Glycerophosphocholine (GPC 16:0/18:1) and 5,5-dimethyl-1-pyrrolidine *N*-oxide (DMPO) were obtained from Sigma (St. Louis, USA) and used without further purification. Iron(II) chloride ($FeCl_2$) and hydrogen peroxide (H_2O_2) used for the peroxidation reaction were purchased from Merck (Darmstadt, Germany).

Preparation of GPC vesicles

Vesicles were prepared from stock solutions (1 mg/mL) dried under a nitrogen stream; ammonium bicarbonate buffer solution (pH 7.4) was added to a final phospholipid concentration of 50 mM, and the mixture was vortexed.[7]

Oxidation of GPC vesicles by Fenton reaction

Oxidative treatments of the GPC were performed by addition of 5 mmol $FeCl_2$ solution and 50 mmol H_2O_2 to 50 μL of phospholipid vesicles in 0.5 mL of solution. This mixture was left to react at 37°C for different periods of time with occasional sonication. Spin-trapping experiments were performed by adding, after different periods of time, 1 μL (9 mmol) of DMPO to the reaction mixture. The control was prepared by replacing the H_2O_2 volume by water. The phospholipid oxidation products and the spin-trap adducts were extracted using a modification of the method of Folch *et al*. with chloroform/methanol (2:1, v/v).[27]

ES-MS

Positive ion mode ES mass spectra and tandem mass spectra were acquired using a Q-TOF2 instrument (Micromass, Manchester, UK) using a MassLynx software system (version 4.0). The samples for ES analyses were prepared by diluting 1 μL of the sample in 1000 μL of chloroform/methanol solution (1:1, v/v). Samples were introduced into the mass spectrometer at a flow rate of 10 μL/min, setting the needle voltage at 3000 V with the ion source at 80°C and cone voltage at 35 V. Tandem mass spectra (MS/MS) of molecular ions were obtained by collision-induced decomposition (CID), using argon as the collision gas (measured pressure on the Penning gauge ~6 h 10^{-6} mbar) and varying the collision energy between 15–35 eV. In MS and MS/MS experiments the TOF resolution was set to approximately 9000 (based on FWHM).

RESULTS AND DISCUSSION

Identification of DMPO radical adducts

The formation of radical glycerophospholipid (GPC 16:0/18:1) products by the hydroxyl radical (under Fenton reaction conditions) was studied by the addition of the spin trap

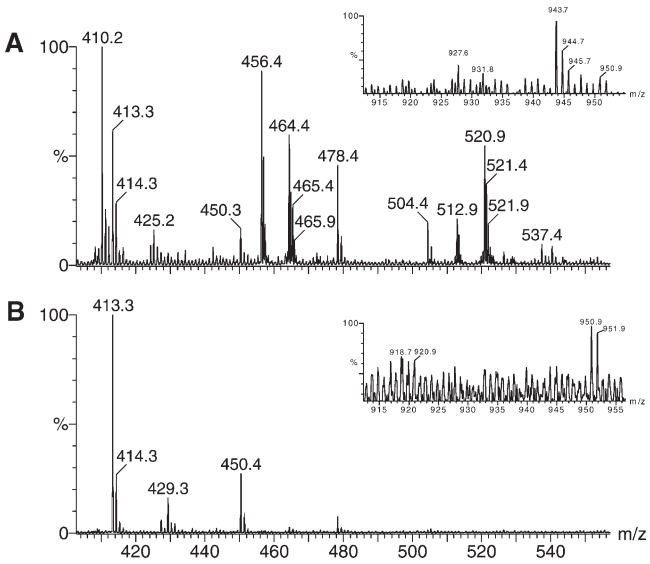

Figure 1. ES-MS spectra obtained for the GPC 16:0/18:1 in the presence of DMPO (A) under oxidative conditions and (B) under non-oxidative conditions.

(DMPO) to the reaction mixture. The ESI-MS spectra of GPC obtained in the presence of DMPO (A) under oxidative ($GPC+Fe^{2+}+DMPO+H_2O_2$) and (B) non-oxidative conditions ($GPC+Fe^{2+}+DMPO$) are shown in Fig. 1. By comparison of the MS spectra obtained, new ions were identified (Fig. 1(A)), and some of these corresponded to the DMPO adducts of radical species formed during GPC oxidation. These adducts were observed at both higher and lower *m/z* values when compared with the ES-MS spectrum of the native phospholipid ($[M+Na]^+$ at *m/z* 782), with the structure shown in Scheme 1.

Adducts observed with low *m/z* in the ES-MS spectrum (Fig. 1(A)), at *m/z* 410, 412, 426 and 442, can be attributed to $[M+H]^+$ ions of spin-trap adducts of oxidized species, while ions at *m/z* 432 and 434 can be attributed to the sodium adduct analogues $[M+Na]^+$ of the $[M+H]^+$ ions at *m/z* 410 and 412, respectively. These ions are assigned as DMPO adducts of radical species arising from oleic acid oxidation, shown in Scheme 2. The release of free fatty acids is known to occur by ester hydrolysis during phospholipid oxidation,[11,13] to form the unsaturated fatty acid chains present at *sn*-1 and/or *sn*-2 positions of the GPC and their oxidized forms with the addition of oxygen atoms.[13] The structures represented in Scheme 2 are similar to the structures proposed for the DMPO adducts of radical species formed during linoleic acid oxidation, monitored by ES-MS.[26] These include alkoxyl (or hydroxy-alkyl) radical adducts (DMPO/LO·), and peroxyl

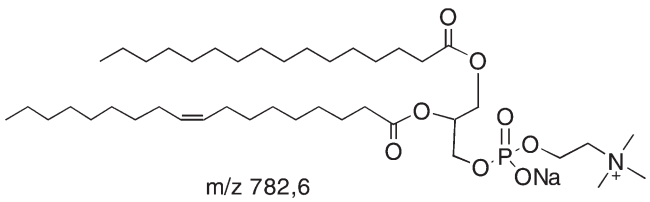

Scheme 1. Structure of the 2-oleoyl-1-palmitoyl-*sn*-glycero-3-phosphocholine (GPC).

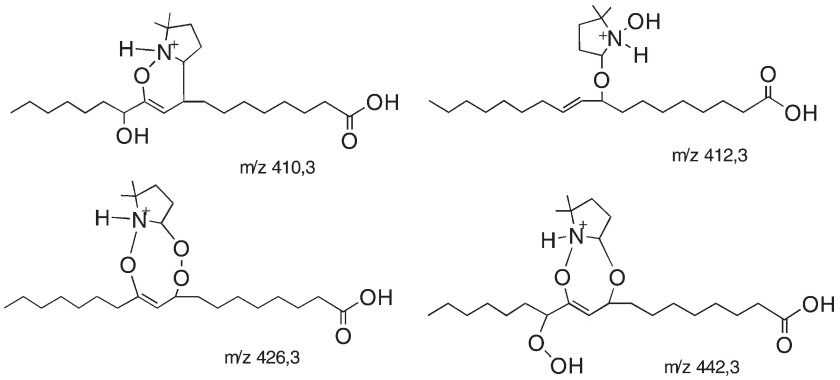

Scheme 2. Proposed structures for the DMPO adducts of radical species of free fatty acids from oxidation of GPC 16:0/18:1, observed at *m/z* 410, 412, 426 and 442.

(or hydroxy-alkoxyl) radical adducts (DMPO/LOO·). The observed adducts are even-electron species, although some are attributed to cyclic radical adducts (at *m/z* 410, 426 and 442). No DMPO adducts derived from the *sn*-1 fatty acid were observed, since saturated fatty acid chains are not susceptible to the peroxidation reaction.

It is known that, in the presence of reactive oxygen species (ROS) such as the hydroxyl radical formed by the Fenton reaction, unsaturated fatty acids can undergo the removal of the allylic hydrogen, leaving an unpaired electron and generating a carbon-centered radical. In oleic acid (present in the studied GPC), the allylic hydrogens are at C_8 and C_{11}, so radical sites can be placed at either C_8 or C_{11}, or even at C_9 and C_{10}, due to double-bond migration. Both carbon radical species may capture the spin trap to form the carbon-centered adducts, or they can take up an oxygen molecule to form an alkyl-peroxyl radical. The alkyl-peroxyl radical may react with DMPO to form adducts, or may capture a hydrogen atom by abstraction from another oleic acid molecule to generate a hydroperoxide. However, these species may also decompose to an alkoxyl radical, which in turn may either be stabilized by hydrogen abstraction to form a hydroxy group, or by capture of a DMPO molecule to form the alkoxyl DMPO adduct.[26]

In Scheme 2, the proposed adduct structures considered the addition of DMPO at C_9. Although on the basis of the MS/MS results the most probable location of the spin-trap bond was found to be at C_8 or C_9, other isomers of DMPO adducts, with radical located at C_{10} or C_{11}, can be formed, as reported above. In the MS/MS experiments, since there was no previous chromatographic separation, all the isomers were selected as precursor ions so different fragmentation pathways derived from different isomers are overlapped. The contributions of these possible locations of the spin site will be considered, and some evidence related to this will be given below.

Other new ions observed in the low mass range of the mass spectrum at *m/z* 478 and 504 are not DMPO adducts, although they do correspond to GPC oxidation products. These ions were attributed to lyso-phosphatidylcholine species and are known to be formed during oxidation of phospholipids[11,13] by release of the *sn*-1 and *sn*-2 fatty acids. Their identification was supported by comparison of ES-MS spectra of GPC obtained under oxidative (GPC+Fe^{2+}+H_2O_2) and non-oxidative conditions (GPC+Fe^{2+}) in the absence of DMPO (data not shown).

In the higher *m/z* range the ions observed at *m/z* 927 and 943 correspond to singly charged ions of the DMPO adducts of oxidized intact GPC species containing two and three oxygen atoms, respectively. The structures proposed for these DMPO adducts are shown in Scheme 3. Oxidized intact GPC containing one oxygen atom (*m/z* 911) is not observed as a singly charged ion, but it is observed as a doubly charged ion.

In the lower *m/z* range, ions observed at *m/z* 456.4, 464.4, 512.9 and 520.9 correspond to doubly charged ions of DMPO adducts of intact GPC radicals, and the proposed structures (as carbon- or oxygen-centered) are represented in Scheme 4. In these doubly charged ions, one charge arising from a sodium ion Na^+ could be located either at the polar head of the GPC, as shown in Scheme 3, or at the DMPO moiety. These adducts have structures similar to those proposed for the singly charged ions at *m/z* 927.6 and 943.7. The ion at *m/z* 456.4 corresponds to the DMPO adduct of oxidized GPC with one oxygen atom, while the ion at *m/z* 464.4 corresponds to the DMPO adduct of GPC with two oxygen atoms. Other doubly charged ions observed at *m/z* 512.9 and 520.9 were attributed to the DMPO adducts of GPC radicals oxidized with one and two oxygen atoms, respectively, but with two DMPO molecules. In this case only one of the DMPO molecules is charged. No triply charged species were observed.

Other ions observed at *m/z* 130, 146, 211, 243 and 257 in the mass spectra of the reaction products obtained under oxidative conditions (data not shown) have already been identified as DMPO oxidation species,[22] while ions at *m/z* 197, 341, 371, 425 and 438 were observed in a control reaction of DMPO, H_2O_2 and Fe(II) in bicarbonate buffer, so they are not spin adducts of GPC species (data not shown).[28]

In order to clarify the structure of the DMPO adducts of the radicals resulting from the GPC peroxidation reaction and identified in the ES mass spectrum, collision induced decomposition (ES-MS/MS) experiments were performed.

MS/MS of adducts of GPC oxidation products with DMPO

The mass spectrometric fragmentation pathway of glycerophosphatidylcholines (GPC) has been extensively studied

RCM

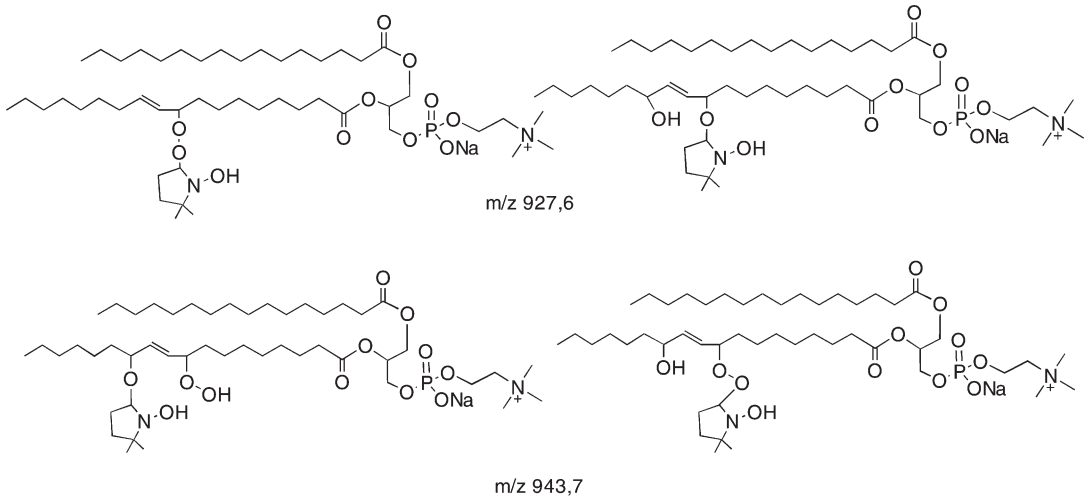

Scheme 3. Proposed structures for the singly charged DMPO adducts of intact GPC radicals at *m/z* 927.6 and 943.7.

by FAB-MS/MS,[29] by ES-MS/MS[30–34] and by MALDI-PSD.[35] These studies allowed the identification of typical fragmentations of sodiated GPC molecules such as loss of $N(CH_3)_3$ (59 Da), of $HPO_4(CH_2)_2N(CH_3)_3$ (183 Da), of $NaPO_4(CH_2)_2N(CH_3)_3$ (205 Da), and loss of the fatty acids at *sn*-1 and *sn*-2; all of these losses are fingerprints for the identification of the GPC structural units. Moreover, previous studies obtained by ES-MS/MS of DMPO adducts with oxidation products of linoleic acid revealed characteristic fragmentation pathways.[26] These characteristic fingerprint fragments, such as the presence of ions due to the loss of the DMPO or to the loss of the oxidized DMPO (DMPO–OH or DMPO–OOH), the ions $[DMPO–OH+H]^+$ and $[DMPO–OOH+H]^+$, , and the preferential cleavage of C–C bonds (α or β) in the

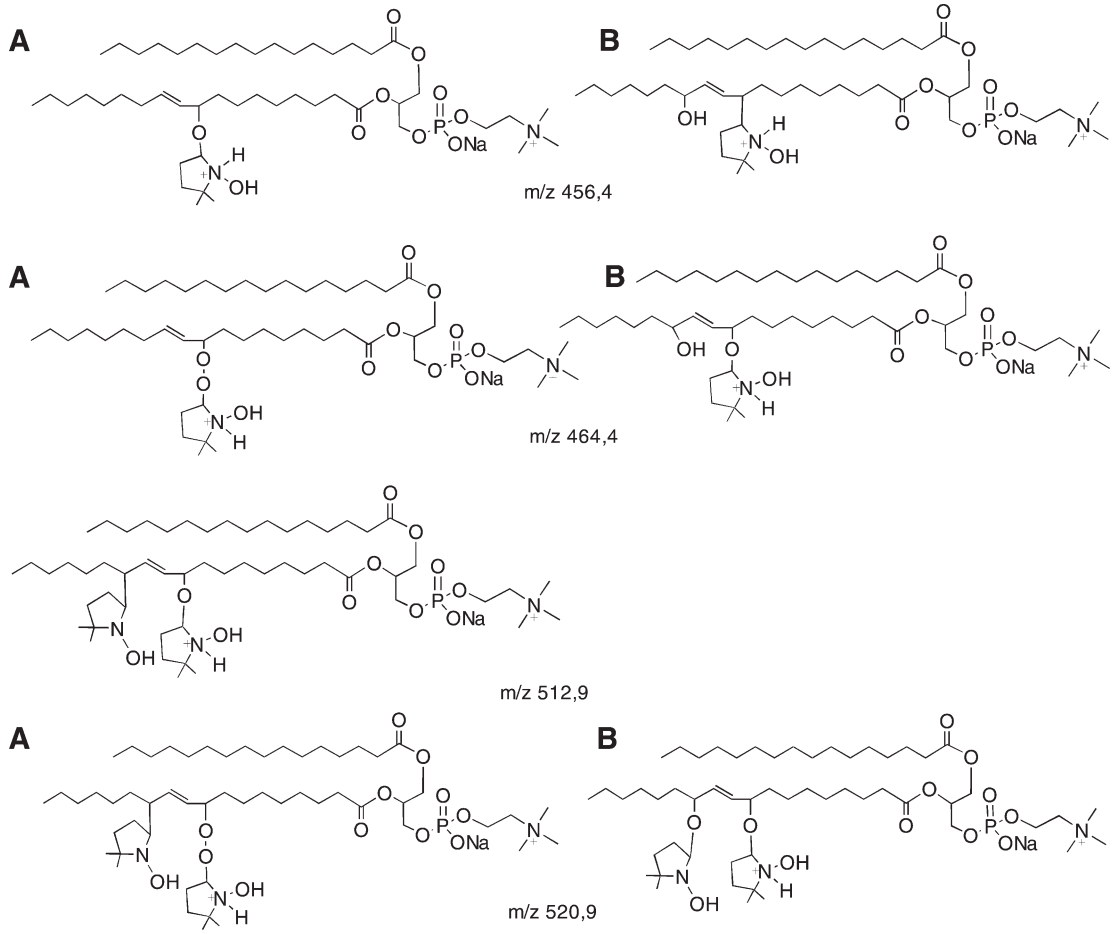

Scheme 4. Proposed structures for the doubly charged DMPO adducts of intact GPC radicals.

Table 1. Main fragment ions observed in the ES-MS/MS spectra of the short-chain DMPO adducts at *m/z* 410, 412, 426, and 442 (intensities normalized to the base peak)

Precursor (*m*/*z*)	410	412	426	442
$[DMPO+H]^+$	114 (<5)	114 (<5)	114 (<5)	114 (<5)
–DMPO (–113 Da)	297 (100)	299 (100)	313 (95)	329 (80)
–DMPO–OH (–129 Da)	—	—	297 (30)	313 (20)
–DMPO–OOH (–145 Da)	—	—	281 (20)	297 (25)

vicinity of the carbon linked to the spin, allowed confirmation of the presence of DMPO adducts and also a possible location for the spin.[26]

Fragmentation pattern of adducts of oxidized free fatty acids

The MS/MS spectra of ions at *m/z* 410, 412, 426 and 442, identified as $[M+H]^+$ ions of DMPO spin-trap adducts of oxidized oleic acid (Scheme 2), show typical fragmentations allowing their identification as DMPO adducts, namely the loss of DMPO (113 Da) from the precursor ion (the base peak of the spectra), similar to what was reported for DMPO adducts of oxidized linoleic acid,[26] and the fragment ion at *m/z* 114 corresponding to $[DMPO+H]^+$. The MS/MS spectra of the ions at *m/z* 432 and 434, the $[M+Na]^+$ versions of the $[M+H]^+$ ions at *m/z* 410 and 412, contain the fragment ion at *m/z* 136 corresponding to $[DMPO+Na]^+$. Table 1 summarizes the main fragment ions observed in these ES-MS/MS spectra.

The MS/MS spectra of the precursor ions at *m/z* 410 and 412 do not show a fragment at *m/z* 130 $[DMPO–OH+H]^+$, or an ion due to loss of DMPO–OH neutral (indicative of the presence of an alkoxyl radical adduct), suggesting the absence of (or a very minor contribution from) the alkoxyl radical, thus supporting the proposed structure of these adducts as an alkyl radical adduct with an additional

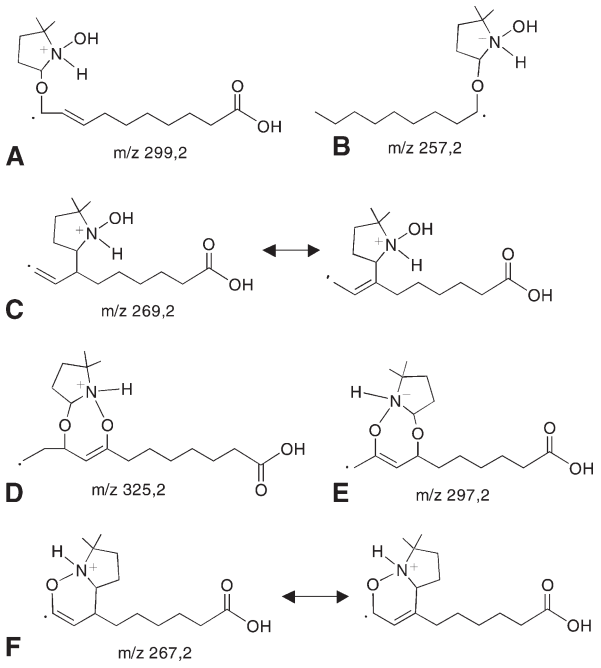

Scheme 5. Proposed structures for some fragment ions formed by homolytic cleavage in the vicinity of the carbon where the DMPO is linked, for the adducts at *m/z* 412 (structures A, B, C) and 410 (structures A, B, C).

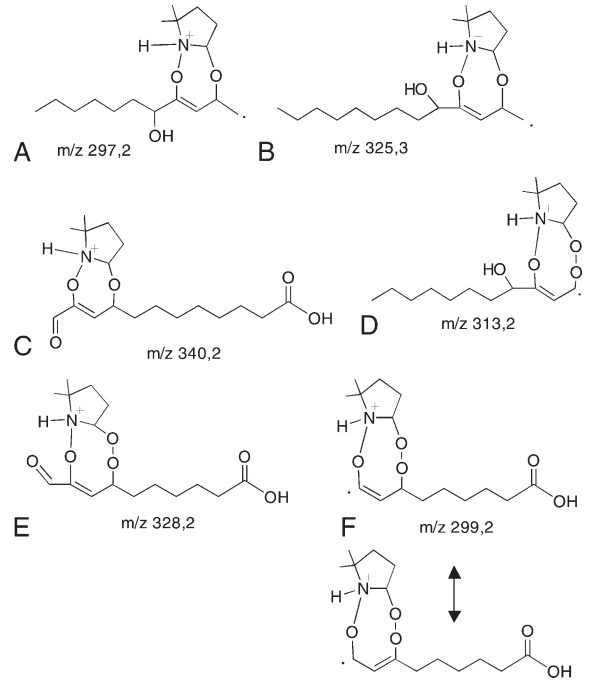

Scheme 6. Proposed structures for some fragment ions formed by cleavage in the vicinity of the carbon where the DMPO is linked for the adducts at *m/z* 426 (structures A, B, C) and at *m/z* 442 (structures D, E and F).

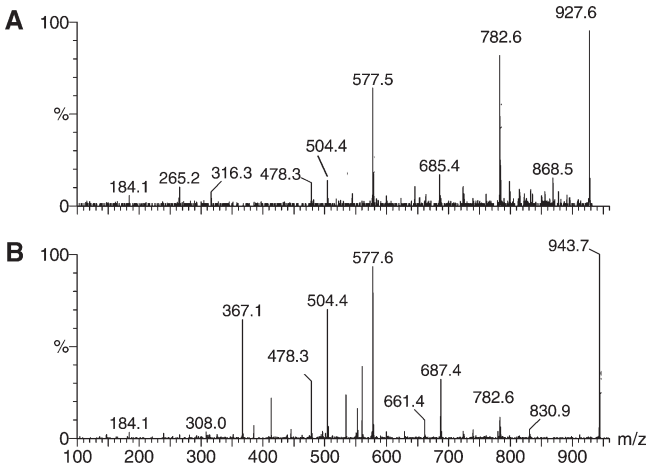

Figure 2. ES-MS/MS spectra obtained for (A) the ion at *m/z* 927.6 and (B) the ion at *m/z* 943.7.

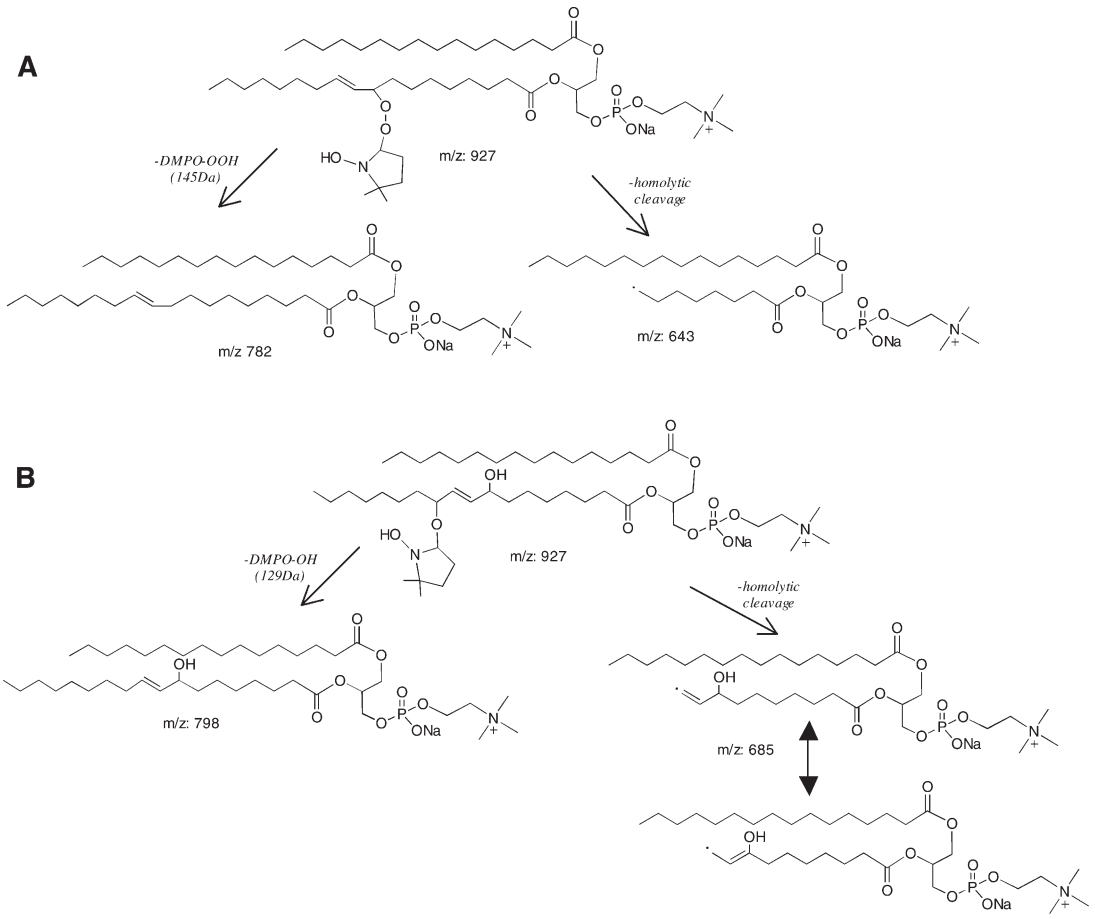

Scheme 7. Fragmentation pathways identified for the ion at *m/z* 927.7.

hydroxy group, in which the DMPO is linked to the carbon-centered radical (Scheme 2, structure A), similar to that described for linoleic acid DMPO adducts.[26] Fragment ions formed by cleavage in the vicinity of the carbon where the DMPO is linked, as represented in Scheme 5, suggests the presence of either hydroxy-alkyl (C and F) or alkoxyl radical structures for these adducts (A, B, D and E). The identification of the carbon-centered radical adducts using DMPO spin trap by MS has recently been reported,[26,28] despite the fact that DMPO is commonly assumed to be suitable for the detection and identification of oxygen-centered radical adducts.[36]

The MS/MS spectrum of the ion at *m/z* 426, attributed to the cyclic derivative of the peroxyl radical, exhibited fragment ions at *m/z* 313 (−113 Da), 297 (−129 Da, i.e., DMPO–OH) and 281 (−145 Da, i.e. DMPO–OOH), suggesting the presence of the alkoxyl and/or peroxyl radical adducts. Loss of O_2 leading to the fragment ion at *m/z* 394 suggested the presence of a hydroperoxide. The fragments that originated from homolytic cleavages in the vicinity where the DMPO is linked are represented in Scheme 6, suggesting the presence of both hydroxy-alkoxyl adducts (structures A, B, and C) and peroxyl adducts (structures D and E). The MS/MS spectrum of the ion at *m/z* 442, attributed to the cyclic radical adduct of the hydroxy-peroxyl derivative, exhibited fragmentation behavior similar to that of the ion at *m/z* 426. The fragment ions at *m/z* 329 (−113 Da), 313 (−129 Da), 297 (−145 Da) and 410 (−32 Da, i.e., O_2) were observed. Other ions observed at *m/z* 299 (structure F), 313 (structure D) and 328 (structure E) suggest the presence of the hydroxy-peroxyl adduct, while the presence of a hydroperoxide-alkoxyl adduct cannot be excluded.

Adducts of oxidized intact GPC

The fragmentation patterns of the singly charged ions of DMPO adducts of oxidized GPC at *m/z* 927 and 943 were also studied. The MS/MS spectra are shown in Figs. 2(A) and 2(B), respectively.

The presence of fragments resulting from loss of DMPO (113 Da), and loss of oxidized DMPO, i.e., DMPO–OH (129 Da) and DMPO–OOH (145 Da), is indicative of the presence of oxygen-centered DMPO adducts. These adducts can have contributions from alkoxyl and/or peroxyl radicals. The loss of O_2 from the precursor ions (*m/z* 927 and 943), leading to the fragment ions at *m/z* 895 and 911, respectively, indicates the presence of the hydroperoxide derivative for both adducts. This fragment, in the case of the adduct at *m/z* 943 (Fig. 2(B)), may in turn undergo loss of 129 Da (DMPO–OH), leading to the fragment at *m/z* 782, suggesting the presence of the alkoxyl radical with a hydroperoxide group in the chain. This identification may be corroborated by the presence of the fragment at *m/z* 152 corresponding to $[DMPO–OH+Na]^+$. In previous results obtained by EPR spectroscopy during glycerophosphocholine peroxidation,[21] the authors were not able to identify oxygen-centered radicals, although they

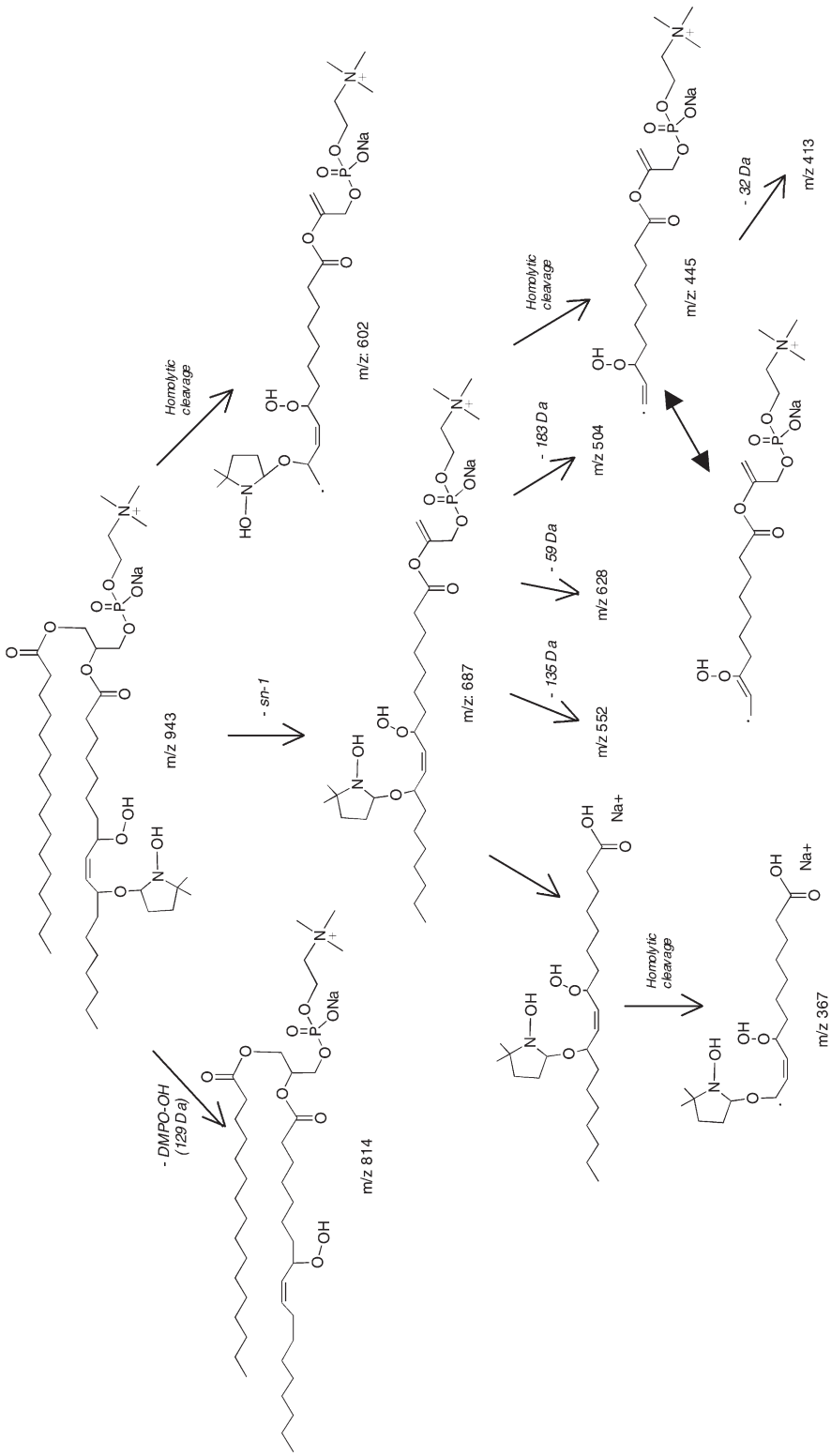

Scheme 8. Fragmentation pathways identified for the ion at *m/z* 943.7.

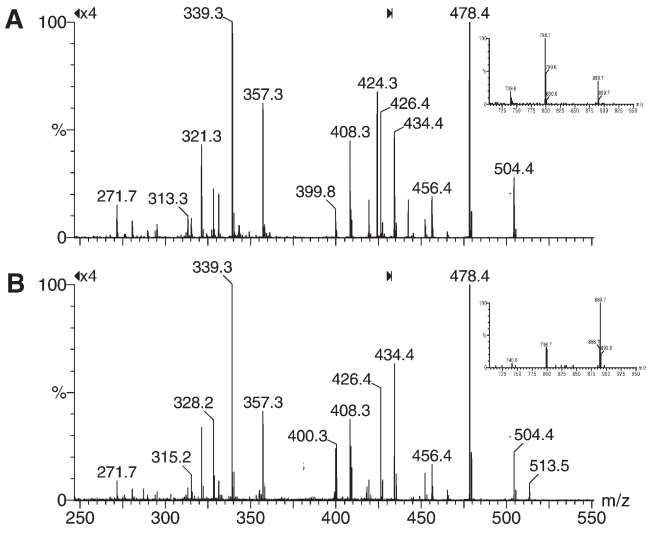

Figure 3. ES-MS/MS spectra of doubly charged ions of the adducts of oxidized GPC with one DMPO at *m/z* 456.4 (A) and with two DMPO molecules at *m/z* 512.9 (B).

were expected to occur. The presence of the alkoxyl radical is a by-product of the lipid peroxidation reaction through the homolytic cleavage of hydroperoxides.[15] The ion at *m/z* 782, corresponding to the $[M+Na]^+$ ion of the native GPC, observed in both MS/MS spectra (*m/z* 927 and 943), may undergo further losses characteristic of GPC species leading to the fragment ions at *m/z* 723, 599, 577, 526 (loss of the *sn*-1 substituent as free acid), 504 (loss of the *sn*-1 substituent as the sodium salt), 500 (loss of the *sn*-2 substituent as the free acid), and 478 (loss of the *sn*-2 substituent as the sodium salt); all of these are observed in the MS/MS spectra. The fragment ions observed in the MS/MS spectra at *m/z* 643 (Scheme 7(A)) and 685 (Scheme 7(B)), with low relative abundance, may be formed by homolytic cleavages in the vicinity of the C–C bond where the spin trap is located (α bond), allowing proposal of the position of the hydroxy group at C_8 and the spin at C_{11}.

In the MS/MS spectrum of the ion at *m/z* 943 (Fig. 2(B)), apart from the fragment ions due to characteristic losses from the precursor ion, some fragments are indicative of the radical species present and also about the location of the spin. The presence of the fragment ion at *m/z* 911 ($-O_2$) combined with the fragment ion at *m/z* 782 (loss of DMPO–OH) suggests the contribution of a hydroperoxide-alkoxyl radical. This identification is corroborated by the presence of the fragment ions at *m/z* 602, 445 and 367 formed by homolytic cleavage of the bonds adjacent to the spin trap (Scheme 8), which place the alkoxyl radical at C_{11} of the oleic acid and the hydroperoxide group at C_8. The fragment ion at *m/z* 445 may undergo loss of O_2 to give the fragment ion at *m/z* 413. On the other hand, a minor contribution from the hydroxy-peroxyl DMPO adduct can also occur, suggested by the presence of the fragment ion at *m/z* 798 (loss of DMPO–OOH), the fragment ion at *m/z* 857 arising from cleavage of the C_{12}–C_{13} bond through a 1,4-hydrogen elimination mechanism involving a hydroxy group placed at C_{12}, and by the fragment ion at *m/z* 532 formed by homolytic cleavage of the C_8–C_9 bond indicating the presence of the peroxyl derivative at C_9. Altogether, these fragmentations suggest that isomeric structures may be contributing to the ion at *m/z* 943.

The MS/MS spectra of the doubly charged ions at *m/z* 456.4 and 512.9, attributed to the adducts of the GPC radicals with one and two DMPO molecules, respectively, are shown in Fig. 3. The fragmentation of doubly charged ions may occur through loss of neutral fragments leaving a doubly charged fragment or by loss of charged fragments yielding two singly charged fragments. The fragment ions observed in the MS/MS spectra of the doubly charged ions (Fig. 3) are due to characteristic losses of GPC species and to loss of a DMPO moiety from the precursor ions, that indicate the radical species present in each ion, and also other fragments in low relative abundance that may suggest the location of the radicals within the structure. The MS/MS spectra of doubly charged ions at *m/z* 456.4 (Fig. 3(A)) and 512.9 (Fig. 3(B)) exhibit fragment ions at *m/z* 114 and 136 identified as the $[M+H]^+$ and $[M+Na]^+$ of DMPO (data not shown),[22] along with the fragment ions at *m/z* 147 and 184 that allowed confirmation of these species as DMPO adducts of oxidized GPC. The MS/MS spectra contained fragment ions due to characteristic losses of GPC species from the precursor ion, and characteristic losses as is the case of the doubly charged fragment ion at *m/z* 328 (loss of the *sn*-1 substituent) that, combined with loss of DMPO (113 Da), leads to the doubly charged fragment ion at *m/z* 271.

The MS/MS spectrum of the ion at *m/z* 456.4 (Fig. 3(A)) includes a fragment ion at *m/z* 478 (singly charged) that is formed by loss of the charged fragment of 434 Da. The fragment at *m/z* 434 corresponds to the $[M+Na]^+$ ion of the DMPO adduct of the oxidized oleic acid containing one oxygen atom (shown in Scheme 9) and may be attributed to either the alkoxyl (oxygen-centered) or to the hydroxy-alkyl (carbon-centered) adduct. The absence of ions at *m/z* 130 ($[DMPO–OH+H]^+$) or 152 ($[DMPO–OH+Na]^+$), attributed to oxidized DMPO species, suggested the absence of the oxygen-centered adduct. The fragment ions observed with low relative abundance at *m/z* 424, 321, 283, and 251 (Scheme 9) were the most informative and point to the presence of the carbon-centered radical adduct.

Altogether, the fragment ions identified in the MS/MS spectrum allow proposal of a contribution of the hydroxy-alkyl radical adduct with the hydroxy group placed at C_8 and the carbon-centered radical at C_{11}. However, a minor contribution from the alkoxyl radical could not excluded due to observation of the fragment ion at *m/z* 295 that places the alkoxyl radical at C_8.

The fragmentation pathway of the ion at *m/z* 512.9 (Fig. 3(B)), corresponding to the adduct of oxidized GPC with two DMPO molecules (Scheme 4), is very similar to that indicated by the MS/MS spectrum of the ion at *m/z* 456.4, with high abundance fragments at *m/z* 478, 434 and 339, which have already been identified (Scheme 9). The similarity to the MS/MS spectrum of the ion at *m/z* 456.4 may be rationalized by considering the loss of one of the DMPO molecules as a neutral (113 Da), thus leading to the doubly charged ion at *m/z* 456.4; in fact, this fragment ion is observed in the MS/MS spectrum (Fig. 3(B)). The observation of the fragment ion at *m/z* 152 (data not shown) suggests that the remaining DMPO molecule is linked to an

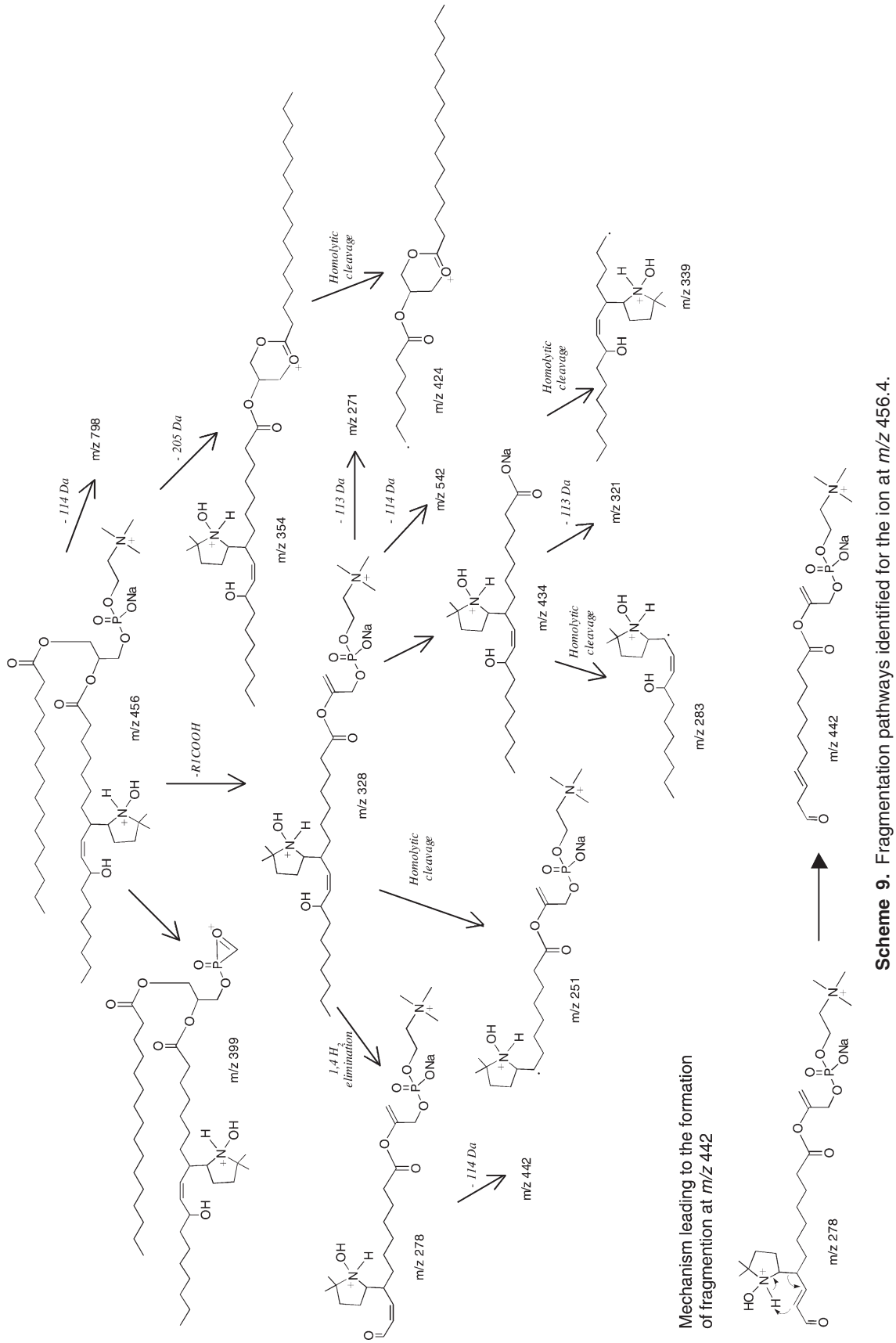

Scheme 9. Fragmentation pathways identified for the ion at *m/z* 456.4.

oxygen atom, indicating the presence of the alkoxyl radical contributing to the ion at *m/z* 512.9. These results support the occurrence of a spin adduct that is simultaneously a carbon- and an oxygen-centered radical species for the ion at *m/z* 512.9.

The MS/MS spectra of the doubly charged ions at *m/z* 464.4 and 520.9, assigned to the adducts of GPC radicals containing two oxygen atoms with one and two DMPO molecules, respectively (Scheme 4), are shown in Fig. 4. The MS/MS spectra of the doubly charged ions (Fig. 4) contain, apart from fragment ions due to characteristic losses from the precursor ion, a singly charged fragment ion at *m/z* 450 formed by loss of a charged moiety of 478 Da, corresponding to the DMPO adduct of oleic acid containing two oxygen atoms that can be attributed to the alkyl-hydroperoxide, to the hydroxy-alkoxyl, or even to the peroxyl derivatives. Also, the fragment ion at *m/z* 136 $[DMPO+Na]^+$, as well as fragment ions formed by homolytic cleavages in the vicinity of the spin trap (α and γ bonds) (Scheme 10), allow the proposal of the location of the radical species within the structure. The fragment ion at *m/z* 292 resulting from cleavage of the double bond placed at C_9–C_{10} indicates the position of the double bond within the structure. The identification of these fragment ions leads to the proposal of the location of an alkyl radical at C_8 and of a hydroperoxide group at C_{11}. The presence of fragment ions at *m/z* 152 $[DMPO–OH + Na]^+$ (data not shown) and at *m/z* 442 (1,4-hydrogen elimination), 365 (homolytic cleavage) and 353 (loss of 129 Da from fragment ion at *m/z* 482) suggest the contribution of the alkoxyl radical with the hydroxy group at C_{11}.

The fragmentation pattern exhibited by the doubly charged ion at *m/z* 520.9 (Fig. 4(B)), assigned to the DMPO adduct of an oxidized form containing two oxygen atoms and one additional DMPO molecule (Scheme 4), is very similar to that discussed above. This result may be rationalized by considering the loss of one uncharged DMPO molecule as a neutral (113 Da, or 129 Da for the oxidized form) leading to the doubly charged fragment ions at *m/z* 464 or 456, both of which are observed in the MS/MS spectrum. Evidence for the contribution of the alkoxyl and alkyl radical species is also provided by the fragments at *m/z* 814 and 798 (inset of Fig. 4(B)) formed through loss of charged fragments with 114 Da $[DMPO+H]^+$ or 130 Da $[DMPO–OH+H]^+$, respectively, from the ion at *m/z* 464, and by the fragment ions at *m/z* 798 and 782 formed by losses of the charged fragments with 114 and 130 Da, respectively, from the ion at *m/z* 456. The occurrence of these fragments indicates the contribution of competitive fragmentation pathways and suggests the presence of both oxygen- and carbon-centered radical adducts.

As shown from the results presented here, the identification of the predominant fragment ions allows proposal of the presence of one, two and three oxygen atoms occurring in phospholipids after they were exposed to oxidation by the hydroxyl radical. However, the fragment ions observed in the MS/MS spectra with low relative abundance are the most informative, as they allow the proposal of the presence of carbon- and oxygen-centered adducts and even to propose the location of the spin trap along the fatty acid carbon chain. The ion observed at *m/z* 464.4, corresponding mainly to the hydroperoxide-alkyl species, is consistent with the identification of radical species containing two DMPO molecules, as they may undergo homolytic scission in the hydroperoxide moiety generating an alkoxyl radical that can form an adduct containing a second DMPO molecule, thus leading to the ion at *m/z* 512.9.

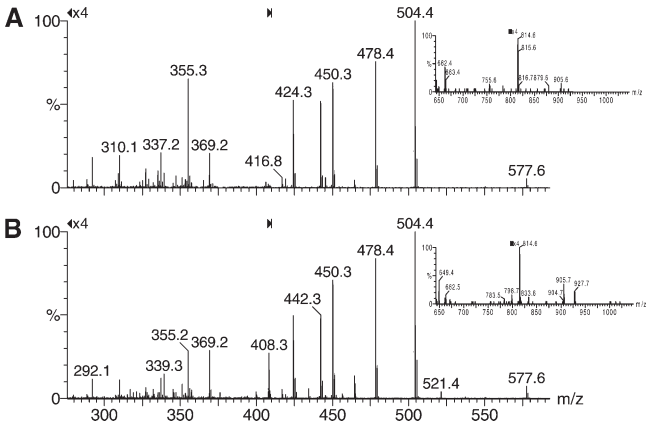

Figure 4. ES-MS/MS spectra of doubly charged ions of the adducts of oxidized GPC with one DMPO at *m/z* 464.4 (A) and with two DMPO molecules at *m/z* 520.9 (B).

CONCLUSIONS

The results obtained by the use of mass spectrometry and tandem mass spectrometry for the identification of radical-derived products of phospholipids oxidized through the Fenton system show the presence of several products formed. Among the products thus formed, adducts of oxidized free fatty acids and of oxidized intact GPC were identified. The intact GPC oxidation products identified, observed as singly and doubly charged ions, were characterized as adducts of carbon- and oxygen-centered phospholipid radical species (hydroxy-alkyl, alkoxyl, hydroxy-alkoxyl, hydroperoxide-alkoxyl and peroxyl), while the adducts of radicals from free fatty acids were also characterized as carbon- and oxygen-centered (alkyl, alkoxyl and peroxyl). The fragment ions present with low relative abundance were the most informative, as they allowed proposal of the location of the spin trap along the fatty acid carbon chain, namely, the occurrence of the alkoxyl DMPO adduct at C_{11} (singly charged) with the hydroperoxide at C_9, and also the presence of the alkoxyl DMPO adduct at C_9 (doubly charged). The identification of radical adducts containing two DMPO molecules is novel, and their characterization made it possible to identify the species that are DMPO adducts of radicals that are simultaneously carbon- and oxygen-centered. The observation of different radicals from the same molecule, due to abstraction of different allylic hydrogens, suggests the possibility that intramolecular radical reactions could occur as the termination step of oxidation. This subject is currently under study. The identification of these compounds suggests the formation of a large number of phospholipid structures that may be responsible for the disruption of the ordered membrane during the peroxidation process of glycerophosphocholine lipids.

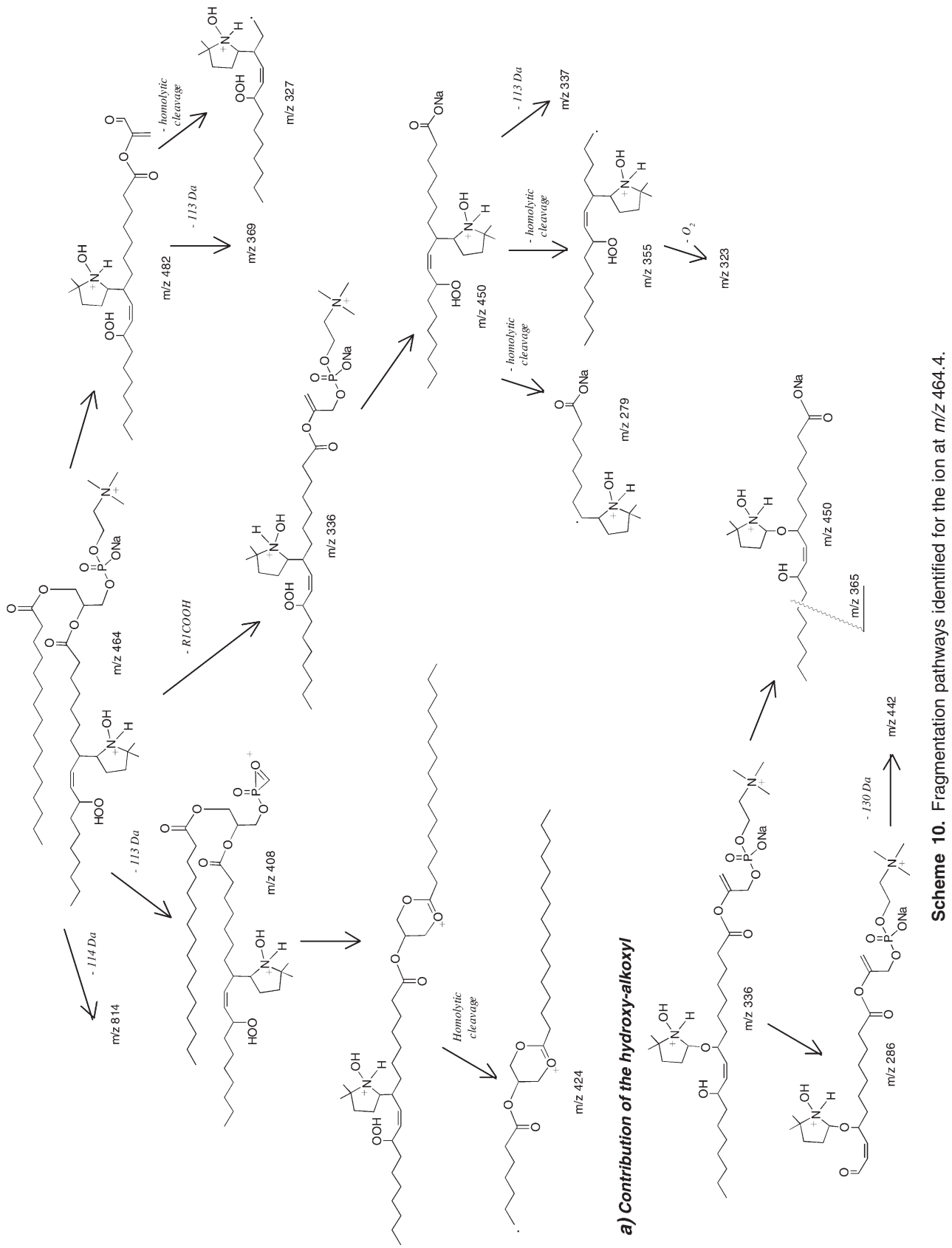

Scheme 10. Fragmentation pathways identified for the ion at *m/z* 464.4.

Acknowledgements

The authors gratefully acknowledge the financial support provided by the project POCTI 33279/99, and the PhD grant to Ana Reis (SFRH/BD/10358/2002), provided by the Foundation for Science and Technology (FCT) and FSE (III Quadro Comunitário de Apoio).

REFERENCES

1. Silvius JR. In *Phospholipid Handbook*, Gregor C (ed). Marcel Dekker: New York, 1993; 1–22.
2. Pincemail J. Free radicals and antioxidants in human diseases. In *Analysis of Free Radicals in Biological Systems*, Favier A, Cadet J, Kalyanaraman B, Fontecave M, Pierre JL (eds). Springer Verlag: Berlin, 1995; 83–98.
3. Jackson MJ. *Free Radicals in the Pathogeneses of Tissue Damage in Calcium, Oxygen Radical and cellular Damage*, Society for Experimental Biology Seminar Series, vol. 46, Duncan CJ (ed). Cambridge University Press: Cambridge, 1991; 11–16.
4. McIntyre TM, Zimmerman GA, Prescott SM. *J. Biol. Chem*. 1999; **274**: 25189.
5. Marathe GK, Harrison KA, Murphy RC, Prescott SM, Zimmerman GA, McIntyre TM. *Free Rad. Biol. Med*. 2000; **28**: 1762.
6. Facino RM, Carini M, Aldini G, Colombo L. *Rapid Commun. Mass Spectrom*. 1996; **10**: 1148.
7. Spickett CM, Pitt AR, Brown AJ. *Free Rad. Biol. Med*. 1998; **25**: 613.
8. Jerlich A, Pitt AR, Schaur RJ, Spickett CM. *Free Rad. Biol. Med*. 2000; **28**: 673.
9. Spickett CM, Rennie N, Winter H, Zambonin L, Landi L, Jerlich A, Schaur RJ, Pitt AR. *Biochem. J*. 2001; **355**: 449.
10. Itabe H, Yamamoto H, Suzuki M, Kawai Y, Nakagwa Y, Suzuki A, Imanaka T, Takano T. *J. Biol. Chem*. 1996; **271**: 33208.
11. Watson AD, Leitinger N, Navab M, Faull KF, Hörkkö S, Witztum JL, Palinski W, Schwenke D, Salomon RG, Sha W, Subbanagounder G, Fogelman AM, Berliner JA. *J. Biol. Chem*. 1997; **272**: 13597.
12. Tokumura A, Sumida T, Toujima M, Kogure K, Fukuzawa K, Takahashi Y, Yamamoto S. *J. Lipid. Res*. 2000; **41**: 953.
13. Khaselev N, Murphy RC. *Free Rad. Biol. Med*. 2000; **29**: 620.
14. Khaselev N, Murphy RC. *J. Lipid Res*. 2000; **41**: 564.
15. Liochev SI. The Mechanism of Fenton-like reactions and their importance for Biological Systems. A Biologist's View. In *Metal Ions in Biological Systems*, vol. 36, Sigel A, Sigel H (eds). Marcel Dekker: New York, 1999; 1–40.
16. Rota C, Barr DP, Martin MV, Guengerich FP, Tomasi A, Mason RP. *Biochem. J*. 1997; **328**: 565.
17. Qian SY, Wang HP, Schafer FQ, Buettner GR. *Free Rad. Cell Med*. 2000; **29**, 568.
18. Iwahashi H. *J. Chromatogr*. 2000; **904**: 197.
19. Dikalov SI, Mason RP. *Free Rad. Biol. Med*. 2001; **30**: 187.
20. Qian SY, Tomer KB, Yue G, Guo Q, Kadiisha MB, Mason RP. *Free Rad. Biol. Med*. 2002; **33**: 998.
21. Yoshida T, Otake H, Aramaki Y, Hara T, Tsuchiya S, Hamada A, Utsumi H. *Biol. Pharm. Bull*. 1996; **19**: 779.
22. Domingues P, Domingues MRM, Amado FML, Ferrer-Correia AJ. *J. Am. Soc. Mass Spectrom*. 2001; **12**: 1241.
23. Iwahashi H, Nishizaki K, Takagi I. *Biochem. J*. 2002; **361**: 57.
24. Qian SY, Yue G, Tomer KB, Mason RP. *Free Rad. Biol. Med*. 2003; **34**: 1017.
25. Qian SY, Guo Q, Mason RP. *Free Rad. Biol. Med*. 2003; **35**: 33.
26. Reis A, Domingues MRM, Amado FML, Ferrer-Correia AJ, Domingues P. *J. Am. Soc. Mass Spectrom*. 2003; **14**: 1250.
27. Folch J, Lees M, Stanley GHS. *J. Biol. Chem*. 1957; **226**: 497.
28. Domingues MRM, Domingues P, Reis A, Fonseca C, Amado FML, Ferrer-Correia AJ. *J. Am. Soc. Mass Spectrom*. 2003; **14**: 406.
29. Domingues P, Domingues MRM, Amado FML, Ferrer-Correia AJ. *Rapid Commun. Mass Spectrom*. 2001; **15**: 799.
30. Han X, Gross RW. *J. Am. Soc. Mass Spectrom*. 1995; **6**: 1202.
31. Larsen A, Uran S, Jacobsen PB, Skotland T. *Rapid Commun. Mass Spectrom*. 2001; **15**: 2393.
32. Pelizzi N, Catinella S, Barboso S, Zanol M. *Rapid Commun. Mass Spectrom*. 2002; **16**: 2215.
33. Ho Y-P, Huang P-C. *Rapid Commun. Mass Spectrom*. 2002; **16**: 1582.
34. Hsu F-F, Turk J. *J. Am. Soc. Mass Spectrom*. 2003; **14**: 352.
35. Al-Saad KA, Siems WF, Hill HH, Zabrouskov V, Knowles NR. *J. Am. Soc. Mass Spectrom*. 2003; **14**: 373.
36. Spin trapping Free Radicals. In *Free Radicals, Biology and Detection by Spin Trapping*, Rosen GM, Britigam BE, Halpern HJ, Pou S (eds). Oxford University Press: New York, 1999; 170–186.

Identification of free radicals of glycerophosphatidylcholines containing ω-6 fatty acids using spin trapping coupled with tandem mass spectrometry

A. Reis, P. Domingues, A.J.V. Ferrer-Correia and M. R. M. Domingues*

Department of Chemistry, University of Aveiro, 3810-193 Aveiro, Portugal

* to whom correspondence should be addressed: Maria R. M. Domingues, Department of Chemistry, University of Aveiro, 3810-193 Aveiro, Portugal.

E-mail: mrd@dq.ua.pt, telephone number: + 351-234-370698, fax number: +351-234-370084

Abbreviations

ESI electrospray ionisation; **ESR** electron spin resonance; **HPLC** high performance liquid chromatography; **MS** mass spectrometry; **MS/MS** tandem mass spectrometry; **DMPO** 5,5-dimethyl-1-pyrrolidine-N-oxide; **POBN** α-(4-pyridil-1-oxide)-N-tert-butylnitrone; **PUFA** polyunsaturated fatty acids; **ROS** reactive oxygen species; **GPC** glycerophosphatidylcholines; **POPC** 1-palmitoyl-2-oleoyl-3-glycerophosphatidylcholine; **PLPC** 1-palmitoyl-2-lineloyl-3-glycerophosphatidylcholine; **PAPC** 1-palmitoyl-2-arachidonoyl-3-glycerophosphatidylcholine.

Abstract

Metal-catalysed radical oxidation of diacyl-glycerophosphatidylcholines (GPC) with ω-6 acyl polyunsaturated fatty acids (PAPC-palmitoyl-arachidonoyl and PLPC-palmitoyl-lineloyl) was studied. Free radical oxidation products were trapped by spin trapping with 5,5-dimethyl-1-pyrrolidine-N-oxide (DMPO) and identified by Electrospray Mass Spectrometry (ES-MS). The spin adducts of oxidised GPC containing one and two oxygen atoms and one and two DMPO molecules were observed as doubly charged ions. Structural characterisation by tandem mass spectrometry (MS/MS) of these ions revealed product ions corresponding to loss of the acyl chains (*sn*-1-palmitoyl and *sn*-2-oxidised spin adduct of lineloyl or arachidonoyl), loss of the spin trap (DMPO) and product ions attributed to oxidised *sn*-2 fatty acid spin adduct (lineloyl and arachidonoyl). Product ions formed by homolytic cleavages near the spin trap and also from 1,4 hydrogen elimination cleavages involving the hydroxy group in the *sn*-2 fatty acid spin adduct allowed to infer the nature of the radical. Altogether, the presence of GPC hydroxy-alkyl/DMPO and hydroxy-alkoxyl/DMPO spin adducts was proposed.

Keywords: *Phospholipids; carbon-centred radicals, oxygen-centred radicals, spin trapping; tandem mass spectrometry.*

Introduction

Oxidative damage of biomolecules triggered by free radicals, such as reactive oxygen species (ROS) formed during aerobic metabolism, is associated with the pathogenesis of several age-related diseases and also with atherosclerosis, lung and liver cancer [1], and for this reason much effort has been dedicated to the identification of the structural changes induced by free radicals in lipids, proteins and DNA bases [1]. Free radical species are very reactive species, and due to their very short lives are difficult to detect and analyse [2], and so the work published is mainly focused on the identification of more chemically stable non-radical products of biomolecules [3]. On the other hand, the addition of a nitroso or nitrone compound (spin trap), with formation of spin-adducts, stabilises the free radicals making their detection possible [2]. In fact, this approach has been used for the mass spectrometric identification of carbon and/or oxygen centred radicals of amino acids [4], proteins [5] and lipids [6,7]. Phospholipids, found as major components of cell membranes provide the physical barrier between different organelles and cells, and are also susceptible to free radical attack. Although, the structural changes induced by free radicals to phospholipids with formation of radical and non-radical oxidation products [8-10], are reported to affect the physical properties of membranes [11-13], the identification of phospholipid free radicals is scarce [8,14]. The detection of phospholipid free radicals was initially attempted through ESR with the identification of phosphatidylcholine spin adducts [14], and through the hyperfine coupling constants was proposed to correspond to a carbon centred spin adduct. However, the ESR data does not provide detailed structural information about the substitutents nor the location of the spin trap along the carbon chain of the acyl residues present in the phospholipids. Information about the point of radical location can be proposed based on the tandem mass spectrometry (MS/MS), which is already described for lipid spin adducts [15,16], and recently applied in the identification of DMPO spin adducts of palmitoyl-oleoyl-glycerophosphatidylcholine (POPC), a structurally simple GPC [8]. The results obtained by tandem mass spectrometry also gave information about the hydroxy groups present (or not) in the fatty acid chain, allowing proposing the presence of both carbon and oxygen centred adducts [8].

In the present work, DMPO spin trapped radicals of glycerophosphatidylcholines containing ω-6 lipids at the *sn*-2 residue, namely palmitoyl-lineloyl-glycerophosphatidylcholine (PLPC) and palmitoyl-arachidonoyl-glycerophosphatidylcholine (PAPC), formed by metal-catalysed radical oxidation, were studied by electrospray ionisation mass spectrometry (ES-MS). The ions observed in the

mass spectra were further characterised by tandem mass spectrometry (MS/MS) in order to determine the type of radical formed and their location along the unsaturated fatty acid chain.

Experimental

Chemicals

Glycerophosphocholine (GPC, 16:0/18:2 and 16:0/20:4) and 5,5-dimethyl-1-pyrrolidine-N-oxide (DMPO) were obtained from Sigma (St. Louis, USA) and used without further purification. Iron (II) chloride ($FeCl_2$) and hydrogen peroxide (H_2O_2) used for the peroxidation reaction were purchased from Merck (Darmstadt, Germany).

Preparation of GPC vesicles

Vesicles were prepared from stock solutions, of 1mg/mL dried under nitrogen stream, and ammonium bicarbonate buffer solution (pH 7.4) was added to a final phospholipid concentration of 50mM, and the mixture vortexed.

Oxidation of GPC vesicles by Fenton reaction

Oxidative treatments performed on the GPC were done by addition of 5 mmol $FeCl_2$ solution and 50 mmol H_2O_2 to 50 μL of phospholipid vesicles in 0.5mL of solution. This mixture was left to react at 37°C for different periods of time with occasional sonication. Spin trapping experiments were performed by adding 1 μL (9 mmol) of 5,5-dimethyl-1-pyrroline-N-oxide (DMPO) to the reaction mixture 30-60 min after the reaction was initiated. The control was prepared by replacing H_2O_2 volume by water. The phospholipid oxidation products and the spin adducts were extracted using the Folch method with chloroform:methanol (2:1, v/v) [17].

ES Mass Spectrometry

Positive ion mode ES mass spectra and tandem mass spectra were acquired in a Q-TOF 2 instrument (Micromass, Manchester, UK) using a MassLynx software system (version 4.0, Micromass, Manchester, UK). The samples for electrospray analyses were prepared by diluting 2 μL of the sample in 1000 μL of chloroform:methanol solution (1:1, v/v). Samples

were introduced into the mass spectrometer using a flow rate of 10 μL/min, setting the needle voltage at 3000V with the ion source at 80ºC and cone voltage at 30V. Tandem mass spectra (MS/MS) of molecular ions were obtained by collision-induced decomposition (CID), using argon as the collision gas (measured pressure in the penning gauge (~ $6x10^{-6}$ mBar) and varying collision energy between 15-25 eV. In MS and MS/MS experiments TOF resolution was set to approximately 9000 (FWHM).

Results and Discussion

A) Characterisation of doubly charged ions of PLPC/DMPO spin adducts

The formation of palmitoyl-lineloyl-GPC free radicals by metal catalysed oxidation (Fenton reaction) coupled with DMPO spin trapping was studied by MS. The ES mass spectra of PLPC obtained in the presence of DMPO, (A) under non-oxidative conditions (PLPC + Fe^{2+}) and (B) under oxidative conditions (PLPC + Fe^{2+} + H_2O_2) are shown in Fig. 1. By comparison of the mass spectra in the *m/z* range of 450-530, some new ions with *m/z* 455.4 and 463.4 are observed, and can be assigned as doubly charged $[MH+Na]^{2+}$ ions of PLPC/DMPO adducts containing one and two oxygen atoms, respectively (Scheme 1).

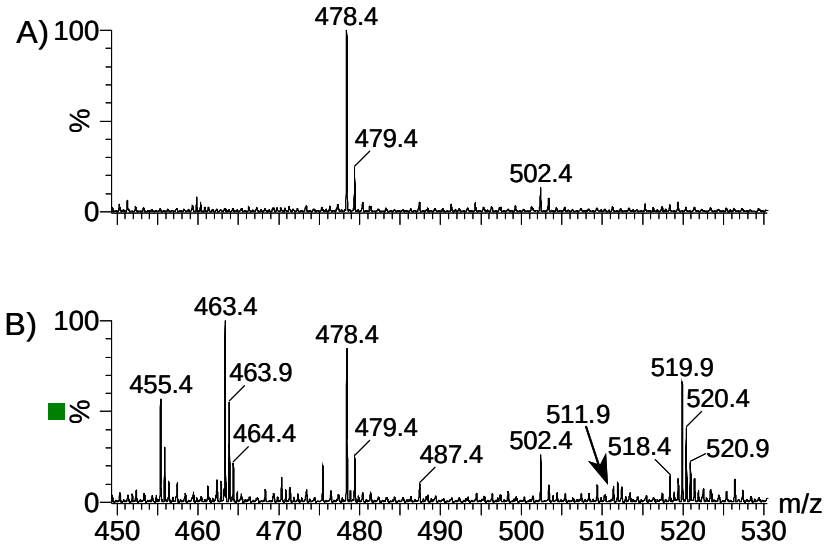

Fig. 1. Mass spectrum of PLPC vesicles obtained under non-oxidative conditions (A) and in the presence of H_2O_2+Fe(II)+DMPO (B). The doubly charged ions correspond to PLPC-DMPO spin adducts.

The structures shown in Scheme 1 are one of the possible structures that may be formed. Doubly charged ions observed at *m/z* 511.9 and 519.9 were attributed to the ions corresponding to DMPO spin adducts containing two DMPO molecules of intact PLPC

with one and two oxygen atoms, respectively, similarly as was reported during the identification of DMPO spin adducts of intact POPC [8].

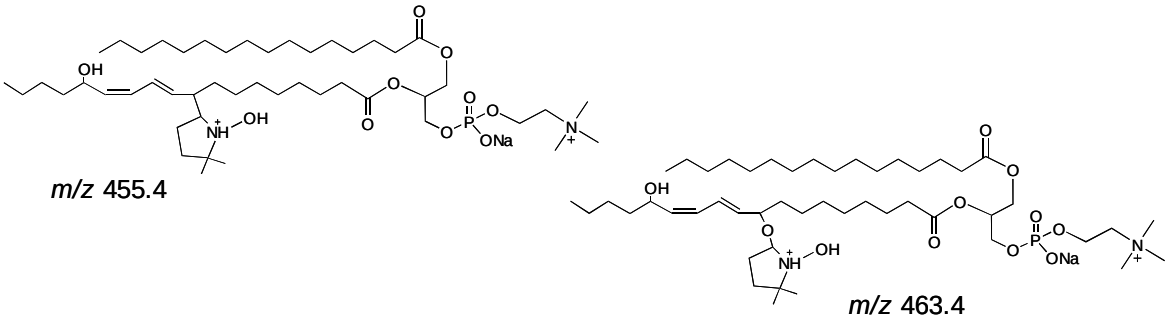

Scheme 1. Proposed structures for the doubly charged of PLPC DMPO spin adducts (*m/z* 455.4 and 463.4).

Other ions observed with very low relative abundance at *m/z* 471.4 and *m/z* 941.8 (data not shown) were attributed, respectively, to sodiated doubly charged and sodiated mono charged ions of DMPO spin adducts of intact PLPC containing three oxygen atoms. However, the low relative abundance of these ions limited the acquisition of tandem mass spectra. The identification of mono and doubly charged ions of oxidised intact GPC is in accordance with previous work [8] performed on the identification of POPC/DMPO spin adducts where doubly charged ions exhibited higher relative abundance over the singly charged ions. In order to identify the free radicals of oxidised PLPC, detailed structural information was obtained by performing tandem mass spectrometry (product ion scanning) on the most abundant doubly charged ions.

The product ion spectra can either exhibit singly charged product ions, formed by loss of charged molecules, and doubly charged ions formed by loss of neutral molecules. The product ion spectra obtained for the doubly charged ions at *m/z* 455.4 and 463.4, and depicted in Fig. 2, exhibit abundant singly charged product ions at *m/z* 478.4 and 502.4 (Scheme 2) that correspond to the $[MH]^+$ ion of the dehydrated 1-palmitoyl-2-lyso-phosphatidylcholine and 2-lineloyl-1-lyso-glycerophosphatidylcholine, respectively. The product ion spectrum of the ion at *m/z* 455.4 (Fig. 2A), which can be assigned to the alkoxyl/DMPO spin adduct or to the hydroxy-alkyl/DMPO spin adduct of the PLPC, exhibits the doubly charged product ion observed at *m/z* 270.7 that was attributed to the [2-lineloyl-1-lyso-phosphatidylcholine(H)+Na]$^{2+}$ ion (Scheme 2), containing the oxygen atom most likely at the lineloyl moiety. This product ion was also observed, with very low relative abundance, as mono charged product ion with *m/z* 540.4 (data not shown). The presence of the oxygen atom and of the DMPO molecule at the linoleoyl moiety is also

evidenced by the singly charged product ion at *m/z* 432.3 $[R_2(O)COONa/DMPO+H]^+$ (Fig. 2A). This product ion at *m/z* 432.3 (Scheme 2), containing both the DMPO molecule and the oxygen atom, can be assigned to the alkoxyl lineloyl spin adduct ($LO^{\bullet}$/DMPO) or to the hydroxy-alkyl lineloyl spin adduct ($L^{\bullet}(OH)$/DMPO).

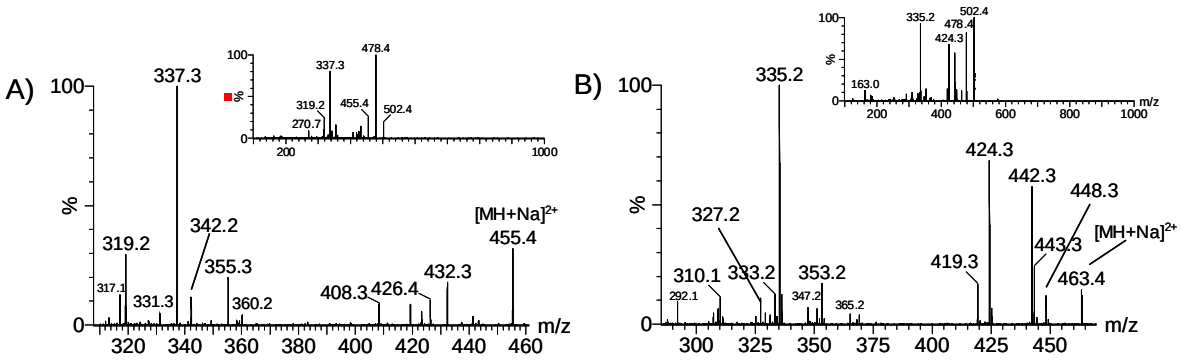

Fig. 2. Product ion spectra of doubly charged ions of PLPC-DMPO spin adducts containing (A) one oxygen atom with m/z 455.4, and (B) two oxygen atoms with m/z 463.4. Insets were included to visualize the complete product ion spectrum.

The product ion at *m/z* 502.4 formed by combined loss of R_1COOH and DMPO-OH may suggest the presence of the alkoxyl spin adduct. The loss of the acyl chains (*sn*-1 and *sn*-2 residues) observed here, lost as free fatty acids (R_1COOH and R_2COOH) and ketene (R_1=C=O and R_2=C=O) in the case of $[MH]^+$ molecular ions, or lost as salts (R_1COONa and R_2COONa) and free fatty acids (R_1COOH and R_2COOH) in the case of $[MNa]^+$ molecular ions, are also observed in the product ion spectra of GPC [18] and GPC oxidation products [19,20]. The product ion spectra of doubly charged POPC spin adducts previously described [8] exhibited charge remote fragmentations, namely homolytic cleavages that were assigned as the result of cleavages occurring in the vicinity of the spin trap. Hence, the product ion at *m/z* 337.3 may result from homolytic cleavage of the γ-bond relative to the carboxylic group (Scheme 2). This product ion involves the cleavage of C_3-C_4 bond, already observed in the product ion spectra of fatty acids [16] and of oxidised fatty acids [21], and is a typical high-energy CID fragmentation [16] although, it has also been observed in low–energy CID spectra [21]. Dehydration of the product ion at *m/z* 337.3 may rationalise the product ion at *m/z* 319.2 (observed in Fig. 2A). The product ion at *m/z* 319.2 may also be attributed to $[R_2(O)COONa+H]^+$ formed by combined loss of DMPO molecule (113 Da) and loss of 1-palmitoyl-lyso-phosphatidylcholine. The odd numbered singly charged product ion observed at *m/z* 295.2 (not shown in Fig. 2A) may be identified as resultant from cleavage occurring in the vicinity of the spin trap (Scheme 2)

allowing proposing the spin trap to be located at C-8. On the other hand, the even numbered singly charged product ion observed at *m/z* 360.2 (Scheme 2) may result from cleavage involving the hydroxy group at C-13. Thus, the structures of the product ions depicted in Scheme 2, are consistent with the presence of the hydroxy derivative of the carbon centred (alkyl at C-13) spin adduct with the hydroxy group placed at C-8 (Scheme 2).

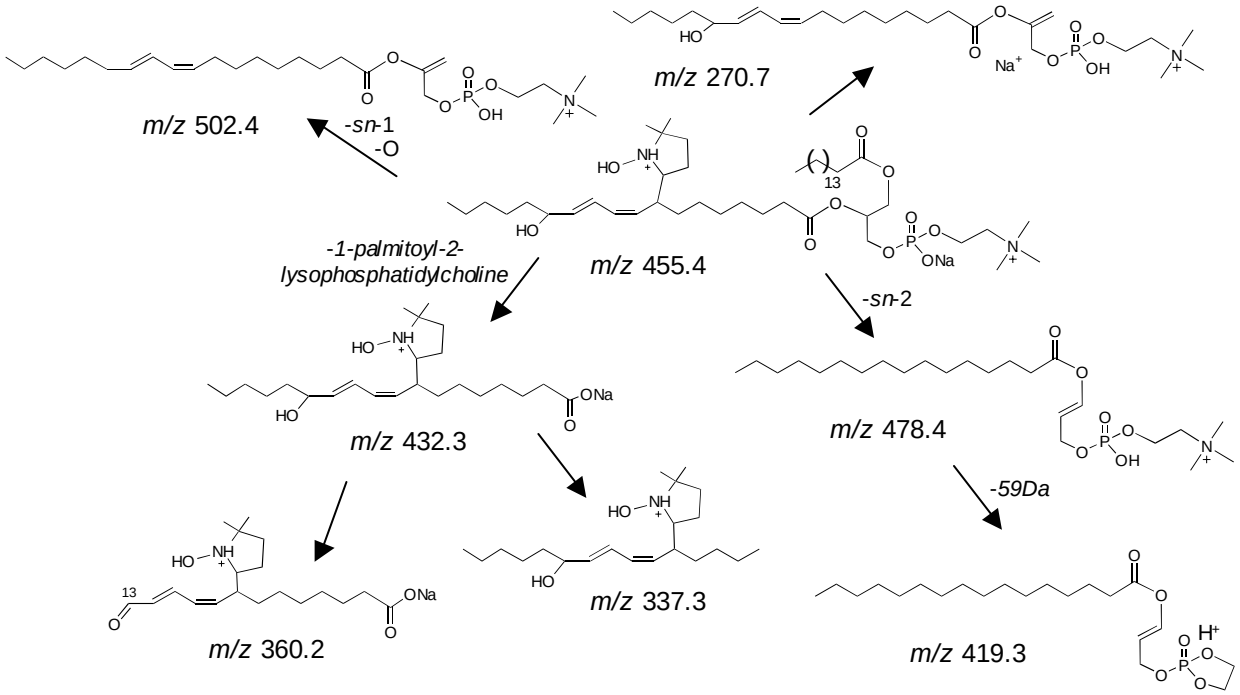

Scheme 2. Proposed structures for the product ions observed in the product ion spectra of ion at *m/z* 455.4.

The product ion spectrum of ion at *m/z* 463.4 (Fig. 2B) shows the typical fragmentation behaviour described for the doubly charged ions of glycerophosphatidylcholines DMPO spin adducts, with abundant product ions attributed to the lyso-phosphatidylcholines at *m/z* 502.4 and 478.4 formed by loss of the *sn*-1 and the oxidised *sn*-2 fatty acid/DMPO, respectively. Also, the singly charged product ions at *m/z* 419.3 and 443.3 (Fig. 2B) formed by loss of the oxidised *sn*-2 and *sn*-1 residues, respectively, combined with loss of $N(CH_3)_3$ are observed. The product ion at *m/z* 448.3) gives information regarding the *sn*-2 acyl residue which is observed attributed to the sodium salt of the oxidised linoleic acid spin adduct $[(OO)R_2COONa/DMPO+H]^+$ (Fig. 2B). The product ion at *m/z* 448.3 can result from the contribution of the hydroperoxide-alkyl, the hydroxy-alkoxyl or the peroxyl DMPO lineloyl spin adduct. Product ions resulting from loss of the acyl chains, of the spin trap and of homolytic cleavages occurring at the γ-bond relative to the carboxylic group

(*m/z* 353.2, Scheme 3A) are fragmentations that do not provide information regarding the location of either the spin trap or the hydroxy groups along the unsaturated acyl chain, as they may be present deriving from either the hydroperoxide-alkyl, the hydroxy-alkoxyl or the peroxyl DMPO lineloyl spin adduct.

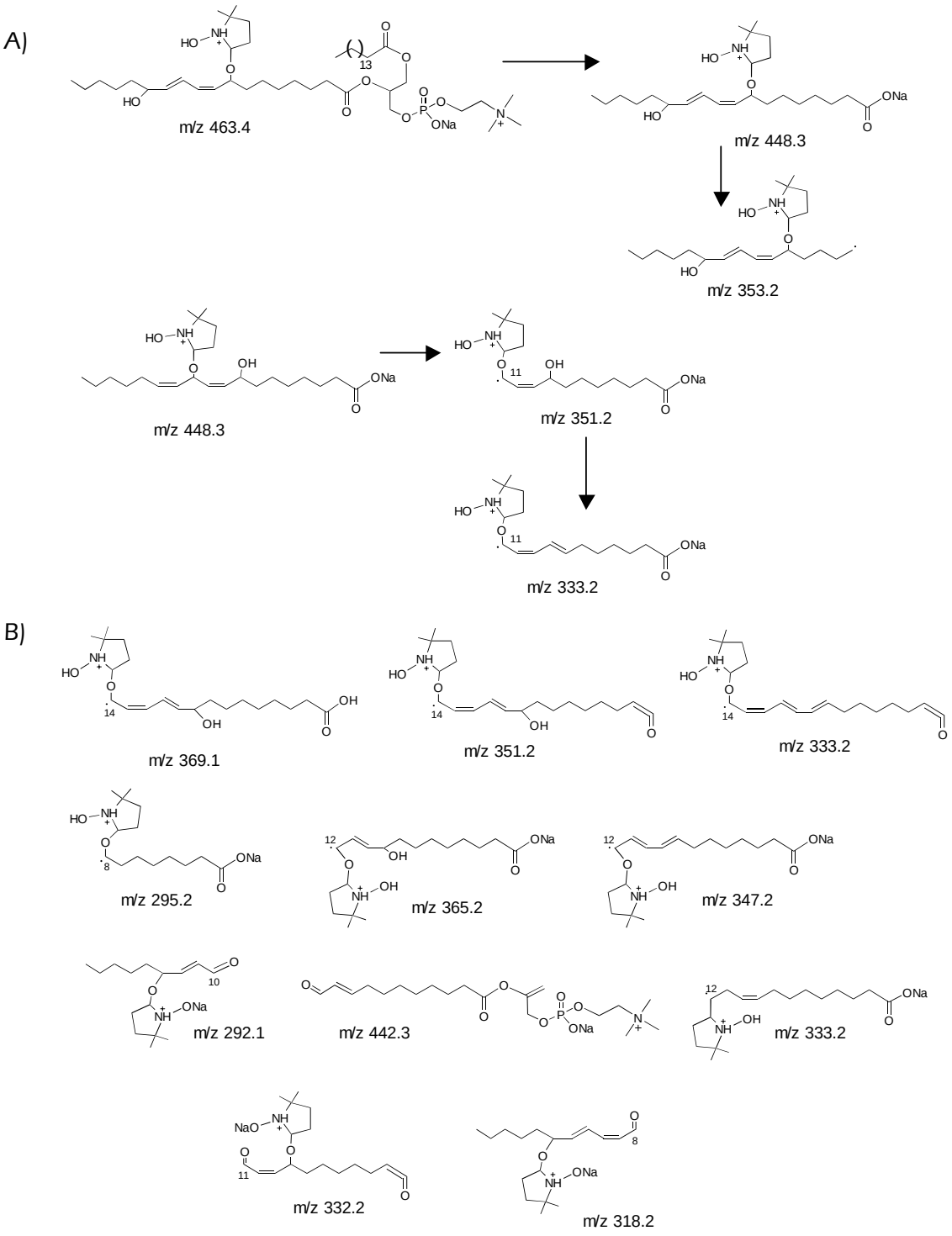

Scheme 3. Proposed structures for the product ions observed in the product ion spectra of ions at *m/z* 463.4.

However, the odd numbered product ions at *m/z* 369.1, 365.2, 351.2, 347.2 and 333.2 (Fig. 2B), occurring with minor relative abundance may be assigned to cleavages in the vicinity of the spin trap (Scheme 3A and 3B), and are consistent with the presence of the spin adducts at C-8, C-11, C-12 or C-14. Also, the even numbered product ion observed at *m/z* 292.1 (Fig. 2B) evidences the presence of the hydroxy group at C-10 (Scheme 3B), although the product ion at *m/z* 442.3 suggests also the hydroxy placed at C-11 (Scheme 3B). The product ions described are consistent with the presence of the hydroxy derivative of the oxygen centred spin adduct (hydroxy-alkoxyl/DMPO). Nonetheless, the product ion at *m/z* 163.0 also observed in the spectrum (Fig. 2B), which exhibits a 16 Da mass increase relative to the sodiated five-membered cyclophosphane ring (*m/z* 147), suggests that the hydroxy group is also at the phosphocholine head and therefore an additional isomer containing the oxidised polar head must be considered. In this case, the alkyl radical may be considered at C-12, as suggested by the product ion at *m/z* 333.2 (Scheme 3B).

The product ion spectra obtained for the PLPC/DMPO sodiated doubly charged $[MH+Na]^+$ spin adducts containing two DMPO molecules with *m/z* 511.9 and 519.9 (insets in Fig. 3A and B), exhibited loss of one uncharged DMPO molecule leading to the product ions with *m/z* 455.4 and 463.4, respectively.

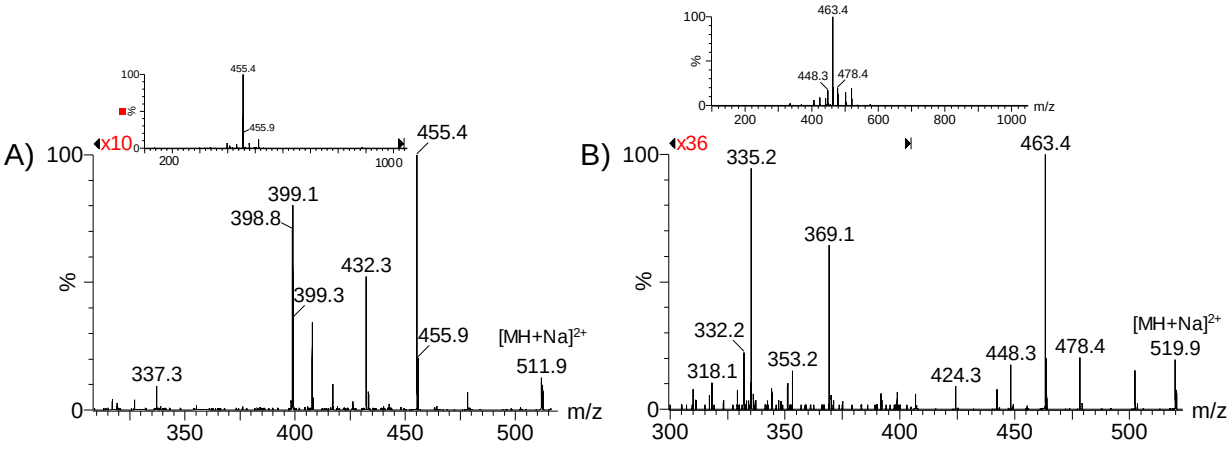

Fig. 3. Product ion spectra of doubly charged ions of PLPC-DMPO spin adducts containing two DMPO molecules and (A) one oxygen atom with *m/z* 511.8, and (B) two oxygen atoms with *m/z* 519.9. Insets were included to visualize the complete product ion spectrum.

Both product ions (*m/z* 455.4 and 463.4) are observed in the respective product ion spectrum and seem to be a first step of the fragmentation pattern of these sodiated doubly charged spin adducts, providing no additional structural information on the location of the second DMPO molecule. This behaviour resulted in product-ion spectra

very similar to the product-ion spectra of *m/z* 455.4 and 463.4 previously described. In the case of POPC/DMPO spin adducts, the presence of the second DMPO together with the presence of the product ion at *m/z* 130.1 $[DMPO\text{-}OH+H]^+$ allowed to propose that the spin adduct containing one oxygen atom and two DMPO molecules (*m/z* 512.9) [8] was simultaneously carbon- and oxygen-centred spin adduct. In the case of the ion at *m/z* 511.9 (Fig. 3A), the doubly charged product ion at *m/z* 398.8, attributed to loss of both DMPO molecules from the precursor ion, does not provide structural information regarding the location of the spin trap nor to the nature of the spin adduct. However, in the case of ion at *m/z* 519.9 (Fig. 3B), the odd numbered product ions observed with minor relative abundance at *m/z* 353.2 may result from γ-bond cleavage (structure in Scheme 3A) with dehydration (*m/z* 335.2), and the product ions at *m/z* 369.1 and 351.2 (Fig. 3B) suggest the presence of the spin trap at the C-14 (Scheme 3B), while even numbered product ions at *m/z* 318.1 and 332.2 (Fig. 3B) provided evidence for the presence of the hydroxy group at C-8 and C-11 respectively (Scheme 3B).

B) Characterisation of doubly charged ions of PAPC/DMPO spin adducts

The ES mass spectra obtained for the extracts containing oxidised PAPC in the presence of DMPO (Fig. 4 B) was plotted against the native PAPC in the presence of DMPO (Fig. 4A). The presence of ions at *m/z* 467.4 and 475.4 were attributed to doubly charged ions of PAPC/DMPO spin adducts containing one and two oxygen atoms, respectively (Scheme 1).

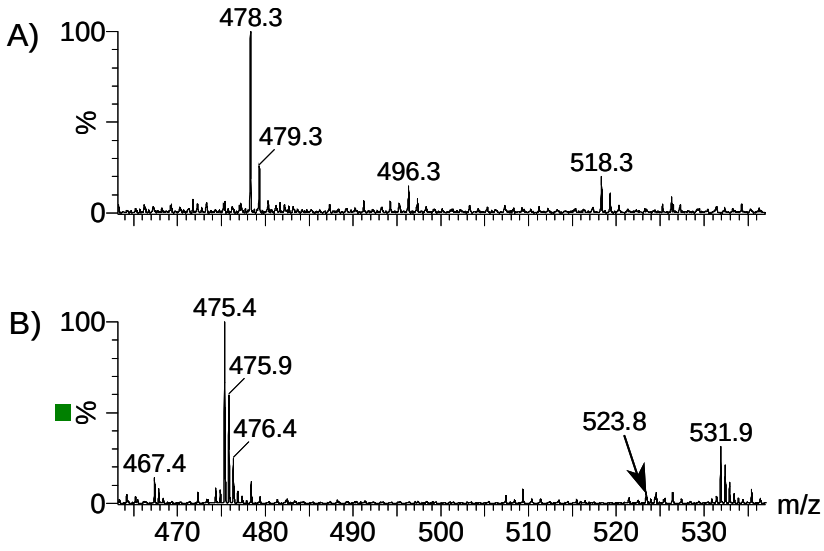

Fig. 4. Mass spectrum of PAPC vesicles obtained under non-oxidative conditions and in the presence of H_2O_2+Fe(II)+DMPO. The doubly charged ions correspond to PAPC-DMPO spin adducts.

The ion with *m/z* 965.7 (data not shown) was also observed although with low relative abundance and may be assigned to the singly charged of the spin adduct PAPC/DMPO containing three oxygen atoms. The ions with *m/z* 523.8 and 531.9 were also observed and may be attributed to doubly charged ions of PAPC spin adducts with one and two oxygen atoms containing two DMPO molecules, similar to previous results. Tandem mass spectra obtained for the ions at *m/z* 467.4 (Fig. 5A) and 475.4 (Fig. 5B), exhibit product ions formed by similar fragmentation pathways, namely the product ions with *m/z* 478.3 and 526.3 were attributed to the dehydrated $[MH]^+$ ion of the 1-palmitoyl-lyso-phosphatidylcholine and 2-arachidonoyl-lyso-phosphatidylcholines, respectively. Also, the doubly charged product ions observed with *m/z* 282.7 (inset Fig. 5A) and 290.7 (inset Fig. 5B) may correspond to the dehydrated [2-arachidonoyl-lyso-phosphatidylcholines(H)+Na]$^{2+}$ ions containing one and two oxygen atoms, respectively, confirming the oxidation at the *sn*-2 acyl residue. Also, the product ion attributed to the unsaturated fatty acid chain (arachidonoyl) containing the DMPO molecule and the oxygen atom(s) are observed at *m/z* 456.3 (Fig. 5A) and 472.3 (Fig. 5B). The product ions at *m/z* 410.7 (Fig. 5A) and 418.7 (Fig. 5B) correspond to the doubly charged product ions formed by loss of DMPO (113 Da) from the correspondent precursor ions.

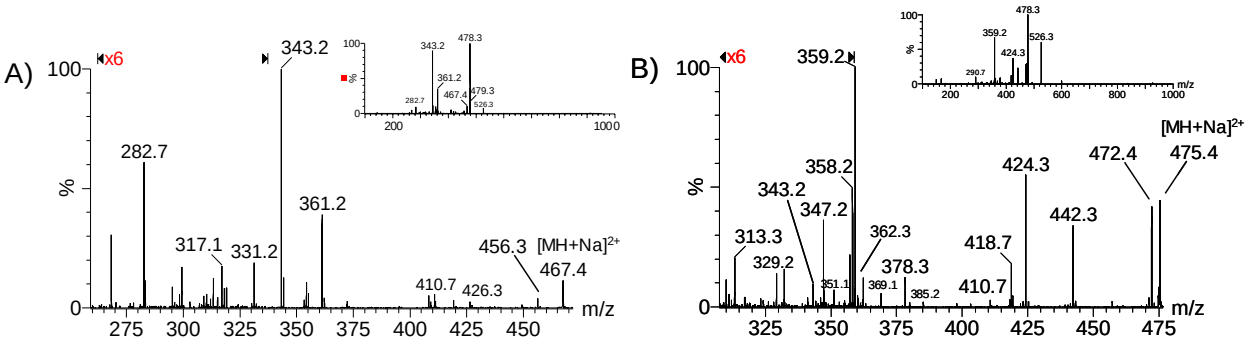

Fig. 5. Product ion spectra of doubly charged ions of PAPC-DMPO spin adducts containing (A) one oxygen atom with *m/z* 467.4, and (B) two oxygen atoms with *m/z* 475.4. Insets were included to visualize the complete product ion spectrum.

In Fig. 5A, the singly charged product ion at *m/z* 361.2 (Scheme 4) is formed by homolytic cleavage of the γ-bond relative to the carboxylic acid, evidencing the presence of the oxygen and DMPO molecule in the *sn*-2 acyl chain. This product ion can also be due to homolytic cleavage occurring in the vicinity of the epoxy derivative (Scheme 4), as is described to occur for epoxy derivatives [22]. The product ion at *m/z* 343.2 may be attributed to loss of DMPO (Scheme 4) suggesting the hydroxy-alkyl spin adduct. The product ion at *m/z* 426.3 may suggest the hydroxy group at C-10 (Scheme 4). In Fig. 5B,

the product ion observed at *m/z* 410.7 can be assigned to the doubly charged product ion formed due to loss of $[DMPO\text{-}OH+H]^+$ (-130Da) from the precursor ion. Also, the loss of the *sn*-1 residue as free fatty acid (R_1COOH) is observed combined with loss of DMPO (-113Da) leading to the doubly charged product ions at *m/z* 290.7. Odd numbered product ions observed at *m/z* 359.2 and 343.2 (Fig. 5B) may be attributed to loss of DMPO (113 Da) and DMPO-OH (129 Da) combined with loss of 1-palmitoyl-2-lyso-phosphatidylcholine from the precursor ion, while the product ions at *m/z* 385.2 and 329.2 (Scheme 4) formed by homolytic cleavages in the vicinity of the spin trap at the C-5 and C-8, respectively, suggesting the presence of the hydroxy-alkoxyl spin adduct.

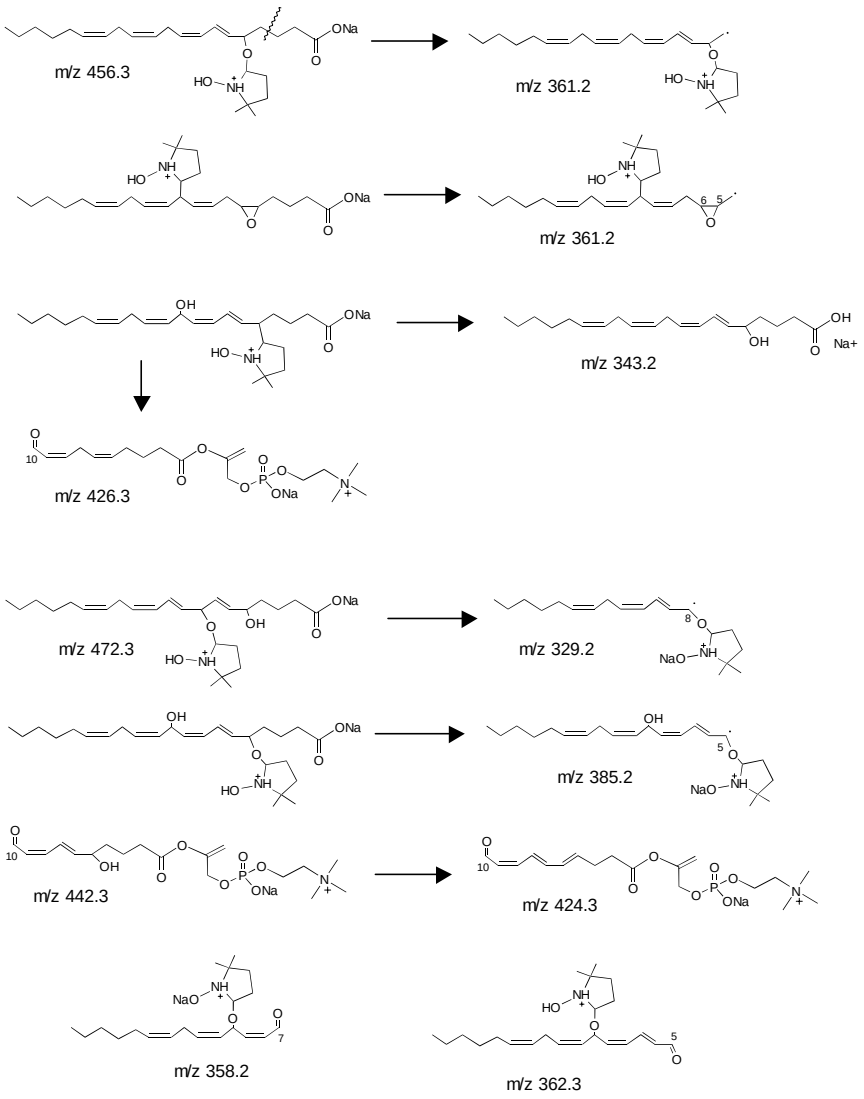

Scheme 4. Proposed structures for the product ions observed in the product ion spectra of ion at *m/z* 467.4.

The even numbered product ions at *m/z* 442.3 and 424.3 (hydroxy at C-10), 362.3 (hydroxy at C-5) and 358.2 (hydroxy at C-7) (Scheme 4) may result by 1,4-hydrogen elimination mechanism and allow proposing the hydroxy group in different locations. The product ion resulting from homolytic cleavage of the γ-bond relative to the carboxylic group (*m/z* 377.3) was not observed in the product ion spectra, as observed in the previous DMPO spin adducts [8]. Altogether, the product ions point out to the predominance of the hydroxy-alkoxyl-arachidonoyl spin adduct to the relative abundance of the spin adduct of PAPC. The product ions at *m/z* 408.3 and 426.4 were observed in the product ion spectra of phospholipid spin adducts containing one oxygen atom, namely PAPC (*m/z* 463.4- Fig. 5A), PLPC (*m/z* 455.4 -Fig. 2A) and POPC (*m/z* 456.4, 8), and can also be attributed to the palmitoyl-glycerol ion with the DMPO molecule attached most probably at one of the carbon atoms of the glycerol moiety since saturated acids are resistant to radical oxidation. Also the product ions at *m/z* 442.3 and 424.3 observed in the product ion spectra of phospholipid spin adducts containing two oxygen atoms, namely for PAPC (*m/z* 475.4 – Fig. 5B), PLPC (*m/z* 463.4 – Fig. 2B) and POPC (*m/z* 464.4, 8), and can also be attributed to the palmitoyl-glycerol ion with one oxygen atom and the DMPO molecule. These structures were never proposed before, although oxidation in other points of the phosphatidylcholine molecule may be susceptible to undergo radical oxidation, as was recently proposed to occur at the phosphocholine polar head [20], which may occur by a mechanism similar to the radical oxidation of amino acids and proteins [23] by hydrogen abstraction from the α-carbon atom of amino acids and proteins, and also from aliphatic side chains [23].

The identification in this study of intact oxidised PAPC free radicals centred at C-5, C-8 and C-10 positions of the arachidonoyl chain, and considering that the arachidonoyl moiety contains 3 bis-allylic hydrogen atoms each equally susceptible to be removed during non-enzymatic radical oxidation [2], suggests that the C-7 bis-allylic hydrogen atom is most accessible to be abstracted by the hydroxyl radical. The bis-allylic hydrogen atom at C-7 is the one closer to the glycerol moiety. Similar conclusions were drawn through the attack of the thiyl radical ($RS^{\bullet}$) during the study of cis-trans isomerisation of PUFA in diacyl-glycerophosphatidylcholine large unilamelar vesicles [24]. The abstraction of the C-7 bis-allylic hydrogen atom generates the alkyl radical centred at C-7 that through isomerisation leads to the alkyl radicals centred at C-5 and C-9. Isomerisation of radical place at C-7 to the C-5 position seems to be favoured due to the predominance of short-chain peroxidation products of PAPC (aldehydes and dicarboxylic terminal groups) with 5 carbon atoms over others during metal catalysed radical peroxidation [25,26], assuming

that no significant differences occur in the ionisation efficiencies of products with various chain lengths.

The product ion spectra of the doubly charged ions with two DMPO molecules containing one (*m/z* 523.8) and two oxygen atoms (*m/z* 531.9) were obtained, and particularly the product ion spectrum of ion at *m/z* 531.9 (Fig. 6), exhibits the product ion at *m/z* 146.1 $[DMPO\text{-}OOH+H]^+$ (Fig. 6) that suggests the presence of the peroxyl derivative for the PAPC/DMPO spin adduct. In previous studies, performed in the characterisation of linoleic acid DMPO spin adducts, the product ion at *m/z* 146.1 was used together with others to suggest the presence of the peroxyl/DMPO linoleic acid spin adduct [15]. In fact, losses of one and two DMPO molecules from the precursor ion are observed by the doubly charged product ions at *m/z* 475.3 and 418.8 (Fig. 6). Also, loss of one DMPO-OH from the precursor ion (*m/z* 467.4) and combined with loss of DMPO molecule at (*m/z* 410.8) are observed as doubly charged ions (Fig. 6). Furthermore, product ions observed with low relative abundance at *m/z* 359.2 (loss of DMPO combined with palmitoyl-lyso-phosphatidylcholine) and particularly the product ions at *m/z* 332.2 (hydroxy at C-9) is consistent with the additional contribution of the hydroxy-alkoxyl derivative.

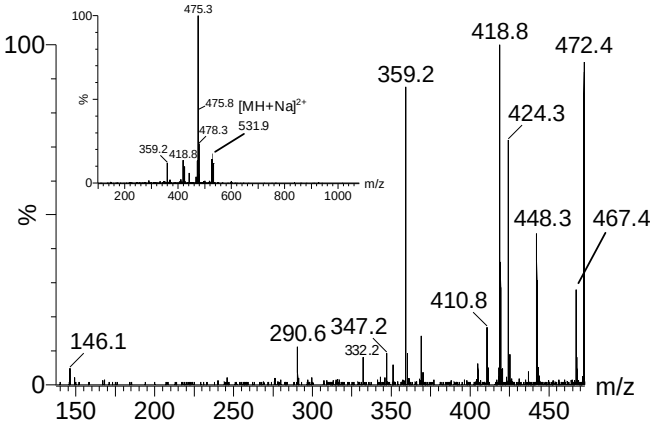

Fig. 6. Product ion spectrum of doubly charged ion of PAPC-DMPO spin adducts containing two DMPO molecules and two oxygen atoms with *m/z* 531.9. Inset was included to visualize the complete product ion spectrum.

The glycerophosphatidylcholines used in this study contained one saturated fatty acid (palmitic acid), which is resistant to radical oxidation, and also linoleic (18:2) and arachidonic acid (20:4), which are ω-6 PUFA. The mass spectra obtained for both glycerophosphatidylcholines (PLPC and PAPC) showed the presence of ions that were assigned to DMPO spin adducts of oxidised intact GPC formed by insertion of up to three

oxygen atoms. In the literature it is acknowledged that the extent of oxidation reaction is related to the number of double bonds (i.e. the number of bis-allylic hydrogen atoms). The presence of 3 bis-allylic hydrogen atoms in the arachidonoyl moiety of PAPC vesicles, would be expected to induce oxidation to a greater extent, when compared to the PLPC vesicles. Thus, the insertion of 3 oxygen atoms may be rationalized considering that the oxidative damage of PUFA by free radicals may not be strictly related to the number of bis-allylic hydrogen atoms or to the surface area [27], but also to the acyl chain conformation in PC bilayers [28]. However, the identification of radical peroxidation products of PAPC containing up to six oxygen atoms, in previous published results obtained during radical oxidation of PAPC vesicles by the Fenton reaction [20], rules out the hypothesis that acyl chain packing might have influence on the accessibility of ROS into the liposomes, as was proposed earlier to explain the higher oxidative stability shown by PDPC vesicles relative to PAPC vesicles [28]. Another explanation is to consider that the DMPO may have a retarding effect on the lipid peroxidation reaction by trapping the glycerophosphatidylcholine radicals and blocking subsequent reactions with the oxygen, as suggested elsewhere [5,29]. On the other hand, some authors have reported that larger alkyl radicals, as is the case of GPC free radicals, are trapped more slowly by DMPO than the smaller ones, such as $^{\bullet}CH_3$ or $^{\bullet}CH_2CH_3$ [30], due either to spin-spin reactions of larger alkyl radicals [30] or to increasing steric hindrance effects [2]. The rate constants of alkyl radicals with DMPO ($k \sim 10^6$-10^7 $M^{-1}s^{-1}$), although with little variations, are chain length-dependent [30], in detriment of the formation of higher carbon chain lengths alkyl DMPO spin adducts. However, in the present study, tandem mass spectrometry data supported the presence of both carbon and oxygen centred radicals of glycerophosphatidylcholines, namely of alkoxyl PLPC/DMPO spin adducts placed at the C-9 and C-11 and the presence of alkoxyl PAPC/DMPO spin adducts that can be placed at the C-5 and C-10, the latter formed by abstraction of the C-7 bis-allylic hydrogen atom.

Evidence for the presence of the alkoxyl radical of the dilinoleoyl-glycerophosphatidylcholine (DLPC), was recently proposed during enzymatic and non-enzymatic oxidation, based on the identification of the $^{\bullet}C_5H_{11}$/POBN spin adduct [31], which was interpreted as indicative of the alkoxyl radical located at the C-13 in one of the linoleoyl residues. However, the authors do not mention the presence of the carbon centred spin adduct resultant from the alkoxyl radical placed at C-9. This would also be expected since both 9-alkoxyl and 13-alkoxyl lipid radicals have previously been described during linoleic acid enzymatic oxidation [6,7,32], although the ratios of POBN/$^{\bullet}C_5H_{11}$ *vs* POBN/$^{\bullet}C_8H_{15}O_2$ observed during lipoxygenase oxidation were consistent with preferential

formation of 13-LO$^{\bullet}$ over 9-LO$^{\bullet}$ [7], which is in accordance with the specificity of the enzyme [33]. Both 9-alkoxyl and 13-alkoxyl lipid radicals were identified as oxidation products of linoleic acid during non-enzymatic metal catalysed oxidation [15,16]. It is assumed that the LO$^{\bullet}$ radicals play a minor role in the propagation steps during lipid peroxidation, and instead undergo cyclisation leading to the carbon centred epoxy-alkyl radical (OL$^{\bullet}$) [34]. Thus, cyclisation of the 13-alkoxyl linoleic radical leads to the epoxy carbon centred lipid radical placed at C-9 and after β-scission the epoxy-alkyl radical may lead to the heptanoic radical ($^{\bullet}C_7H_{13}O_2$). Similarly, the 9-alkoxyl linoleic radical would, through the same route, lead to the butyl radical ($^{\bullet}C_4H_9$). Interestingly, the heptanoic acid DMPO spin adduct (*m/z* 244), but not the butyl DMPO spin adduct (*m/z* 172), was identified during the study of linoleic acid radicals by tandem mass spectrometry coupled with liquid chromatography (LC-MS/MS) [16], thus suggesting the presence of the carbon centred radical (epoxy-alkyl) at the C-9. These findings suggest that in the case of linoleic acid, after C-11 bis-allylic hydrogen abstraction, the isomerisation would be preferably towards the formation of the radicals at C-9 over the C-13 position, leading to the more favourable or more stable formation of the C_9 short-chain products. Other studies performed on the identification of peroxidation products of glycerophosphatidylcholines in model liposomes [19] and in oxLDL [35,36] revealed the 1-palmitoyl-2-(9-oxo-nonanoyl)-3-glycerophosphatidylcholine to be one of the major aldehyde products, among the short-chain products with terminal aldehyde at *sn*-2 acyl residues esterified to the 1-palmitoyl-GPC moiety. On the other hand, the predominance of C_9 aldehydes (9-oxo-nonanoyl) over C_{12} aldehydes (12-oxo-dodecenoyl) may be related to the higher ionisation efficiency, which is also dependent on the acyl chain length [37].

In the present study, the mass spectrum of ion at *m/z* 531.9 exhibited the product ion at *m/z* 146.1 identified as $[DMPO\text{-}OOH+H]^+$, which was earlier used to proposed the presence of the peroxyl linoleic acid DMPO adduct [15] may be corroborated by the product ion at *m/z* 526.4 (data not shown) formed by combined loss of R1COOH and DMPO-OOH. Although the lipid peroxyl radicals are reported to give unstable spin adducts [38] these have shown to be stable enough to allow DMPO trapping [15]. Lipid alkoxyl radicals, and particularly the hydroperoxide derivatives, are intermediate lipid peroxidation products known to be the precursors of cytotoxic α,β-unsaturated aldehydes, such as acrolein, crotonaldehyde and 4-hydroxy-nonenal (HNE), among others [39,40]. The citoxicity of these secondary products is reported to be related to the chain length [41] and also to the electrophilicity at C-3 given by electron-withdrawing groups [42,43]. The chemical stability of unsaturated aldehydes, when compared to the lipid radicals, the

ability to permeate across the lipid bilayer membrane, and the nucleophilic reaction that they undergo with primary amino groups, found in proteins and DNA bases [23], is though to be responsible for the initiation of apoptotic events that different cells exhibited [41-43].

In conclusion, carbon and oxygen centred free radicals of intact diacyl-glycerophosphatidylcholines were identified using the DMPO as spin adducts, and based on the tandem mass spectrometry data, the free radicals were identified to occur in carbon atoms closer to the glycerol moiety. The product ions observed with minor relative abundance were the most informative regarding the location of the spin trap and of the hydroxy groups.

Acknowledgements

The authors gratefully acknowledge the financial support provided to Ana Reis (PhD grant SFRH/BD/10358/2002) by the Foundation for Science and Technology (FCT) and FSE (III Quadro Comunitário de Apoio).

References

[1] Pincemail J. "Free radicals and antioxidants in human diseases". *In* Analysis of free radicals in biological systems. Ed. Favier, Cadet, Kalyanaraman, Fontecave, Pierre, 1995, Verlag, Berlin, p. 83-98.

[2] Spin trapping Free Radicals. In *Free Radicals, Biology and Detection by Spin Trapping*; Rosen, G.M.; Britigan, B.E.; Halpern, H.J.; Pou, S., Eds.; Oxford University Press: N.Y. 1999; pp 170-186.

[3] De Zwart LL, Meerman JHN, Commandeur JNM and Vermeulen NPE. Biomarkers of free radical damage: applications in experimental animals and in humans. Free Rad. Biol. Med. 1999; 26: 202-226.

[4] Domingues, M.R.M.; Domingues, P.; Reis, A.; Fonseca, C.; Amado, F.M.L.; Ferrer-Correia, A. J. V. Identification of oxidation products and free radicals of tryptophan by Mass Spectrometry. J. Am. Soc. Mass Spectrom. 2003, 14: 406-416.

[5] Deterding LJ, Ramirez DC, Dubin JR, Mason RP, Tomer KB. Identification of free radicals on hemoglobin from its self-peroxidation using mass spectrometry and immuno-spin trapping. J. Biol. Chem. 2004; 279: 11600-11607.

[6] Qian SY, Yue G, Tomer KB, Mason RP. Identification of all classes of spin-trapped carbon-centered radicals in soybean lipoxygenase-dependent lipid peroxidation of ω-6 polyunsaturated fatty acids via LC/ESR, LC/MS and tandem MS. Free Rad. Biol. Med. 2003a; 34: 1017-1028.

[7] Qian SY, Guo Q, Mason RP. Identification of spin trapped carbon-centered radicals in soybean lipoxygenase-dependent peroxidations of ω-3 polyunsaturated fatty acids by LC/ESR, LC/MS and tandem MS. *Free Rad. Biol. & Med.* 2003b, 35, 33-44.

[8] Reis A, Domingues P, Ferrer-Correia AJ, Domingues MRM. Identification by Electrospray Tandem Mass Spectrometry of spin trapped free radicals from oxidized 2-oleoyl-1-palmitoyl-sn-glycero-3-phosphocholine. Rapid Commun. Mass Spectrom. 2004a; 18: 1047-1058.

[9] Vitrac H, Courrègelongue M, Couturier M, Collin F, Thérond P, Rémita S, Peretti P, Dore D, Gardès-Albert M. Radiation-induced peroxidation of small unilamellar vesicles of phosphatidylcholine generated by sonication. Can. J. Physiol. Pharmacol. 2004, 82, 153-160.

[10] Berry KAZ, Murphy RC. Free radical oxidation of plasmalogen glycerophosphocholine containing esterified docosahexaenoic acid: structure determination by mass spectrometry. Antioxid. Redox Signal. 2005, 7, 157-169.

[11] Borst JW, Visser NV, Kouptsova O, Visser AJWG. Oxidation of unsaturated phospholipids in membrane bilayer mixtures is accompanied by membrane fluidity changes. Biochim. Biophys. Acta. 2000; 1487: 61-73.

[12] Megli FM, Sabatini K. Mitochondrial phospholipid bilayer structure is ruined after liver oxidative injury in vivo. FEBS Lett. 2004; 573: 68-72.

[13] Megli FM, Sabatini K. Oxidized phospholipids induce phase separation in lipid vesicles. FEBS Lett. 2005; 579: 4577-4584.

[14] Yoshida T, Otake H, Aramaki Y, Hara T, Tsuchiya S, Hamada A, Utsumi H. Free radicals from 1-palmitoyl-2-arachidonoyl-phosphatidylcholine liposomes in Fe^{2+}/ascorbic acid solution. Biol. Pharm. Bull. 1996; 19: 779-782.

[15] Reis A, Domingues MRM, Amado FML, Ferrer-Correia AJ, Domingues P. Detection and characterisation by mass spectrometry of radicals adducts produced by linoleic acid oxidation. J. Am. Soc. Mass Spectrom. 2003; 14: 1250-1261.

[16] Reis A, Domingues MRM, Amado FML, Ferrer-Correia AJ, Domingues P. Identification of linoleic acid free radicals and other breakdown products using spin trapping with liquid-chromatography electrospray tandem mass spectrometry. Biomed. Chromatogr. 2006; 20: 109-118.

[17] Folch J, Lees M, Stanley GHS. A simple method for the isolation and purification of total lipids from animal tissues. J. Biol. Chem. 1957; 226: 497-509.

[18] Hsu F, Turk J. Electrospray ionisation/tandem quadrupole mass spectrometric studies on phosphatidylcholines: the fragmentation processes. J. Am. Soc. Mass Spectrom. 2003; 14: 352-363.

[19] Reis A, Domingues P, Ferrer-Correia AJV, Domingues MRM. Fragmentation study of short-chain products derived from oxidation of diacyl-phosphatidylcholines by electrospray tandem mass spectrometry: identification of novel short-chain products. Rapid Commun. Mass Spectrom., 2004b; 18: 2849-2858.

[20] Reis A, Domingues P, Ferrer-Correia AJV, Domingues MRM. Tandem mass spectrometry of intact oxidation products of diacyl-phosphatidylcholines: evidence for the occurrence of the oxidation of the phosphocholine head and differentiation of isomers. J. Mass Spectrom. 2004c; 39: 1513-1522.

[21] Cheng C, Gross ML. Fragmentation mechanisms of oxofatty acids via high-energy collisional activation. J. Am. Soc. Mass Spectrom. 1998; 9: 620-627.

[22] Giuffrida F, Destaillats F, Skibsted LH, Dionisi F. Structural analysis of hydroperoxy- and epoxy-triacylglycerols by liquid chromatography mass spectrometry. Chem. Phys. Lipids. 2004, 131, 41-49.

[23] Stadtman ER, Levine RL. Free radical mediated oxidation of free amino acids and aminoacid residues in proteins. Aminoacids 2003, 25, 207-218.

[24] Chatgilialoglu C, Ferreri C. Trans lipids: the free radical path. Accounts of Chem. Res. 2005; 38: 441-448.

[25] Khaselev N, Murphy RC. Peroxidation of arachidonate containing plasmenyl glycerophosphocholines: facile oxidation of esterified arachidonate at carbon-5. Free Rad. Biol. Med. 2000; 29: 620-632.

[26] Reis A, Domingues MRM, Amado FML, Ferrer-Correia AJ, Domingues P. Separation of peroxidation products of diacyl-phosphatidylcholines by reverse phase Liquid Chromatography-Mass Spectrometry. Biomed. Chromatogr. 2005; 19: 129-137.

[27] Li Q-T, Yeo MH, Tan BK. Lipid peroxidation in small and large phospholipid unilamelar vesicles induced by water-soluble free radical sources. Biochem. Biophys. Res. Commun. 2000; 273: 72-76.

[28] Araseki M, Yamamoto K, Miyashita K. Oxidative stability of polyunsaturated fatty acid in phosphatidylcholine liposomes. Biosci. Biotechnol. Biochem. 2002; 66: 2573-2577.

[29] Barclay LRC, Vinqvist MR. Do spin traps also act as classical chain-breaking antioxidants? A quantitative kinetic study of phenyl tert-butyl nitrone (PBN) in solution and in liposome. *Free Rad. Biol. & Med.* 2000, **28**, 1079-1090.

[30] Taniguchi H, Madden KP. An *in situ* time-resolved ESR study of the kinetics of spin trapping by 5,5-dimethyl-1-pyrroline-N-oxide. J. Am. Chem. Soc. 1999; 121: 11875-11879.

[31] Kumamoto K, Hirai T, Kishioka S, Iwahashi H. Identification of a radical formed in the reaction mixtures of oxidised phosphatidylcholines with ferrous ions using HPLC-ESR and HPLC-ESR-MS. Free Rad. Res. 2005; 39: 987-993.

[32] Iwahashi H, Nishizaki K, Takagi I. Cytochrome c catalyses the formation of pentyl radical and octanoic acid radical from linoleic acid hydroperoxide. Biochem J. 2002; 361: 57-66.

[33] Kitaguchi H, Ohkubo K, Ogo S, Fukuzumi S. Direct ESR detection of pentadienyl radicals and peroxyl radicals in lipid peroxidation: mechanistic insight into regioselective oxygenation in lipoxygenases. *J. Am. Chem. Soc.* 2005, 127, 6605-6609.

[34] Venkataraman S, Schafer FQ, Buettner GR. Detection of lipid radicals using EPR. Antioxid. Redox Signal. 2004; 6: 631-638.

[35] Itabe H, Yamamoto H, Suzuki M, Kawai Y, Nakagwa Y, Suzuki A, Imanaka T, Takano T. *J. Biol. Chem.* 1996; 271: 33208-33217.

[36] Harrison KA, Davies SS, Marathe GK, McIntyre T, Prescott S, Reddy KM, Falck JR, Murphy RC. Analysis of oxidized glycerophosphocholine lipids using electrospray ionisation mass spectrometry and microderivatization techniques. J. Mass Spectrom. 2000; 35: 224-236.

[37] Koivusalo M, Haimi P, Heikinheimo L, Kostiainen R, Somerharju P. Quantitative determination of phospholipid compositions by ESI-MS: effects of acyl chain length, unsaturation and lipid concentration on instrument response. J. Lipid Res. 2001; 42,: 663-672.

[38] Dikalov SI, Mason RP. Spin trapping of polyunsaturated fatty acid-derived alkyl peroxyl radicals: reassignment to alkoxyl radical adducts. Free Rad. Biol. & Med. 2001; 30: 187-197.

[39] Spiteller P, Kern W, Reiner J, Spiteller G. Aldehydic lipid peroxidation products derived from linoleic acid. Biochim. Biophys. Acta. 2001; 1531: 188-208.

[40] Lee SH, Oe T, Arora JS, Blair IA. Analysis of Fe(II)-mediated decomposition of a linoleic acid-derived lipid hydroperoxide by liquid chromatography/mass spectrometry. *J. Mass Spectrom.* 2005, **40**, 661-668.

[41] Niknahad H, Siraki AG, Shuhendler A, Khan S, Teng S, Galati G, Easson E, Poon R, O'Brien PJ. Modulating carbonyl cytotoxicity in intact rat hepatocytes by inhibiting carbonyl-metabolizing enzymes. I. Aliphatic alkenals. Chem. Biol. Interact. 2003; 143-144: 107-117.

[42] Haynes RL, Szweda L, Pickin K, Welker ME, Townsend AJ. Structure-activity relationship for growth inhibition and induction of apoptosis by 4-hydroxy-2-nonenal in raw 264.7 cells. Mol. Pharmacol. 2000; 58: 788-794.

[43] Jian W, Arora JS, Oe T, Shuvaev VV, Blair IA. Induction of endothelial cell apoptosis by lipid hydroperoxide-derived bifunctional electrophiles. Free Rad. Biol. Med. 2005; 39: 1162-1176.

4. Phosphatidylcholine non-radical products

Manuscript V: Tandem mass spectrometry of intact oxidation products of diacyl-phosphatidylcholines: evidence for the occurrence of the oxidation of the phosphocholine head and differentiation of isomers

Manuscript VI: Radical oxidation of palmitoyl-lineloyl-glycerophosphocholine liposomes : identification of long-chain oxidized products by liquid-chromatography/tandem mass spectrometry

Manuscript VII: Fragmentation study of short-chain products derived from oxidation of diacyl-phosphatidylcholines by electrospray tandem mass spectrometry: identification of novel short-chain products

Manuscript VIII: Separation of peroxidation products of diacyl-phosphatidylcholines by reverse-phase liquid chromatography/mass spectrometry

JOURNAL OF MASS SPECTROMETRY
J. Mass Spectrom. 2004; **39**: 1513–1522
Published online in Wiley InterScience (www.interscience.wiley.com). DOI: 10.1002/jms.751

JMS

Tandem mass spectrometry of intact oxidation products of diacylphosphatidylcholines: evidence for the occurrence of the oxidation of the phosphocholine head and differentiation of isomers

A. Reis, P. Domingues, A. J. V. Ferrer-Correia and M. R. M. Domingues*

Department of Chemistry, University of Aveiro, 3810-193 Aveiro, Portugal

Received 1 July 2004; Accepted 17 September 2004

Three glycerophosphatidylcholine (GPC) phospholipids (oleoyl-, linoleoyl- and arachidonoylpalmitoylphosphatidylcholine) were oxidized under Fenton reaction conditions (H_2O_2 and Fe^{2+}), and the long-chain oxidation products were detected by electrospray mass spectrometry (ES-MS) and characterized by ES-MS/MS. The intact oxidation products resulted from the insertion of oxygen atoms into the phospholipid structure. The tandem mass spectra of the $[MNa]^+$ molecular ion showed, apart from the characteristic fragments of GPC, fragment ions resulting from neutral losses from $[MNa]^+$, and combined with loss of 59 and 183 Da from $[MNa]^+$. These ions resulted from cleavage of the bond near the hydroxy group by a charge-remote fragmentation mechanism, allowing its location to be pinpointed. The fragments thus formed reflected the positions of the double bonds and of the derivatives along the unsaturated fatty acid chain, giving very useful information, as they allowed the presence of structural isomers and positional isomers to be established. The identification of the fragment ion at *m/z* 163, which is 16 Da higher than the five-membered cyclophosphane ion (*m/z* 147), in some tandem mass spectra, is consistent with the oxidation of the phosphocholine head. Some ions were found to occur with the same *m/z* value; in two of the phospholipids and based on the MS/MS data, structural and positional isomers were differentiated. Our findings indicate that MS/MS is a valuable tool for the identification of the wide complexity of structural features occurring in oxidized phosphatidylcholines during lipid peroxidation in cellular membranes. Copyright © 2004 John Wiley & Sons, Ltd.

KEYWORDS: phosphatidylcholines; hydroxyl radical; peroxidation products; tandem mass spectrometry

INTRODUCTION

Phospholipids, namely glycerophosphatidylcholines (GPC), comprise the majority of the lipid membranes and are composed of a phosphocholine polar head linked to the glycerol moiety and fatty acid chains linked to the *sn*-2 and *sn*-1 positions.[1] These fatty acid chains may be either saturated or unsaturated chains. Among the unsaturated fatty acid chains occurring in biological samples, linoleic and arachidonic acids predominate.[2] Owing to the presence of double bonds, these compounds are susceptible to oxidative damage by reactive oxygen species (ROS), of which one of the most reactive is the hydroxyl radical,[3] formed under aerobic conditions. The lipid peroxidation process is a radical reaction that may induce the formation of oxidized intact phospholipids, known as long-chain products, such as hydroxy and/or hydroperoxide derivatives. The formation of such products is responsible for the increase in the phospholipid is polarity and consequently the decrease in the fluidity of the membrane or even disruption of the membrane integrity.[4,5] The lipid peroxidation process has been implicated in lung and liver cancer, diabetes and also in the pathogenesis of several neurodegenerative diseases.[6] In consequence, the study of the structure of oxidized phospholipid products has recently become of great interest.

Mass spectrometry (MS) has been applied to the identification of phosphatidylcholine oxidation products resulting from radical reactions.[7–9] Among the intact oxidized products identified by MS, the mass increments of +16, +32, +48 and +64 Da relative to the molecular mass of the native GPCs suggested the occurrence of hydroxy,[7] monohydroperoxy,[7–9] hydroxyhydroperoxide[8] and dihydroperoxide derivatives.[8,9] However, the characterization of peroxidation products based on MS results is very limited since no information regarding structural features is obtained. This limitation can be overcome by using tandem mass spectrometry (MS/MS) as it allows structural information to be obtained.

*Correspondence to: M. R. M. Domingues, Department of Chemistry, University of Aveiro, 3810-193 Aveiro, Portugal.
E-mail: mrd@dq.ua.pt
Contract/grant sponsor: PhD grant to Ana Reis (SFRH/BD/10358/2002), Foundation for Science and Technology;
Contract/grant number: POCTI 33279/99.
Contract/grant sponsor: FSE.

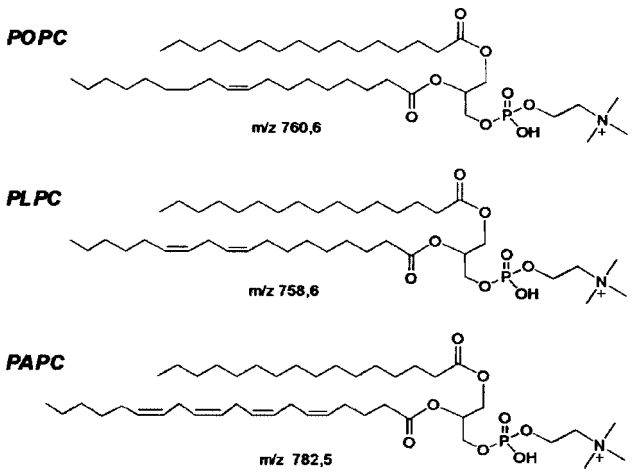

Scheme 1. Structure of the glycerophosphatidylcholines studied. POPC, 1-palmitoyl-2-oleoylglycerophosphatidylcholine; PLPC, 1-palmitoyl-2-lineloylglycerophosphatidylcholine; PAPC, 1-palmitoyl-2-arachidonoylphosphatidylcholine.

The identification of intact glycerophospholipids has been extensively studied by MS/MS using the fragmentation pattern characteristic for each class of phospholipids.[10,11] GPC assignment is based on the identification of fragments formed by loss of $N(CH_3)_3$ (59 Da), $HPO_4(CH_2)_2N(CH_3)_3$ (183 Da), $NaPO_4(CH_2)_2N(CH_3)_3$ (205 Da) and *sn-1* and *sn-2*.[11–14] So far, work dedicated to the investigation of the chemical structure of long-chain oxidized phosphatidylcholines using MS/MS is scarce,[7,15,16] relating mainly to the characterization of oxidized fatty acids obtained after saponification of oxidized phosphatidylcholine extracts[17–22] and later inferring the structures determined in the oxidized phospholipids. However, this procedure increases sample handling and also the possibility for misinterpretation of structural features.

In this paper we present and discuss the electrospray (ES) MS results obtained for the long-chain products formed by radical oxidation of phosphatidylcholines (oleoyl-, linoleoyl- and arachidonoylpalmitoylphosphatidylcholine). The structures of GPCs contain a common *sn*-1 chain (palmitic acid) and variation of the *sn*-2 chain (oleic, linoleic and arachidonic acid), and are shown in Scheme 1. The ions observed in the mass spectra were characterized by ES-MS/MS.

EXPERIMENTAL

Chemicals

The GPCs were obtained from Sigma (St. Louis, MO, USA) and used without further purification. Ammonium bicarbonate, $FeCl_2$ and H_2O_2 used for the peroxidation reaction were purchased from Merck (Darmstadt, Germany).

Preparation of GPC vesicles

Vesicles were prepared from stock solutions of 1 mg ml^{-1} and were dried under nitrogen stream. Ammonium bicarbonate buffer (pH 7.4) was added to a final phospholipid concentration of 50 mM and vortex mixed.[8]

Oxidation of GPC vesicles by Fenton reaction

Oxidative treatments performed on the GPC vesicles were performed by addition to 50 µl of phospholipid vesicles, 5 mmol $FeCl_2$ solution and 50 mmol of hydrogen peroxide (H_2O_2) in 0.5 ml of solution. This mixture was left to react in the dark at 37 °C for different periods of time with occasional sonication. The control was obtained by replacing H_2O_2 with water. The phospholipid oxidation products were extracted using a modification of the Folch method with chloroform–methanol (2 : 1, v/v).[23]

ES-MS

Positive ion mode ES mass spectra and tandem mass spectra were acquired in a Q-TOF 2 instrument (Micromass, Manchester, UK) using MassLynx software (version 4.0). The samples for electrospray analyses were prepared by diluting 5 µl of the sample in 1000 µl of chloroform–methanol (1 : 1, v/v). Samples were introduced into the mass spectrometer using a flow rate of 10 µl min^{-1}, setting the needle voltage at 3000 V with the ion source at 80 °C and the cone voltage at 35 V. Tandem mass spectra of molecular ions were obtained by collision-induced decomposition (CID), using argon as the collision gas (measured pressure in the Penning gauge $\sim 6 \times 10^{-6}$ mbar) and varying the collision energy between 15 and 35 eV. In MS and MS/MS experiments the time-of-flight (TOF) resolution (50% valley) was set to ~9000.

RESULTS AND DISCUSSION

Oxidation of 1-palmitoyl-2-oleoylglycerophosphatidylcholine (POPC)

The formation of POPC intact oxidation products through the hydroxyl radical was studied by ES-MS. The ES mass spectra obtained, in the presence (Fig. 1(A)) and absence (Fig. 1(B)) of H_2O_2, were compared. The ES mass spectra were constructed with the same number of scans and normalized to the base peak. As can be seen, in the absence of H_2O_2, the ES mass spectrum shows the molecular ion of the native PLPC as $[MH]^+$ (*m/z* 760.6) and $[MNa]^+$ (*m/z* 782.6), and the presence of both ions was taken into account

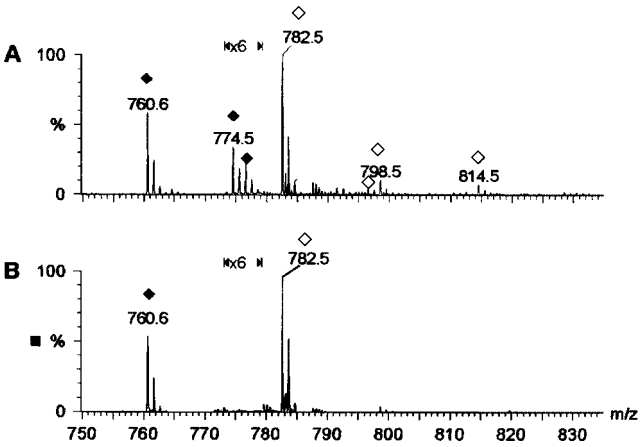

Figure 1. ES mass spectra of POPC obtained in the presence (A) and absence (B) of H_2O_2. Different symbols are shown for $[MH]^+$ molecular ions (solid diamonds) and for the $[MNa]^+$ molecular ions (empty diamonds).

in the interpretation of the ES mass spectrum obtained in the presence of H_2O_2 for the identification of long-chain oxidation products. In Fig. 1 the ES mass spectra show different symbols for $[MH]^+$ ions and $[MNa]^+$ ions for easier identification. The long-chain products identified resulted from the insertion of oxygen atoms in the unsaturated fatty acid chain. Some of the observed peroxidation products have already been observed during oxidative studies and their structure proposed, namely at m/z 796.6, 798.6 and 814.6[7,24] although the ion, observed with very low relative abundance, at m/z 830.6 (putative insertion of three oxygen atoms), was never reported. The presence of a double bond at C-9 leads to the presence of two monoallylic hydrogen atoms at C-8 and C-11 in the oleic acid moiety that are likely to be removed by the hydroxyl radical, leading to the occurrence of the oxidation reaction at very specific points of the unsaturated fatty acid chain.

In order to clarify the structure of the ions identified in the mass spectrum, and since $[MNa]^+$ molecular ions show higher relative abundance in the ES mass spectra than the $[MH]^+$ molecular ions and that cationized adducts are more informative,[14] structural characterization by CID was focused on the sodium adducts.

Tandem mass spectrometry of POPC long-chain products

The tandem mass spectra obtained for the $[MNa]^+$ molecular ions at m/z 782.6, 796.6, 798.6, 814.6 and 830.6 are shown in Fig. 2. The tandem mass spectra show abundant fragment ions due to loss of 59, 183 and 205 Da from the precursor ion, and also low-abundance fragment ions at m/z 147 and 184, all of them characteristic of the GPC derivatives.[10,11] These fragmentation pathways do not provide any structural information about the location of the oxygen atoms inserted during peroxidation; however, other fragment ions observed in the tandem mass spectra, with low relative abundance, may give an insight.

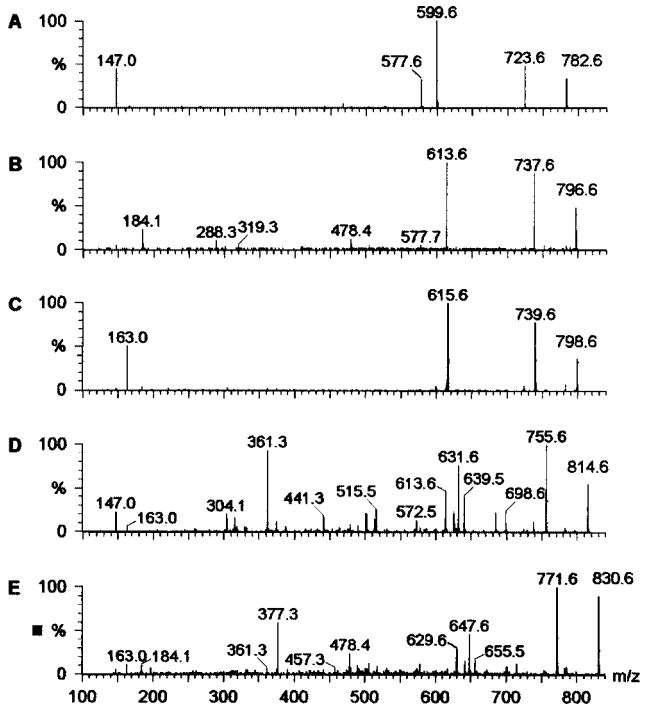

Figure 2. ES tandem mass spectra of the $[MNa]^+$ ions at (A) *m/z* 782.6, (B) *m/z* 796.6, (C) *m/z* 798.6, (D) *m/z* 814.6 and (E) *m/z* 830.6.

The tandem mass spectrum of ion at m/z 796.6 (Fig. 2(B)) shows fragment ions, with very low relative abundance, that may be attributed to homolytic cleavage of the β-bond (relative to the keto group) combined with loss of R_1COOH from the $[MNa]^+$ ion, namely observed at m/z 441, indicating cleavage of the carbon bond between C-11 and C-12, and observed at m/z 429 by cleavage of the carbon bond between C-10 and C-11 (Scheme 2) considering the keto group at C-10 and C-9, respectively. The fragmentation of the β-carbon bond relative to the keto group is in agreement with the fragmentation behaviour described for the keto derivatives of saturated fatty acids.[25]

The tandem mass spectrum of ion at m/z 798.6 (Fig. 2(C)) exhibits an abundant fragment ion at m/z 163. This fragment ion, which is 16 Da higher than that at m/z 147 (sodiated five-membered cyclophosphane[25]), was new and was proposed to be formed by the insertion of the hydroxy group at the phosphocholine head. This result suggests that the hydroxy derivative with the hydroxy group located at the polar head can also be formed (Scheme 3). This result is supported by the presence of the fragment ions observed at m/z 599 due to loss of 199 Da (183 + 16), and at m/z 575 due to loss of 221 Da (205 + 16). The identification of GPC oxidation products containing the hydroxy group at the polar head is, to our knowledge, novel, thus being the first time that this structural feature is identified and reported. Also, the presence of fragment ions due to loss of 59, 183 and 205 Da from the precursor ion in all the tandem mass spectra, along with the fragment ion at m/z 147, indicate the presence of the hydroxy derivative with the hydroxy group located at the unsaturated fatty acid chain. Overall, these results indicate the contribution of two very distinct, hydroxy derivatives one containing the hydroxy group at the polar head and the other with the hydroxy group on the unsaturated carbon chain. When present in the unsaturated fatty acid chain, it is proposed that the hydroxy group is most probably located either at C-8 or C-11.

The tandem mass spectrum of the ion at m/z 814.6 (Fig. 2(D)) exhibits fragment ions at m/z 698 and 684 resulting from loss of 116 ($C_7H_{14}O$) and 130 Da ($C_8H_{16}O$), respectively, from the precursor ion $[MNa]^+$. The fragment ions formed by combined loss of 116 and 130 Da with 59 Da from $[MNa]^+$ leading to the fragment ions at m/z 639 and 625, and combined with loss of 183 Da from $[MNa]^+$ leading to the fragment ions at m/z 515 and 501, are also observed (Scheme 2), in addition to the combined loss of 18 Da with 59 and 183Da. These fragment ions formed by charge-remote fragmentations involving one hydroxy group (Scheme 4) give an indication of the location of the hydroxy group along the unsaturated fatty acid chain, and are similar to those described for polyhydroxy derivatives of unsaturated fatty acids.[17] These fragment ions were consistent with the presence of a dihydroxy derivative, with both hydroxy

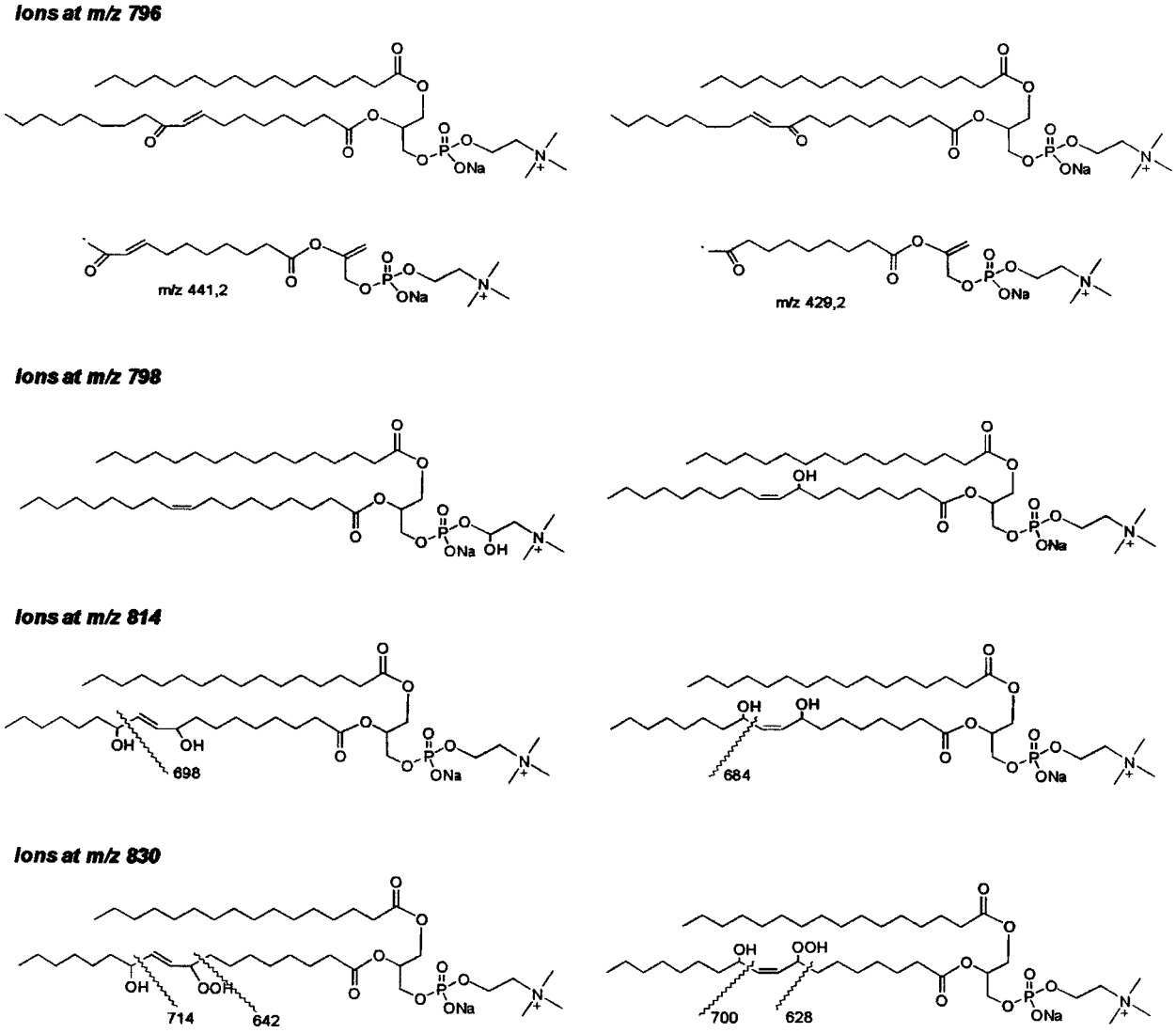

Scheme 2. Proposed structures for the POPC long-chain products observed in the mass spectrum at *m/z* 796.6, 798.6, 814.6 and 830.6.

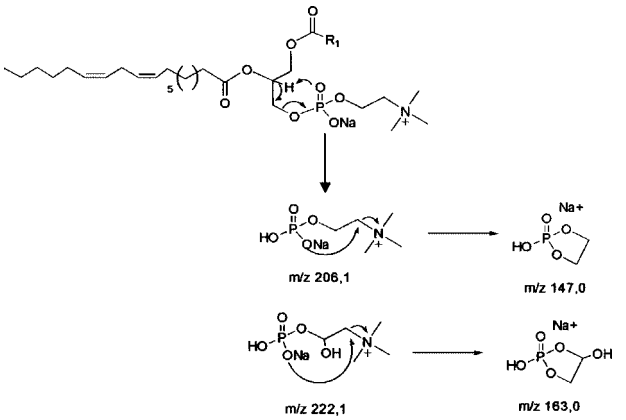

Scheme 3. Proposed structure for the fragment ion at *m/z* 163 observed in some of the tandem mass spectra.

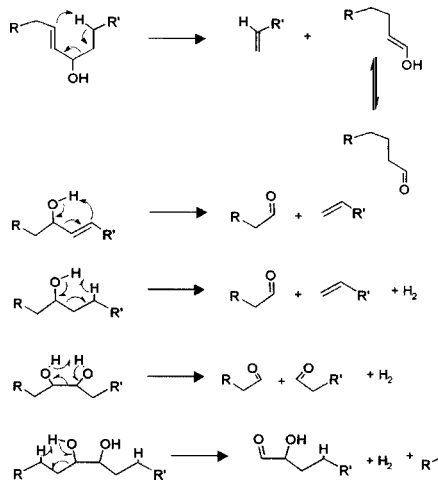

Scheme 4. Proposed fragmentation pathways involving the hydroxy group resulting in the cleavage of the carbon chain.

groups at the unsaturated fatty acid chain, namely at C-8/C-11 and C-9/C-12 (Scheme 2). On the other hand, the presence of the fragment ion at m/z 163 is indicative of a minor contribution of the dihydroxy derivative with one of the hydroxy groups placed at the polar head and the other at the unsaturated fatty acid chain. The fragment ion

formed by loss of 32Da (O_2) from the precursor ion, and indicative of the presence of the hydroperoxide derivative, was absent. Altogether, these results suggest the presence of the dihydroxy derivative over the hydroperoxide derivative and are in accordance with results reported elsewhere.[26]

The tandem mass spectrum of ion at *m/z* 830.6 (Fig. 2(E)), attributed to the hydroxyhydroperoxide derivative, exhibited the loss of 116 ($C_7H_{14}O$) and 130 Da ($C_8H_{16}O$) from the $[MNa]^+$ molecular ion, and combined with the loss of 59 Da and with the loss of 183 Da from $[MNa]^+$, similar to what was observed earlier for the dihydroxy derivative (*m/z* 814). Moreover, the fragment ion due to loss of 32 Da (*m/z* 798) is observed, confirming the presence of the hydroperoxide group. As can be seen, the fragment ions formed by loss of 116 (*m/z* 714) and 130 Da (*m/z* 700) allow the hydroxy group to be placed at C-12 (−116 Da) and at C-11 (−130 Da). Hence the fragment ions observed allowed the proposal of the occurrence of two structural isomers substituted at C-11(OH)/C-8(OOH) and also C-12(OH)/C-9(OOH) (Scheme 2). The proposal for the occurrence of hydroperoxide located at C-8 and C-9 is in full agreement with earlier proposed structures of phospholipid radical adducts with formation of alkoxyl at C-8 and at C-9 of POPC.[27] Once again, the fragment ion at *m/z* 163 is observed in the tandem mass spectrum (Fig. 2(E)) and therefore an additional structure with the hydroxy group at the polar head should be considered to contribute to the ion at *m/z* 830.6.

Oxidation of 1-palmitoyl-2-lineloylglycerophosphatidylcholine (PLPC)

The oxidation of PLPC by the Fenton reaction was monitored by ES-MS and upon comparison of the mass spectra obtained (Fig. 3), in the presence (A) and absence (B) of H_2O_2, new ions were observed. In the ES mass spectra, the native PLPC was observed as $[MH]^+$ molecular ions (solid diamonds) (*m/z* 758.6) and as $[MNa]^+$ molecular ions (crossed diamonds) (*m/z* 780.6). The peroxidation products observed in the ES mass spectrum (Fig. 3(A)) corresponded to the insertion of one to five oxygen atoms, where the most abundant ion was observed at *m/z* 812.6, with an increase of 32 Da relative to the native phospholipid,

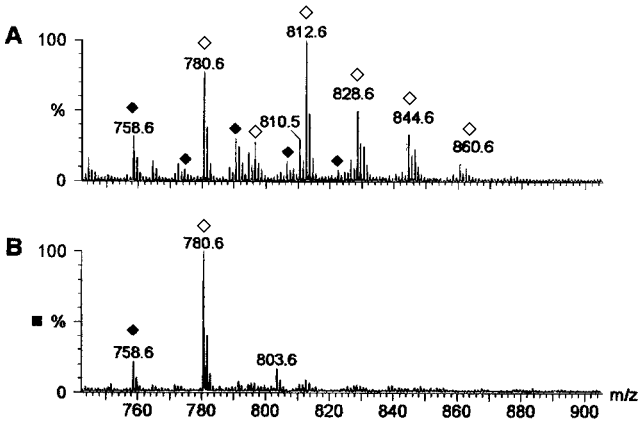

Figure 3. ES mass spectra of PLPC obtained in the presence (A) and absence (B) of H_2O_2. Different symbols are shown for $[MH]^+$ molecular ions (solid diamonds) and for the $[MNa]^+$ molecular ions (empty diamonds).

corresponding to the insertion of two oxygen atoms. This ion was previously reported by other workers and can be attributed to the hydroperoxide derivative[9] or to the dihydroxy derivative, as suggested by others.[26] The ion at *m/z* 794.6, 2 Da lower than the hydroxy derivative (*m/z* 796.6), was attributed to 1-palmitoyl-2-(ketooctadecadienoic acid)phosphatidylcholine, and although it has not yet been been described as a peroxidation product of PLPC, it is in accordance with the finding of 13-oxo-9,11-octadecadienoic during the peroxidation of linoleic acid.[9] To our knowledge, the remaining long-chain products have not been identified. The unsaturated fatty acid chain present as the *sn*-2 residue in PLPC is the linoleic acid that has one bis-allylic hydrogen atom at C-11 and can readily be abstracted by ROS leading, after double bond migration, to two stable radical species (C-9 and C-13). The insertion of oxygen can take place at those carbons. Subsequently, the linoleic acid may undergo further oxidation by abstraction of the remaining allylic hydrogen atoms at C-14 (in the C-9 isomer) or at C-8 (in the C-13 isomer).

In order to determine the structures formed, MS/MS experiments were performed on the $[MNa]^+$ molecular ions.

Tandem mass spectrometry of PLPC long-chain products

Tandem mass spectra obtained for the $[MNa]^+$ ions at *m/z* 796.6, 812.6, 828.6, 844.6 and 860.6, and shown in Fig. 4, exhibited the characteristic fragment ions due to loss of 59, 183 and 205 Da from the precursor ion. Other fragment ions observed in the tandem mass spectra resulted from loss of molecules combined with loss of 59 and 183 Da from $[MNa]^+$ ions.

The tandem mass spectrum of the ion at *m/z* 796.6 attributed to the hydroxy derivative shows an abundant fragment ion at *m/z* 163 (Fig. 4(A)). As discussed above, the presence of this fragment ion suggests the contribution of one hydroxy group placed at the phosphocholine polar head. This may be corroborated by the fragment ion due to loss of an *sn*-2 residue without the hydroxy group (*m/z* 516).

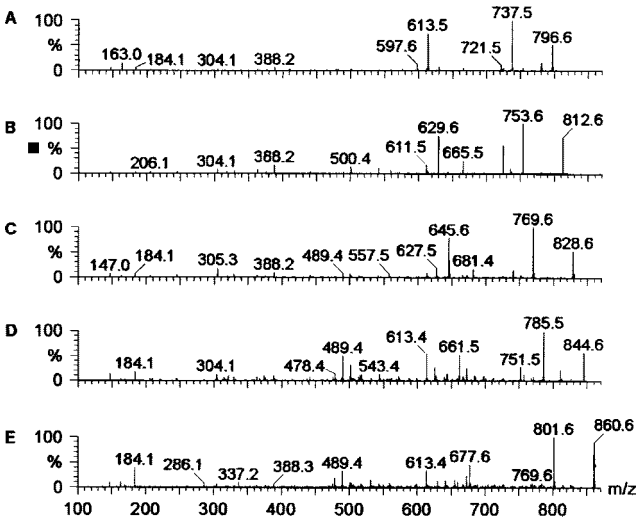

Figure 4. ES tandem mass spectra of the $[MNa]^+$ ions at (A) *m/z* 796.6, (B) *m/z* 812.6, (C) *m/z* 828.6 (D) *m/z* 844.6, and (E) *m/z* 860.6.

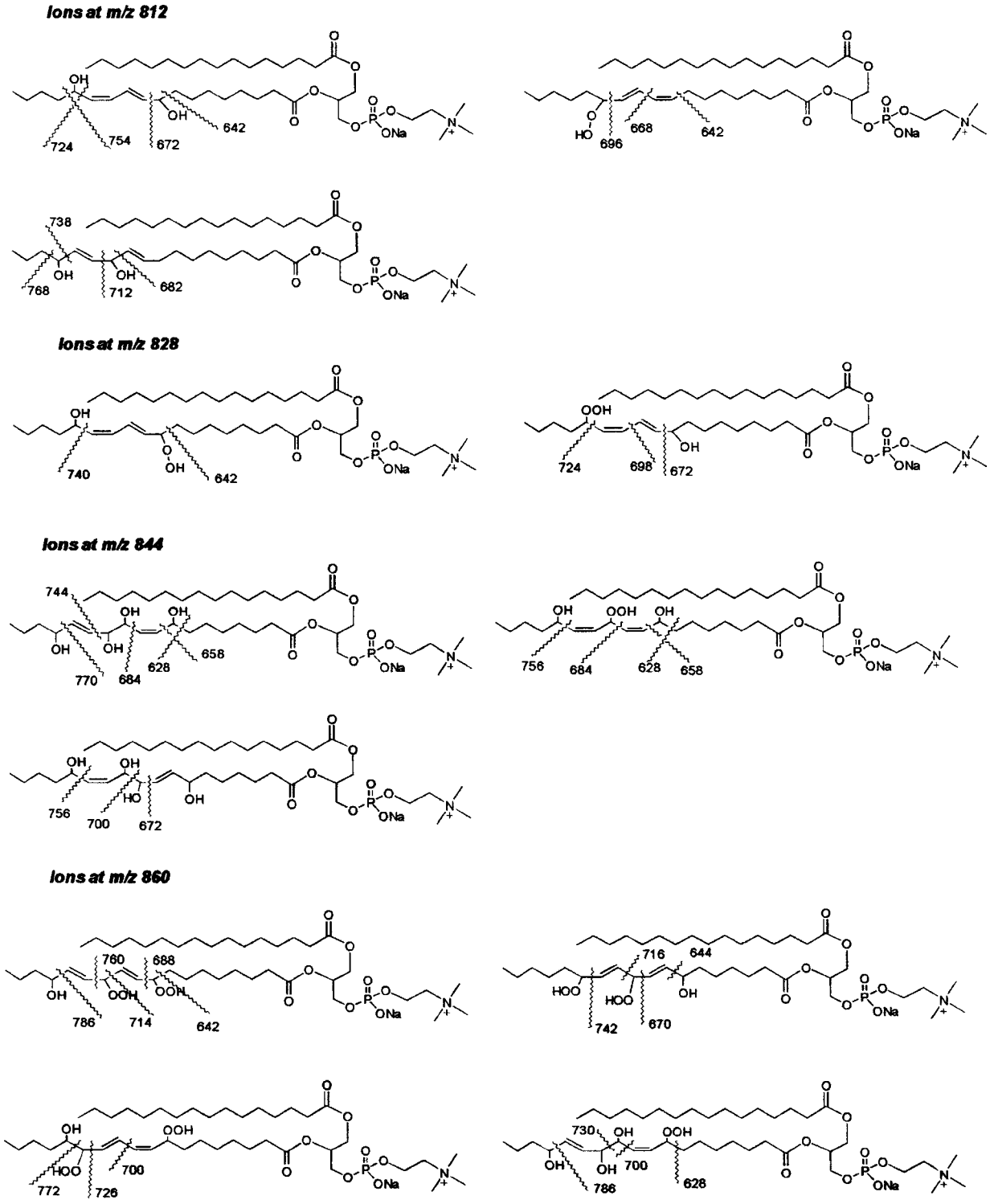

Scheme 5. Proposed structures for the PLPC long-chain products observed in the mass spectrum at *m/z* 812.6, 828.6, 844.6 and 860.6.

On the other hand, the presence of the fragment ion at *m/z* 500, formed by loss of a hydroxylated *sn*-2 residue from the precursor ion, suggests the presence of a second isomer with the hydroxy on the unsaturated fatty acid chain. The location of the hydroxy group in this isomer can be ascertained by the fragment ion at *m/z* 724 formed by loss of 72 Da (C_5H_{12}) from the precursor ion (Scheme 5), suggesting the presence of the 13-hydroxyoctadecadienoic acid derivative. Fragment ions due to loss of 72 Da combined with loss of 59 Da (*m/z* 665) and 183 Da (*m/z* 541) were also observed. Other fragment ions observed at *m/z* 725 resulting from homolytic cleavages (cleavage of the C-13—C-14 bond), also support the presence of the 13-hydroxyoctadecadienoic acid derivative, although the minor contribution of other isomers cannot be excluded.

The ion at *m/z* 812.6, with a 32 Da mass increase relative to the native PLPC (*m/z* 780.6), can be attributed either to the hydroperoxide or to the dihydroxy derivatives. The tandem mass spectrum of this ion (Fig. 4(B)) revealed the loss 18

(H_2O), 32 (O_2), 88 ($C_5H_{12}O$), 100 ($C_6H_{12}O$), 130 ($C_7H_{14}O_2$) and 140 Da ($C_9H_{16}O$) from the $[MNa]^+$ ion, combined with the loss of 59 and 183 Da from $[MNa]^+$. Particularly, the fragment ions due to loss of 88 Da may be formed by cleavage of the C-13—C-14 bond involving the hydroxy group at C-14 (Scheme 5), whereas the loss of 140 Da resulting from cleavage between C-9 and C-10 supports the contribution of the hydroxy groups at C-9, both supporting the contribution of the dihydroxy derivative with the hydroxy groups and C-9 and the remaining hydroxy group at C-14. Furthermore, the fragment due to loss of 32 Da in the tandem mass spectrum (Fig. 4(B)) confirms the contribution of the hydroperoxide derivative. The charge-remote fragmentation pathways for the formation of fragment ions involving the hydroxy groups are shown in Scheme 4, as described earlier for hydroxy fatty acids.[17]

The tandem mass spectrum of the ion at m/z 828.6 (Fig. 4(C)), attributed to the hydroxyhydroperoxide derivative, exhibited fragment ions due to loss of 18 (H_2O), 34 (H_2O_2), 74 ($C_4H_{10}O$), 88 ($C_5H_{12}O$), 104 ($C_5H_{12}O_2$), 130 ($C_7H_{14}O_2$) and 156 Da ($C_9H_{16}O_2$) from $[MNa]^+$, combined with the loss of 59 and 183 Da from $[MNa]^+$. The fragment ions formed by loss of 88 Da (m/z 740, 681 and 557, by cleavage of the C-13—C-14 bond suggest the occurrence of a hydroxy group at C-14 (Scheme 5), while the fragment ions due to loss of 74 Da (m/z 754, 695 and 571) place the hydroperoxide group at C-14 (Scheme 5). Also observed in the tandem mass spectrum is the loss of 34 Da from $[MNa]^+$, combined with the loss of 59 and 183 Da from $[MNa]^+$ that can be attributed to loss of H_2O_2. This loss can only be rationalized considering the occurrence of hydroxy groups in vicinal positions (as shown in Scheme 6). Hence the presence of the trihydroxy derivative should also be considered to be contributing to the relative abundance of the molecular ion at m/z 828.6. The occurrence of hydroxy groups in vicinal positions has already been proposed to occur during the analysis oxidation products of linoleic acid by gas chromatography/mass spectrometry (GC/MS).[9]

The tandem mass spectrum of the ion at m/z 844.6 (Fig. 4(D)), with a 64 Da mass increase relative to the native GPC (m/z 780.6), can be attributed either to the dihydroperoxide, to the dihydroxyhydroperoxide or to the tetrahydroxy derivative of PLPC. However, the abundant fragment ion due to loss of 34 Da (H_2O_2) from $[MNa]^+$, and combined with loss of 59 and 183 Da from $[MNa]^+$, suggested the preferential occurrence of the hydroxy derivatives over the hydroperoxide derivatives, with the hydroxy groups in vicinal positions, although fragments due to loss of 32 Da (O_2) from $[MNa]^+$, and combined with loss of 59 and 183 Da from $[MNa]^+$, were also observed. The loss of 74 ($C_4H_{10}O$), 88 ($C_5H_{12}O$), 118 ($C_6H_{14}O_2$), 144 ($C_8H_{16}O_2$), 160 ($C_8H_{16}O_3$) and 172 Da ($C_9H_{16}O_3$) from $[MNa]^+$, combined with the loss of 59 and 183 Da from $[MNa]^+$, were observed. The fragment ions due to loss of 74 Da (at m/z 770, 711 and 587) supported the presence of one hydroxy group at C-15, the fragment due to loss of 88 Da (at m/z 756, 697 and 573) places one hydroxy group at C-14, the fragment ions due to loss of 118 Da (at m/z 726, 667 and 543) place one hydroperoxide at C-13 and the fragment ions due to loss of 172 Da (at m/z 672, 613 and 489) place one hydroxy group at C-9 (Scheme 5). Overall, these data suggested the presence of several isomers contributing to the ion at m/z 844.6.

In the tandem mass spectrum of the ion at m/z 860.6 (Fig. 4(E)), the loss of 32 (O_2), 34 (H_2O_2), 74 ($C_4H_{10}O$), 88 ($C_5H_{12}O$), 100 ($C_6H_{12}O$), 118 ($C_6H_{14}O_2$), 146 ($C_7H_{14}O_3$), 160 ($C_8H_{16}O_3$) and 172 Da ($C_9H_{16}O_3$) from $[MNa]^+$, combined with the loss of 59 and 183 Da from $[MNa]^+$ ion, was observed, and the proposed structures are shown in Scheme 5. Based on the fragment ions identified, we suggest the presence of the hydroxydihydroperoxide derivative, although the trihydroxyhydroperoxide derivative cannot be excluded, owing to the presence of fragment ions due to loss of 34 Da, and also the minor contribution of the isomer containing the hydroxy group at the polar head.

Oxidation of 1-palmitoyl-2-arachidonoylphosphatidylcholine (PAPC)

The oxidation of PAPC by the Fenton reaction was monitored by ES-MS and on comparison of the mass spectra obtained (Fig. 5), in the presence (A) and absence (B) of H_2O_2, new ions were observed in the mass spectrum obtained after addition of H_2O_2. In the ES-mass spectra, the native PAPC and the peroxidation products were observed as $[MH]^+$ and $[MNa]^+$. Peroxidation products observed at m/z 836.5, 852.5, 868.5, 884.5, and 900.5 can be attributed to $[MNa]^+$ ions of hydroxy and hydroperoxide derivatives formed by insertion of 1–6 oxygen atoms in the unsaturated fatty acid, where some of them have already been proposed to occur by other workers.[8,9] On the other hand, peroxidation products showing a 2 Da decrease relative to the hydroxy

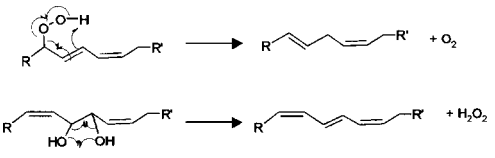

Scheme 6. Proposed fragmentation mechanism for the loss of O_2 (A) and H_2O_2 (B) observed in the tandem mass spectra of ions at *m/z* 828.6, 844.6 and 860.6.

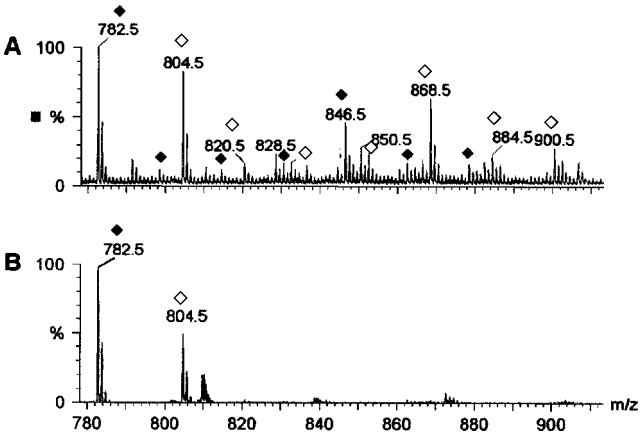

Figure 5. ES mass spectra of PAPC obtained in the presence (A) and absence (B) of H_2O_2. Different symbols are shown for $[MH]^+$ molecular ions (solid diamonds) and for the $[MNa]^+$ molecular ions (empty diamonds).

and hydroperoxide derivatives observed at *m/z* 850.5, 866.5, 882.5 and 898.5 can be attributed to the ketohydroxy or ketohydroperoxide derivatives, which in this case have never been reported. The most abundant ion at *m/z* 868.5 showing a 64 Da (four oxygen atoms) increase relative to the native phospholipid (*m/z* 804.5) can be attributed to the dihydroperoxide derivative, and is in accordance to what was observed in other studies.[8,9]

In order to confirm the proposed structures, MS/MS experiments were performed on these ions.

Tandem mass spectrometry of PAPC long-chain products

The tandem mass spectra of the ions at *m/z* 820.5, 836.5, 852.5, 868.5, 884.5 and 900.5, attributed to $[MNa]^+$ ions, are shown in Fig. 6. The tandem mass spectra of the ions studied exhibited increased fragmentation as the number of oxygen atoms in the structure increased, with loss of molecules from $[MNa]^+$, combined with the loss of 59 and 183 Da from the $[MNa]^+$ ion. The ion at *m/z* 820.5 was attributed to the hydroxy derivative, and the fragment ion due to loss of 32 Da (O_2) and the absence of fragment formed by loss of 34 (H_2O_2) and 36 Da ($2H_2O$) in the tandem mass spectrum of ion at *m/z* 836.5, suggested the presence of the hydroperoxide derivative. The tandem mass spectrum of the parent ion at *m/z* 852.5 exhibited fragments formed by loss of 36 Da ($2H_2O$) and no fragment ions due to loss of 32 and 34 Da, suggesting the presence of the trihydroxy derivative. The fragment ions due to loss of 32 (O_2) and 64 Da ($2O_2$) from the precursor ion observed in the tandem mass spectrum of ion at *m/z* 868.5 suggested the contribution of the dihydroperoxide derivative. The tandem mass spectrum of the parent ion at *m/z* 884.5 shows fragments formed by loss of 18 (H_2O) and 34 Da (H_2O_2) from the precursor ion that suggested the contribution of the pentahydroxy derivative, with some of the hydroxy groups occurring in vicinal positions. In the tandem mass spectrum of the parent ion at *m/z* 900.5, the presence of fragments formed by loss of 18 (H_2O) and 34 Da (H_2O_2) and the absence of fragments formed by loss of 32 Da (O_2) from the precursor ion suggested the contribution of the hexahydroxy derivative.

The results described here indicate that the formation of polyhydroxy derivatives is more favourable, or more stable, than the formation of polyhydroperoxide derivatives during *in vitro* peroxidation of PAPC. However, with the increase in oxygen atoms inserted in the unsaturated fatty acid chain, the number of possible structures (considering hydroxy and hydroperoxide groups) also increases, hence leading to a wide variety of structures that in the mass spectra are present as overlapping peaks. A detailed investigation of the possible isobaric structures (due to the presence of structural or positional isomers) that are contributing for each of the ions is currently being undertaken.

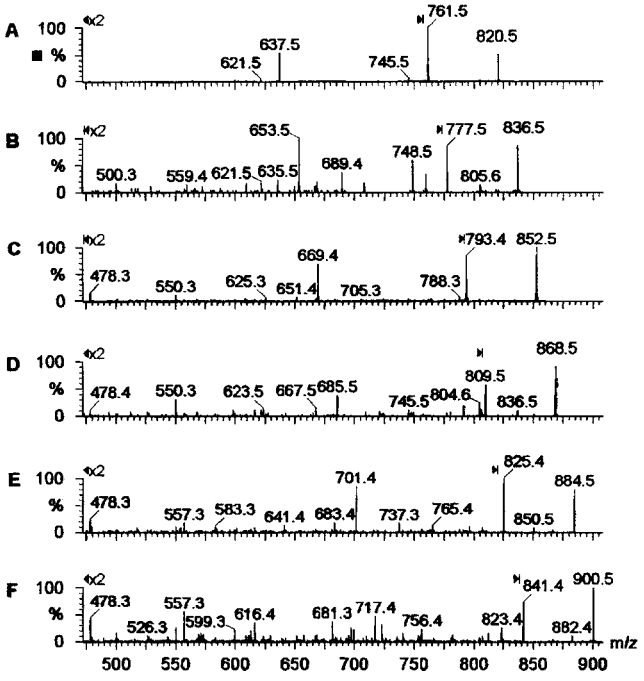

Figure 6. ES tandem mass spectra of the $[MNa]^+$ ions at (A) *m/z* 820.5, (B) *m/z* 836.5, (C) *m/z* 852.5, (D) *m/z* 868.5, (E) *m/z* 884.5 and (F) *m/z* 900.5.

Differentiation of structures occurring in different glycerophospholipids

The study performed on the intact peroxidation products of phosphatidylcholines evidenced the occurrence of oxidation products, with the same *m/z* value in different phosphatidylcholines observed at *m/z* 796.6, 812.6, 828.6, 830.6, 844.6 and 850.5. Considering all the ions identified, one example is described below.

The ion at *m/z* 830.6 was observed as an $[MNa]^+$ ion in POPC and in PLPC, and the tandem mass spectra (shown in Fig. 7) exhibit common fragments, due to loss of 59 and 183 Da from $[MNa]^+$, that are characteristic of GPC species. The tandem mass spectrum from POPC (Fig. 7(A)), discussed in the POPC section, shows the fragment at *m/z* 798 ($-O_2$), supporting the hydroxyhydroperoxide structure, and the fragments at *m/z* 700 and 714 place the substituent groups at C-11 and C-12, respectively. The tandem mass spectrum of ion from PLPC (Fig. 7(B)) shows fragment ions due to loss of 36 Da combined with the loss of 59 Da (*m/z* 735), but not of 32 Da, supporting the presence of the trihydroxy derivative, and the fragments due to loss of 88 Da from $[MNa]^+$ (*m/z* 742) and combined with loss of 59 Da (*m/z* 683) (Scheme 7)

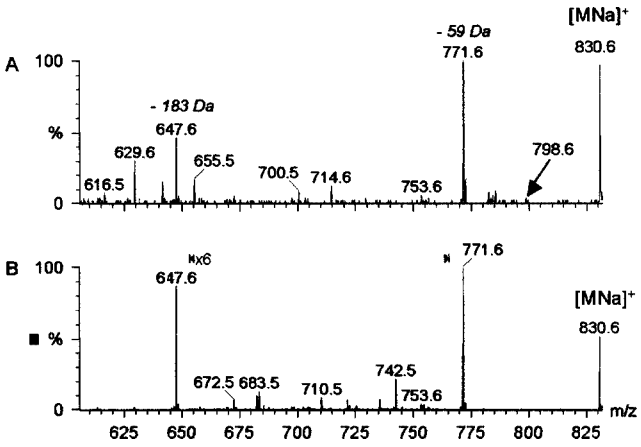

Figure 7. ES tandem mass spectra of the $[MNa]^+$ ions at *m/z* 830.6 observed in (A) POPC and (B) PLPC.

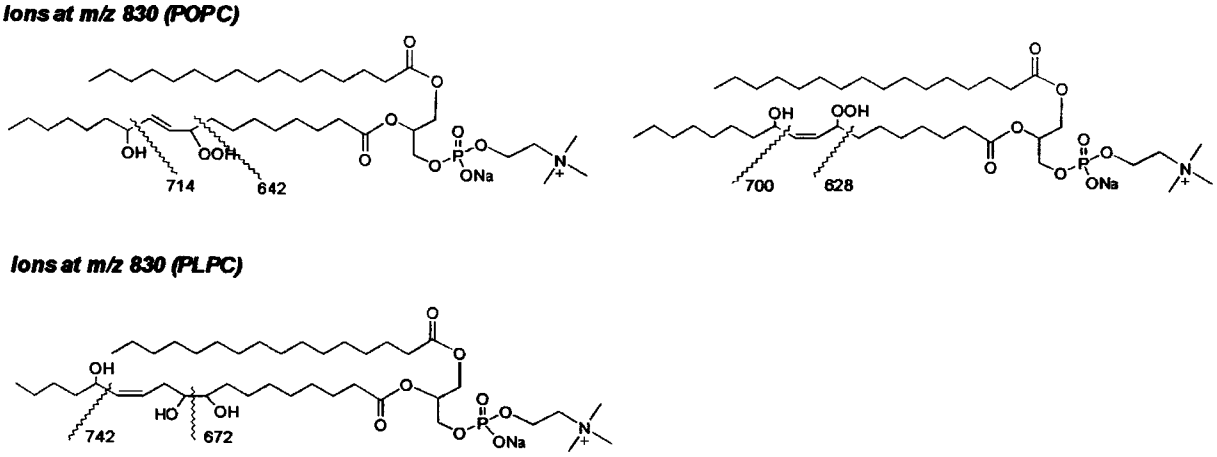

Scheme 7. Proposed structures for the ion at *m/z* 830.6 $[MNa]^+$ (PLPC).

suggest the presence of one of the hydroxy groups at C-14 and together with loss of 158 Da from $[MNa]^+$ (*m/z* 672), the remaining hydroxy groups at C-9 and C-10. Overall, the fragment ions described allow the differentiation of the ions at *m/z* 830.6 from POPC and PLPC. The occurrence of the trihydroxy derivative, with vicinal hydroxy groups, has never been reported in phosphatidylcholines, although other workers initially identified the 9,10,13-trihydroxyoctadecenoic group during the oxidation of linoleic acid.[28]

CONCLUSIONS

The formation of long-chain oxidation products of diacylglycerophosphatidylcholine species by reaction with the hydroxyl radical was monitored by ES-MS. The long-chain products resulting from the insertion of oxygen atoms into the unsaturated fatty acid chain corresponded to keto-, hydroxy-, hydroperoxide, dihydroperoxide, ketohydroxy and hydroxyhydroperoxide derivatives. The tandem mass spectra showed that under CID conditions, fragmentation pathways involving mainly by charge-remote processes were occurring involving the hydroxy groups present in the structure. This fragmentation pattern gave an indication of where the substituting groups were located. Additionally, it also allowed the proposal of the presence of several structural and positional isomers contributing to the ion with same *m/z* value. These results suggest that during lipid peroxidation, the formation of hydroxy derivatives is favoured over the formation of hydroperoxides. This may reflect the instability of hydroperoxides and the occurrence of homolytic decomposition in solution.

Furthermore, the identification of the fragment ion at *m/z* 163 in the tandem mass spectra of some radical-derived phospholipid products indicated that oxidation of the GPC polar head can also occur. This is the first time that oxidized phospholipid products with the hydroxy group placed at the polar head have been reported.

Acknowledgements

The authors gratefully acknowledge the financial support provided by the project POCTI 33279/99 and a PhD grant to Ana Reis (SFRH/BD/10358/2002), provided by the Foundation for Science and Technology (FCT) and FSE (III Quadro Comunitário de Apoio).

REFERENCES

1. Silvius JR. Structure and nomenclature. In *Phospholipid Handbook*, Gregor, Cevc G (eds). Marcel Dekker: New York, 1993; 1.
2. Yorek MA. Biological distribution. In *Phospholipid Handbook*, Gregor, Cevc G (eds). Marcel Dekker: New York, 1993; 745.
3. Pierre J-L. Chemistry of dioxygen and its activated species. In *Analysis of Free Radicals in Biological Systems*, Favier AE, Cadet J, Kalyanaraman B, Fontecave M, Pierre JL (eds). Springer Verlag: Berlin, 1995; 1.
4. Gupta CM. Phospholipids in Disease. In *Phospholipid Handbook*, Gregor, Cevc G (eds). Marcel Dekker: New York, 1993; 895.
5. Megli FM, Sabatini K. EPR studies of phospholipid bilayers after lipoperoxidation. 1. Inner molecular order and fluidity gradient. *Chem. Phys. Lipids* 2003; **125**: 161.
6. Spiteller G. Linoleic acid peroxidation—the dominant lipid peroxidation process in low density lipoprotein—and its relationship to chronic diseases. *Chem. Phys. Lipids* 1998; **95**: 105.
7. Facino RM, Carini M, Aldini G, Colombo L. Characterization of the intermediate products of lipid peroxidation in phosphatidylcholine liposomes by fast-atom bombardment mass spectrometry and tandem mass spectrometry techniques. *Rapid Commun. Mass Spectrom.* 1996; **10**: 1148.
8. Spickett CM, Pitt AR, Brown AJ. Direct observation of lipid hydroperoxides in phospholipid vesicles by electrospray mass spectrometry. *Free Rad. Biol. Med.* 1998; **25**: 613.
9. Spickett CM, Rennie N, Winter H, Zambonin L, Landi L, Jerlich A, Schaurs RJ, Pitt AR. Detection of phospholipid oxidation in oxidatively stressed cells by reverse-phase HPLC coupled with positive-ionisation electroscopy MS. *Biochem. J.* 2001; **355**: 449.
10. Han X, Gross RW. Structural determination of picomole amounts of phospholipids via electrospray ionisation tandem mass spectrometry. *J. Am. Soc. Mass Spectrom.* 1995; **6**: 1202.
11. Pelizzi N, Catinella S, Barboso S, Zanol M. Different electrospray tandem mass spectrometric approaches for rapid characterisation of phospholipid classes of Curosurf, a natural pulmonary surfactant. *Rapid Commun. Mass Spectrom.* 2002; **16**: 2215.
12. Domingues P, Amado FML, Santana-Marques MGO, Ferrer-Correia AJ. Constant neutral loss scanning for the characterization of glycerol phosphatidylcholine phospholipids. *J. Am. Soc. Mass Spectrom.* 1998; **9**: 1189.
13. Larsen A, Uran S, Jacobsen PB, Skotland T. Collision-induced dissociation of glycero phospholipids using electrospray ion-trap mass spectrometry. *Rapid Commun. Mass Spectrom.* 2001; **15**: 2393.
14. Hsu F, Turk J. Electrospray ionisation/tandem quadrupole mass spectrometric studies on phosphatidylcholines: the

fragmentation processes. *J. Am. Soc. Mass Spectrom.* 2003; **14**: 352.
15. Watson AD, Leitinger N, Navab M, Faull KF, Hörkö S, Witztum JL, Palinski W, Schwenke D, Salomon RG, Sha W, Subbanagounder G, Fogelman AM, Berliner JA. Structural identification by mass spectrometry of oxidized phospholipids in minimally oxidized low density lipoprotein that induce monocyte/endothelial interactions and evidence for their presence *in vivo*. *J. Biol. Chem.* 1997; **272**: 13 597.
16. Khaselev N, Murphy RC. Structural characterization of oxidised phospholipid products derived from arachidonate-containing plasmenyl glycerophosphocholine. *J. Lipid Res.* 2000; **41**: 564.
17. Wheelan P, Zirrolli JA, Murphy RC. Electrospray ionisation and low energy tandem mass spectrometry of polyhydroxy unsaturated fatty acids. *J. Am. Soc. Mass Spectrom.* 1996; **7**: 140.
18. Hall LM, Murphy RC. Electrospray mass spectrometric analysis of 5-hydroperoxy and 5-hydroxyeicosatetraenoic acids generated by lipid peroxidation of red blood cell ghost phospholipids. *J. Am. Soc. Mass Spectrom.* 1998; **9**: 527.
19. Nakamura T, Bratton DL, Murphy RC. Analysis of epoxyeicosatetraenoic and monohydroxyeicosatetraenoic acids esterified to phospholipids in human red blood cells by electrospray tandem mass spectrometry. *J. Mass Spectrom.* 1997; **32**: 888.
20. Nakamura T, Henson PM, Murphy RC. Occurrence of oxidized metabolites of arachidonic acid esterified to phospholipids in murine lung tissue. *Anal. Biochem.* 1998; **262**: 23.
21. Khaselev N, Murphy RC. Peroxidation of arachidonate containing plasmenyl glycerophosphocholines: facile oxidation of esterified arachidonate at carbon-5. *Free Rad. Biol. Med.* 2000; **29**: 620.
22. Dickinson JS, Murphy RC. Mass spectrometric analysis of leukotriene A4 and other chemically reactive metabolites of arachidonic acid. *J. Am. Soc. Mass Spectrom.* 2002; **13**: 1227.
23. Folch J, Lees M, Stanley GHS. A simple method for the isolation and purification of total lipids from animal tissues. *J. Biol. Chem.* 1957; **226**: 497.
24. Reis A, Domingues MRM, Amado FML, Ferrer-Correia AJV, Domingues P. Separation of peroxidation products of diacylphosphatidylcholines by reverse phase liquid chromatography-mass spectrometry. *Biomed. Chromatogr.* (accepted for publication).
25. Cheng C, Gross ML. Fragmentation mechanisms of oxofatty acids via high-energy collisional activation. *J. Am. Soc. Mass Spectrom.* 1998; **9**: 620.
26. Itabe H, Yamamoto H, Suzuki M, Kawai Y, Nakagwa Y, Suzuki A, Imanaka T, Takano T. Oxidized phosphatidylcholines that modify proteins: analysis by monoclonal antibody against oxidized low density lipoprotein. *J. Biol. Chem.* 1996; **271**: 33 208.
27. Reis A, Ferrer-Correia AJV, Domingues P, Domingues MRM. Identification by electrospray tandem mass spectrometry of spin trapped free radicals from oxidized 2-oleoyl-1-palmitoyl-*sn*-glycero-3-phosphocholine. *Rapid Commun. Mass Spectrom.* 2004; **18**: 1047.
28. Spiteller P, Kern W, Reiner J, Spiteller G. Aldehydic lipid peroxidation products derived from linoleic acid. *Biochim. Biophys. Acta* 2001; **1531**: 188.

Radical peroxidation of palmitoyl-lineloyl-glycerophosphocholine liposomes: Identification of long-chain oxidised products by liquid chromatography-tandem mass spectrometry

*Ana Reis, M.R.M. Domingues, F.M.L. Amado, A.J. Ferrer-Correia, P. Domingues **
Chemistry Department, University of Aveiro, 3810-193 Aveiro, Portugal

Abstract

Liquid chromatography coupled with electrospray tandem mass spectrometry (LC-MS/MS) was used to identify palmitoyl-lineloyl-glycerophosphatidylcholine oxidation products (PL[O_{1-5}]PC). The product-ion spectra of $[MH]^+$ ions exhibited product ions characteristic of phosphatidylcholines, product ions formed by loss of nH_2O and H_2O_2 from $[MH]^+$ ions suggesting the presence of the keto, hydroxy, epoxy or hydroperoxide groups, and product ions involving the hydroxy group, that were structurally informative about the position of these groups and of the double bonds along the carbon chain of lineloyl moiety. Based on the LC-MS/MS data, structural and positional isomers of oxPLPC were identified.

Correspondence should be sent to:
Pedro Domingues, Department of Chemistry, University of Aveiro, 3810-193 Aveiro, Portugal
e-mail address: pedrom@dq.ua.pt, telephone number: +351-234-370699, fax number: +351-234-370084

Introduction

Free radicals are formed within the cell during aerobic processes, and generally are trapped by enzymatic and/or non-enzymatic antioxidant systems [1]. However, when an imbalance between the radicals formed and the antioxidant systems occurs oxidative damage takes place. For this reason, in recent years, oxidative damage of biomolecules by free radicals has received increasing attention due to the growing evidence of its involvement in many age related diseases, such as atherosclerosis, Alzheimer, Parkinson, multiple sclerosis, and some liver and lung diseases [1]. Free radicals possess high reactivity towards unsaturated compounds such as DNA bases, amino acid residues and polyunsaturated fatty acids (PUFA) [2]. Among the radical species, one of the most reactive is the hydroxyl radical ($HO^{\bullet}$) that may be formed through the reaction of hydrogen peroxide (H_2O_2) in the presence of ferrous ions (Fe^{2+}) [3], released during erythrocyte senescence and/or from heme-proteins [4]. Most of the work performed to identify the modifications induced during oxidative damage to biomolecules is focused on the structural changes induced to peptides and proteins. However, phospholipids present in cell membranes, low density lipoproteins (LDL), cholesterol and triglycerides [2], play an important role in membrane structure, metabolism and signal transduction [5], and have not been so extensively studied. The changes induced by free radicals to phospholipids occur on the PUFA acyl chains, which are esterified to the polar head, and can result in the formation of peroxidation products with a shortened chain with an oxo or carboxy terminal [6], or products resulting from the insertion of oxygen atoms in the intact chain [7-9], or radical species that in turn propagate the peroxidation reaction [10-12]. The structural changes caused by radical peroxidation in phospholipids, such as phosphatidylcholines, affect the physical properties of the membrane bilayers [13,14] which are reflected in membrane integrity [15]; and are also responsible for covalent cross-linking between oxidised lipid moieties and proteins [16,17] leading to inactivation of membrane proteins and/or receptors [18]. In some cases, oxidised phospholipids show biological activity similar to platelet aggregating factors (PAF) [19], or may act as promoters in the expression of several genes, as proposed in the tumorogenesis of breast cancer cells [20].

The literature reporting on the study of oxidised phosphatidylcholines by mass spectrometry (MS) is focused on the identification of either short-chain products [21-23] or long-chain products [24-27]. In the case of long-chain products the increase of oxygen atoms inserted into the unsaturated fatty acid increases structural variability (structural and positional isomers), limiting the identification [28,29]. The knowledge about the structure of phospholipid peroxidation products is of major importance as, for example, for

the identification of products proposed as potential biomarkers [9,30]. For example, the concentration of phosphatidylcholine hydroperoxide (PCOOH) was found to be significantly higher in the plasma of patients with blood alcohol when compared with controls [30]. The use of HPLC coupled with Mass Spectrometry (LC-MS) [26,27,31] already used for the screening of short-chain phosphatidylcholine products [31] and for the separation of long chain phosphatidylcholine products [26,27,31] may in association with tandem mass spectrometry (MS/MS), provide further insight to the structure of products formed. To date, most of the studies performed on the study of oxidation products of phosphatidylcholines by LC-MS/MS report the characterisation of oxidised fatty acids obtained by saponification [7,8,28,29], and the results obtained were further extrapolated to the intact phosphatidylcholine peroxidation products. To our knowledge, attempts made on the analysis of the oxidised long-chain phosphatidylcholine products itself by LC-MS/MS were recently reported, in which the authors have identified oxo-, hydroxy-, hydroperoxide- and tri-hydroxy derivatives of PLPC based on the presence of the product ions due to loss of water molecules from the precursor ion to propose [32]. No further structural information, regarding the location of the proposed substitutents along the unsaturated carbon chain, were made by the authors. For the long-chain PLPC products, the structural diversity that can occur for a single ion, as was reported by the observation of the increase of the number of chromatographic peaks as the number of oxygen atoms augmented [26,27,31,32], suggested the contribution of isomers, which can only be interpreted by LC coupled with MS/MS.

In this work, we present and discuss the results obtained by liquid chromatography coupled with electrospray tandem mass spectrometry (LC-MS/MS) of radical oxidised long-chain palmitoyl-lineloyl-glycerophosphatidylcholine (PLPC) phospholipid liposomes. Using the LC-MS/MS fragmentation patterns, namely the product ions due to loss of water and hydrogen peroxide together with other product ions attributed to cleavages in the unsaturated fatty acid chain, different peroxidation products will be identified in more detail, with focus on the formation of the different isomers, as the result of GPC radical oxidation.

Experimental

Preparation and oxidation of GPC vesicles

Vesicles were prepared from stock solutions of 1mg/mL of phospholipids and were dried under nitrogen stream. Ammonium bicarbonate buffer (5 mM, pH 7.4) was added to a final phospholipid concentration of 50mM, and the mixture was vortexed. Oxidative treatments performed on the GPC vesicles were done as described elsewhere [31]. Briefly, oxidative treatments using Fe (II) and hydrogen peroxide (H_2O_2) were carried out by adding to 50 μL of phospholipid vesicles, 5 mmol $FeCl_2$ solution and 50 mmol of H_2O_2 in 0.5 mL solution. This mixture was left to react at 37˚C in the dark for 24 hours with occasional sonication. The phospholipid oxidation products were extracted using the Folch method with chloroform:methanol (2:1, v/v) [33].

Liquid Chromatography-electrospray mass spectrometry (LC-MS and LC-MS/MS)

The HPLC-MS study was performed with a Waters Alliance (Milford, USA) Model 2690 equipped with a UV detector (Knauer K-2500). An APEX 300 C4 7μm (250 mm x 4.6mm I.D., Jones Chromatography) column with a flow rate of 1.0 mL/min was used for the separation of 50 μL injections. The column temperature was maintained at 30ºC. A gradient of acetonitrile (eluent B) and ammonium acetate, 5mM (acetonitrile/ammonium acetate, 5mM (50/50) (eluent A)) was employed to obtain suitable separation. The linear gradient used was as follows: 20%B (10 minutes), followed by a linear increase from 20% to 80%B (30 minutes) remaining in 80%B (5 minutes). A 1:20 home made splitter, redirected the flow (50 μL) to the MS interface through a capillary (i.d. 150 μm) of approximately 20 cm long.

The Q-TOF2 (Micromass, Manchester, UK) mass spectrometer using a MassLynx software system (version 4.0) was operated in the positive ion mode with a capillary voltage of 3000V, the cone voltage of 35V, the source block temperature set to 100ºC and the desolvation temperature set to 200ºC. Mass spectra were obtained over a mass range of *m/z* 50-1000. The LC-MS/MS experiments were performed by selecting the precursor ion of interest using Q1 and collisionally inducing fragmentation, using argon as the collision gas. The collision energy varied according to the ion of interest (between 30-35 eV). For accurate mass measurements of each of the ion species studied, the lock mass in each product ion mass spectrum was the calculated monoisotopic mass/charge ratio of the precursor ion.

Results and Discussion

Long-chain PLPC products resultant from radical oxidation observed as $[MH]^+$ ions at *m/z* 774.6, 790.6, 806.6, 822.6 and 838.6 [31], resulted from the insertion of one to five oxygen atoms into the *sn*-2 unsaturated fatty acid chain of the linoleic acid, since the palmitic acid (saturated fatty acid as *sn*-1 residue) is resistant to radical oxidation [34]. The RIC chromatogram obtained for each ion was plotted against the RIC chromatogram of the native PLPC (*m/z* 758.6) and is depicted in Fig. 1. Ions exhibiting the same *m/z* values were also reported during radiation-induced peroxidation of PLPC liposomes [26].

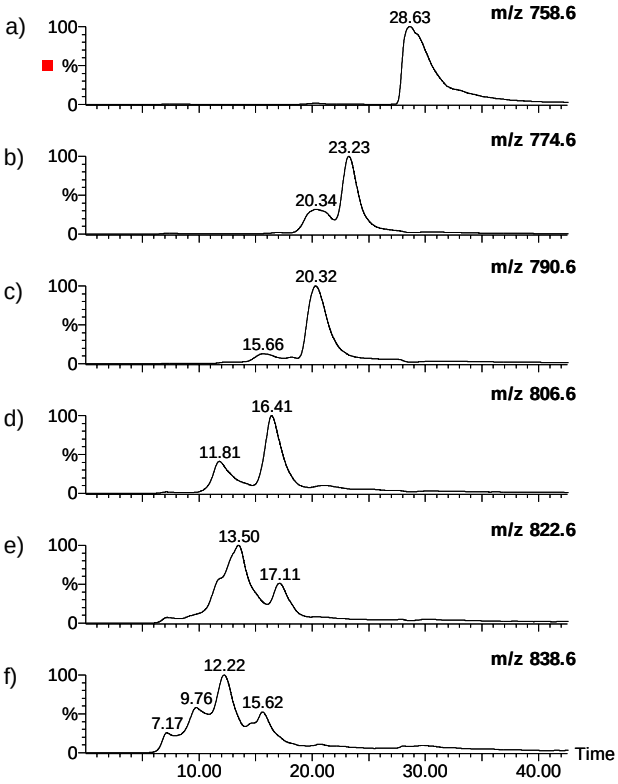

Fig. 1. Reconstructed Ion Chromatograms (RIC) of $[MH]^+$ ions of PLPC (*m/z* 758.6) and PLPC radical peroxidation products with *m/z* 774.6, 790.6, 806.6, 822.6 and 838.6.

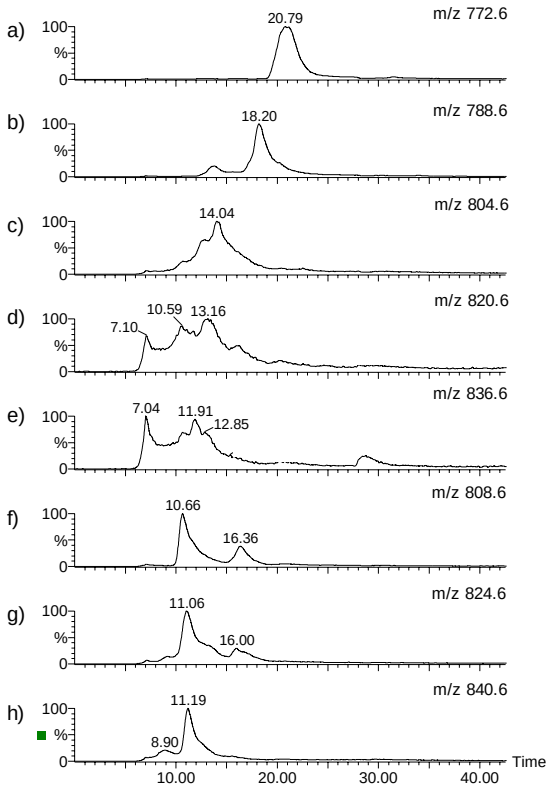

Fig. 2. Reconstructed Ion Chromatograms (RIC) of $[MH]^+$ ions of PLPC radical peroxidation products with *m/z* 772.6, 788.6, 804.6, 820.6, 836.6, 808.6, 824.6 and 840.6.

Other peroxidation products observed in the LC-MS spectrum at *m/z* 772.6, 788.6, 804.6, 820.6 and 836.6 (Fig. 2), exhibiting 2 Da mass decrease relative to the previous ions, were also resultant from the insertion of oxygen atoms and were attributed to $[MH]^+$ of the keto, keto-hydroxy, keto-hydroperoxy and keto-poly hydroxy derivatives. The RIC chromatograms obtained for the keto derivatives (*m/z* 772.6, 788.6, 804.6, 820.6 and 836.6) showed the elution of peaks with different retention times (Fig. 2) when compared with the products with the same number of oxygen atoms (*m/z* 774.6, 790.6, 806.6, 822.6 and 838.6), shown in Fig. 1. Oxo PLPC derivatives (*m/z* 772.6, 788.6 and 804.6) were identified in oxidised LDL [21] and more recently in the rat heart tissue [32]. Other ions with *m/z* 808.6, 824.6 and 840.6 (Fig. 2), exhibited 2 Da increase relative to the ions at *m/z* 806.6, 822.6 and 838.6, and were only observed for the peroxidation products containing 3 or more oxygen atoms. The LC-MS/MS spectra for the different ions present in each chromatographic peak were obtained and will be discussed in the following sections and used for structure elucidation. The ions with *m/z* 820.6, 824.6, 836.6, 838.6 and 840.6 were formed with very low relative abundance, which restricted the acquisition of the product-ion spectra.

Peroxidation products by insertion of one oxygen atom (m/z 774.6 and 772.6)

The ion at *m/z* 774.6, showed two major peaks eluting at 20.4 and 23.2 min (Fig. 1b), and the LC-MS/MS spectra obtained are shown in Fig. 3.

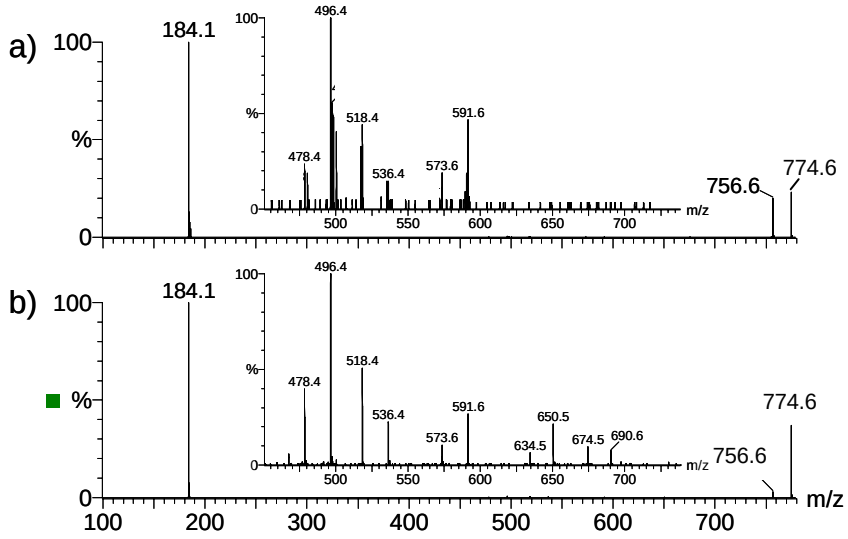

Fig. 3. LC-MS/MS spectra of $[MH]^+$ ion at *m/z* 774.6, a) rt= 20.3 min and b) 23.2 min.

The insertion of one oxygen atom in the linoleic acid moiety may correspond to the hydroxy- or the epoxy-derivatives of PLPC. The LC-MS/MS spectrum obtained for each

peak and selecting the parent ion at *m/z* 774.6 (Fig. 3a and b) showed the presence of common product ions at *m/z* 756.6 (-H_2O), 518.4 (-R_1COOH), 496.4 (-R_2=C=O), 478.4 (-R_2COOH) and 184.1 (phosphocholine head), which are characteristic losses during GPC fragmentation [35,36]. The LC-MS/MS spectrum obtained for the major peak (rt 23.2 min, Fig. 3b) exhibited the product ions at *m/z* 634.5 (-$C_9H_{16}O$), 650.5 (-C_9H_{16}), 674.5 (-$C_6H_{12}O$) and 690.6 (-C_6H_{12}), with loss of aldehydes and alkenes molecules. These losses resulted from cleavage of the C-C bond near the hydroxy group through a McLafferty like rearrangement with hydrogen transfer [25].

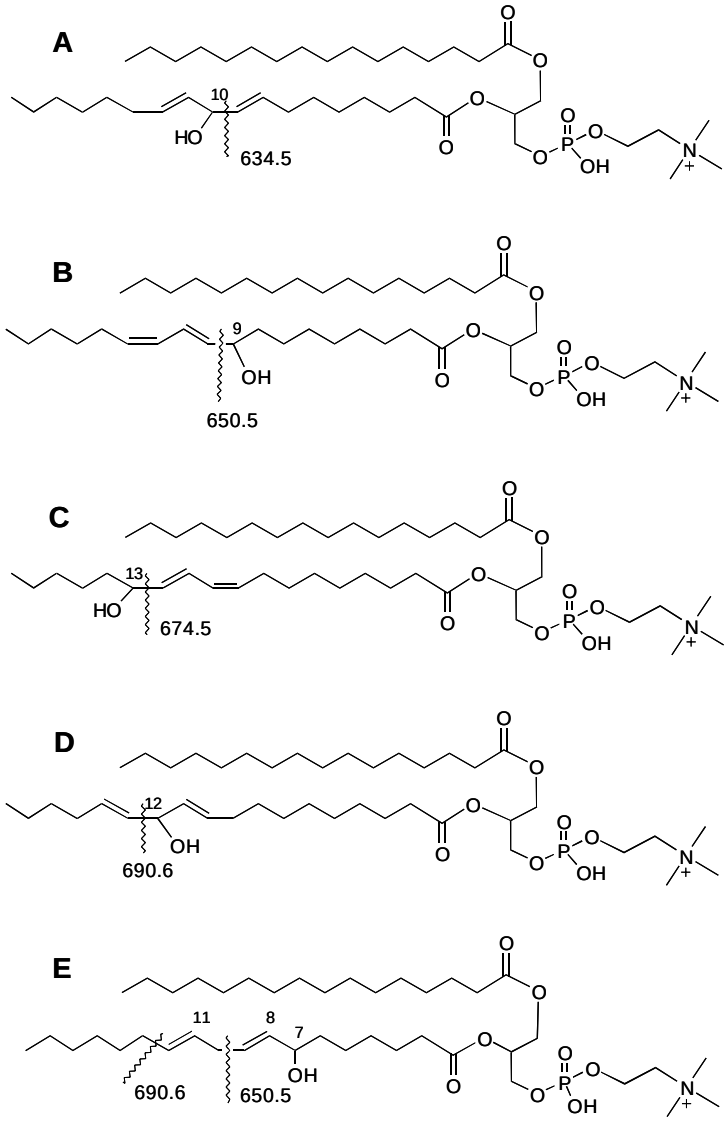

Scheme 1. Proposed structures for the ions at *m/z* 774.6 of PLPC oxidation products.

The cleavages are charge remote fragmentations and structurally informative allowing pinpointing the hydroxy groups at C-10, C-9, C-13 and C-12, respectively (Scheme 1A-D). Previously, other authors described the product ion spectra of oxidised

phosphatidylcholines obtained in QTOF instruments in which product ions observed in the *m/z* region between 600 and 750 were not object of discussion [27,32]. The elemental composition determined for each product ion by accurate mass measurements (Table 1), allows to confirm the proposed structure, as can be seen for the product ion at *m/z* 650.5, $C_{33}H_{65}NO_9P^+$, showing an error of 10.1 mDa (15.5 ppm) between the observed and calculated masses. The lock mass of the product ion spectrum was calculated using the monoisotopic mass/charge of the precursor ion (*m/z* 774.5649).

Table 1. Empirical formula, observed and calculated mass/charge ratios, double bond equivalents (DBE), and mass errors of the main fragments observed in the LC-MS/MS spectra for the ion at *m/z* 774.6.

Precursor ion $[MH]^+$	Product Ion Predicted formula	Observed mass	Calculated mass	DBE	error (mDa)	error (ppm)
774.6	$C_{33}H_{65}NO_8P^+$	634.4442	634.4448	2.5	-0.6	-0.9
	$C_{33}H_{65}NO_9P^+$	650.4498	650.4397	2.5	10.1	15.5
	$C_{36}H_{69}NO_8P^+$	674.4614	674.4761	3.5	-14.7	-21.8
	$C_{36}H_{69}NO_9P^+$	690.4786	690.4710	3.5	7.6	11.0

The difference of 40 Da that is observed between the product ions at *m/z* 634.5 and 674.5, and also between the product ions at *m/z* 650.5 and 690.6 is, according to Hsu and Turk [37], indicative of allylic cleavages between double bonds. Taking this into consideration, the product ions at *m/z* 650.5 and 690.6 indicate the presence of the 7-hydroxy octadecadienoyl derivative (Scheme 1E), instead of the proposed 9-hydroxy and 12-hydroxy *sn*-2 acyl derivatives. However, for the product ions at *m/z* 634.5 and 674.5, which are also 40Da apart, a secondary alternative structure cannot be rationalised for these product ions. For this reason it is assumed that the product ions at *m/z* 634.5, 650.5, 674.5 and 690.6 are due to fragmentation in the vicinity of the hydroxy groups. The identification of the 9-, 10-, 12- and 13-hydroxy *sn*-2 acyl derivatives suggest that, although separation between positional isomers was not achieved under the elution conditions (one peak observed in Fig. 2a), these isomers can be discriminated through their LC-MS/MS data. The LC-MS/MS data could be of value since, for example, the 9-hydroxy derivative of PLPC was proposed as biomarker in diabetic patients as was found to be elevated in erythrocyte membranes [9].

The LC-MS/MS spectrum of the ion at *m/z* 774.6 (Fig. 3a) for the peak eluting at 20.4 min (Fig 1b) only showed the product ions at *m/z* 756.6 (-H_2O), 591.6 (-183 Da), 573.6 (-183-18 Da), 496.4 (-R_2=C=O) and *m/z* 184.1 ($[H_2PO_4(CH_2)_2N(CH_3)_3]^+$), giving no specific structural information. It is proposed that these ions may be attributed to epoxy derivatives of the linoleoyl moiety. Although, no fragmentation was observed under

low-energy conditions, under high-energy conditions, epoxy fatty acids are described to undergo cleavage in the vicinity of the epoxy ring [8, 38]. Furthermore, epoxy derivatives of eicosatetraenoic acids were considered to be unstable at 25ºC and decrease their stability with increasing temperature, as reported earlier [39]. Nonetheless, both epoxy- and hydroxy- derivatives of eicosatetraenoic acid have been identified and quantified in human red blood cells, although, as stated by the authors, no statistical differences were observed for the epoxy derivatives, relative to the controls upon oxidative damage [8]. The peroxidation products identified with the suggested location for the substituting groups are summarised in Table 4.

The LC-MS/MS spectrum obtained for the ion at *m/z* 772.6 (data not shown), attributed to the conjugated keto derivative eluting at 20.8 min (Fig. 2a), exhibited the product ions at *m/z* 754.6, 589.5, 534.4, 516.4, 496.4 and 478.4, together with the product ion at *m/z* 184.1 (phosphocholine head) are characteristic losses from phosphatidylcholines [35,36], and did not provide any specific structural information about the location of the keto group other than the presence of the keto group at the oxidised *sn*-2 fatty acyl chain, which is given by the 2-oxolineloyl-lyso-phosphatidylcholine product ion (*m/z* 534.4) and its dehydration product ion with *m/z* 516.4. Thus, the 9-keto-10,12-octadecadienoic acid and the 13-keto-9,11-ocatadecadienoic acid, which are the most probable oxo derivatives, can be proposed as *sn*-2 acyl chains contributing to the relative abundance of the ion at *m/z* 772.6.

Peroxidation products by insertion of two oxygen atoms (m/z 790.6 and 788.6)

The LC-MS/MS spectra obtained for the ion at *m/z* 790.6, which eluted in two peaks (Fig. 1c), is shown in Fig. 4. The insertion of two oxygen atoms in the linoleic acid moiety may result in the formation of hydroperoxide, epoxy-hydroxy and di-hydroxy derivatives.

The LC-MS/MS spectra (Fig. 4) exhibit the product ions characteristic of $[MH]^+$ diacyl GPC ions such as loss of 183 Da, loss of R_2=C=O and of R_2COOH. The product ion at *m/z* 754.6 is due to the loss of two H_2O molecules (Fig. 4a, rt 15.6 min) and at *m/z* 756.6 is due to loss of H_2O_2 (Fig. 4b, rt 20.3 min) from the precursor ion.

The LC-MS/MS spectrum of the major peak at 20.3 min (Fig. 4b) exhibited, apart from the product ions characteristic of [MH]+ diacyl GPC ions, product ions due to loss of H_2O and H_2O_2. In previous studies, the product ion due to the loss of 34 Da (H_2O_2) from the precursor ion was proposed to be indicative for the presence of the monohydroperoxide derivatives [27] using the synthetic palmitoyl-lineloyl hydroperoxide as standard [27]. The presence of hydroperoxide derivatives was also proposed through the product ions due to loss of 32 ($-O_2$) from the precursor ion [25].

Nonetheless, the loss of 34 Da from the precursor ion may also be attributed to the presence of vicinal hydroxy groups, and is formed due to a combined homolytic cleavage mechanism, as proposed previously [25]. The loss of oxygen atoms in the form of water, peroxide hydrogen or oxygen prevent from obtaining structural information regarding the location of the substituting groups along the unsaturated fatty acid chain, however the product ions observed between *m/z* 600 and 750 allow proposing several locations.

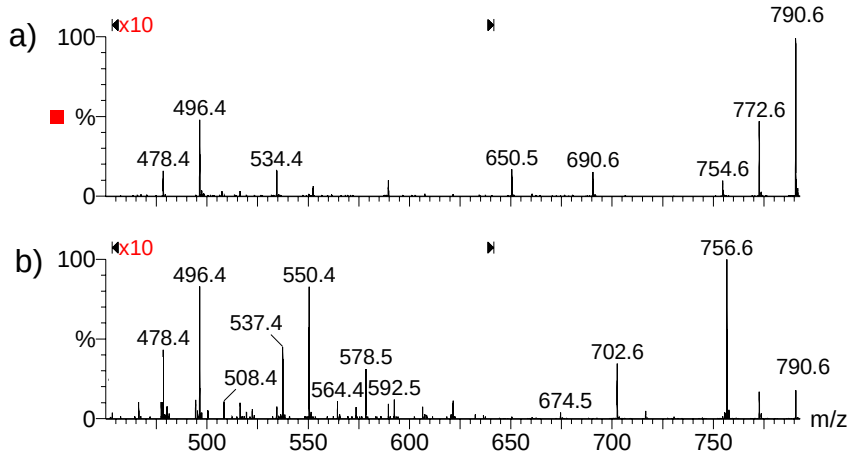

Fig. 4. LC-MS/MS spectra of $[MH]^+$ ion at *m/z* 790.6, a) rt= 15.6 min and b) rt=20.3 min.

These product ions are most likely resultant from charge-remote fragmentations, either by homolytic or heterolytic cleavages, may give structural information regarding the positions of functional groups (double bonds, hydroxy, epoxy and cyclopropane) in the oxidised PLPC, in a manner similar to what is described for lipids [Cheng and Gross, 2000]. The product ion at *m/z* 702.6 ($-C_5H_{12}O$) supports the presence of the hydroxy group placed at C-14, as shown in Scheme 2A, while the product ion observed at *m/z* 674.5 ($-C_6H_{12}O_2$) may result from vynillic fragmentation occurring in the same structure, suggesting the presence of the di-hydroxy derivative, with the hydroxy groups in vicinal positions. On the other hand, the product ion at *m/z* 674.5, with the structure $C_{36}H_{69}NO_8P^+$ (Table 2), may also be assigned to the 13-hydroperoxide derivative (B, Scheme 2), which would also lead to the loss of 34 Da (H_2O_2), similar to previous published results using hydroperoxide standards [27] and of triacylglycerols [40]. Thus, both isomers, namely 13,14-di-hydroxy-9,11-octadecadienoyl and 13-hydroperoxy-9,11-octadecadienoyl, may contribute as *sn*-2 residues linked to the 1-palmitoyl-3-glycerophosphatidylcholine in the peak with rt 20.3 min. Other product ions observed at *m/z* 550.4, 564.4, 578.5, 592.5, 606.5 and 620.5 (Fig. 4b), exhibit differences of 14 Da from each other and may be assigned to fragmentations occurring in the saturated moiety (alkyl chain) of the *sn*-2 residue by 1,4 hydrogen elimination mechanism [41],

starting from the γ-bond of the ester group. These product ions derive from charge remote fragmentations typical of high-energy collisional activation, although they have also been described in the low energy product ion spectra of short-chain phosphatidylcholines [42] and in triacylglycerols [41].

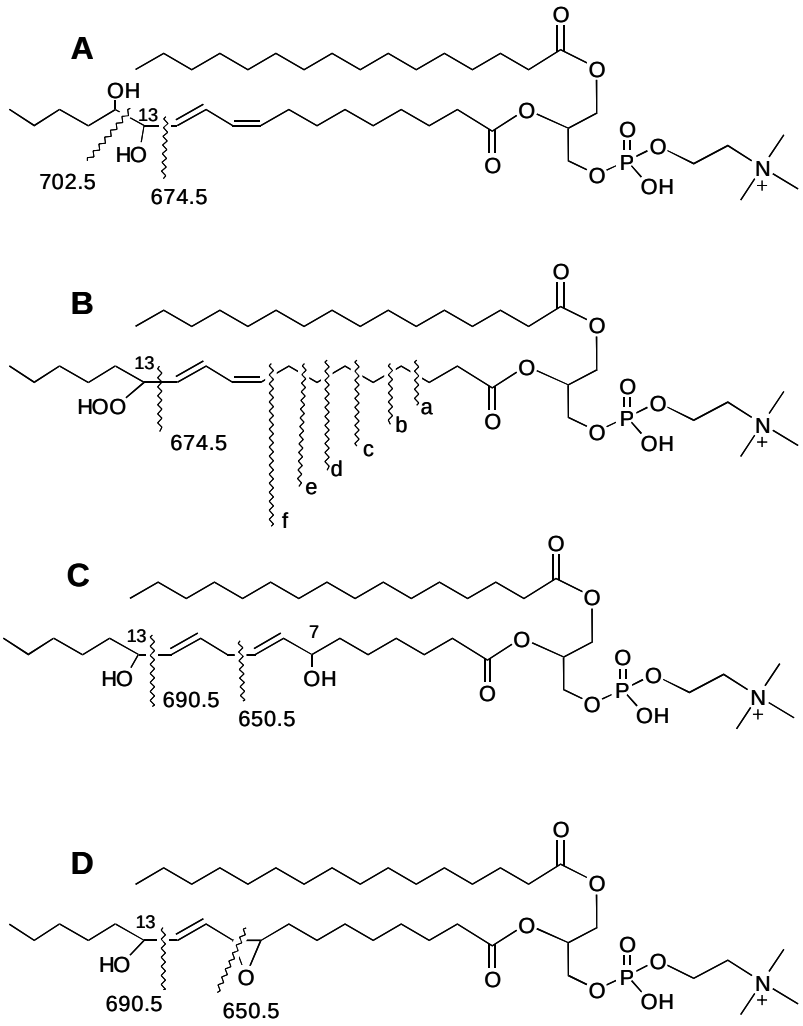

Scheme 2. Proposed structures for the ions at *m/z* 790.6 of PLPC oxidation products.

The LC-MS/MS spectrum obtained for the peak eluting at 15.6 min (Fig. 4a) exhibited product ions at *m/z* 650.5 (-140 Da) and 690.6 (-100 Da), which may reflect the presence of the hydroxy at C-7 and the product ion at *m/z* 690.6 due to cleavage of C_{12}-C_{13} carbon bond indicating the presence of the 7,13-di-hydroxy-8,11-octadecadienoyl (C, Scheme 2). On the other hand, both product ions (at *m/z* 650.5 and 690.6) may also be rationalised to the epoxy-hydroxy derivative (D, Scheme 2), resulting from the cleavage in the vicinity of the epoxy group by a mechanism similar to the one proposed earlier for linoleic acid epoxy-peroxyl DMPO adducts [12]. This would

suggest the presence of the 13-hydroxy-9,10-epoxy-11-octadecenoyl as the *sn*-2 residue (D, Scheme 2) attached to the phospholipid moiety.

Table 2. Empirical formula, observed and calculated mass/charge ratios, double bond equivalents (DBE), and mass errors of the main fragments observed in the LC-MS/MS spectra for the ions resultant from the insertion of two oxygen atoms observed at *m/z* 788.6 and 790.6 with different retention times.

$[MH]^+$	Predicted formula	Observed mass	Calculated mass	DBE	error (mDa)	error (ppm)
788.6	$C_{33}H_{65}NO_9P^+$	650.4373	650.4397	2.5	-2.4	-3.7
(rt 13.8 min)	$C_{35}H_{67}NO_9P^+$	676.4418	676.4553	3.5	-13.5	-20.0
(rt 18.2 min)	$C_{33}H_{65}NO_9P^+$	650.4269	650.4397	2.5	-12.8	-19.7
	$C_{36}H_{67}NO_9P^+$	688.4515	688.4553	4.5	-3.5	-5.2
790.6	$C_{33}H_{65}NO_9P^+$	650.4434	650.4397	2.5	3.7	5.7
(rt 15.6 min)	$C_{36}H_{69}NO_8P^+$	674.4683	674.4761	3.5	-7.8	-11.5
	$C_{36}H_{69}NO_9P^+$	690.4764	690.4710	3.5	5.4	7.8
(rt 20.3 min)	$C_{37}H_{69}NO_9P^+$	702.4758	702.4710	4.5	4.8	6.8

Thus, the product ions at *m/z* 650.5 and *m/z* 690.6 may be originated from the fragmentation of the di-hydroxy (C, Scheme 2) and/or the epoxy-hydroxy derivatives (D, Scheme 2), although formed through different fragmentation pathways, exhibit the same elemental composition (observed with an error of 5.7 ppm and 7.8 ppm, respectively (Table 2)). The presence of epoxy-hydroxy derivatives as radical products of linoleic acid, as well as their degradation products, is described in the literature [6], and can thus be assumed to account for the ion at *m/z* 790.6 in oxidised PLPC.

The RIC chromatogram of the ion at *m/z* 788.6, attributed to the keto-hydroxy and keto-epoxy derivatives, eluted between 12-22 min with maxima of elution at 13.8 and 18.2 min (Fig. 2b). The LC-MS/MS product ion spectra obtained in the different peaks (Fig. 5) showed common product ions at *m/z* 478.4 ($-R_2COOH$), 496.4 ($-R_2{=}C{=}O$), 532.4 ($-R_1COOH$), 550.4 ($-R_1{=}C{=}O$), 605.5 (-183Da), 587.5 (-183 Da and H_2O), 711.6 (-59Da and H_2O) and 770.6 ($-H_2O$). The product ion observed at *m/z* 650.5 ($-C_9H_{14}O$) may, by cleavage of the C_9-C_{10} bond, suggest the hydroxy placed at C-9 (Scheme 3 A), although the presence of the epoxy derivative can also be proposed (Scheme 3A1), the product ion at *m/z* 676.5 ($-C_7H_{12}O$) in Fig. 5a (rt 13.8 min) may be attributed to cleavage of the C_{11}-C_{12} denoting the presence of the keto group at C-9 and most probably with the hydroxy group at C-14 (Scheme 3B).

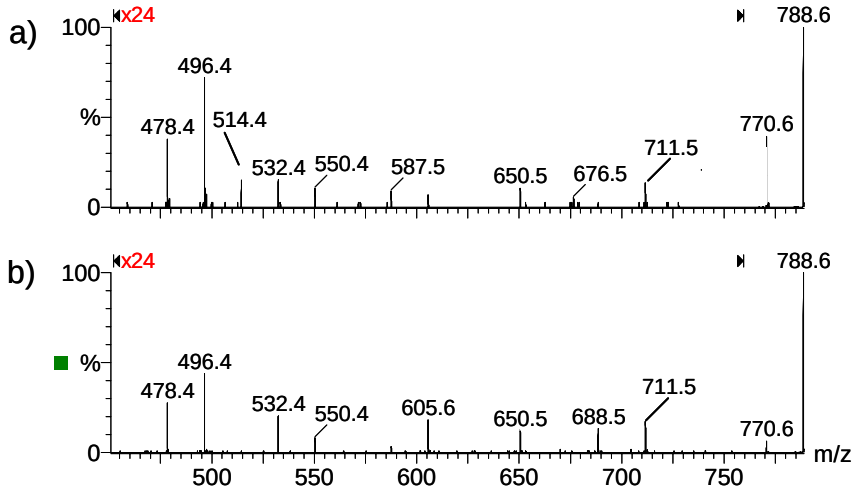

Fig. 5. LC-MS/MS spectra of $[MH]^+$ ion at *m/z* 788.6, a) rt=13.8 min and b) rt=18.2 min.

The product ion observed at *m/z* 688.5 in Fig. 5b may result from cleavage of the C_{12}-C_{13} bond placing the keto group at C-10 with the hydroxy group at C-13 (Scheme 3C). In fact, these product ions are formed by cleavage of the γ-bond, earlier described as the asymmetrical cleavage in oxofatty acids [41]. On the other hand, as noted so far, the fragmentation which is governed by the functional groups, in the case of keto-hydroxy derivatives, may be primarily governed by the hydroxy group since the product ion spectra of keto derivatives (*m/z* 772.6, data not shown) exhibits no fragmentation, other than the one characteristic of glycerophosphatidylcholines. Thus, the product ion at *m/z* 650.5 suggests the hydroxy group at C-9 resulting from the 9-hydroxy-14-keto-10,12-octadecadienoyl (Scheme 3A), while the product ion at *m/z* 676.5 places the hydroxy group at C-11 suggesting the 11-hydroxy-14-keto-9,12-octadecadienoyl (Scheme 3B1), and the product ion at *m/z* 688.5 ($-C_6H_{12}O$), with the structure $C_{36}H_{67}NO_9P^+$ and an error of -3.5 mDa (-5.2 ppm, Table 2), places the hydroxy group at C-13 suggesting the 13-hydroxy-8-keto-9,11-octadecadienoyl (Scheme 3C1). All the structures proposed are feasible to occur as peroxidation products of lineloyl chain, and are in accordance with previous published results [21]. The peroxidation products proposed and identified based on the LC-MS/MS data are summarised in Table 4.

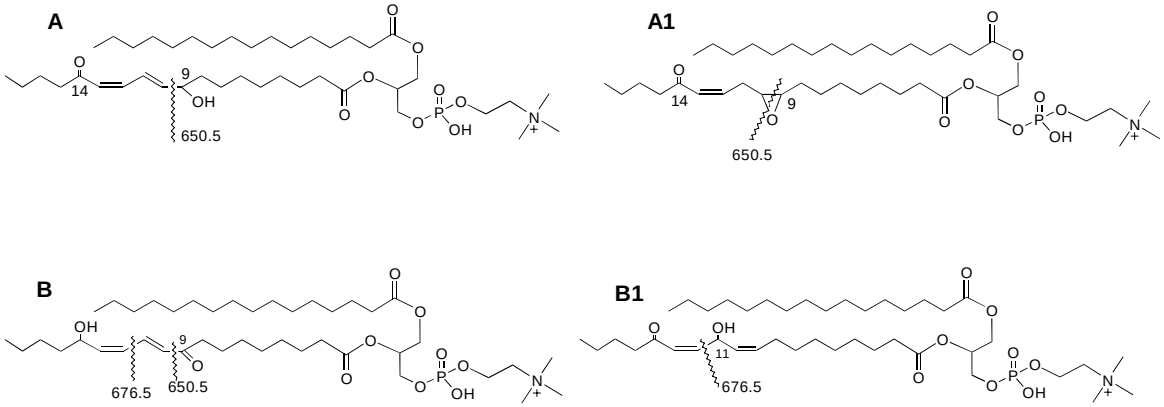

Scheme 3. Proposed structures for the ions at *m/z* 788.6 of PLPC oxidation products.

Peroxidation products by insertion of three oxygen atoms (m/z 806.6, 808.6 and 804.6)

The ion at *m/z* 806.6 (RIC on Fig. 1d), resultant from the insertion of three oxygen atoms in the unsaturated fatty acid chain, can be attributed to the hydroxy-hydroperoxy or to the tri-hydroxy derivatives. The ions observed at *m/z* 804.6 (RIC on Fig. 2c), may be attributed to the keto-di-hydroxy or to the keto-hydroperoxy, and the ion at *m/z* 808.6 (Fig. 2f) may be attributed to other tri-hydroxy derivatives deriving from the epoxy-hydroxy derivatives, as suggested by Spiteller *et al.* [6]. The RIC chromatograms obtained for each of these ions showed maximum of elution at different retention times (Fig. 1 and 2), and were studied by LC-MS/MS. The fragmentation pattern observed will be discussed and structures will be tentatively assigned.

The LC-MS/MS spectra obtained for the ion at *m/z* 806.6, eluting between 10-20 min with two maxima at 11.8 and 16.4 min (Fig. 1d), are depicted in Fig. 6. Product ions common to both spectra were observed at *m/z* 788.6 (-H_2O) and 184.1 ($[H_2PO_4(CH_2)_2N(CH_3)_3]^+$) [36]. However, as can be seen, the main differences observed in the LC-MS/MS spectra are related with the major losses from the precursor ion, namely the loss of $2H_2O$ (*m/z* 770.6) and loss of $3H_2O$ (*m/z* 752.6) for the peak at 11.8 min (Fig. 6a) and the loss of H_2O_2 (*m/z* 772.6) and H_2O_2 with H_2O (*m/z* 754.6) for the peak at 16.4 min (Fig. 6b). Other product ions observed in the region of *m/z* 600 to 750, observed in Fig. 6a, at *m/z* 650.5 (-$C_9H_{16}O_2$) and 706.5 (-$C_6H_{12}O$), together with product ions at *m/z* 770.6 (-$2H_2O$) and 752.6 (-$3H_2O$) are consistent with the presence of the 7,10,13-tri-hydroxy-8,11-octadecadienoyl as *sn*-2 residue (A, Scheme 4).

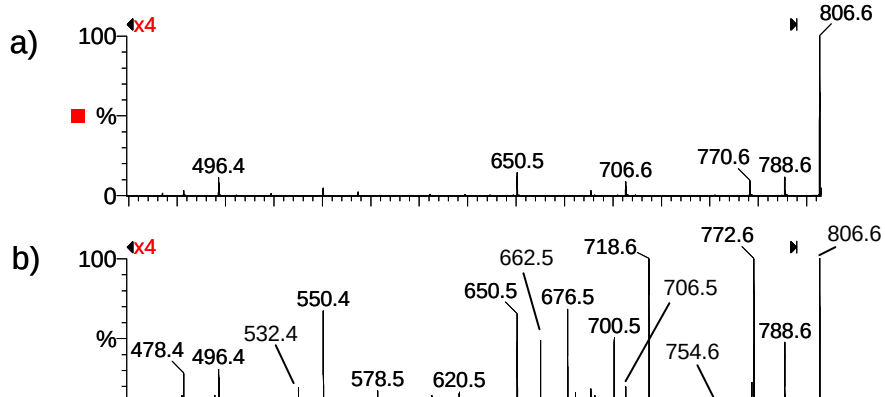

Fig. 6. LC-MS/MS spectra of $[MH]^+$ ion at *m/z* 806.6, a) rt=11.8 min and b) rt=16.4 min.

The elemental composition determined for each product ion and the error associated are summarised in Table 3. The product ions observed in the LC-MS/MS mass spectrum of the peak eluting at 16.4 min (Fig. 6b) at *m/z* 718.6 ($-C_5H_{12}O$), 706.5 ($-C_6H_{12}O$), 676.5 ($-C_7H_{14}O_2$), 662.5 ($-C_8H_{16}O_2$) and 650.5 ($-C_9H_{16}O_2$), together with the product ion resulting from loss of 34 Da (*m/z* 772.6), suggest the presence of three different structures that can be attributed to the 13-hydroxy-8-hydroperoxy-9,11-octadecadienoyl, the 10,13,14-tri-hydroxy-9,11-octadecadienoyl, or also to the 11,12,15-tri-hydroxy-9,13-octadecadienoyl as *sn*-2 residues of PLPC (Scheme 4). The elemental composition determined for each product ion (Table 3) support the structures proposed. Product ions observed in Fig. 6b at *m/z* 550.4, 564.4, 578.5, 592.5, 606.5 and 620.5 are attributed to cleavages of the saturated alkyl moiety in the lineloyl chain. Based on the LC-MS/MS data here described, the ion at *m/z* 806.6 eluting in two peaks is resultant from the contribution of 4 different oxidation products, which are summarised in Table 4.

As can be observed in (Fig. 1 and 2, the tri-hydroxy (*m/z* 808.6) and the keto-hydroxy derivatives (*m/z* 804.6) exhibit different retention times corroborating that the keto derivatives are formed in solution during the radical peroxidation and not formed by dehydration phenomena due to in-source chemistry.

As can be seen by the RIC chromatogram the elution of the ion at *m/z* 804.6 occurred in a broad band between 7-20 min with the maximum at 14.0 min (Fig. 2c) and the LC-MS/MS spectrum obtained for the peak (Fig. 7b) with a rt of 14.0 min exhibited the product ions due to loss of H_2O_2 (*m/z* 770.6), while the LC-MS/MS spectrum obtained for the peaks eluting prior to 14.0 min (Fig. 7a) showed the loss of $2H_2O$ (*m/z* 768.6), but not the product ions due to loss of $3H_2O$ (*m/z* 750.6), nor to the combined loss of H_2O_2 with H_2O (*m/z* 752.6). The neutral losses of water and peroxide hydrogen observed from the precursor ion point out to the presence of keto-di-hydroxy derivative and keto-hydroperoxide derivatives to the RIC chromatogram of ion at *m/z*

804.6, although the contribution of epoxy-hydroxy-keto derivatives cannot be excluded.

Table 3. Empirical formula, observed and calculated mass/charge ratios, double bond equivalents (DBE), and mass errors of the main fragments observed in the LC-MS/MS spectra for the ions resultant from the insertion of three oxygen atoms observed at *m/z* 804.6, 806.6 and 808.6 with different retention times.

$[MH]^+$	Predicted formula	Observed mass	Calculated mass	DBE	error (mDa)	error (ppm)
804.6						
(rt 12.9 min)	$C_{33}H_{65}NO_9P^+$	650.4387	650.4397	2.5	-1.0	-1.5
(rt 14.0 min)	$C_{36}H_{67}NO_9P^+$	688.4651	688.4553	4.5	9.8	14.2
	$C_{37}H_{69}NO_9P^+$	702.4719	702.4710	4.5	0.9	1.3
	$C_{37}H_{67}NO_{10}P^+$	716.4451	716.4503	5.5	-5.2	-7.2
	$C_{38}H_{69}NO_{10}P^+$	730.4677	730.4659	5.5	1.8	2.4
806.6	$C_{33}H_{65}NO_9P^+$	650.4498	650.4397	2.5	10.1	15.5
(rt 11.8 min)	$C_{36}H_{67}NO_9P^+$	688.4544	688.4553	4.5	-0.9	-1.4
	$C_{36}H_{69}NO_{10}P^+$	706.4673	706.4659	3.5	1.4	2.0
806.6	$C_{33}H_{65}NO_9P^+$	650.4509	650.4397	2.5	11.2	17.2
(rt 16.4 min)	$C_{34}H_{65}NO_9P^+$	662.4495	662.4397	3.5	9.8	14.8
	$C_{35}H_{67}NO_9P^+$	676.4556	676.4553	3.5	0.3	0.4
	$C_{36}H_{67}NO_9P^+$	688.4553	688.4553	4.5	0.0	-0.1
	$C_{36}H_{69}NO_9P^+$	690.4871	690.4710	3.5	16.1	23.3
	$C_{36}H_{69}NO_{10}P^+$	706.4789	706.4659	3.5	13.0	18.4
	$C_{37}H_{69}NO_{10}P^+$	718.4673	718.4659	4.5	1.4	1.9
808.6	$C_{33}H_{65}NO_9P^+$	650.4438	650.4397	2.5	4.1	6.3
(rt 10.6 min)	$C_{36}H_{69}NO_9P^+$	690.4773	690.4710	3.5	6.3	9.1
808.6	$C_{33}H_{65}NO_9P^+$	650.4532	650.4397	2.5	13.5	20.8
(rt 16.8 min)	$C_{36}H_{69}NO_9P^+$	690.4872	690.4710	3.5	16.2	23.5
	$C_{36}H_{71}NO_{10}P^+$	708.4875	708.4816	2.5	5.9	8.4
	$C_{37}H_{71}NO_{10}P^+$	720.4883	720.4816	3.5	6.7	9.4

A) Ions at *m/z* 806.6

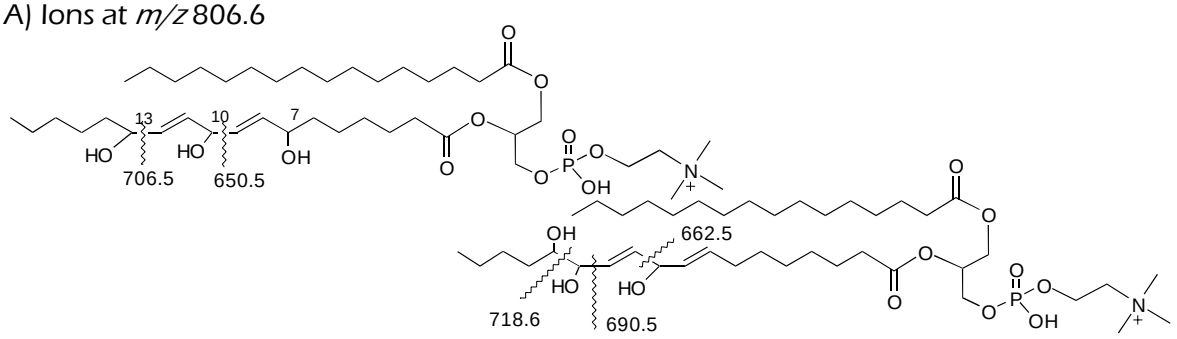

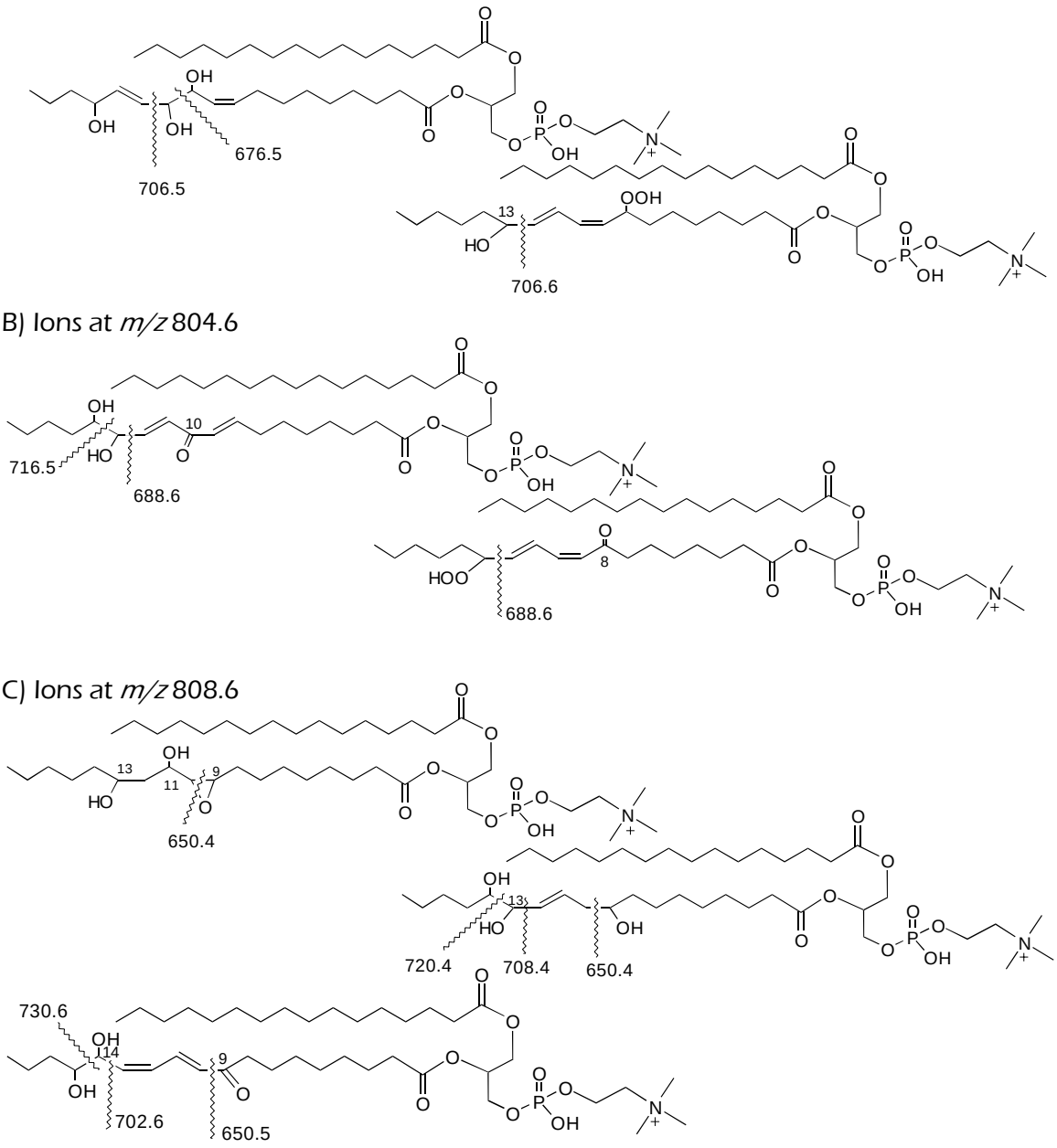

Scheme 4. Proposed structures for the ions at *m/z* 806.6, 804.6 and 808.6 of PLPC oxidation products.

The expected structural heterogeneity of the radical peroxidation products may explain the occurrence of unresolved chromatographic peaks, still, some product ions, observed in Fig. 7b at *m/z* 730.6 (hydroxy at C-15), 716.5 (hydroxy group at C-14) allow proposing the substitutents in the higher carbon atoms, while in Fig. 7a the product ions at *m/z* 688.5 allow proposing the hydroperoxide at C-13 and 650.5 the hydroxy at C-9. On the other hand, other product ions give ambiguous information, which, as seen for the product at *m/z* 688.5 (B, Scheme 4), can either suggest the presence of the hydroperoxide or the di-hydroxy derivatives. Overall, based on the product ions

observed it is suggested the presence of the 13,14-di-hydroxy-10-keto-8,11-octadecadienoyl or the 13-hydroperoxide-8-keto-9,11-octadecadienoyl, and the 14,15-di-hydroxy-9-keto-10,12-octadecadienoyl. The elemental composition determined for each product ion is shown in Table 3, and support the proposed structures (Table 4).

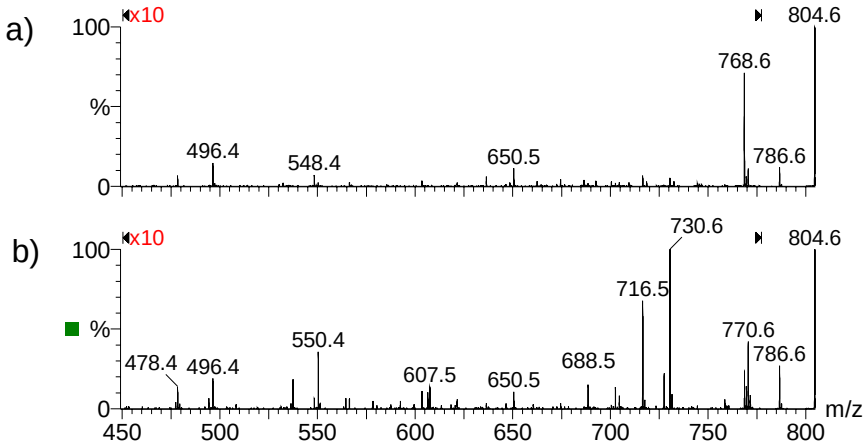

Fig. 7. LC-MS/MS spectra of $[MH]^+$ ion at *m/z* 804.6, a) average on unresolved peaks present before 14 min and b) rt=14.0 min.

The RIC for the ion at *m/z* 808.6 (Fig. 2f) showed elution in two well resolved peaks with maxima of elution at 10.7 and 16.4 min. The LC-MS/MS obtained for the ion with rt 10.7 min (data not shown) exhibited the product ions at *m/z* 790.5 ($-H_2O$) and 772.5 ($-2H_2O$), and the product ion resultant from loss of R_1COOH, which indicated the oxygen atoms to be placed at the *sn*-2 residue. The product ion at *m/z* 650.4, with the structure $C_{33}H_{65}NO_9P^+$ (Table 3), resulted from cleavage between C_9-C_{10} carbon bond and the product ion at *m/z* 690.5, with the structure $C_{36}H_{69}NO_9P^+$ (Table 3), resulted from cleavage between C_{12}-C_{13} and can be attributed to the 11,13-di-hydroxy-9,10-epoxy-octadecanoyl as the *sn*-2 acyl residue (C, Scheme 4). The LC-MS/MS obtained for the ion with rt 16.4 min (data not shown) exhibited the product ions at *m/z* 790.5 ($-H_2O$), 774.5 ($-H_2O_2$) and the product ions resultant from losses of *sn*-1 and *sn*-2 and due to loss of $N(CH_3)_3$ and $HPO_4(CH_2)_2N(CH_3)_3$ from the precursor ion. Other product ions observed at *m/z* 650.4 and 708.4, and 720.4, resultant from cleavages in the vicinity of the double bond or hydroxy groups suggest the presence of the 9,13,14-tri-hydroxy-11-octadecenoyl (C, Scheme 4) as the *sn*-2 residue. The presence of tri-hydroxy derivatives of the linoleic acid bearing vicinal hydroxy groups were earlier proposed as linoleic peroxidation products formed by hydrolysis of the epoxy-hydroxy linoleic acid derivatives [6], and also as peroxidation products in cardiolipin-cytochrome c system [43]. More recently, in a study aimed at the identification of enzymatic oxidised diacyl-phosphatidylcholines isolated from rat heart tissue the ion at *m/z* 808.6 was attributed

to the tri-hydroxy PLPC derivative based on the loss of one, two and three water molecules, although information regarding the location of the hydroxy groups was not attempted [32].

Peroxidation products by insertion of four oxygen atoms (m/z 822.6)

The RIC chromatogram obtained for the ions at *m/z* 822.6 eluted in a broad band between 10-20 min (Fig. 1e), with unresolved peaks that can be attributed to the elution of several structural and positional isomers. The LC-MS/MS spectra obtained in each peak (Fig. 8a-c) exhibit, apart from the product ions at *m/z* 184.1, 478.4 and 496.4, the product ions formed by loss of H_2O, of H_2O_2 and of both combined, as is the case of product ions at *m/z* 804.5 (-H_2O), 788.5 (-H_2O_2), 786.5 (-2H_2O), 770.5 (-H_2O_2 and H_2O), and 768.5 (-3H_2O). The product ion at *m/z* 754.5 (Fig. 8b and c), in particular, may be due to either combined loss of 2H_2O_2 or, to combined loss of 2H_2O with O_2, since the product ion at *m/z* 786.5 (-2H_2O) is also observed in the LC-MS/MS spectra (Fig. 8b).

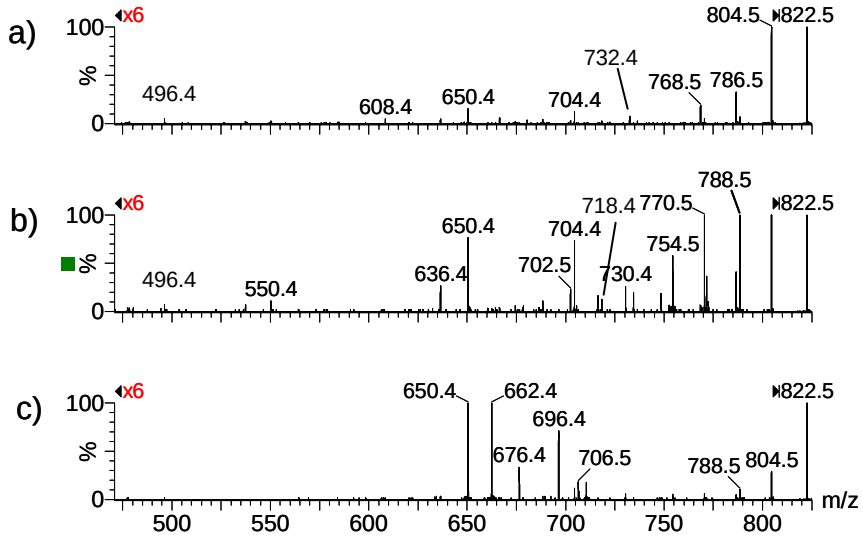

Fig. 8. LC-MS/MS spectra of $[MH]^+$ ion at *m/z* 822.6, a) rt=11.8 min; b) rt=13.5 min; and c) rt=17.1 min.

The loss of the oxygen molecule may occur by a mechanism similar to what was earlier proposed suggesting the presence of a conjugated hydroperoxide derivative [25]. Due to the different possible isomers generated by the insertion of high number of oxygen atoms into the *sn*-2 acyl chain (lineloyl), co-elution of different structures may take place. The LC-MS/MS spectrum obtained for the ion at *m/z* 822.6 with the peak maximum at 11.8 min (Fig. 8a) showed the product ions at *m/z* 650.4, 704.4 and 732.4 that may suggest the contribution of the 7,10,14-tri-hydroxy-12,13-epoxy-8-octadecenoyl as the *sn*-2 residue derivative (A, Scheme 5), which may also account for

the observed loss of $3H_2O$ (*m/z* 768.5). The product ions observed for the peak at 13.5 min (Fig. 8b) at *m/z* 636.4, 718.5, 788.5 and the product ion at *m/z* 754.5 (loss $2H_2O$ and O_2), may account for the presence of 8,13-di-hydroxy-14-hydroperoxy-9,11-octadecadienoyl acid (B, Scheme 5).

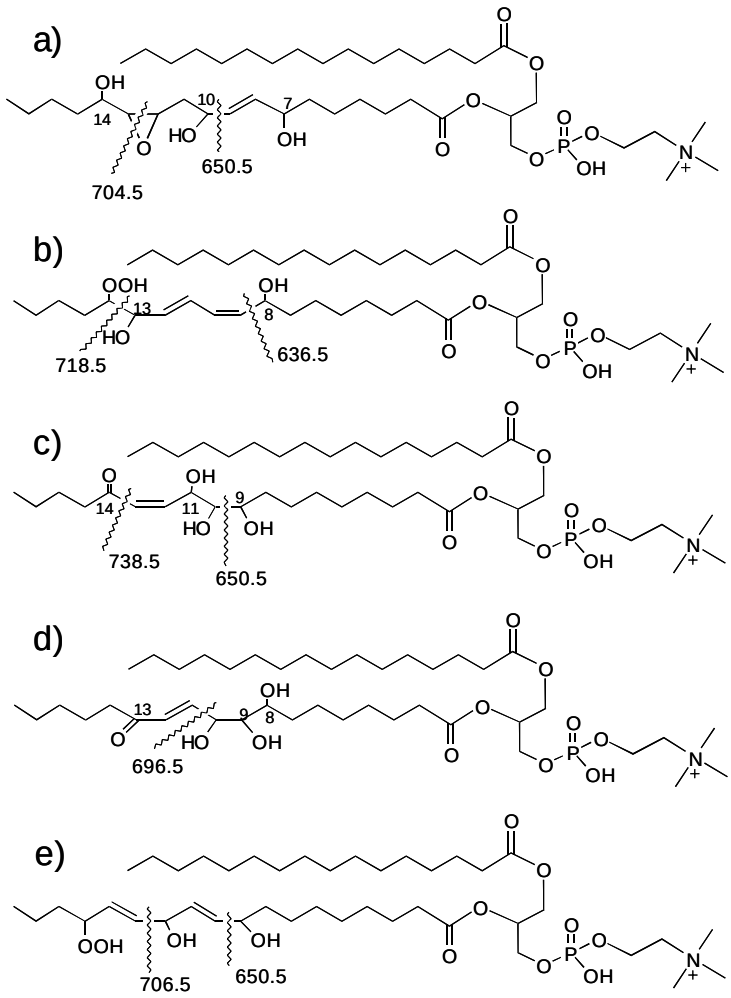

Scheme 5. Proposed structures for the ions at *m/z* 822.6 of PLPC oxidation products.

On the other hand, the contribution of 9,10,11-tri-hydroxy-14-keto-12-octadecenoyl (C, Scheme 5) also supports the observation of the product ions at *m/z* 650.5 and 738.5 and the loss of 34Da observed from the precursor ion, and in turn may account for the presence of the product ion at *m/z* 704.5 by loss of 34Da combined with the cleavage between C_{13}-C_{14}.

Table 4. Retention times of the of the oxidised acyl fatty acid chains present as *sn*-2 acyl residues in oxidised PLPC identified based on the LC-MS/MS data.

Retention times	*m/z* value $[MH]^+$	Peroxidation product

(min)		
10.7	808.6	1-palmitoyl-2-(11,13-di-hydroxy-9,10-epoxy-octadecanoyl)-GPC
11.8	822.6	1-palmitoyl-2-(7,10,14-tri-hydroxy-12,13-epoxy-8-octadecenoyl)-GPC
11.8	806.6	1-palmitoyl-2-(7,10,13-tri-hydroxy-8,11-octadecadienoyl)-GPC
12.9	804.6	1-palmitoyl-2-(14,15-di-hydroxy-9-keto-10,12-octadecadienoyl)-GPC
13.5	822.6	1-palmitoyl-2-(8,13-di-hydroxy-14-hydroperoxy-9,11-octadecadienoyl)-GPC
13.5	822.6	1-palmitoyl-2-(9,10,11-tri-hydroxy-14-keto-12-octadecenoyl)-GPC
13.8	788.6	1-palmitoyl-2-(9,10-epoxy-14-keto-12-octadecenoyl)-GPC
14.0	804.6	1-palmitoyl-2-(13,14-di-hydroxy-10-keto-8,11-octadecadienoyl)-GPC
14.0	804.6	1-palmitoyl-2-(13-hydroperoxy-8-keto-9,11-octadecadienoyl)-GPC
15.6	790.6	1-palmitoyl-2-(7,13-di-hydroxy-8,11-octadecadienoyl)-GPC
15.6	790.6	1-palmitoyl-2-(13-hydroxy-9,10-epoxy-11-octadecenoyl)-GPC
16.4	806.6	1-palmitoyl-2-(13-hydroxy-8-hydroperoxy-9,11-octadecadienoyl)-GPC
16.4	806.6	1-palmitoyl-2-(10,13,14-tri-hydroxy-9,11-octadecadienoyl)-GPC
16.4	806.6	1-palmitoyl-2-(11,12,15-tri-hydroxy-9,13-octadecadienoyl)-GPC
16.4	808.6	1-palmitoyl-2-(9,13,14-tri-hydroxy-11-octadecenoyl)-GPC
17.1	822.6	1-palmitoyl-2-(9,12-di-hydroxy-15-hydroperoxy-10,13-octadecadienoyl)-GPC
17.1	822.6	1-palmitoyl-2-(8,9,10-tri-hydroxy-13-keto-10-octadecenoyl)-GPC
18.2	788.6	1-palmitoyl-2-(9-hydroxy-14-keto-10,12-octadecadienoyl)-GPC
18.2	788.6	1-palmitoyl-2-(11-hydroxy-14-keto-9,12-octadecadienoyl)-GPC
18.2	788.6	1-palmitoyl-2-(13-hydroxy-8-keto-9,11-octadecadienoyl)-GPC
20.3	790.6	1-palmitoyl-2-(13,14-di-hydroxy-9,11-octadecadienoyl)-GPC
20.3	790.6	1-palmitoyl-2-(13-hydroperoxy-9,11-octadecadienoyl)-GPC
20.3	774.6	1-palmitoyl-2-(9,10-epoxy-10,12-octadecadienoyl)-GPC
20.8	772.6	1-palmitoyl-2-(9-keto-10,12-octadecadienoyl)-GPC
20.8	772.6	1-palmitoyl-2-(10-keto-8,11-octadecadienoyl)-GPC
20.8	772.6	1-palmitoyl-2-(12-keto-10,13-octadecadienoyl)-GPC
20.8	772.6	1-palmitoyl-2-(13-keto-9,11-octadecadienoyl)-GPC
23.2	774.6	1-palmitoyl-2-(9-hydroxy-10,12-octadecadienoyl)-GPC
23.2	774.6	1-palmitoyl-2-(10-hydroxy-8,11-octadecadienoyl)-GPC
23.2	774.6	1-palmitoyl-2-(12-hydroxy-10,13-octadecadienoyl)-GPC
23.2	774.6	1-palmitoyl-2-(13-hydroxy-9,11-octadecadienoyl)-GPC
28.6	758.6	1-palmitoyl-2-(9,12-octadecadienoyl)-GPC

GPC is abbreviation of glycero-phosphatidylcholine

The 8,9,10-tri-hydroxy-13-keto-10-octadecenoyl (D, Scheme 5) and the 9,12-di-hydroxy-15-hydroperoxy-10,13-octadecadienoyl derivatives (E, Scheme 5) allow rationalising the product ions at *m/z* 650.4, 662.5, 696.5 and 706.5, and the loss of one H_2O_2 (-34Da) observed for the maximum rt with 17.1 min (Fig. 8c). By plotting the RIC chromatogram of the product ions with *m/z* 636.4, 650.5, 662.5, 696.5, 704.5, 706.5, 718.5 and 738.5 used for structural characterisation of ion at *m/z* 822.5 (data not shown) it is possible to group the product ions according to the differences in the retention times observed corroborating the elution of different PLPC oxidation products. The elemental

composition determined for each product ion observed in the LC-MS/MS spectra and the errors associated were calculated (data not shown) and the identification was accepted when mass errors were inferior to 25 ppm. The peroxidation products identified based on the LC-MS/MS data are summarised in Table 4. Bearing in mind the results here described it is, therefore, feasible to assume that the presence of unresolved peaks seen in the RIC chromatograms of the several ions studied is the result of the considerable heterogeneity of the oxidised *sn*-2 acyl chains that may arise from radical oxidation of the linoleic acid moiety in PLPC.

The ions that may also result from the insertion of four oxygen atoms (*m/z* 820.6 and 824.6) and those resulting from the insertion of five oxygen atoms (*m/z* 836.6 and 840.6) were also formed (Fig. 2). As can be seen, all the ions exhibited different retention times, suggesting that were in fact different peroxidation products formed during the radical reaction of PLPC. However, the acquisition of the LC-MS/MS spectra in the different chromatographic peaks observed was restricted by the low ion current obtained for these ions, constraining our ability to perform structural characterisation. Nevertheless, the presence of peroxidation products with high number of oxygen atoms may be responsible for the increase of the hydrophilic character described for membrane bilayers [14,15]. The identification of these products suggests that the hydroxyl radical was able to penetrate into the lipophilic packing of the liposomes and thus initiate/propagate the radical reaction. In fact, Vitrac et al. [26], through light-scattering studies, have concluded that approximately 90% of PLPC vesicles were of low diameter, when formed during sonication [26]. The occurrence of a phospholipid dispersion comprised of low diameter vesicles would contain highly curved surface and, therefore, a looser packing of the lipid chains facilitating ROS penetration [44]. In the case of LC-MS/MS analysis of long-chain PLPC products, among the isomers identified several contained the C-9 position substituted, which suggests this carbon atom to be easily oxidised or the oxidation product to be very stable. Remarkably, the identification of short-chain product with *m/z* 650.4 assigned to 1-palmitoyl-2-(9-oxo-nonanoyl)-glycerophosphocholine during the LC-MS analysis of radical oxidised PLPC liposomes [31] and in oxidised LDL [21,22] was found to be one of the predominant PLPC peroxidation product among the short-chain products.

The LC-MS conditions used for the separation of PLPC peroxidation products showed splitting of chromatographic peaks (broader elution bands) as the number of oxygen atoms increased. This chromatographic behaviour is in accordance with the results obtained by Vitrac and co-workers (2004) also performed with liposome model. This chromatographic behaviour reflects the wide variety of the lipid peroxidation

products formed during non-enzymatic radical oxidation in PUFA with several points susceptible to be modified, leading to the formation of positional isomers. In a recent study, several derivatives of phosphatidylcholine oxidation products were proposed [32]. These derivatives eluted in single chromatographic peaks, unlike the elution in multiple peaks that was observed in this study, most likely due to the specificity of the enzymatic oxidation reaction (lipoxygenase), suggesting a greater structural homogeneity for the products formed. Nonetheless, differences in the chromatographic conditions used, namely composition of stationary phase, column length, composition of mobile phase, and column flow, could also account for the separation achieved for the oxidised long-chain PLPC products. As can be seen, most of the RIC chromatograms were not fully resolved, thus the LC-MS/MS data only provided some isomeric differentiation. Still, the tandem mass spectrometric data obtained for the various ions allowed the distinction of isomeric peroxidation products (structural and positional features) when present in the same chromatographic peak, such as di-hydroxy and hydroperoxide derivatives, identified by their retention times and distinctive fragmentation pattern, namely the loss of water (H_2O) or hydrogen peroxide (H_2O_2) combined with product ions resulting from charge remote fragmentations in the unsaturated backbone. These types of fragmentations, although present in the product ion spectra of enzymatically oxidised diacyl-phosphatidylcholines, were not discussed [32]. However, as pointed out in this study, the detailed structural information that can be obtained from tandem mass spectra for the ions corresponding to the insertion of one and two oxygen atoms, although with some limitations for the ions containing higher oxygen atoms since the fragmentation patterns overlap.

Based on the peroxidation products here described, the poly-hydroxy derivatives identified as *sn*-2 acyl derivatives in oxidised PLPC, either with hydroxy groups in vicinal positions or in distant positions, are apparently predominant over the hydroperoxide derivatives. These results suggest that radical oxidation of GPC under the Fenton conditions, the hydroxy derivatives appear to be more stable, or its formation more favourable. In *in vivo* conditions, the action of glutathione peroxidases (GPx) are described to reduce the hydroperoxides to their hydroxy derivatives [5,46]. Moreover, the presence of epoxy (and epoxy-hydroxy) derivatives, isomers of di-hydroxy and hydroperoxide derivatives, was not excluded and its formation during the Fenton radical reaction may be reinforced due to the identification of ions with 2 Da higher than the hydroxy derivatives (i.e. ions at *m/z* 808.6, 824.6 and 840.6), that can be originated from the hydration of epoxy derivatives [2].

The distinction of isomeric and positional isomers described in this study was achieved using only one phospholipid, thus it is expected that the identification of

radical peroxidation products in biological samples may turn out to be a more difficult task considering that ω-3, ω-6 and ω-9 fatty acids are present in biological membranes [45]. On the other hand, considering that in *in vivo* conditions the formation of phospholipid peroxidation products is not only promoted by ROS but also by enzymatic reactions, the formation of some phospholipid peroxidation products may be enhanced or promoted over others, which might simplify the composition of the oxidised phospholipids thus facilitating their identification in a complex mixture. Furthermore, the presence of the lyso-phosphatidylcholine product ions present in all product ion spectra allows drawing information about the oxidised acyl chain. This, together with the product ions resulting from charge remote cleavages, facilitates the structural characterisation of oxidised phospholipids. In summary, the PLPC peroxidation products identified based on these fragmentation pathways will allow widening the products monitored in biological samples since, the monitorisation of intact peroxidation products esterified to glycerophosphocholine formed in *in vivo* conditions is currently focused on a small number of products [47,48].

In the overall, the structural changes that take place in membrane phospholipids, either with formation of long-chain products or of the short-chain products, with terminal aldehyde and carboxylic groups [31], may account for the decrease of membrane packing and increase of membrane disorder [14,15], and may further promote ROS penetration and the propagation of the damage, with consequences to the membrane bilayer shape and in the diffusion capacity of red blood cells with major implications in tissue oxygenation. Propagation of the damage may induce to the loss of membrane integrity, essential for proper phospholipid-phospholipid and protein-phospholipid interactions [18].

Conclusions

The use of tandem mass spectrometry (MS/MS) together with chromatography allowed establishing the presence of several PLPC long-chain peroxidation products formed by radical peroxidation of PLPC vesicles. Based on the differences observed in the retention times of the different ions, coupled with the product ion spectra obtained for each ion in each chromatographic peak, the LC-MS/MS data allowed the differentiation of oxidation products with the same number of oxygen atoms, as is the case of keto and hydroxy derivatives, and the identification of structural and positional PLPC isomers. This information may be further used in the proposal of reliable GPC biomarkers during the analysis of biological samples, particularly of cell membranes

exposed to free radicals, in the hope of biomarker identification of specific pathologies related to oxidative stress.

Acknowledgements

The authors gratefully acknowledge the financial support provided to Ana Reis (PhD grant SFRH/BD/10358/2002) by the Foundation for Science and Technology (FCT) and FSE (III Quadro Comunitário de Apoio).

References

[1] J. Pincemail "Free radicals and antioxidants in human diseases". In *Analysis of free radicals in biological systems*. Eds. Favier AE, Cadet J, Kalyanaraman B, Fontecave M, Pierre JL, 1995, Verlag, Berlin, p. 83-98.

[2] G. Spiteller, Chem. Phys. Lipids 95 (1998) 105.

[3] S.I. Liochev, The Mechanism of "Fenton-like" reactions and their importance for Biological Systems. A Biologist's View" in Metal Ions in Biological Systems, Ed. Sigel, A. and Sigel H, vol 36 Marcel Dekker, INC. New York, 1999, p 1-40.

[4] M. Comporti, C. Signorini, G. Buonocuore and L. Ciccoli, Free Rad. Biol. Med. 32 (2002) 568.

[5] A. Girotti, J. Lipid Res. 39 (1998) 1529.

[6] P. Spiteller, W. Kern, J. Reiner and G. Spiteller, Biochim. Biophys. Acta. 1531 (2001) 188.

[7] P. Wheelan, J.A. Zirrolli and R.C. Murphy, J. Am. Soc. Mass Spectrom. 7 (1996) 140.

[8] T. Nakamura, D.L. Bratton and R.C. Murphy, J. Mass Spectrom. 32 (1997) 888.

[9] M. Inouye, T. Moi and K. Sumino, Biochim. Biophys. Acta. 1438 (1999) 204.

[10] H. Iwahashi, K. Nishizaki and I. Takagi, Biochem J. 361 (2002) 57.

[11] S.Y. Qian, G-H. Yue, K.B. Tomer and R.P. Mason, Free Rad. Biol. Med. 34 (2003) 1017.

[12] A. Reis, M.R.M. Domingues, F.M.L. Amado, A.J. Ferrer-Correia and P. Domingues, J. Am. Soc. Mass Spectrom., 14 (2003) 1250.

[13] J.W. Borst, N.V. Visser, O. Kouptsova and A.J.W.G. Visser, Biochim. Biophys. Acta. 1487 (2000) 61.

[14] F.M. Megli and K. Sabatini, Chem. Phys. Lipids. 125 (2003) 161.

[15] F.M. Megli and K. Sabatini, FEBS Lett. 573 (2004) 68.

[16] M. Carini, G. Aldini and R.M. Facino, Mass Spectrom. Rev. 23 (2004) 281.

[17] A. Reis, P. Domingues, A.J. Ferrer-Correia and M.R.M. Domingues. J. Am. Soc. Mass Spectrom. 17 (2006) 657.

[18] F. van Voorst and B. de Kruijff, Biochem. J. 347 (2000), 601.

[19] T.M. McIntyre, G.A. Zimmerman and S.M. Prescott, J. Biol. Chem. 274 (1999) 25189.

[20] C.E. Clay, A.M. Namen, G.-I. Atsumi, M.C. Willingham, K.P. High, T.E. Kute, A.J. Trimboli, A.N. Fonteh, P.A. Dawson and F.H. Chilton, Carcinogenesis. 20 (1999) 1905.

[21] H. Itabe, H. Yamamoto, M. Suzuki, Y. Kawai, Y. Nakagwa, A. Suzuki, T. Imanaka and T. Takano, J. Biol. Chem. 271 (1996) 33208.

[22] G.K. Marathe, K.A. Harrison, R.C. Murphy, S.M. Prescott, G.A. Zimmerman and T.M. McIntyre. Free Rad. Biol. Med. 28 (2000) 1762.

[23] E.A. Podrez, E. Poliakov, Z. Shen, R. Zhang, Y. Deng, M. Sun, P.J. Finton, L. Shan, B. Gugiu, P.L. Fox, H.F. Hoff, R.G. Salomon and S.L. Hazen. J. Biol. Chem. 277 (2002) 38503.

[24] J.-R. Zhang, A.R. Cazers, B.S. Lutzke and E.D. Hall. Free Rad. Biol. Med. 18 (1995) 1.

[25] A. Reis, P. Domingues, A.J. Ferrer-Correia and M.R.M. Domingues, J. Mass Spectrom., 39 (2004) 1513.

[26] H. Vitrac, M. Courrègelongue, M. Couturier, F. Collin, P. Thérond, S. Rémita, P. Peretti, D. Jore and M. Gardès-Albert, Can. J. Physiol. Pharmacol. 82 (2004) 153.

[27] J. Adachi, N. Yoshida, R. Funae, H. Nushida, M. Asano and Y. Ueno, J. Chromatogr. B. 806 (2004) 41.

[28] D.K. MacMillan and R.C. Murphy, J. Am. Soc. Mass Spectrom. 6 (1995) 1190.

[29] K.A. Harrison and R.C. Murphy, J. Biol. Chem. 270 (1995) 17273.

[30] J. Adachi, S. Matsushita, N. Yoshioka, R. Funae, T. Fujita, S. Higuchi and Y. Ueno, J. Lipid. Res. 45 (2004) 967.

[31] A. Reis, M.R.M. Domingues, F.M.L. Amado, A.J. Ferrer-Correia and P. Domingues, Biomed. Chromatogr. 19 (2005) 129.

[32] J. Adachi, N. Yoshida, M. Sato, K. Nakagawa, Y. Yamamoto and Y. Ueno, J. Chromatogr. B. 823 (2005) 37.

[33] J. Folch, M. Lees and G.H.S. Stanley, J. Biol. Chem. 226 (1957) 497.

[34] O. Sergent, I. Morel and J. Cillard "Involvement of metal ions in lipid peroxidation: biological implications " in Metal Ions in Biological Systems, ed. Sigel, A. and Sigel H, Vol 36, Marcel Dekker, INC. New York, 1999, p 251-262.

[35] N. Pelizzi, S. Catinella, S. Barboso and M. Zanol, Rapid Commun. Mass Spectrom. 16 (2002) 2215.

[36] F.-F. Hsu and J. Turk, J. Am. Soc. Mass Spectrom. 14 (2003) 352.

[37] F.-F. Hsu and J. Turk, J. Am. Soc. Mass Spectrom. 10 (1999) 600.

[38] L.M. Hall and R.C. Murphy, J. Am. Soc. Mass Spectrom. 9 (1998) 527.

[39] F.A. Fitzpatrick, D.R. Morton and M.A. Wynalda. J. Biol. Chem. 257 (1982) 4680.

[40] F. Giuffrida, F. Destaillats, L.H. Skibsted and F. Dionisi, Chem. Phys. Lipids 131 (2004) 41.

[41] C. Cheng and M.L. Gross, Mass Spectrom. Rev. 19 (2000) 398.

[42] A. Reis, P. Domingues, A.J. Ferrer-Correia and M.R.M. Domingues, Rapid Commun. Mass Spectrom., 18 (2004) 2849.

[43] H. Iwase, T. Talatori, M. Nagao, H. Nijima, K. Iwadate, Y. Matsuda and M. Kobayashi, Free Rad. Biol. Med. 24 (1998) 1492.

[44] Q-T. Li, M.H. Yeo and B.K. Tan, Biochem. Biophys. Res. Commun. 273 (2000) 72.

[45] M.A. Yorek, "Biological Distribution" *In* Phospholipids Handbook; Gregor, Cevc, Ed.; Marcel Dekker: New York, 1993; p 745-775.

[46] E. Niki, Y. Yoshida, Y. Saito and N. Nguchi, Biochem. Biophys. Res. Commun. 338 (2005) 668.

[47] A.D. Watson, N. Leitinger, M. Navab, K.F. Faull, S. Horkkö, J.L. Witztum, W. Palinski, D. Schwenke, R.G. Salomon, W. Sha, G. Subbannagounder, A.M. Fogelman, J.A. Berliner, J. Biol. Chem. 272 (1997) 13597.

[48] A. Jerlich, R.J. Schaur, A.R. Pitt and C.M. Spickett. Free Rad. Res. 37 (2003) 645.

RAPID COMMUNICATIONS IN MASS SPECTROMETRY
Rapid Commun. Mass Spectrom. 2004; **18**: 2849–2858
Published online in Wiley InterScience (www.interscience.wiley.com). DOI: 10.1002/rcm.1686

RCM

Fragmentation study of short-chain products derived from oxidation of diacylphosphatidylcholines by electrospray tandem mass spectrometry: identification of novel short-chain products

A. Reis, P. Domingues, A. J. V. Ferrer-Correia and M. R. M. Domingues*
Chemistry Department, University of Aveiro, 3810-193 Aveiro, Portugal

Received 13 June 2004; Revised 22 September 2004; Accepted 22 September 2004

Lineloyl-palmitoyl (PLPC) and arachidonoyl-palmitoyl (PAPC) phosphatidylcholine were oxidized under Fenton reaction conditions (H_2O_2 and Fe^{2+}), and the short-chain products formed were identified by electrospray ionization mass spectrometry (ESI-MS). The short-chain products resulted from *β*-cleavage of oxygen-centered radicals and comprised aldehydes, hydroxyaldehydes and dicarboxylic acids that yielded both $[MH]^+$ and $[MNa]^+$ ions. The fragmentation of the $[MH]^+$ and $[MNa]^+$ ions of the peroxidation products was studied by tandem mass spectrometry (MS/MS). The MS/MS spectra of both ions showed ions resulting from characteristic losses of glycerophosphatidylcholine. Other product ions, resulting from C–C cleavages occurring in the vicinity of the functional group, and fragmentations involving the hydroxy groups, were the most informative since they allowed us to obtain structural information relating to the *sn*-2 acyl residue. Both fragmentation pathways are due to charge-remote fragmentation occurring by a 1,4-hydrogen elimination mechanism and/or by homolytic cleavage. Furthermore, the fragmentation pathway of some ions observed in the ESI-MS spectrum was not consistent with the fragmentation behavior expected for some of the short-chain species identified in the literature and allowed the reassignment of the ions as different structures. Isobaric ions were observed in the ESI-MS spectra of both oxidized phospholipids, and were differentiated based on distinct fragmentation. The detailed knowledge of lipid peroxidation degradation products is of major importance and should be very valuable in providing new markers for oxidative stress signaling and for disease states monitoring. Copyright © 2004 John Wiley & Sons, Ltd.

Glycerophosphatidylcholines (GPCs) comprise the majority of the phospholipids in membranes and are composed of a phosphocholine polar head linked to the glycerol moiety, and fatty acid chains linked to the *sn*-2 and *sn*-1 positions, that may either be saturated or unsaturated chains.[1] Among the unsaturated fatty acid chains occurring in biological samples, the linoleic and arachidonic acids predominate.[2] Due to the presence of double bonds in the fatty acid chains these compounds are susceptible to oxidative damage by reactive oxygen species (ROS). One of the most reactive species is the hydroxyl radical ($HO^{\cdot}$)[3] that is formed under aerobic conditions. In biological systems this radical species is formed by a Fenton-like reaction with implications in oxidative stress and diseases.[4] The oxidative process is a complex radical reaction leading to the formation of oxidized intact phospholipids, and to short-chain products containing a short acyl fatty acid formed through a *β*-cleavage mechanism. The GPC peroxidation products are responsible for increasing the polarity of the phospholipids and consequently decrease the fluidity of the membrane, or even cause disruption of the membrane integrity.[5] This is thought to be the cause of several pathological conditions such as atherosclerosis, Alzheimers disease, Parkinsons disease, cataracts, diabetes and others age-related diseases.[6,7] On the other hand, some of the oxidized phosphatidylcholines have been found to possess biological activity similar to platelet-activating factor (PAF).[8,9]

In the last decade, short-chain products derived from phospholipid oxidation have been studied by mass spectrometry (MS); however, most of the studies involved derivatization strategies prior to MS analysis.[10–14] More recently, soft ionization methods have been used in the analysis of underivatized short-chain products of GPCs.[15,16] Based on MS data some short-chain products were identified, namely aldehydes, hydroxyaldehydes and dicarboxylic acids, formed from radical-derived reactions in linoleate- and arachidonate-containing phospholipids.[10–16] However, very little work has been dedicated to the study by tandem mass

**Correspondence to*: M. R. M. Domingues, Department of Chemistry, University of Aveiro, 3810-193 Aveiro, Portugal.
E-mail: mrd@dq.ua.pt

spectrometry (MS/MS) of the short-chain phospholipids. So far, the work published describes the fragmentation pattern of specific peroxidation products that were derivatized.[10–13] To our knowledge, no work has been dedicated to the investigation of the fragmentation pattern, by MS/MS, of underivatized GPC short-chain peroxidation products. This lack of information should be overcome since MS/MS will be very useful for the structural identification of short-chain products, and particularly important when applied to the analysis of individual peroxidation products in complex mixtures, such as the ones obtained from *in vivo* analysis. Moreover, detailed knowledge of lipid peroxidation degradation products should be very valuable in providing new markers for oxidative stress signaling and for disease state monitoring, giving new insights into the pathogenesis process.

The purpose of the present study was to identify the short-chain oxidation products formed during oxidation of phosphatidylcholines (16:0/18:2 and 16:0/20:4) under Fenton reaction conditions. Oxidation reactions were monitored, analyzing the reaction solution by electrospray ionization mass spectrometry (ESI-MS). Structural characterization of the identified products was performed by MS/MS. Detailed fragmentation observed in the MS/MS spectra will be discussed, allowing the identification of typical fragmentations pathways of short-chain products formed and permitting the confirmation (or not) of the proposed structures for short-chain oxidation products.

EXPERIMENTAL

Chemicals

Glycerophosphocholine phospholipids (16:0/18:2 and 16:0/20:4) were obtained from Sigma (St. Louis, MO, USA) and used without further purification. $FeCl_2$ and H_2O_2 used for the peroxidation reactions were purchased from Merck (Darmstadt, Germany).

Preparation of GPC vesicles

Vesicles were prepared from stock solutions of 1 mg/mL and dried under a nitrogen stream. Ammonium bicarbonate buffer (pH 7.4) was added to a final phospholipid concentration of 50 mM, and the mixture vortexed.[17]

Oxidation of GPC vesicles by Fenton reaction

Oxidative treatments performed on the GPC vesicles were conducted by addition to 50 μL of phospholipid vesicles, 5 mmol $FeCl_2$ solution and 50 mmol of hydrogen peroxide (H_2O_2) in 0.5 mL of solution. This mixture was left to react at 37°C in the dark for different periods of time with occasional sonication. The controls were prepared by replacing H_2O_2 with water. The phospholipid oxidation products were extracted using a modification of the Folch method with chloroform/methanol (2:1, v/v).[18] The extent of oxidation was monitored by ESI-MS.

ESI-MS

Positive ion mode ESI mass spectra and tandem mass spectra were acquired in a Q-TOF 2 instrument (Micromass, Manchester, UK) using a MassLynx software system (version 4.0). The samples for ESI analyses were prepared by diluting 5 μL of the sample in 1000 μL of chloroform/methanol solution (1:1, v/v). Samples were introduced into the mass spectrometer using a flow rate of 10 μL/min, setting the needle voltage at 3000 V with the ion source at 80°C and cone voltage at 35 V. Tandem mass spectra (MS/MS) of $[MH]^+$ and $[MNa]^+$ ions produced by ESI-MS were obtained by collision-induced decomposition (CID), using argon as the collision gas (measured pressure in the Penning gauge $\sim 6 \times 10^{-6}$ mbar) and varying collision energy between 15–35 eV. In MS and MS/MS experiments time-of-flight (TOF) resolution was set to approximately 9000.

RESULTS AND DISCUSSION

MS of peroxidation products of PLPC and PAPC

The peroxidation reaction of 1-palmitoyl-2-lineloyl-glycerophosphatidylcholine (PLPC) under Fenton conditions was monitored by ESI-MS and the spectra obtained in the presence (Fig. 1(A)) and absence (Fig. 1(B)) of H_2O_2 were compared. As can be seen, additional ions were observed in the MS spectrum obtained under oxidative conditions (in the presence of H_2O_2). In both ESI-MS spectra the native PLPC was observed as $[MH]^+$ (*m/z* 758) and $[MNa]^+$ (*m/z* 780); thus the short-chain products formed are observed in the MS spectrum also as $[MH]^+$ and $[MNa]^+$ ions. This fact will be considered in the assignment of additional ions observed in the ESI-MS spectrum obtained under oxidative conditions.

PLPC phospholipid contains palmitic acid (saturated fatty acid chain) at the *sn*-1 position and linoleic acid (unsaturated fatty acid chain) at the *sn*-2 position. The saturated fatty acid is not expected to undergo radical oxidation, so the short-chain products are formed as the result of *β*-cleavage oxidation of the linoleic acid. In the linoleic acid moiety the bis-allylic hydrogen at C-11 is more likely to be abstracted by the hydroxyl radical than the mono-allylic hydrogen atoms at C-8 or C-14. By double-bond migration, the oxidation at C-9 and C-13 positions occurs and through *β*-scission generates short-chain products of different chain length with terminal aldehydic function (Scheme 1),[19] which can further be oxidized to a terminal dicarboxylic function. Both can undergo further oxidation to other short-chain products.

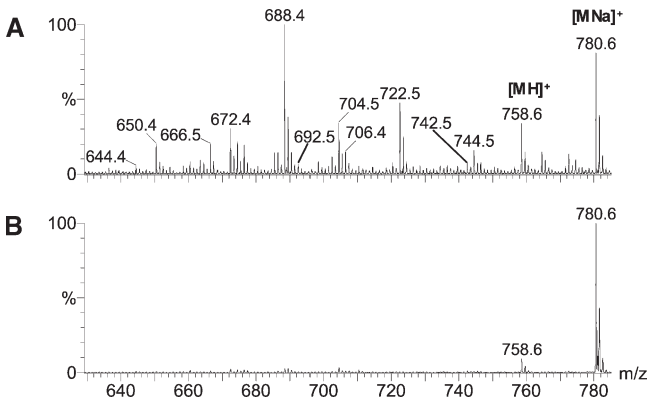

Figure 1. ESI-MS spectra obtained for PLPC in the presence (A) and absence (B) of H_2O_2. The ESI-MS spectra were constructed with the same number of scans and normalized to the base peak.

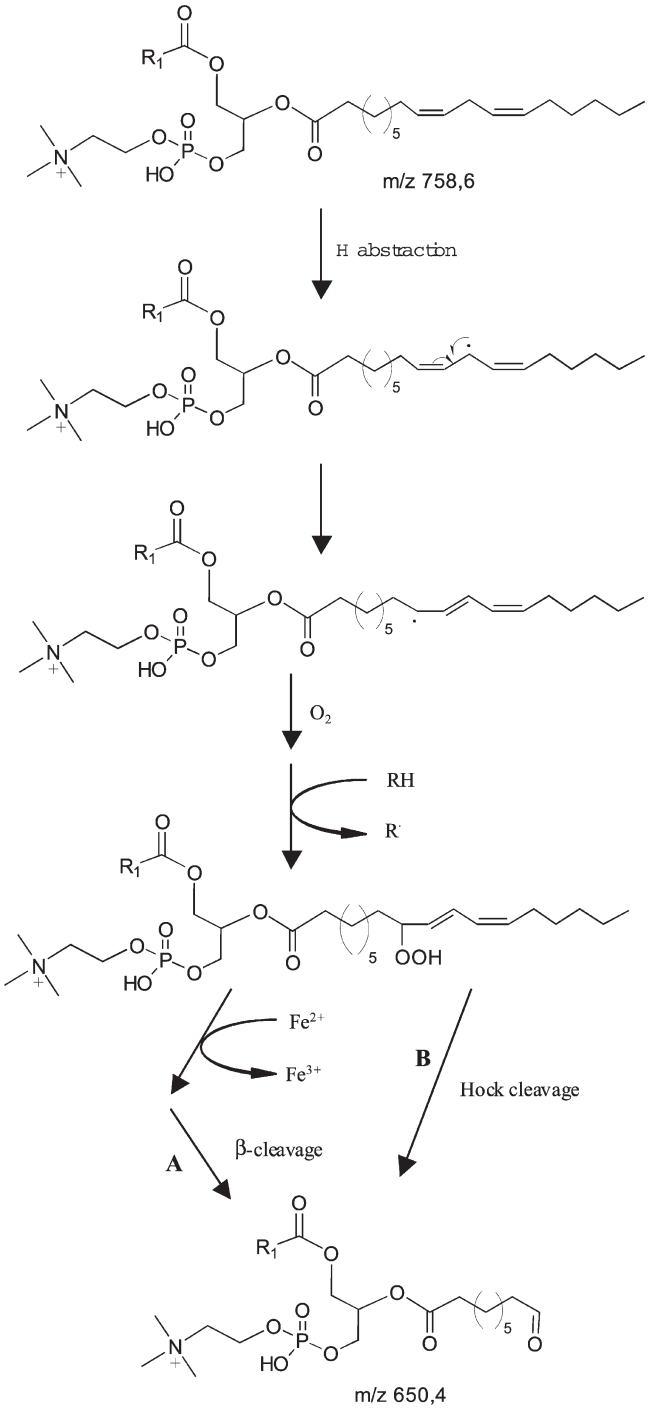

Scheme 1. Proposed formation of 1-palmitoyl-2-(9-oxo-nonanoic acid)-phosphatidylcholine observed at *m/z* 650 ($[MH]^+$) in the ESI-MS spectrum of PLPC after oxidation.

Based on this knowledge the predominant ion observed in the ESI-MS spectrum at *m/z* 688 (Fig. 1(A)) was attributed to the $[MNa]^+$ of 1-palmitoyl-2-(nonadioic acid)-glycerophosphatidylcholine. This short-chain product is a C_9 dicarboxylic acid, suggesting that the intermediate radical at C-9 is more favorable or more stable relative to the intermediate radical species at C-13. This dicarboxylic acid may result from oxidation in solution of the oxo derivative as previously suggested.[20] The corresponding oxo derivative, 1-palmitoyl-2-(9-oxo-nonanoic acid)-glycerophosphatidylcholine, was observed at *m/z* 672 ($[MNa]^+$). These products have already been reported by Spiteller and coworkers during the identification of peroxidation products of linoleic acid by gas chromatography/mass spectrometry (GC/MS).[21] Other ions observed in the ESI-MS spectrum (Fig. 1(A)) give evidence for radical oxidation in other positions along the *sn*-2 carbon chain, such as the ion at *m/z* 658 reflecting the initial contribution of an oxygen-centered radical (alkoxyl radical) placed at the C-8 position, and the ion at *m/z* 714 from an alkoxyl radical at the C-11 position. The corresponding protonated molecules of the identified short chains were observed but with lower relative abundance. Other short-chain products identified in the MS spectra as $[MH]^+$ and $[MNa]^+$ ions are summarized in Table 1, comprising terminal aldehydic and terminal dicarboxylic products some of them being saturated or unsaturated, and being substituted (or not) with keto or hydroxy groups. Some of the identified ions described here have already been reported during peroxidation studies of GPC, and the references are identified in Table 1.

The peroxidation reaction of 1-palmitoyl-2-arachidonoyl-glycerophosphatidylcholine (PAPC) under Fenton conditions ($H_2O_2 + Fe^{2+}$) was also monitored by ESI-MS and the spectra obtained in the presence (Fig. 2(A)) and absence (Fig. 2(B)) of H_2O_2 are shown in Fig. 2. By comparison of the spectra, additional ions were observed in the MS spectrum obtained under oxidative conditions (in the presence of H_2O_2).

In PAPC the oxidation occurred in the arachidonic acid (20:4) at the *sn*-2 position, which contains three bis-allylic hydrogen atoms at C-7, C-10 and C-13. These hydrogen atoms may be readily abstracted by the hydroxyl radical, providing several places of oxidation that through a *β*-scission mechanism break down to short-chain phospholipid products with terminal aldehydic and dicarboxylic functions, as described for PLPC and shown in Scheme 1.

With this knowledge, the ion at *m/z* 616 observed in the ESI-MS spectrum was attributed to the $[MNa]^+$ ion of a C_5 aldehyde (1-palmitoyl-2-(5-oxo-pentanoic acid)-glycerophosphatidylcholine), suggesting the occurrence of an intermediate radical at C-5; the ion at *m/z* 642 to the $[MNa]^+$ ion of the C_7 aldehyde (1-palmitoyl-2-(7-oxo-5-heptenoic acid)-glycerophosphatidylcholine); and the ion at *m/z* 672 to the $[MNa]^+$ ion of the C_8 aldehyde (1-palmitoyl-2-(5-hydroxy-8-oxo-6-octenoic acid)-glycerophosphatidylcholine). The corresponding protonated molecules are also observed. The identification of saturated, unsaturated and hydroxyaldehydes are consistent with the results obtained by oxidation of the arachidonic acid.[21,22] Ions observed in the ESI-MS spectrum were attributed to unsaturated hydroxyaldehydes, although hydroxyaldehydes containing more than one double bond were not identified during oxidation of arachidonic acid.[22] Dicarboxylic acids were also identified in this study, such as the ion at *m/z* 632 observed in the ESI-MS spectrum and attributed to the $[MNa]^+$ ion of a C_5 dicarboxylic acid (1-palmitoyl-2-(pentandioic acid)-glycerophosphatidylcholine). Overall, the short-chain products of PLPC and PAPC identified could be summarized into two different classes: the products with an oxo terminal functional group among which are included saturated,

Table 1. Aldehydic and dicarboxylic acids identified as short-chain peroxidation products formed by oxidation of PLPC and PAPC and observed in the ESI-MS spectra as $[MNa]^+$ and $[MH]^+$ ions

Structural feature	GPC*	Peroxidation product	*m/z*	Value	Ref.
Aldehydes	PLPC	1-palmitoyl-2-(7-oxoheptanoic acid)-GPC	622	644	
		1-palmitoyl-2-(8-oxooctanoic acid)-GPC	636	658	15
		1-palmitoyl-2-(9-oxononanoic acid)-GPC	650	672	15
		1-palmitoyl-2-(11-oxo-9-undecenoic acid)-GPC	676	698	
		1-palmitoyl-2-(8-hydroxy-11-oxo-9-undecenoic acid)-GPC	692	714	
		1-palmitoyl-2-(9-keto-12-oxo-10-dodecenoic acid)-GPC	704	726	15
		1-palmitoyl-2-(8-hydroperoxide-9-oxo-nonanoic acid)-GPC	704	726	
		1-palmitoyl-2-(9-hydroxy-12-oxo-10-dodecenoic acid)-GPC	706	728	
		1-palmitoyl-2-(12-oxo-8,10-dodecedienoic acid)-GPC	710	732	
	PAPC	1-palmitoyl-2-(5-oxopentanoic acid)-GPC	594	616	12
		1-palmitoyl-2-(7-oxo-5-heptenoic acid)-GPC	620	642	
		1-palmitoyl-2-(4-hydroxy-7-oxo-5-heptenoic acid)-GPC	636	658	
		1-palmitoyl-2-(5-keto-8-oxo-6-octenoic acid)-GPC	648	—	16
		1-palmitoyl-2-(4-hydroperoxide-5-oxopentanoic acid)-GPC	648	—	
		1-palmitoyl-2-(5-hydroxy-8-oxo-6-octenoic acid)-GPC	650	672	16
		1-palmitoyl-2-(10-oxo-6,8-decedienoic acid)-GPC	660	682	
		1-palmitoyl-2-(5-hydroxy-6,8-undecedienoic acid)-GPC	690	—	
		1-palmitoyl-2-(10-hydroxy-5,8,11-tridecatrienedioic acid)-GPC	732	754	
Dicarboxylic acids	PLPC	1-palmitoyl-2-(octanedioic acid)-GPC	652	674	
		1-palmitoyl-2-(nonadioic acid)-GPC	666	688	16
		1-palmitoyl-2-(9-keto-10-dodecenedioic acid)-GPC	720	742	16
		1-palmitoyl-2-(9-hydroxy-10-dodecenedioic acid)-GPC	722	744	
		1-palmitoyl-2-(8-oxo-9,11-tridecedienedioic acid)-GPC	732	754	
	PAPC	1-palmitoyl-2-(pentanedioic acid)-GPC	610	632	16
		1-palmitoyl-2-(4-hexenedioic acid)-GPC	622	644	
		1-palmitoyl-2-(5-heptenedioic acid)-GPC	636	658	
		1-palmitoyl-2-(6-octenedioic acid)-GPC	650	672	
		1-palmitoyl-2-(5-hydroxy-6-octenedioic acid)-GPC	666	688	

*GPC is the abbreviation for glycerophosphatidylcholine.

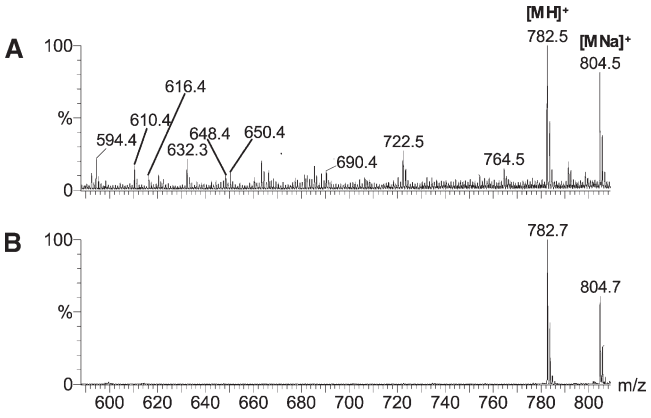

Figure 2. ESI-MS spectra obtained for PAPC in the presence (A) and absence (B) of H_2O_2. The ESI-MS spectra were constructed with the same number of scans and normalized to the base peak.

unsaturated, keto- and hydroxyaldehydes; and also products with a carboxy terminal functional group (dicarboxylic acids) where saturated, unsaturated aldehydes, keto- and hydroxyaldehydes are also included. In Table 1 the short-chain products are identified. Some of the identified ions have already been reported during peroxidation studies of PAPC and the references are identified in Table 1.

The fragmentations of $[MH]^+$ and $[MNa]^+$ ions of the PLPC and PAPC short-chain products were studied by MS/MS.

MS/MS of short-chain products

To date, fragmentation studies have focused on intact GPCs allowing the identification of characteristic fragment ions for each class of phospholipids.[23–25] In the case of GPC assignment, this is based on the identification of fragment ions due to loss of $N(CH_3)_3$ (59 Da), loss of $HPO_4(CH_2)_2N(CH_3)_3$ (183 Da), loss of $NaPO_4(CH_2)_2N(CH_3)_3$ (205 Da), and loss of *sn-1* and *sn-2*. These fragmentations occurred in the MS/MS spectra of sodiated GPC, while in the MS/MS spectra of protonated molecules a fragment ion at *m/z* 184 with high abundance is present. Other fragment ions are absent in low-energy (LE) MS/MS spectra.[23,26]

Analyzing the MS/MS spectra of the short-chain products obtained (Table 1), the MS/MS spectra of $[MH]^+$ and $[MNa]^+$ ions showed distinct fragmentation patterns. The MS/MS spectra of $[MNa]^+$ ions showed characteristic fragmentation, namely loss of 59, 183 and 205 Da, loss of the *sn*-2 residue as a free fatty acid ($-R_2COOH$) and as a sodium salt ($-R_2COONa$), and also fragment ions at *m/z* 147 and 184. On the other hand, the MS/MS spectra of $[MH]^+$ ions exhibit an ion at *m/z* 184 as the base peak. Other fragment ions due to loss of 59 and 183 Da, loss of the *sn*-2 fatty acid chain as a free fatty acid ($-R_2COOH$) and as a ketene ($-R_2=C=O$) were also observed with very low relative abundance. The loss of the fatty acid chain as ($-R_2COOH$) and as a ketene ($-R_2=C=O$) is in accordance with the fragmentation behavior described for protonated molecules of intact GPC species.[25] The MS/MS spectra, both of $[MNa]^+$ and of $[MH]^+$ ions, also showed product ions resulting from

Table 2. Product ions observed in the MS/MS spectra of $[MNa]^+$ ions of PLPC at *m/z* 644, 658, 672, 688, 698, 710, 742 and 744, and of PAPC at *m/z* 616 and 632

	$[MNa]^+$ ions									
	644	658	672	688	698	710	742	744	616	632
−59 Da	585 (70)	599 (72)	613 (100)	629 (100)	639 (100)	651 (40)	683 (100)	685 (100)	557 (100)	573 (100)
−183 Da	461 (100)	475 (100)	489 (80)	505 (75)	515 (80)	527 (100)	559 (90)	561 (80)	433 (90)	449 (90)
−205 Da	439 (25)	453 (6)	467 (10)	483 (5)	493 (<5)	505 (30)	537 (5)	539 (<5)	411 (6)	427 (<5)
$-R_1COOH$	388 (5)	402 (<5)	416 (<5)	432 (5)	442 (<5)	454 (6)	486 (<5)	488 (5)	360 (<5)	376 (<5)
$-R_2COOH$	500 (<5)	500 (<5)	500 (<5)	500 (<5)	500 (<5)	500 (<5)	500 (<5)	500 (<5)	500 (<5)	500 (<5)
$-R_2COONa$	478 (<5)	478 (<5)	478 (<5)	478 (<5)	478 (<5)	478 (25)	478 (40)	478 (<5)	478 (<5)	478 (5)
$-H_2O$				670 (<5)			724 (<5)	726 (<5)		614 (<5)
$-CO_2$										588 (<5)
γ-bond*		550 (<5)	550 (<5)	551 (<5)	551 (<5)		550 (<5)	550 (<5)	551 (<5)	550 (<5)
γ-bond							671 (<5)			
γ-bond (keto)							614 (<5)			
α-bond (hydroxy)								670 (<5)		
$[MNa-205-CO_2]^+$								494 (<5)		
γ-bond $[MNa-205]^+$				409 (<5)		409 (<5)				
β-bond $[MNa-205]^+$		410 (<5)								
α-bond $[MNa-sn1]^+$	359 (<5)							387 (<5)		
γ-bond $[MNa-sn1]^+$				358 (<5)	387 (<5)		415 (<5)			

combined losses of characteristic fragments, such as ions formed by loss of 59 and of *sn*-2. As can be seen, the characteristic ion in the MS/MS spectra of the $[MNa]^+$ ion of short-chain products was at *m/z* 147, while, in the MS/MS spectra of the $[MH]^+$ ion of short-chain products, it was the ion at *m/z* 496 (loss of R_2=C=O). Altogether, these fragments did not provide any structural information regarding the structure of the short *sn*-2 acyl residue.

Other fragments, observed with low abundance in the MS/MS spectra of $[MNa]^+$ and $[MH]^+$, resulted from cleavages in the vicinity of the functional group at the *sn-2* chain, by charge-remote fragmentation, either by homolytic cleavage or a 1,4-elimination mechanism and gave very useful structural information. These charge-remote fragmentations also occur combined with loss of 183 Da and with loss of R_1COOH. Charge-remote fragmentations have already been observed in MS/MS spectra obtained with a Q-TOF2 instrument of anilide derivatives of fatty acids[27] and of linoleic acid spin adducts.[28] These fragment ions allowed the identification of the functional groups present in the *sn*-2 moiety, and the information regarding the location of substituents along the *sn*-2 chain, since CID spectra of the intact GPC $[MH]^+$ ions gives essentially a single product ion at *m/z* 184.[29] The occurrence of ions as charge-remote fragmentations resulting from cleavage in the vicinity of the functional group was earlier described in oxo-fatty acids.[30] Tables 2 and 3 summarize the main ions observed in the MS/MS spectra of $[MNa]^+$ and $[MH]^+$ ions, respectively, of short-chain products identified in PLPC and PAPC. Common fragmentation pathways will be described for each group of short-chain products with the same functional group.

The dicarboxylic acids, occurring as saturated and as unsaturated, exhibited characteristic product ions formed by loss of CO_2 from the precursor ion, denoting cleavage of the α-bond relative to the terminal functional group. The loss of CO_2 was also observed combined with loss of 205 Da (Table 2) and loss of 183 Da (Table 3), or even combined with the loss of *sn*-1. Other ions observed in the MS/MS spectra of dicarboxylic acids were the cleavage of the γ-bond relative to the terminal carboxy function, and ions due to the cleavage of the γ-bond in the carboxy group esterified to the phosphocholine moiety (γ-bond*). The cleavage of the carbon chain involved homolytic and/or 1,4-elimination mechanisms. Aldehydic short-chain compounds, either saturated or unsaturated, exhibited product ions attributed to cleavage of the β-bond (loss of 43 Da) relative to the terminal oxo function. The location of the hydroxy group, identified both in hydroxy acids and in hydroxyaldehydes, could also be determined since cleavage of the α-bond involving the hydroxy group was identified.[28] The presence of the keto group induces fragmentation by cleavage of the γ-bond relative to this group.[30] Some ions could result from two different fragmentation pathways, which may make the assignment difficult. The fragmentation pathways described are summarized in Scheme 2.

As an example of the $[MNa]^+$ ion fragmentation, the MS/MS spectrum of the ion at *m/z* 688 (dicarboxylic acid), which is the most abundant ion in the ESI-MS spectrum, is shown in Fig. 3 and the schematic representation of the fragmentation pathways identified in the MS/MS spectrum is also shown (Scheme 3). The ions at *m/z* 409 and 358 may result from cleavage of the C_6–C_7 carbon bond (γ bond) by a 1,4-hydrogen elimination mechanism from $[MNa-R_1COOH]^+$ and from $[MNa-205]^+$ (*), respectively. These ions, along with others observed at *m/z* 460 and 373 resulting from homolytic cleavages in the α- and in β-bond (Scheme 3), provide evidence for the fragmentation pattern described for dicarboxylic acids. Other ions observed in the MS/MS spectrum at *m/z* 227 and 249 result from combined loss of *sn*-1 and 205 or 183 Da, respectively.

Table 3. Product ions observed in the MS/MS spectra of $[MH]^+$ ions of PLPC at *m/z* 636, 650, 666, 692, 720 and 722, and of PAPC at *m/z* 594, 610, 620, 622, 636, 650, 666 and 690.

	$[MH]^+$ ions												
	636	650	666	692	720	722	594	610	620	622	636	650	666	690
−59 Da	577 (<5)	591 (<5)	607 (<5)	633 (18)	661 (25)	663 (30)	535 (<5)	551 (<5)	561	563 (<5)	577	591 (10)	607 (<5)	631
−183 Da	453 (<5)	467 (<5)	483 (<5)	509 (<5)	537 (<5)	539 (8)	411 (<5)	427 (<5)	437	439 (<5)	453	467 (<5)	483 (<5)	507
$-R_1COOH$	380 (<5)	394 (<5)	410 (<5)	436 (<5)	464 (12)	466 (<5)	338 (<5)	354 (<5)	364	366 (<5)	380	394 (15)	410 (<5)	434
$-R_2{=}C{=}O$	496 (<5)	496 (<5)	496 (<5)	496 (<5)	496 (<5)	496 (<5)	496 (<5)	496 (<5)	496	496 (<5)	496 (<5)	496 (<5)	496 (<5)	496
$-R_2COOH$	478 (<5)	478 (<5)	478 (<5)	478 (<5)	478 (25)	478 (13)	478 (<5)	478 (<5)	478	478 (<5)	478 (<5)	478 (<5)	478 (40)	478
$-H_2O$			648 (<5)	674 (<5)	702 (<5)	704 (<5)		592 (<5)			618 (<5)	632 (<5)	648 (<5)	
$-CO_2$								566 (<5)		578 (<5)	592 (<5)		—	
γ-bond*	551 (<5)	551 (<5)	550 (<5)	551 (<5)		551 (<5)	551 (<5)	551 (<5)	551 (<5)	550 (<5)	551 (<5)	550 (<5)	550 (25)	550 (<5)
γ-bond			593 (<5)		650 (<5)			536 (<5)			565 (<5)			
γ-bond (keto)					592 (<5)									
β-bond (oxo)	607 (<5)													
α-bond (hydroxy)				607 (<5)							581 (<5)	564 (<5)	595 (<5)	595 (<5)
α-bond [MH−*sn*1]					419 (<5)	365 (<5)			335 (<5)				309 (<5)	
$[MH-183-CO_2]^+$					495 (<5)	497 (<5)		383 (<5)		395 (<5)				
γ-bond $[MH-183]^+$											409 (<5)			
β-bond $[MH-183]^+$	410 (<5)	424 (<5)												
α-bond $[MH-183]^+$				438 (<5)		365 (<5)						411 (<5)	411 (<5)	

An example of the $[MH]^+$ ion fragmentation is given in the MS/MS spectrum of the ion at *m/z* 692 (Fig. 4) attributed to the 1-palmitoyl-2-(8-hydroxy-11-oxo-9-undecenoic acid)-glycerophosphatidylcholine (inset in Fig. 4). In this MS/MS spectrum it is possible to observe the characteristic GPC fragments at *m/z* 633 (−59 Da), 509 (−183 Da) and 478 ($-R_2COOH$), as well as ions at *m/z* 607 (A) and 551 (B) formed by a homolytic cleavage mechanism (as exemplified in Scheme 2(A)) that occur in the *sn*-2 chain in the vicinity of the functional group. 1-Palmitoyl-2-(8-hydroxy-11-oxo-9-undecenoic acid)-glycerophosphatidylcholine has never been reported as a peroxidation product of 1-palmitoyl-2-linoleoyl-glycerophosphocholines, although the 11-oxo-9-undecenoic acid was earlier identified during non-enzymatic linoleic acid peroxidation.[31]

Some of the ions observed in the ESI-MS spectrum of oxidized PLPC and PAPC, and identified in the literature based on the *m/z* values as $[MNa]^+$ or $[MH]^+$ ions, were reassigned based on the fragmentation pattern obtained, such as the ions at *m/z* 648 (PAPC), 704 (PLPC) and 710 (PLPC). The ion at *m/z* 648 was initially attributed to the $[MH]^+$ of 1-palmitoyl-2-(5-keto-8-oxo-6-octenoic acid)-glycerophosphatidylcholine,[16] but the MS/MS spectrum (Fig. 5) showed the presence of the product ion at *m/z* 147 and the ion due to loss of R_2COONa, both indicative of an $[MNa]^+$ ion. These product ions indicate that the ion at *m/z* 648 should have the contribution of the $[MNa]^+$ ion corresponding to another short-chain PAPC product, in addition to the presence of the initially proposed $[MH]^+$ ion. The ions at *m/z* 616, 557 and 433 due to loss of 32 Da (O_2) from the precursor ion, and combined with loss of 59 and 183 Da from the precursor ion, respectively, were observed in the MS/MS spectrum. Based on the ions observed in the MS/MS spectrum, the $[MNa]^+$ ion was assigned to the hydroperoxide derivative of 1-palmitoyl-2-(5-oxo-pentanoic acid)-glycerophosphatidylcholine (*m/z* 616). The ion at *m/z* 367, resulting from cleavage of the $[MH-183]^+$ ion between C_3–C_4 of the *sn*-2 fatty acid chain (described in Scheme 4), gives support to the structure of the hydroperoxy-alkanal.

The ion at *m/z* 704 (obtained from PLPC) was initially attributed to the $[MH]^+$ ion of 1-palmitoyl-2-(8-keto-12-oxo-10-dodecenoic acid)-glycerophosphatidylcholine,[16] but the MS/MS spectrum (data not shown) revealed product ions due to loss of 205 Da from the precursor ion, as well as the ions at *m/z* 478 and 147 formed by loss of the *sn*-2 as R_2COONa, and the phosphocholine head, respectively. These ions are characteristic of $[MNa]^+$ MS/MS spectra of GPCs. The ions at *m/z* 672, 613 and 489 due to loss of 32 Da (O_2) from the precursor ion, and combined with loss of 59 and 183 Da from the precursor ion, respectively, were observed in the MS/MS spectrum. Based on the fragmentation pattern described, the ion at *m/z* 704 was identified as the $[MNa]^+$ of 1-palmitoyl-2-(8-hydroperoxide-9-oxo-nonanoic acid)-glycerophosphatidylcholine, although the presence of the initially proposed $[MH]^+$ ion cannot be excluded.

Interestingly, the occurrence of hydroperoxy-alkanals, predicted as peroxidation products of ω-6-polyunsaturated fatty acids,[32] has never been reported in *in vitro* phospholipid peroxidation studies. Similarly, the presence of hydroperoxy-alkenals is expected, although they were not identified

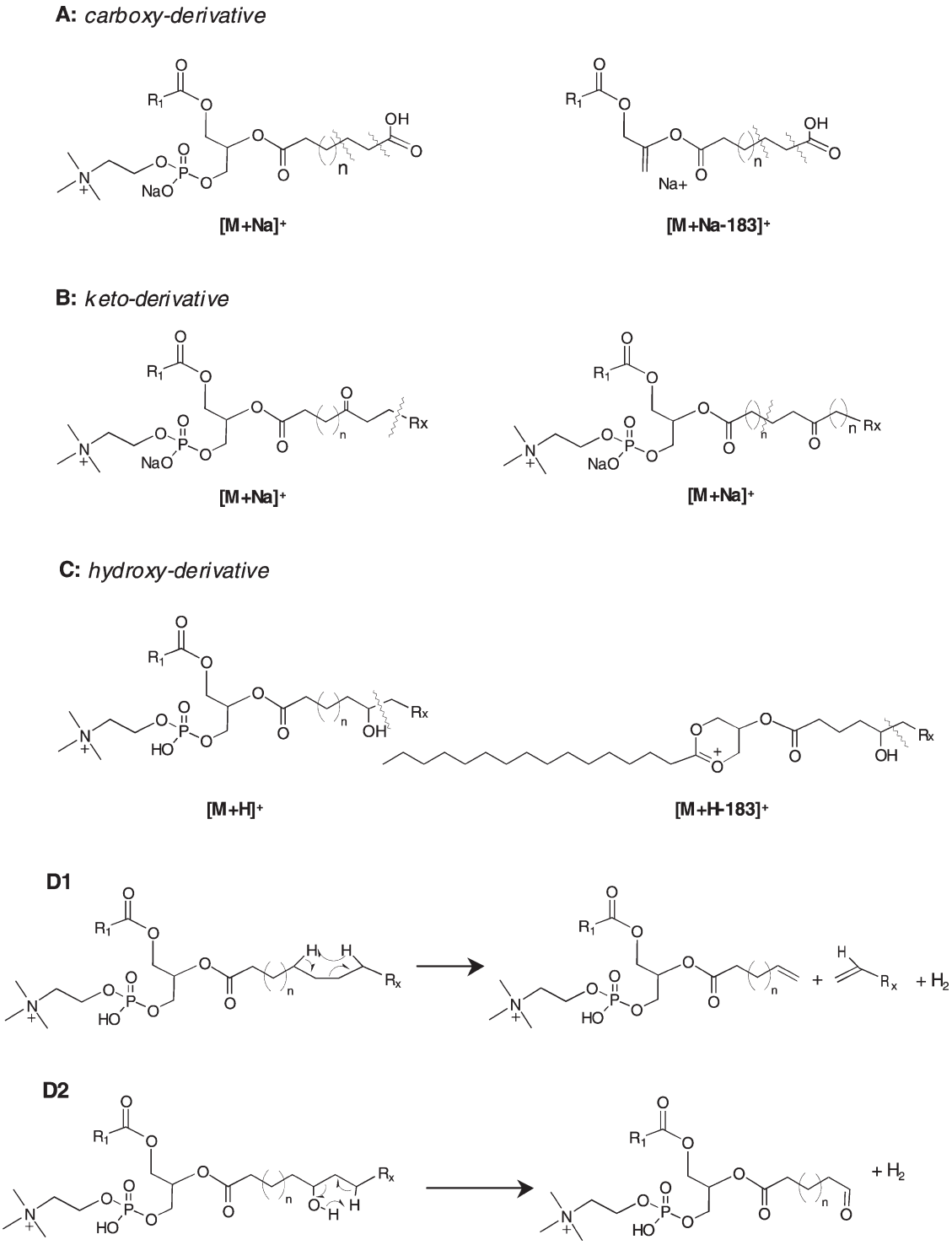

Scheme 2. Schematic representation of the fragmentation pathways identified for $[MNa]^+$ ions by homolytic cleavage mechanisms in carboxy derivatives (A), in keto derivatives (B), in hydroxyl derivatives (C), and by 1,4-hydrogen elimination mechanism involving the saturated fatty acid chain (D1) and involving the hydroxy group (D2) (R_x: carbon chain).

during this study, which may probably be due to the high tendency of unsaturated aldehydes to undergo further decomposition.[22]

The MS/MS spectrum of the ion observed at *m/z* 710 (Fig. 6), initially attributed to the $[MNa]^+$ of 1-palmitoyl-2-(12-oxo-8,10-dodecedienenoic acid)-glycerophosphatidylcholine reflecting the presence of the intermediate alkoxyl radical at C-12, exhibited the product ion formed by loss of 205 Da confirming it to be a $[MNa]^+$ ion of GPC. The ion at *m/z* 147 was absent and in turn the fragment ion at *m/z* 169 was observed. Thus the ion was identified as corresponding to the doubly sodiated ion of the dicarboxylic acid containing the second sodium atom at the terminal carboxylic group. This identification may be corroborated by the presence of the

RCM

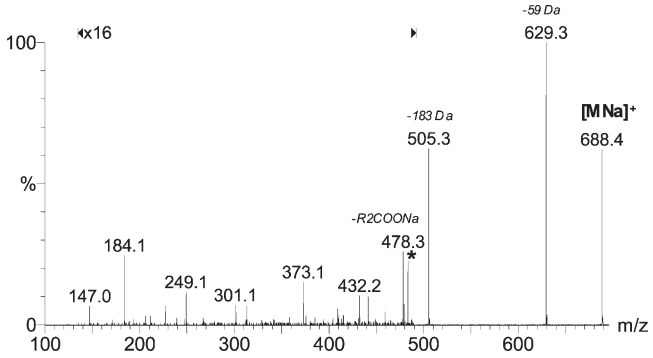

Figure 3. MS/MS spectrum of the $[MNa]^+$ ion at *m/z* 688. The asterisk corresponds to the product ion due to loss of 205 Da.

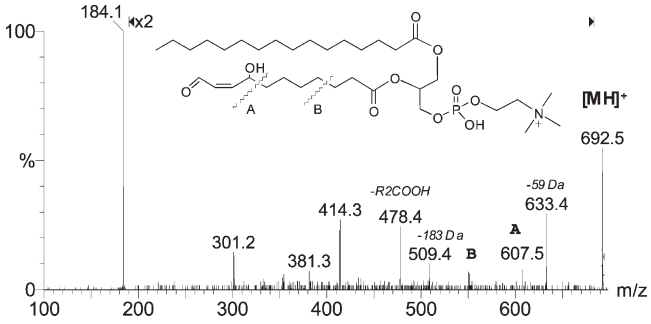

Figure 4. MS/MS spectrum of the $[MH]^+$ ion at *m/z* 692. The insets show the proposed structures for each product ion.

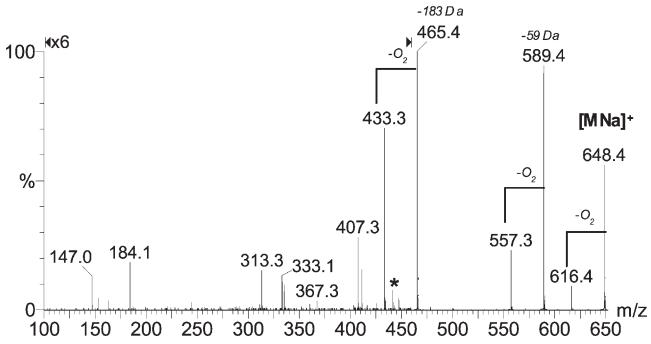

Figure 5. MS/MS spectrum of the $[MNa]^+$ ion at *m/z* 648. The asterisk corresponds to the ion due to loss of 205 Da.

product ion at *m/z* 228 that corresponds to the five-membered cyclophosphane containing an additional sodium atom at the phosphoric acid moiety (monocharged). No other ions containing this feature were identified for the oxidized PLPC.

Overall, of the oxidized phosphatidylcholines products studied in this work, it is possible to notice the contribution of ions with the same *m/z* value in the MS spectra of the phosphatidylcholines after oxidation, although they correspond to different structures. Isobaric ions identified in both PLPC and PAPC were observed at *m/z* 636, 650, 666 and 732 (see Table 1). These peroxidation products were identified since each phospholipid was analyzed separately; however, when monitoring short-chain products as markers of oxidative stress in *in vivo* samples, each of the peroxidation products deriving from PLPC or PAPC will contribute to the total ion current at a given *m/z* value. The characteristic fragmentation pattern identified for dicarboxylic acids and for aldehydic products will provide their differentiation since, due to their different structures, they show different MS/MS spectra.

As an example, the ion at *m/z* 650 was attributed to the $[MH]^+$ of 1-palmitoyl-2-(9-oxo-nonanoic acid)-glycerophosphatidylcholine for PLPC and to 1-palmitoyl-2-(5-hydroxy-8-oxo-octenoic acid)-glycerophosphatidylcholine for PAPC. Their MS/MS spectra are shown in Figs. 7(A) and 7(B), respectively. Both MS/MS spectra exhibit common ions characteristic of GPC such as *m/z* 591 (−59 Da), 467 (−183 Da), and 184 (base peak as expected from the precursor $[MH]^+$ ion), and the ions formed by loss of *sn*-1 (*m/z* 394 and 412) and loss of *sn*-2 (*m/z* 478 and 496); however, differences in the fragmentations were also identified. The MS/MS spectrum of

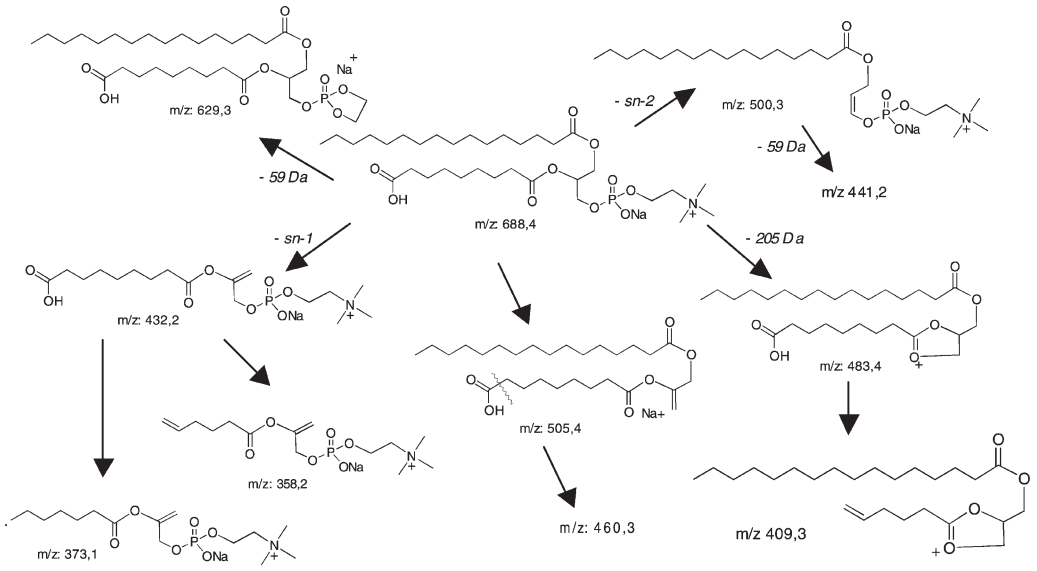

Scheme 3. Proposed fragmentation pathways identified in the ESI-MS/MS spectrum for the ion at *m/z* 688.

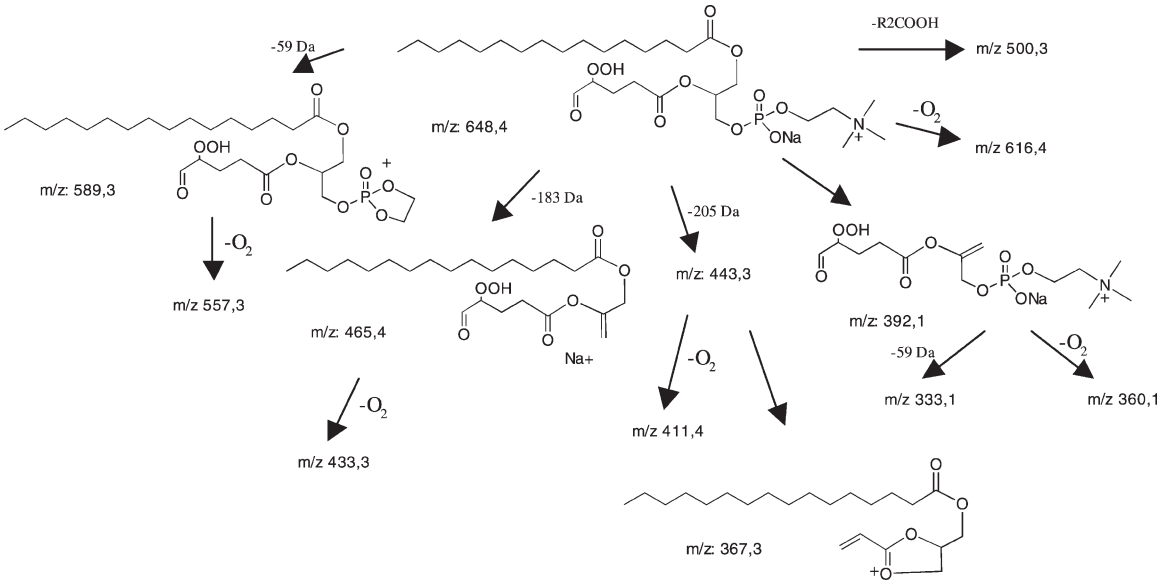

Scheme 4. Proposed fragmentation pathways identified in the ESI-MS/MS spectrum for the ion at *m/z* 648.

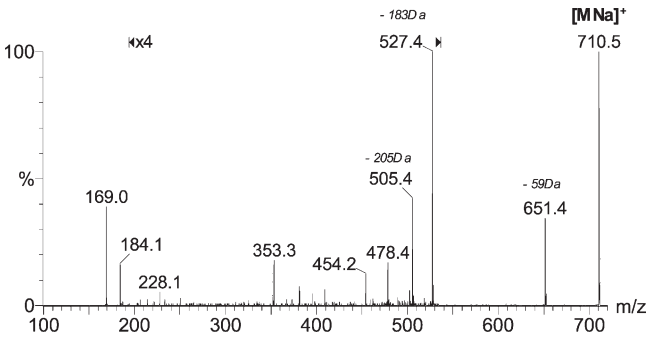

Figure 6. MS/MS spectra of the ion observed at *m/z* 710 in ESI-MS.

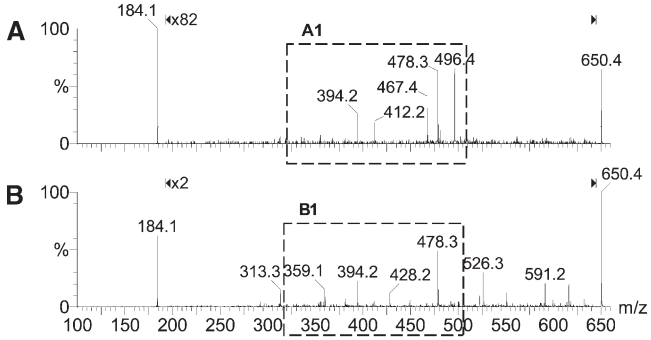

the peroxidation product from PLPC, containing a saturated aldehyde in the *sn*-2 position, showed less fragmentation apart from that described earlier (Fig. 7(A)). In contrast, the MS/MS spectrum of the short-chain product from PAPC, that contains an unsaturated hydroxyaldehyde in the *sn*-2 position, shows additional ions at *m/z* 381, 411 and 449 (Fig. 7(B)) due to cleavage in the vicinity of the hydroxy group, supporting the presence of the hydroxyaldehyde. Still, the fragments at *m/z* 526, 428 and 359 could not be rationalized through the proposed structure and therefore it is expected that another structure may be contributing to the total ion current.

Another example of ions with the same *m/z* value common to both PLPC and PAPC phospholipids is the ion at *m/z* 660, where both ions exhibit common fragment ions at *m/z* 601 (−59 Da), 477 (−183 Da) and 184 (phosphocholine head), although with different relative abundance (data not shown). However, in this case, the identification was facilitated by the fact that one MS/MS spectrum showed the fragment at *m/z* 147 and the ion due to loss of 205 Da consistent with a $[MNa]^+$ ion, while the other MS/MS spectrum showed the ion at *m/z* 496 due to loss of R_2=C=O consistent with the fragmentation pattern of $[MH]^+$ ion.

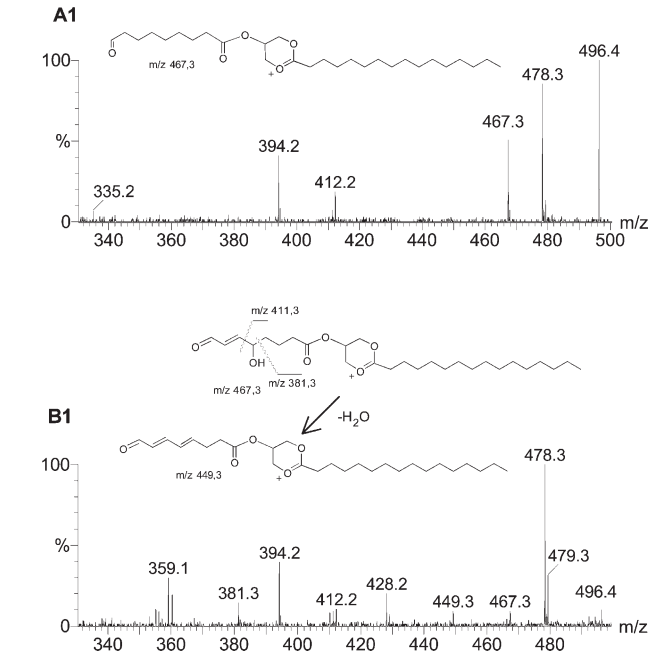

Figure 7. MS/MS spectra of the ion observed at *m/z* 650 in ESI-MS.

CONCLUSIONS

The short-chain products formed by reaction with the hydroxyl radical of glycerophosphatidylcholine phospholipids and identified by electrospray mass spectrometry comprised saturated and unsaturated short-chain products containing terminal aldehyde and carboxylic groups, some of them substituted with hydroxy, keto and hydroperoxide groups. The short-chain species yielded both $[MNa]^+$ and $[MH]^+$ ions. Tandem mass spectrometry was applied to the study of the fragmentation of $[MNa]^+$ and $[MH]^+$ ions of short-chain peroxidation products obtained, leading to different fragmentation patterns. The MS/MS spectra of $[MNa]^+$ ions gave a characteristic ion at *m*/*z* 147, while the MS/MS spectra of $[MH]^+$ ions gave the ion at *m*/*z* 496 (loss of R_2=C=O) as the characteristic product ion, and this will facilitate the identification of the precursor ion, $[MNa]^+$ versus $[MH]^+$. The low abundance ions due to C–C cleavages occurring in the vicinity of the functional group, as well as fragmentations involving the hydroxy groups, resulting from charge-remote fragmentations, either by 1,4-hydrogen elimination or by a homolytic mechanism, were the most informative since they allowed us to obtain structural information relating to the *sn*-2 acyl residue. These ions were crucial for the correct assessment of the structure of oxidized phospholipids. Furthermore, the fragmentation pathway of some ions was not consistent with the fragmentation behavior expected for some of the short-chain compounds identified in the literature and allowed the reassignment of the ions as different structures. Some of the structures corresponded to novel oxidized short-chain phospholipid products. The results obtained by MS/MS showed that the Q-TOF, in spite of being a low-energy fragmentation instrument, is still energetic enough to induce high-energy fragmentations, which were helpful in the identification of the short-chain products.

The fragmentation behavior described for the studied short-chain products can be useful in the determination of structural features of phosphatidylcholine peroxidation products obtained from mixtures. The detailed knowledge of lipid peroxidation degradation products is of major importance and should be very valuable in providing new markers for oxidative stress signaling and for disease state monitoring, giving new insights in the pathogenesis process.

Acknowledgements

The authors gratefully acknowledge the financial support provided by the project POCTI 33279/99 and the PhD grant to Ana Reis (SFRH/BD/10358/2002) provided by the Foundation for Science and Technology (FCT) and FSE (III Quadro Comunitário de Apoio).

REFERENCES

1. Silvius JR. Structure and nomenclature. In *Phospholipids Handbook*, Cevc G (ed). Marcel Dekker: New York, 1993; 1–22.
2. Yorek MA. Biological distribution. In *Phospholipids Handbook*, Cevc G (ed). Marcel Dekker: New York, 1993; 745–775.
3. Pierre J-L. Chemistry of dioxygen and its activated species. In *Analysis of Free Radicals in Biological Systems*, Favier A, Cadet J, Kalyanaraman B, Fontecave M, Pierre JL (eds). Springer Verlag: Berlin, 1995; 1–10.
4. Liochev SI. The mechanism of 'Fenton-like' reactions and their importance for biological systems: a biologist's view. In *Metal Ions in Biological Systems*, vol. 36, Sigel A, Sigel H (eds). Marcel Dekker: New York, 1999; 1–40.
5. Gupta CM. Phospholipids in disease. In *Phospholipids Handbook*, Cevc G (ed). Marcel Dekker: New York, 1993; 895–908.
6. Shigenaga MK, Hagen TM, Ames BN. *Proc. Natl. Acad. Sci.* 1994; **91**: 10771.
7. Pincemail J. Free radicals and antioxidants in human diseases. In *Analysis of Free Radicals in Biological Systems*, Favier A, Cadet J, Kalyanaraman B, Fontecave M, Pierre JL (eds). Springer Verlag: Berlin, 1995; 83–98.
8. McIntyre TM, Zimmerman GA, Prescott SM. *J. Biol. Chem.* 1999; **274**: 25189.
9. Marathe GK, Harrison KA, Murphy RC, Prescott SM, Zimmerman GA, McIntyre TM. *Free Rad. Biol. Med.* 2000; **28**: 1762.
10. Kayganich-Harrison KA, Murphy RC. *Anal. Biochem.* 1994; **221**: 16.
11. Schlame M, Haupt R, Wiswedel I, Kox WJ, Rüstow B. *J. Lipid Res.* 1996; **37**: 2608.
12. Watson AD, Leitinger N, Navab M, Faull KF, Hörkö S, Witztum JL, Palinski W, Schwenke D, Salomon RG, Sha W, Subbanagounder G, Fogelman AM, Berliner JA. *J. Biol. Chem.* 1997; **272**: 13597.
13. Frey B, Haupt R, Alms S, Holzmann G, König T, Kern H, Kox W, Rüstow B, Schlame M. *J. Lipid Res.* 2000; **41**: 1145.
14. Tokumura A, Sumida T, Toujima M, Kogure K, Fukuzawa K, Takahashi Y, Yamamoto S. *J. Lipid Res.* 2000; **41**: 953.
15. Itabe H, Yamamoto H, Suzuki M, Kawai Y, Nakagwa Y, Suzuki A, Imanaka T, Takano T. *J. Biol. Chem.* 1996; **271**: 33208.
16. Podrez EA, Poliakov E, Shen Z, Zhang R, Deng Y, Sun M, Finton PJ, Shan L, Gugiu B, Fox PL, Hoff HF, Salomon RG, Hazen SL. *J. Biol. Chem.* 2002; **277**: 38503.
17. Spickett CM, Pitt AR, Brown AJ. *Free Rad. Biol. Med.* 1998; **25**: 613.
18. Folch J, Lees M, Stanley GHS. *J. Biol. Chem.* 1957; **226**: 497.
19. Spiteller G. *Chem. Phys. Lipids* 1998; **95**: 105.
20. Spiteller P, Kern W, Reiner J, Spiteller G. *Biochim. Biophys. Acta* 2001; **1531**: 188.
21. Loidl-Stahlhofen A, Spiteller G. *Biochim. Biophys. Acta* 1994; **1211**: 156.
22. Mlakar A, Spiteller G. *Chem. Phys. Lipids* 1996; **79**: 47.
23. Han X, Gross RW. *J. Am. Soc. Mass Spectrom.* 1995; **6**: 1202.
24. Pelizzi N, Catinella S, Barboso S, Zanol M. *Rapid Commun. Mass Spectrom.* 2002; **16**: 2215.
25. Hsu F, Turk J. *J. Am. Soc. Mass Spectrom.* 2003; **14**: 352.
26. Hsu F-F, Turk J, Thukkani AK, Messner MC, Wildsmith KR, Ford DA. *J. Mass Spectrom.* 2003; **38**: 752.
27. Crow FW, Cragun JD, Johnson KL, Ruiz MV, Paz MP, Naylor S. *Biomed. Chromatogr.* 2002; **16**: 311.
28. Reis A, Domingues MRM, Amado FML, Ferrer-Correia AJV, Domingues P. *J. Am. Soc. Mass Spectrom.* 2003; **14**: 1250.
29. Easton C, Johnson DW, Poulos A. *J. Lipid Res.* 1988; **29**: 109.
30. Cheng C, Gross ML. *J. Am. Soc. Mass Spectrom.* 1998; **9**: 620.
31. Schneider C, Tallman KA, Porter NA, Brasch AR. *J. Biol. Chem.* 2001; **276**: 20831.
32. Zwart LL, Meerman JHN, Commandeur JNM, Vermeulen NPE. *Free Rad. Biol. Med.* 1999; **26**: 202.

BIOMEDICAL CHROMATOGRAPHY
Biomed. Chromatogr. **19**: 129–137 (2005)
Published online in Wiley InterScience (www.interscience.wiley.com).
DOI: 10.1002/bmc.429

ORIGINAL RESEARCH

Separation of peroxidation products of diacyl-phosphatidylcholines by reversed-phase liquid chromatography–mass spectrometry

A. Reis, M. R. M. Domingues, Francisco M. L. Amado, A. J. V. Ferrer-Correia and P. Domingues*

Chemistry Department, University of Aveiro, 3810-193 Aveiro, Portugal

Received 1 June 2004; accepted 12 July 2004

ABSTRACT: Lipid peroxidation process has attracted much attention due to the growing evidence of its involvement in the pathogenesis of age-related diseases. The monitoring of the lipid peroxidation products in phospholipids, formed under oxidative stress conditions, may provide new markers for oxidative stress signaling and for disease states, giving new insights in the pathogenesis process. Reversed-phase liquid chromatographic method coupled to mass spectrometry was developed for the separation of oxidized glycero-phosphatidylcholine (GPC) peroxidation products formed by the Fenton reaction that mimic *in vivo* oxidative stress conditions. The LC-MS conditions were applied for the separation of peroxidation products of oleoyl- (POPC), lineloyl- (PLPC) and arachidonoyl-palmitoyl phosphatidylcholine (PAPC). The peroxidation products separated included products resulting from the insertion of oxygen atoms in the *sn*-2 chain (long-chain), and products with the *sn*-2 chain shortened resulting from cleavage of oxygen-centered radicals (short-chain). Among long-chain products were the keto, hydroxy, hydroperoxide and poly-hydroxy derivatives, while short-chain products included dicarboxylic acids, aldehydes and hydroxy-aldehydes. Separation of long-chain products formed in each phosphatidylcholine was observed, and the reconstructed ion chromatogram of each ion showed an increase in the number of peaks with the increase in the number of oxygen atoms inserted into the phospholipid. Separation of short-chain products took place according to the functional group present at the *sn*-2 moiety that allowed the elution of dicarboxylic acids distinct from aldehydes. Separation between isomeric structures that were present in short- and long-chain products was also achieved. Copyright © 2004 John Wiley & Sons, Ltd.

KEYWORDS: diacyl-phosphatidylcholines; oxidative stress; LC-MS; short-chain products; long-chain products

INTRODUCTION

Lipid peroxidation process has attracted much attention due to the growing evidence of its involvement in several inflammatory processes, in diabetes, cancer, liver and lung diseases (Gupta, 1993), and in the pathogenesis of age-related diseases, such as Parkinson, Alzheimer and atherosclerosis (Pincemail, 1995).

Lipid peroxidation is a complex reaction, mediated by free radicals, that generates a wide range of oxidized products formed via a radical reaction initiated by reactive oxygen species (ROS). One of the most reactive species is the hydroxyl radical (·OH), which is formed during cell metabolism in aerobic conditions by a Fenton-like reaction (Liochev, 1999). During lipid peroxidation, the allylic hydrogen atoms present in fatty acyl chains (linoleic and arachidonic acids, for example) esterified to phospholipids of cell membranes and of low density lipoproteins (LDL), are removed by the hydroxyl radical (Liochev, 1999). The removal of allylic hydrogen atoms generates a radical species (carbon-centered radical) that, due to its high reactivity, readily uptakes an oxygen molecule, leading to a hydroperoxide (Girotti, 1998). Lipid hydroperoxides can undergo homolytic scission of the hydroperoxide group, forming an alkoxyl radical (oxygen centered radical). This radical product can further react, by a β-cleavage mechanism, originating products with the unsaturated fatty acid moiety shortened, called short-chain products. The alkoxyl radical can also, by an alternative pathway, abstract a hydrogen atom from a neighboring molecule, forming a hydroxy group (Sergent *et al.*, 1999). The hydroxy derivatives together with the hydroperoxide derivatives, formed as a result of the insertion of oxygen atoms without breakdown of the phospholipid structure, are called long-chain products. The products resulting from β-cleavage mechanism are usually aldehydes that can undergo further oxidation leading to hydroxy-aldehydes, keto-aldehydes, dicarboxylic acids, keto-acids and others (Loidl-Stahlhofen and Spiteller,

*Correspondence to: P. Domingues, Department of Chemistry, University of Aveiro, 3810-193 Aveiro, Portugal.
E-mail: pedrom@dq.ua.pt

Abbreviations used: GPC, glycero-phosphatidylcholine; LDL, low density lipoproteins; PAPC, arachidonoyl-palmitoyl phosphatidylcholine; PLPC, lineloyl-palmitoyl phosphatidylcholine; POPC, oleoyl-palmitoyl phosphatidylcholine; ROS, reactive oxygen species; TIC, total ion current.

Published online 23 November 2004

1994; Lee and Blair, 2000; Spiteller *et al.*, 2001). Short-chain products with an aldehydic moiety are known to be cytotoxic (Aldini *et al.*, 2002; Hoff *et al.*, 2003). Other products formed by peroxidation of phosphatidylcholines are lyso-phosphatidylcholines, known to be present in human plasma (Yorek, 1993), and, although they are not radical mediated peroxidation products, their concentration is increased during peroxidation reaction of LDL by hydrolysis of *sn*-1 and *sn*-2 fatty acid chains (McIntyre *et al.*, 1999). Generally, these products increase membrane polarity, leading to a decrease in membrane fluidity and permeability, or are involved in reactions with amino compounds and DNA bases, interfering with the functional integrity of the cell membranes (Sergent *et al.*, 1999).

Several groups have focused their work on the study of phosphatidylcholine peroxidation products by mass spectrometry both in positive and negative modes. The experimental procedures involved the analysis of fractions mainly by FAB-MS, collected after high-performance liquid chromatography, in conjunction with several derivatization reactions (Kayganich-Harrison and Murphy, 1994; Schlame *et al.*, 1996; Watson *et al.*, 1997; Frey *et al.*, 2000). So far, the use of mass spectrometry (MS) coupled with HPLC separation techniques (HPLC-MS) for the study of phosphatidylcholine peroxidation products is scarce and has focused on the analysis of either short-chain products (Itabe *et al.*, 1996; Podrez *et al.*, 2002), or long-chain products (Zhang *et al.*, 1995; Spickett *et al.*, 2001). To our knowledge, there has not yet been performed a thorough study of the peroxidation products occurring from several phosphatidylcholines by LC-MS.

The purpose of this work is the development of a reverse-phase liquid chromatography method coupled to electrospray mass spectrometry for the separation of glycero-phosphatidylcholine peroxidation products formed by the Fenton reaction, to be further applied to the analysis of potential GPC biomarkers in biological samples under oxidative stress conditions. In this paper, we present and discuss the results obtained by LC-MS on three glycero-phosphatidylcholines containing a common *sn*-1 chain (palmitic acid) and varying the *sn*-2 chain (oleic, linoleic and arachidonic acid).

EXPERIMENTAL

Chemicals. The glycerophospholipids, 2-oleoyl-, 2-lineloyl- and 2-arachidonoyl-1-palmitoyl-glycerophosphatidylcholines (Scheme 1), were obtained from Sigma (St Louis, MO, USA) and used without further purification. $FeCl_2$ and H_2O_2 (30%, w/v) used for the peroxidation reaction were purchased from Merck (Darmstadt, Germany). All solvents were HPLC grade.

Preparation of oxidized GPC vesicles. Vesicles were prepared from stock solutions of 1 mg/mL and dried under nitrogen stream. Ammonium bicarbonate buffer (pH 7.4) was added to a final phospholipid concentration of 50 mM and the mixture vortexed (Spickett *et al.*, 1998). Oxidative treatments using Fe (II) and H_2O_2 were carried out by adding to 50 µL of phospholipid vesicles, 5 mmol $FeCl_2$ solution and 50 mmol of hydrogen peroxide (H_2O_2) in 0.5 mL solution. This mixture was left to react at 37°C in the dark for different periods of time with occasional sonication. The phospholipid oxidation products were extracted using a modification of the Folch method with chloroform–methanol (2:1, v/v; Folch *et al.*,

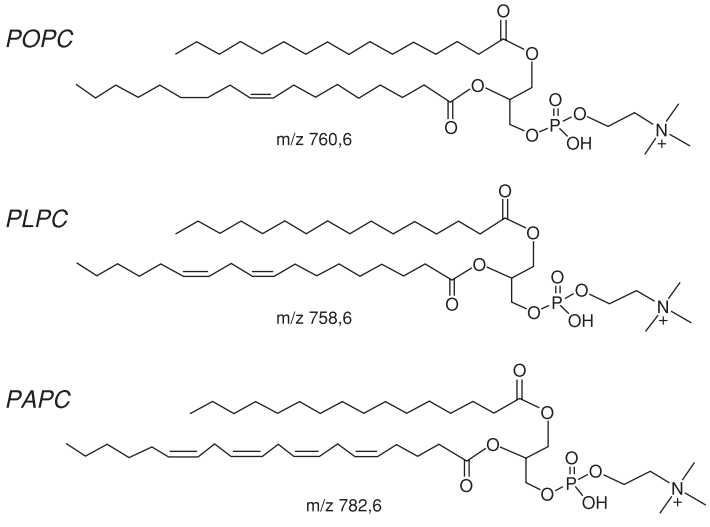

Scheme 1. Structures of the studied phosphatidylcholines (POPC, 1-palmitoyl-2-oleoyl-3-glycerophosphocholine; PLPC, 1-palmitoyl-2-lineloyl-3-glycerophosphocholine; and PAPC, 1-palmitoyl-2-arachidonoyl-3-glycerophosphocholine). The *m*/*z* value of the $[MH]^+$ ions is indicated.

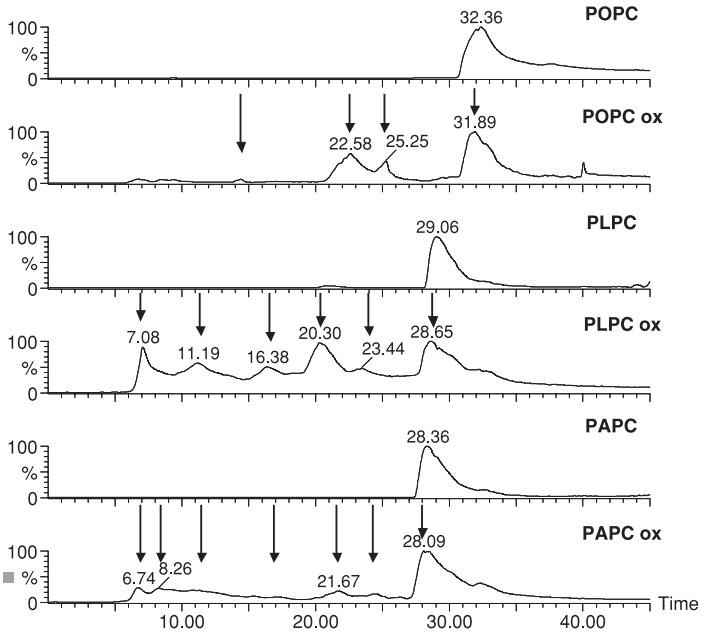

Figure 1. LC-MS profile of POPC, PLPC and PAPC phospholipids obtained under oxidative ($POPC_{ox}$, $PLPC_{ox}$ and $PAPC_{ox}$) and non-oxidative conditions (POPC, PLPC and PAPC).

1957). Controls were performed by replacing H_2O_2 with water. The extent of oxidation was monitored by electrospray mass spectrometry (ES-MS).

Liquid chromatography–electrospray mass spectrometry (LC-MS). Phospholipid oxidation products were separated by LC performed on an HPLC system (Waters Aliance 2690) with UV detection (Knauer K-2500) set at λ = 205 nm. The reaction mixture (50 µL) was introduced into a APEX 300 C_4 column (250 × 4.6 mm i.d., 7.0 µm, Jones Chromatography, kept at 30°C). The mobile phase consisted of acetonitrile–aqueous ammonium acetate (5 mM; 50/50; eluent A) and acetonitrile (eluent B). The solvent gradient was programmed as follows: 20% B for 10 min followed by a linear increase to 80% B at 40 min and held isocratically for 5 min. The flow rate through the column was 1.0 mL/min. After the detector the flow was redirected to the MS interface with a 1:20 home-made split.

The Q-TOF2 (Micromass, Manchester, UK) mass spectrometer using a MassLynx software system (version 4.0) was operated in the positive ion mode with a capillary voltage of 3000 V, cone voltage 35 V, the source block temperature set to 100°C and the desolvation temperature set to 200°C. Mass spectra were obtained over a mass-to-charge ratio (m/z) of 50–1000 at a resolution of 10,000 (50% valley).

RESULTS AND DISCUSSION

Separation and identification of peroxidation products

The LC-MS total ion current chromatograms (TIC) obtained before oxidation of 1-palmitoyl-2-oleoyl-3-glycerophosphocholine (POPC), 1-palmitoyl-2-lineloyl-3-glycerophosphocholine (PLPC) and 1-palmitoyl-2-arachidonoyl-3-glycerophosphocholine (PAPC) are shown in Fig. 1. The retention times (R_t) of the non-oxidized glycero-phosphatidylcholines were 32.4 min for POPC, 29.1 min for PLPC and 28.4 min for PAPC. The ES-MS spectra obtained for these peaks show the presence of the molecular ions ($[MH]^+$) of m/z 760, 758 and 804, respectively (Fig. 2D, 3F). The chromatographic behaviour observed for the GPC studied shows, as expected, that elution time decreased with increasing double bonds (POPC vs PLPC), and with increasing carbon chain. In Fig. 1 are also depicted the TIC chromatograms obtained for the GPC after the oxidation reaction ($POPC_{ox}$, $PLPC_{ox}$ and $PAPC_{ox}$). Comparing the TIC chromatogram between the unoxidized POPC and the corresponding oxidized POPC chromatogram ($POPC_{ox}$), it is possible to observe that, at the conditions used, the elution of the peroxidation products occurred between 20 and 26 min. The TIC chromatogram of PLPC when compared with the chromatogram of $PLPC_{ox}$ showed the elution of peroxidation products between 7 and 27 min in several peaks, revealing that a wide range of oxidation products was formed. Similarly, comparison between the TIC chromatograms obtained for PAPC and $PAPC_{ox}$ showed the elution of peroxidation products in multiple peaks with retention times between 7 and 26 min. The increase of the chromatographic peaks observed for $PLPC_{ox}$ and $PAPC_{ox}$, when compared with $POPC_{ox}$, reflects an increase in the number of oxidation products formed and is due to

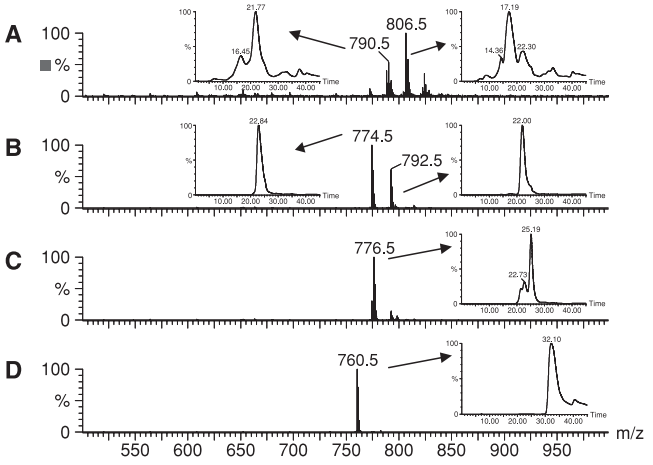

Figure 2. ES-MS spectra of the predominant chromatographic peaks observed during elution of $POPC_{ox}$. The insets show the RIC chromatogram of the ions observed in the ES-MS.

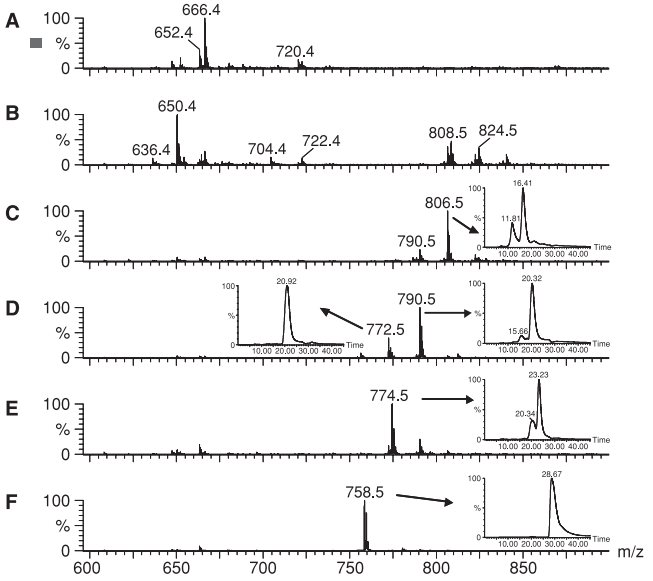

Figure 3. ES-MS spectra of the predominant chromatographic peaks observed during elution of $PLPC_{ox}$. The insets show the RIC chromatogram of the ions observed in the ES-MS.

the presence of more double bonds in the linoleic and arachidonic acids (*sn*-2 residues) and in consequence the increase in the number of possible places where the oxidation reaction might occur.

The peroxidation products formed from POPC eluted in two predominant peaks with retention times of 22.6 and 25.3 min. Other minor peaks were also observed. The ES-MS mass spectrum obtained for the peak at 22.6 min (Fig. 2) showed the presence of ions at *m*/*z* 792 and 774, attributed to the protonated molecule of the hydroperoxide and the keto derivatives, respectively. Although, these peroxidation products appear together in the MS spectrum, they exhibit different retention times, as can be seen by the RIC chromatogram of the ion at *m*/*z* 792 and 774 (inset in Fig. 2). The location of the hydroxy and hydroperoxide derivatives within the unsaturated fatty acid chain is likely to be at C-8 or C-11, or even at C-9 or C-10 by double bond rearrangement, as was identified for POPC DMPO adducts by electrospray mass spectrometry (Reis *et al.*, 2004). The ES-MS mass spectrum of the chromatographic peak at 25.3 min showed the contribution of the ion at *m*/*z* 776 that can be attributed to the hydroxy derivative. The ion at *m*/*z* 776 attributed to the hydroxy derivative showed two peaks at 25.3 and 23.5 min that may correspond to isomeric structures. The ES-MS mass spectrum obtained for the minor peak at 14.4 min showed the presence of the ions at *m*/*z* 790 and 806 that can be attributed to the keto-hydroxy and the keto-hydroperoxide derivatives, respectively. These peroxidation products were separated under the elution conditions used, as can be seen by the RIC chromatograms of the ions at *m*/*z* 790 and 806 (inset in Fig. 2). The chromatographic peak observed at 32.4 min corresponds to the unoxidized phospholipid. No short-chain products resulting from β-scission of alkoxyl radicals were identified, although other peroxidation products resulting from loss of *sn*-1 and *sn*-2 were observed namely ions at *m*/*z* 496 and 522 corresponding to 1-palmitoyl-lyso-phosphatidylcholine and 2-oleoyl-lyso-phosphatidylcholine, eluting at 8.3 and 8.5 min, respectively (data not shown).

The TIC chromatogram obtained for $PLPC_{ox}$ (Fig. 1) showed several peaks eluting prior to the unoxidized phospholipid (R_t 29 min). These peaks were observed at 7.1, 11.2, 16.4, 20.3, 23.4 and 28.7 min, and the ES-MS mass spectrum obtained for each peak is shown in Fig. 3(A–F). As can be seen by the ES-MS spectra (Fig. 3), these peaks corresponded to the elution of short- and long-chain products. The formation of short- and long-chain products result from the oxidation reaction of the linoleic acid (*sn*-2 substituent) since the palmitic acid (*sn*-1 substituent) is a saturated fatty acid that is unaffected during radical peroxidation reaction due to the lack of allylic hydrogen atoms (Sergent *et al.*, 1999). The linoleic acid contains two double bonds (C-9 and C-12), and by hydrogen abstraction of the bis-allylic hydrogen atom at C-11, triggered by the hydroxyl radical, may generate an alkyl radical centered at C-11. The radical species, by rearrangement of the double bonds, leads to two structures with the radical placed at C-9 or C-13, stabilized by resonance. This species can react with an oxygen molecule, and by alkoxyl formation ultimately lead to long-chain products by insertion of oxygen atoms, or to short-chain products by β-scission of the alkoxyl radical, thus generating a variety of peroxidation products.

The ES-MS mass spectrum of peak 1 [Fig. 3(A)] shows several abundant ions at *m*/*z* 652, attributed to

Table 1. Identification of the most abundant ions observed in the ES-MS mass spectra and the proposed structure obtained for the chromatographic peaks observed in $PLPC_{ox}$

m/*z* value	GPC assignment
636	1-Palmitoyl-2-(8-oxo-octanoic acid)-GPC
650	1-Palmitoyl-2-(9-oxo-nonanoic acid)-GPC
652	1-Palmitoyl-2-(octandioic acid)-GPC
666	1-Palmitoyl-2-(nonandioic acid)-GPC
704	1-Palmitoyl-2-(9-keto-12-oxo-10-dodecenoic acid)-GPC
720	1-Palmitoyl-2-(9-keto-10-dodecendioic acid)-GPC
722	1-Palmitoyl-2-(9-hydroxy-10-dodecendioic acid)-GPC
758	1-Palmitoyl-2-(octadecadienoic acid)-GPC
772	1-Palmitoyl-2-(keto-octadecadienoic acid)-GPC
774	1-Palmitoyl-2-(hydroxy-octadecadienoic acid)-GPC
790	1-Palmitoyl-2-(hydroperoxide-octadecadienoic acid)-GPC
806	1-Palmitoyl-2-(hydroxy-hydroperoxide-octadecadienoic acid)-GPC
808	1-Palmitoyl-2-(tri-hydroxy-octadecadienoic acid)-GPC
824	1-Palmitoyl-2-(tetra-hydroxy-octadecadienoic acid)-GPC

GPC, glycerophosphatidylcholine.

1-palmitoyl-2-(octandioic acid)-GPC, at *m*/*z* 666, attributed to 1-palmitoyl-2-(nonandioic acid)-GPC and at *m*/*z* 720, attributed to 1-palmitoyl-2-(9-keto-10-dodecendioic acid)-GPC. The proposed peroxidation products contain the carboxy function as terminal function of the *sn*-2 shortened chain, thus corresponding to dicarboxylic acids. These ions, as well as others observed in the ES-MS mass spectrum with lower relative abundance, are summarized in Table 1. The ES-MS mass spectrum of peak 2 [Fig. 3(B)] exhibits the ions at *m*/*z* 636, 650, 704 and 722 attributed to peroxidation products with an aldehydic moiety at the *sn*-2 short-chain residue, and ions at *m*/*z* 808, 824 and 840 can be attributed to long-chain products due to the insertion of oxygen atoms into the carbon chain. The ES-MS mass spectra obtained for peaks 3, 4 and 5 [Fig. 3(C–E)] exhibited ions in the high mass region at *m*/*z* 806, 790, 774 and 772 that can be attributed to the hydroxy-hydroperoxide, hydroperoxide, hydroxy and keto derivatives, respectively. Peak 6 corresponds to the unoxidized PLPC, as can be seen by the ion at *m*/*z* 758 in the ES-MS mass spectrum [Fig. 3(F)]. ES-MS data obtained for each chromatographic peak, clearly shows that separation between short- and long-chain products was achieved. However, long-chain products containing high number of oxygen atoms, which confer on them high polar character, co-eluted with short-chain products containing a terminal aldehydic moiety.

The short-chain products, when formed, can provide evidence for the location of oxidation on a specific carbon of the unsaturated fatty acid chain. Thus, the occurrence of ions at *m*/*z* 666 (carboxylic acid with C_9) and 650 (aldehyde with C_9), predominant among the short-chain products formed by radical oxidation, suggest that although two stable structures may be formed, namely isomer with radical at C-9 and at C-13, the alkoxyl intermediate radical located at C-9 is favored or more stable than the radical specie located at C-13. The occurrence of oxidation in C-13, although less abundant, is inferred by the presence of the ion at *m*/*z* 732 [1-palmitoyl-2-(8-keto-9,11-tridecadienedioic acid)-GPC]. Furthermore, the ES-MS data shows that short-chain dicarboxylic acids eluted with lower retention time in the first peak [Fig. 3(A)], followed by elution of short-chain aldehydic products. Long-chain derivatives, with high number of oxygen atoms inserted, co-eluted with aldehydes [Fig. 3(B)], followed by the elution of hydroperoxide derivatives [Fig. 3(C)], di-hydroxy derivatives [Fig. 3(D)], mono-hydroxy derivatives [Fig. 3(E)] and finally the unoxidized phosphatidylcholine [Fig. 3(F)]. For the aldehydic short-chain products, the retention times of saturated short-chain aldehydes were observed at 10.6 min (*m*/*z* 636) and at 11.1 min (*m*/*z* 650), while for dicarboxylic short-chain products the retention times were 7.02 min (*m*/*z* 666) and at 6.98 min (*m*/*z* 720). For the long-chain products each envelope showed an increase of the number of peaks in each RIC chromatogram as the number of oxygen atoms inserted into the phospholipid increases. This is more evident for the ions with the same *m*/*z* value and with four or five oxygen atoms, where it may be due to the increase in the number of possible structures (either structural and/or positional isomers).

The TIC mass chromatogram obtained for $PAPC_{ox}$ (Fig. 1) showed several peaks eluting prior to the unoxidized phospholipid (R_t 28 min), and were attributed to short- and long-chain products, as was confirmed by the ES-MS mass spectra (data not shown). The peroxidation products resulted from oxidation of the arachidonic acid (*sn*-2 residue). The arachidonic acid (AA) contains three bis-allylic hydrogen atoms at C-7, C-10 and C-13 that may, equally, be abstracted by the hydroxyl radical generating a wide variety of peroxidation products. The ES-MS spectra (data not

Table 2. Identification of the most abundant ($[MH]^+$) ions observed in the ES-MS mass spectra, and the proposed structure, obtained for the chromatographic peaks observed in $PAPC_{ox}$

m/z value	GPC assignment
496	1-Palmitoyl-lyso-glycerophosphatidylcholine
544	2-Arachidonoyl-lyso-glycerophosphatidylcholine
594	1-Palmitoyl-2-(5-oxo-pentanoic acid)-GPC
610	1-Palmitoyl-2-(pentadioic acid)-GPC
650	1-Palmitoyl-2-(5-hydroxy-8-oxo-6-octenoic acid)-GPC
660	1-Palmitoyl-2-(4-keto-9-oxo-5,7-nonadienoic acid)-GPC
664	1-Palmitoyl-2-(5-keto-6-octendioic acid)-GPC
666	1-Palmitoyl-2-(5-hydroxy-6-octendioic acid)-GPC
722	1-Palmitoyl-2-(5,10-dihydroxy-6,8-undecedienedioic acid)-GPC
732	1-Palmitoyl-2-(10-hydroxy-5,8,11-tridecatrienoic acid)-GPC
782	1-Palmitoyl-2-(eicosatetraenoic acid)-GPC
798	1-Palmitoyl-2-(hydroxy-eicosatetraenoic acid)-GPC
814	1-Palmitoyl-2-(hydroperoxide-eicosatetraenoic acid)-GPC
828	1-Palmitoyl-2-(D2/E2-isoprostanes)-GPC
830	1-Palmitoyl-2-(hydroxy-hydroperoxide-eicosatetraenoic acid)-GPC
844	1-Palmitoyl-2-(keto-hydroxy-hydroperoxide-eicosatetraenoic acid)-GPC
846	1-Palmitoyl-2-(di-hydroperoxide-eicosatetraenoic acid)-GPC
862	1-Palmitoyl-2-(hydroxy-di-hydroperoxide-eicosatetraenoic acid)-GPC
878	1-Palmitoyl-2-(tri-hydroperoxide-eicosatetraenoic acid)-GPC
894	1-Palmitoyl-2-(hydroxy-tri-hydroperoxide-eicosatetraenoic acid)-GPC

GPC, glycerophosphatidylcholine.

shown) obtained for the chromatographic peaks show the predominance of ions at *m/z* 594, 610 and 660, that can be attributed to 1-palmitoyl-2-(5-oxo-pentanoic acid)-GPC and 1-palmitoyl-2-(pentanedioic acid)-GPC and to 1-palmitoyl-2-(9-oxo-4-keto-5,7-nonedienenoic acid)-GPC, respectively. The ions identified in the ES-MS mass spectra along with others observed with low relative abundance, are summarized in Table 2. The identification of short-chain products with C_5, C_7 and C_9 carbon chain lengths suggests that oxidation took place, preferably at C-5, C-7 and C-9 by abstraction of the bis-allylic hydrogen atom at C-7. The abstraction of the bis-allylic hydrogen atom at C-7 seems to be favoured, in spite of the presence of other bis-allylic hydrogen atoms along the unsaturated chain, namely at C-10 and C-13. The identification of the ions formed by abstraction of the hydrogen atom at C-7 is in accordance with previous published results (Watson *et al.*, 1997; Nakamura *et al.*, 1997; Khaselev and Murphy, 2000). Long-chain peroxidation products resulting from oxidation of AA were identified containing one to seven oxygen atoms. Based on the *m/z* value observed in the ES-MS spectra (data not shown), they can be attributed to keto, hydroxy and hydroperoxide derivatives. Other products resulting from non-enzymatic radical oxidation in AA, such as isoprostanes E2, D2, A2 and J2 (Lawson *et al.*, 1999), can also be proposed.

As shown for PLPC, separation between dicarboxylic acids, lyso-phosphatidylcholines and aldehydes was achieved with the used chromatographic method. Also, and similarly to what was observed for POPC and PLPC long-chain products, separation between isomeric structures of long-chain products was achieved.

Differentiation of peroxidation products

Among the short-chain peroxidation products identified for the three GPC studied (POPC, PLPC and PAPC) several products with terminal aldehydic and carboxy moieties at the *sn*-2 shortened residue, substituted with hydroxy and keto groups, as well as lyso-phosphatidylcholines, were identified. This data is in accordance with what is described in the literature regarding lipid peroxidation (Loidl-Stahlhofen and Spiteller, 1994; Mkalar and Spiteller, 1996; Marathe *et al.*, 2000), where a wide range of short-chain products is described.

Plotting the RIC chromatograms of several short-chain products obtained from oxidation of PLPC and PAPC (Fig. 4), it can be established that the dicarboxylic acids eluted between 6 and 7 min, the lyso-phosphatidylcholines eluted between 7 and 9 min, and the aldehydes eluted between 9 and 13 min. For aldehydic short-chain products it was possible to obtain better resolution as shown in Fig. 4, revealing that the separation that took place according to the chain length, the number of double bonds and the presence of keto and/or hydroxy groups (occurring as substituents). Thus, for aldehydes the retention time increased as the chain length increased, but decreased as the insaturations and the presence of additional keto

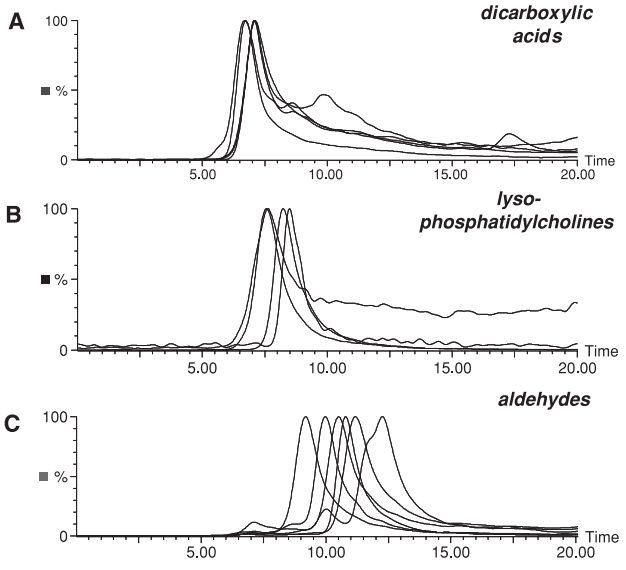

Figure 4. Reconstructed ion chromatograms (RICs) of (a) dicarboxylic acids, (b) lyso-phosphatidylcholines and (c) aldehydes identified as short-chain peroxidation products of phosphatidylcholines.

or hydroxy groups increased. Table 3 summarizes the short-chain peroxidation products depicted in Fig. 4, as well as others identified for $PLPC_{ox}$ and $PAPC_{ox}$.

These results show that the screening of the TIC chromatogram in particular elution zones allows estimation of the structural feature of short-chain products. Moreover, distinction between ions resulting from oxidation of phosphatidylcholines that occur with the same *m*/*z* value, but in different diacyl-phosphatidylcholines, was possible. Several ions were found to be common to both phosphatidylcholines, namely at *m*/*z* 636, 650, 666, 722, 732, 774, 790 and others. As an example, the RIC chromatogram of ion observed at *m*/*z* 636 in $PLPC_{ox}$ corresponding to the 1-palmitoyl-2-(8-oxo-octanoic acid)-GPC, and in $PAPC_{ox}$ to two short-chain products resulting from the oxidation of unsaturated aldehydes, namely the unsaturated hydroxy-aldehyde and dicarboxylic acid, are shown in Fig. 5. As can be seen, the elution of the α,β-hydroxy-aldehyde (PAPC) at 8.21 min occurred earlier than the elution of the saturated aldehyde (PLPC) at 10.5 min, formed by β-scission of the alkoxyl located at C-8 of the *sn*-2 fatty acid. The other product that may be formed by oxidation of unsaturated aldehydes and attributed to dicarboxylic acid eluted at 6.80 min. Data obtained with the RIC chromatograms also shows that for hydroxy and keto derivatives, which contain the same number of oxygen atoms, exhibit different retention times. Thus, the differentiation between the keto derivative from $POPC_{ox}$ and the hydroxy derivative from $PLPC_{ox}$, both occurring at *m*/*z* 774 (Fig. 6) can be achieved.

Since peroxidation products with different structural features can be formed during radical mediated reactions, the results described here are of particular importance and may be useful in the differentiation of isomeric structures and/or the differentiation of ions with the same *m*/*z* value, either occurring in the same phosphatidylcholines or in different phosphatidylcholines. The detailed interpretation and description of LC-

Table 3. Retention times of $[MH]^+$ ions of several lyso-phosphatidylcholines, aldehydes, dicarboxylic acids and hydroxy-aldehydes, identified as peroxidation products of POPC, PLPC and PAPC by LC-MS

Structural feature	GPC	Peroxidation products	Retention time
Lyso-PC		1-Palmitoyl-lyso-GPC (*m*/*z* 496)	8.24
	POPC	2-Oleoyl-lyso-GPC (*m*/*z* 522)	8.49
	PLPC	2-Lineloyl-lyso-GPC (*m*/*z* 520)	7.64
	PAPC	2-Arachidonoyl-lyso-GPC (*m*/*z* 544)	7.57
Dicarboxylic acids	PLPC	1-Palmitoyl-2-(octandioic acid)-GPC (*m*/*z* 652)	7.10
		1-Palmitoyl-2-(nonandioic acid)-GPC (*m*/*z* 666)	7.02
		1-Palmitoyl-2-(9-undecendioic acid)-GPC (*m*/*z* 692)	7.10
		1-Palmitoyl-2-(8-hydroxy-9-undecendioic acid)-GPC (*m*/*z* 708)	7.10
		1-Palmitoyl-2-(9-keto-10-dodecendioic acid)-GPC (*m*/*z* 720)	6.98
	PAPC	1-Palmitoyl-2-(pentandioic acid)-GPC (*m*/*z* 610)	6.67
		1-Palmitoyl-2-(5-heptendioic acid)-GPC (*m*/*z* 636)	6.82
		1-Palmitoyl-2-(5-keto-6-octendioic acid)-GPC (*m*/*z* 664)	6.61
		1-Palmitoyl-2-(5-hydroxy-6-octendioic acid)-GPC (*m*/*z* 666)	6.89
Aldehydes	PLPC	1-Palmitoyl-2-(8-oxo-octanoic acid)-GPC (*m*/*z* 636)	10.5
		1-Palmitoyl-2-(9-oxo-nonanoic acid)-GPC (*m*/*z* 650)	11.2
		1-Palmitoyl-2-(8-hydroxy-11-oxo-9-undecenoic acid)-GPC (*m*/*z* 692)	9.95
	PAPC	1-Palmitoyl-2-(5-oxo-pentanoic acid)-GPC (*m*/*z* 594)	9.18
		1-Palmitoyl-2-(7-oxo-5-heptenoic acid)-GPC (*m*/*z* 620)	9.96
		1-Palmitoyl-2-(4-hydroxy-7-oxo-5-heptenoic acid)-GPC (*m*/*z* 636)	8.21
		1-Palmitoyl-2-(5-hydroxy-8-oxo-6-octenoic acid)-GPC (*m*/*z* 650)	8.55
		1-Palmitoyl-2-(4-keto-9-oxo-5,7-nonadienoic acid)-GPC (*m*/*z* 660)	10.8

GPC, glycerophosphatidylcholine.

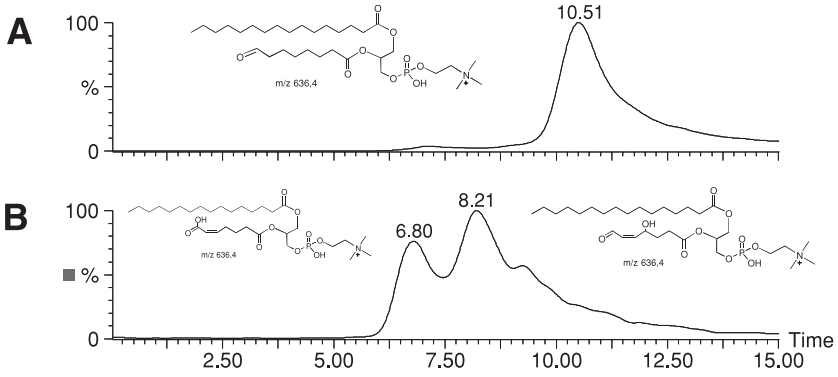

Figure 5. Reconstructed ion chromatograms of ions at m/z 636 identified as short-chain peroxidation products of (a) PLPC and (b) PAPC. The insets show the proposed structures.

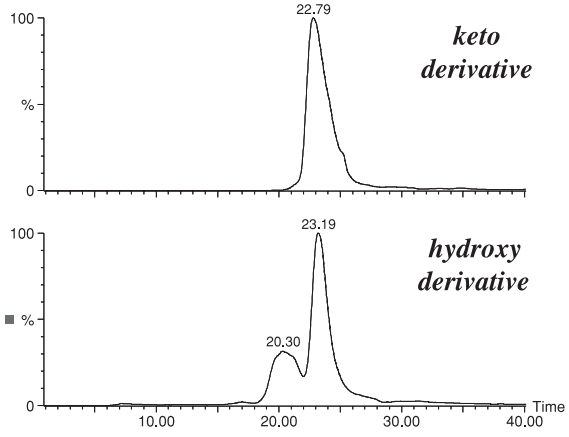

Figure 6. Reconstructed ion chromatograms of ions at m/z 796 identified as long-chain peroxidation products of (a) POPC and (b) PLPC.

MS/MS results, obtained for long-chain peroxidation products of phosphatidylcholine, is currently being undertaken.

CONCLUSIONS

The methodology presented here allowed the separation of short- and long-chain peroxidation products formed by radical mediated reactions in diacylphosphatidylcholines. The identification of the major short-chain peroxidation products by the LC-MS data suggests that radical mediated peroxidation of diacylphosphatidylcholine liposomes occurs preferably in the carbon closer to the polar head, in spite of the presence of other allylic hydrogen atoms equally susceptible to being abstracted, as is the case of arachidonic acid in PAPC. The LC-MS data also showed that the elution conditions allowed separation between short and long chain products, although long-chain products with high polar characteristics co-eluted with aldehydic short-chain products. The separation of short-chain products occurred according to the functional group present at the shortened *sn*-2 moiety. This chromatographic behaviour allowed the grouping of short-chain products in elution zones occurring from the most polar (dicarboxylic acids), followed by the elution of lysophosphatidylcholines, to the least polar products (aldehydes). Separation of long-chain products formed in each phosphatidylcholine was also observed, where the RIC chromatograms of long-chain products exhibited an increase in the number of peaks as the number of oxygen atoms increased, reflecting separation between isomeric structures.

Acknowledgements

The authors gratefully acknowledge the financial support provided by the project POCTI 33279/99 and the PhD grant to Ana Reis (SFRH/BD/10358/2002) provided by Foundation for Science and Technology (FCT) and FSE (III Quadro Comunitário de Apoio).

REFERENCES

Aldini G, Granata P and Carini M. Detoxification of cytotoxic α,β-unsaturated aldehydes by carnosine: characterization of conjugated adducts by electrospray ionisation tandem mass spectrometry and detection by liquid chromatography/mass spectrometry in rat skeletal muscle. *Journal of Mass Spectrometry* 2002; **37**: 1219.

Folch J, Lees M and Stanley GHS. A simple method for the isolation and purification of total lipids from animal tissues. *Journal of Biological Chemistry* 1957; **226**: 497.

Frey B, Haupt R, Alms S, Holzmann G, König T, Kern H, Kox W, Rüstow B and Schlame M. Increase in fragmented phosphatidylcholine in blood plasma by oxidative stress. *Journal of Lipid Research* 2000; **41**: 1145.

Girotti AW. Lipid hydroperoxide generation, turnover, and effector action in biological systems. *Journal of Lipid Research* 1998; **39**: 1529.

Gupta CM. Phospholipids in disease. In *Phospholipids Handbook*, Gregor Cevc (ed.). Marcel Dekker: New York, 1993; 895–908.

Hoff HF, O'Neil J, Wu Z, Hoppe G and Salomon RL. Phospholipid hydroxyalkenals: biological and chemical properties of specific

oxidized lipids present in atherosclerotic lesions. *Arteriosclesos, Thrombosis and Vascular Biology* 2003; **23**: 275.

Itabe H, Yamamoto H, Suzuki M, Kawai Y, Nakagwa Y, Suzuki A, Imanaka T and Takano T. Oxidized phosphatidylcholines that modify proteins: analysis by monoclonal antibody against oxidized low density lipoprotein. *Journal of Biological Chemistry* 1996; **271**: 33208.

Kayganich-Harrison KA and Murphy RC. Characterization of chain-shortened oxidized glycerophosphocholines lipids using fast atom bombardment and tandem mass spectrometry. *Analytical Biochemistry* 1994; **221**: 16.

Khaselev N and Murphy RC. Peroxidation of arachidonate containing plasmenyl glycerophosphocholines: facile oxidation of esterified arachidonate at carbon-5. *Free Radicals Biology and Medicine* 2000; **29**: 620.

Lawson JA, Rokach J and FitzGerald GA. Isoprostanes: formation, analysis and use as indices of lipid peroxidation *in vivo*. *Journal of Biological Chemistry* 1999; **274**: 24441.

Lee SH and Blair IA. Characterization of 4-oxo-2-nonenal as a novel product of lipid peroxidation. *Chemical Research and Toxicology* 2000; **13**: 698.

Liochev SI. The mechanism of 'Fenton-like' reactions and their importance for biological systems. A biologist's view. In *Metal Ions in Biological Systems*, Sigel A and Sigel H (eds), Vol. 36. Marcel Dekker: New York, 1999; 1–40.

Loidl-Stahlhofen A and Spiteller G. α-hydroxyaldehydes, products of lipid peroxidation. *Biochimica Biophysica Acta* 1994; **1211**: 156.

Marathe GK, Harrison KA, Murphy RC, Prescott SM, Zimmerman GA and McIntyre TM. Bioactive phospholipid oxidation products. *Free Radicals Biology and Medicine* 2000; **28**: 1762.

McIntyre TM, Zimmerman GA and Prescott SM. Biologically active oxidized phospholipids. *Journal of Biological Chemistry* 1999; **274**: 25189.

Mlakar A and Spiteller G. Previously unknown aldehydic lipid peroxidation compounds of arachidonic acid. *Chemistry and Physics of Lipids* 1996; **79**: 47.

Nakamura T, Bratton DL and Murphy RC. Analysis of epoxyeicosatrienoic and monohydroxyeicosatetraenoic acids esterified to phospholipids in human red blood cells by electrospray tandem mass spectrometry. *Journal of Mass Spectrometry* 1997; **32**: 888.

Pincemail J. Free radicals and antioxidants in human diseases. In *Analysis of Free Radicals in Biological Systems*, Favier AE, Cadet J, Kalyanaraman B, Fontecave M, Pierre JL (eds). Verlag: Berlin, 1995; 83–98.

Podrez EA, Poliakov E, Shen Z, Zhang R, Deng Y, Sun M, Finton PJ, Shan L, Gugiu B, Fox PL, Hoff HF, Salomon RG and Hazen SL. Identification of a novel family of oxidized phospholipids that serve as a ligand for the macrophage scavenger receptor CD36. *Journal of Biological Chemistry* 2002; **277**: 38503.

Reis A, Domingues P, Ferrer-Correia AJ and Domingues MRM. Identification by Electrospray Tandem Mass Spectrometry of spin trapped free radicals from oxidized 2-oleoyl-1-palmitoyl-*sn*-glycero-3-phosphocholine. *Rapid Communications in Mass Spectrometry* 2004; **18**: 1047.

Schlame M, Haupt R, Wiswedel I, Kox WJ and Rüstow B. Identification of short-chain oxidized phosphatidylcholine in human plasma. *Journal of Lipid Research* 1996; **37**: 2608.

Sergent O, Morel I and Cillard J. Involvement of metal ions in lipid peroxidation: biological implications. In *Metal Ions in Biological Systems*, Sigel A and Sigel H (eds), Vol. 36. Marcel Dekker: New York, 1999; 251–262.

Spickett CM, Pitt AR and Brown AJ. Direct observation of lipid hydroperoxides in phospholipid vesicles by electrospray mass spectrometry. *Free Radicals Biology and Medicine* 1998; **25**: 613.

Spickett CM, Rennie N, Winter H, Zambonin L, Landin L, Jerlich A, Schaurs RJ and Pitt AR. Detection of phospholipid oxidation in oxidatively stressed cells by reverse-phase HPLC coupled with positive-ionisation electroscopy MS. *Biochemistry Journal* 2001; **355**: 449.

Spiteller P, Kern W, Reiner J and Spiteller G. Aldehydic lipid peroxidation products derived from linoleic acid. *Biochimica Biophysica Acta* 2001; **1531**: 188–208.

Watson AD, Leitinger N, Navab M, Faull KF, Hörkö S, Witztum JL, Palinski W, Schwenke D, Salomon RG, Sha W, Subbanagounder G, Fogelman AM and Berliner JA. Structural identification by mass spectrometry of oxidized phospholipids in minimally oxidized low density lipoprotein that induce monocyte/endothelial interactions and evidence for their presence *in vivo*. *Journal of Biological Chemistry* 1997; **272**: 13597.

Yorek MA. Biological distribution. In *Phospholipids Handbook*, Gregor C (ed.). Marcel Dekker: New York, 1993; 745–775.

Zhang J-R, Cazers AR, Lutzke BS and Hall ED. HPLC-chemiluminescence and thermospray LC/MS study of hydroperoxides generated from phosphatidylcholine. *Free Radicals Biology and Medicine* 1995; **18**: 1.

5. Cross-linking reactions

Manuscript IX: Peptide-phospholipid cross-linking reactions: Identification of leucine-enkephalin-alka(e)nal-glycerophosphatidylcholine adducts by tandem mass spectrometry

Peptide-Phospholipid Cross-Linking Reactions: Identification of Leucine Enkephalin-Alka(e)nal-Glycerophosphatidylcholine Adducts by Tandem Mass Spectrometry

Ana Reis, Pedro Domingues, António J. V. Ferrer-Correia, and M. Rosário M. Domingues
Department of Chemistry, University of Aveiro, Aveiro, Portugal

The covalent interactions between peptides and lipid oxidation products, with formation of Schiff and Michael adducts, are known to occur during free radical oxidative damage. In this study, leucine-enkephalin-glycerophosphatidylcholine alka(e)nal adducts were analyzed by electrospray tandem mass spectrometry (MS/MS). Upon collision-induced dissociation of the Leucine enkephalin-2-(9-oxo-nonanoyl)-1-palmitoyl-3-glycerophosphatidylcholine, an alkanal Schiff adduct observed at *m/z* 1187.7, the main product ions were attributed to the phosphocholine polar head and loss of the peptide. Also, product ions resulting from characteristic losses of phosphatidylcholines and cleavages of the peptide chain (mainly b-type) were observed. Additional product ions formed by combined peptide and phosphatidylcholine fragmentations were identified. The fragmentation pattern of the leucine enkephalin-alkanal Schiff adduct and the leucine enkephalin-alkenal phosphatidylcholine Schiff and Michael adducts were similar, although the loss of the peptide for the Michael adduct should occur through a distinct mechanism. These fragmentation pathways differ greatly from those described for peptide-lipid Schiff and Michael adducts, in which only peptide chain cleavages are reported, probably due to charge retention in the glycerophosphatidylcholine polar head in peptide-glycerophosphatidylcholine adducts. (J Am Soc Mass Spectrom 2006, 17, 657–660) © 2006 American Society for Mass Spectrometry

Oxidative damage of peptides/proteins has received increasing attention due to the growing evidence of being associated with diabetes, cancer, and several age-related diseases [1]. The damage can be induced by the structural modification of the peptide/protein by reactive oxygen species (ROS) and other radicalar species, or by cross-linking reactions between peptide/protein and the oxidation products of other biomolecules (lipids, phospholipids, and DNA bases) [1]. The peptide-lipid adducts occur by reaction of the primary amine group (1) with the terminal carbonyl group (named as Schiff adduct), or (2) with the double-bond present in unsaturated aldehydes (named as Michael adduct). Currently, the work published on the peptide-lipid covalent interactions has focused on the identification of peptide adducts formed with the 4-hydroxy-nonenal (4-HNE) [2], which is a secondary oxidation product of ω-6 lipids (such as linoleic and arachidonic acids) found in membrane phospholipids, in triglycerides, and in low density lipoprotein [3]. The studies published allowed to propose that the lipid interactions with key amino acids in proteins were responsible for major structure alterations, not just by modification of the catalytic site [4], but also by reaction with surface amino acids [2], which ultimately leads to structural (conformational) changes. Tandem mass spectrometry (MS/MS) studies performed on the peptide-lipid Schiff and Michael adducts [2] report only product ions formed by peptide cleavages. Considering the formation of peptide/protein-lipid adducts, peptide-phospholipid covalent interactions analogous to the ones described with 4-HNE could occur through reaction between peptide and phosphatidylcholine-alka(e)nals. To our knowledge, the identification of peptide-phospholipid interactions was not yet investigated by Mass Spectrometry (MS). As part of an ongoing research on the identification of biomolecules radical oxidation products by MS, the purpose of this study is the characterization of leucine enkephalin-phosphatidylcholine alka(e)nal adducts by MS/MS.

Published online March 6, 2006

Address reprint requests to Dr. M. R. M. Domingues, Department of Chemistry, University of Aveiro, 3810-193 Aveiro, Portugal.E-mail: mrd@dq.ua.pt

1044-0305/06/$32.00
doi:10.1016/j.jasms.2006.01.006

Received October 10, 2005
Revised January 17, 2006
Accepted January 17, 2006

Experimental

Phospholipid Oxidative Treatment

The 1-palmitoyl-2-lineloyl-sn-glycero-3-phosphocholine (PLPC) vesicles were prepared from stock solutions of 1 mg/mL in chloroform and dried under stream of nitrogen, by adding HCO_3NH_4 buffer (5 mM, pH 7.4) to a final concentration of 50 mM. Metal catalyzed oxidation of PLPC vesicles was performed by the Fenton reaction, as described elsewhere [5].

Peptide-Phospholipid Adduct Incubation

Twenty μL of 1 mg/mL leucine enkephalin (LeuEnk) (Sigma, Darmstadt, Germany) stock solution in HCO_3NH_4 buffer (5 mM, pH 7.4) was allowed to react with 100μ L of the extract containing the PLPC oxidation products (PLPCox) and left to incubate at 37 °C in the dark (4–6 h) in inert atmosphere, with occasional stirring. The reaction evolution was monitored by ES-MS.

Electrospray (ES) Mass Spectrometry

ES mass spectra and tandem mass spectra were acquired in a Q-TOF 2 instrument (Mass Lynx 4.0, Micromass, Manchester, UK) using MassLynx 4.0 software. The peptide-phospholipid adduct analysis was done after diluting 5 μ L of the sample in 200 μ L of MeOH. The flow rate was 10 μ L/min, needle voltage was set at 3 kV, cone voltage at 35 V, and ion source at 80 °C. Product-ion spectra (MS/MS) were obtained using argon as the collision gas (measured pressure in the penning gauge $\sim 6 \times 10^{-6}$ mBar) and collision energy of 55 eV.

Results and Discussion

Previous work performed on the identification of PLPC radical oxidation products by MS [5–7], reported the presence of the 1-palmitoyl-2-(9-oxo-nonanoyl)-GPC ($[MH]^+$ at *m/z* 650.4), as the major aldehyde product, among the short-chain products with terminal aldehyde at *sn*-2 acyl residues esterified to the 1-palmitoyl-GPC moiety [5, 7]. Other aldehydes with C_7 to C_{12} carbon chain length were also identified and characterized by MS/MS [5] and LC-MS [7], such as the ion at *m/z* 692.5 identified as the 1-palmitoyl-2-(8-hydroxy-11-oxo-9-undecenoyl)-GPC [5, 7]. The formation of peptides and GPC alka(e)nals Schiff and Michael adducts was attempted by incubation of LeuEnk with an extract containing GPC alka(e)nals and monitored by ES-MS. The ES mass spectrum obtained (Supplementary Figure 1a which can be found in the electronic version of this article.) was compared with the mass spectrum of the PLPCox extract in the absence of the peptide (Supplementary Figure 1b). Several ions were observed corresponding to the protonated molecules of the peptide (*m/z* 556.3), the native PLPC (*m/z* 758.5), the PLPC short-chain oxidation products [5], the PLPC long-chain products [9], and also ions observed at *m/z* 1187.7, 1193.8, 1205.7, 1209.7, 1221.8, 1225.7, 1229.7, 1243.7, and 1247.7 that were assigned to LeuEnk-GPC alka(e)nal adducts (Supplementary Figure 1a). **1** The ion at *m/z* 1187.7 may correspond to the Schiff adduct of the LeuEnk-(1-palmitoyl-2-(9-oxo-nonanoyl)-GPC) (Supplementary Scheme **1** which can be found in the electronic version of this article.), formed by reaction of the primary amino group (N-terminal) of LeuEnk with the terminal carbonyl group of the C_9 short-chain aldehyde, in a manner similar to what is described for peptide-HNE adducts [1]. The ions at *m/z* 1229.7 and 1247.7 may be attributed to the Schiff and Michael adducts, respectively, of LeuEnk-1-palmitoyl-2-(8-hydroxy-11-oxo-9-undecenoyl)-GPC (*m/z* 692.5). The ion at *m/z* 1229.7 showed a very low relative abundance, but the product-ion spectrum obtained confirmed the proposed attribution. Preliminary work performed by MS on LeuEnk incubated with hexanal and 2-hexenal (data not shown), known as secondary radical peroxidation products of ω-6 fatty acids, showed abundant ions attributed to Schiff adducts (for hexanal and 2-hexenal) and Michael adducts (only for 2-hexenal). The LeuEnk-GPC alka(e)nal adducts may also be present as doubly charged ions $[MH + H]^{2+}$, however they were not assigned due to their low relative abundance in the mass spectrum.

The ions of the LeuEnk-GPC alka(e)nal adducts at *m/z* 1187.7, 1229.7, and 1247.7 were studied by tandem mass spectrometry (ES-MS/MS).

MS/MS of Peptide-GPC Alkanal Adducts

The product-ion spectrum of the $[MH]^+$ ion of LeuEnk-(1-palmitoyl-2-(9-oxo-nonanoyl)-GPC) adduct at *m/z* 1187.7 (Figure 1a) exhibits abundant product ions at *m/z* 184.1 ($[H_2PO_4(CH_2)_2N(CH_3)_3)]^+$), which is the base peak, product ions at *m/z* 478.4 attributed to the dehydration ion of the 1-palmitoyl-2-lyso-GPC, and also at *m/z* 632.2 that may be formed by loss of the LeuEnk (555 Da). The elimination of LeuEnk cannot be rationalized by direct cleavage of the imine bond formed between the peptide and the GPC alkanal, however this fragmentation can be rationalized considering an initial nucleophilic attack of the nitrogen on the carbonyl group with formation of a six-membered ring structure (Supplementary Scheme **2a** which can be found in the electronic version of this article), which leads to double-bond migration and finally to cleavage of the amine bond by a 1,4 elimination mechanism with loss of H_2O. In the mass range of *m/z* 780 to 1180 of this spectrum (Figure 1b), the product ions at *m/z* 1128.7 (−59 Da) and 1004.7 (−183 Da) can be observed, and correspond to loss of $N(CH_3)_3$ and $HPO_4(CH_2)_2N(CH_3)_3$ from the precursor ion, respectively. These are characteristic losses of GPC $[MH]^+$ and $[MNa]^+$ ions [8], and of GPC

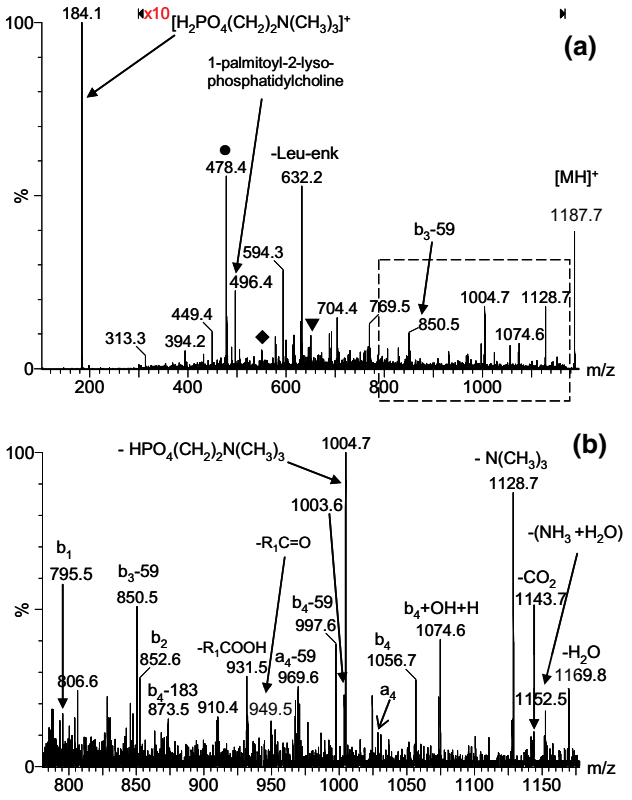

Figure 1. (**a**) Product-ion spectrum of the $[MH]^+$ ion of LeuEnk-1-palmitoyl-2-(9-oxo-nonanoyl)-GPC Schiff adduct. (**b**) Same as (**a**) showing the mass range of *m/z* 780 to 1180 (filled circle, product ion at *m/z* 478.4, filled diamond, product ion at *m/z* 550.4, filled inverted triangle, product ion at *m/z* 650.5).

oxidation products [5, 9]. On the other hand, the product ions observed at *m/z* 931.5 and 949.5, attributed to loss of palmitic acid as a neutral ($-R_1COOH$) and as ketene ($-R_1 = C = O$) from the precursor ion, respectively, are characteristic fragmentations of the phospholipid $[MH]^+$ ions [5, 8, 9]. Overall, the product ions formed by loss of *sn*-1 residue (R_1COOH and $R_1 = C = O$), and the product ion at *m/z* 496.4 attributed to the 1-palmitoyl-2-lyso-GPC (Pathway b in Scheme **1**) along with its dehydration product ion at *m/z* 478.4 (filled circle in Figure 1a), showed that the peptide was linked to the *sn*-2 acyl residue. The higher relative abundance observed for the 1-palmitoyl-2-lyso-GPC (*m/z* 496.4), resulting from loss of peptide-$R_2 = C = O$, when compared to the product resulting from loss of $R_1 = C = O$ (*m/z* 949.5), observed in Figure 1b, was earlier described [8], thus allowing identification of the *sn*-1 fatty acid residue. The product ions at *m/z* 1152.5 ($-NH_3$ and H_2O), 1143.7 ($-CO_2$), 1074.6 (b_4+OH), 1056.7 (b_4), 1028.6 (a_4), 852.6 (b_2), and 795.5 (b_1) observed in Figure 1b, were identified as peptide cleavages corroborating the presence of the LeuEnk linked to the alkanal moiety. The predominance of b-type peptide cleavages is common to product ion spectra obtained with Q-TOF instruments [10], which contrasts with the predominance of y-type product ions in high-energy CID spectra of peptide $[M + H]^+$ ions [11]. Minor product ions observed at *m/z* 806.6 (Figure 1b) and 650.5 (filled inverted triangle in Figure 1a) may be attributed to cleavage of the β-bond of the esterified carboxylic group in the *sn*-1 and *sn*-2 residues, respectively. These fragmentations occur probably by heterolytic cleavage through a McLafferty-like mechanism, and were previously described in tandem mass spectra of oxo fatty acids [12] and of radical peroxidation products of diacyl-GPC [5]. Also, the product ions at *m/z* 1003.6 and 550.4 (filled diamond in Figure 1a) result from cleavage of the γ-bond (Pathway a in Scheme **1**), relative to the carboxylic group, occurring at the *sn*-1 and *sn*-2 residues, respectively, possibly through the 1,4 hydrogen elimination mechanism. Additionally, product ions formed by loss of $N(CH_3)_3$ combined with peptide cleavages were observed at *m/z* 573.4 (loss of LeuEnk), 708.5 (a_1), 765.5 (a_2), 850.5 (b_3), 969.6 (a_4), 997.5 (b_4), and 1015.6 (b_4+OH), as exemplified in Scheme **1**; and product ions formed by loss of $HPO_4(CH_2)_2N(CH_3)_3$ and peptide cleavages at *m/z* 726.5 (b_3), 873.5 (b_4) and 449.4 (loss of LeuEnk) (Scheme **1**). The loss of $R_1 = C = O$ (238 Da) combined with loss of LeuEnk (*m/z* 394.2) was also observed.

The fragmentation pathways here described differ greatly from those identified for the lipid-peptide adducts [2], where only peptide chain cleavages are described. The dissimilarity between the fragmentation

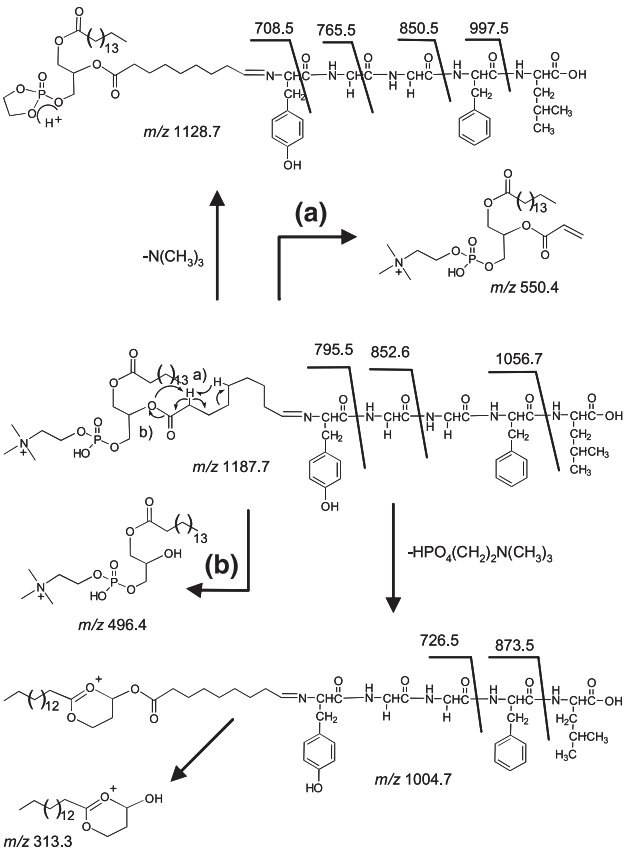

Scheme 1. Proposed fragmentation pathways for the product ions observed in the product ion spectrum of the ion at *m/z* 1187.7.

pattern of peptide-lipid and peptide-GPC adducts is most probably due to charge retention on the GPC polar head, in contrast with the peptide-lipid adducts where the charge is retained in the peptide moiety. The identification of fragmentation pathways occurring in the peptide and in the phosphatidylcholine moieties gives structural information about the two components of the adducts.

Peptide-Phosphatidylcholine Alkenal Adducts

The product-ion spectra obtained for the LeuEnk-(1-palmitoyl-2-(8-hydroxy-11-oxo-9-undecenoyl)-GPC)) Schiff and Michael adducts (Supplementary Figure 2 which can be found in the electronic version) exhibited similar fragmentation patterns, with the product ion at *m/z* 184.1 (base peak) and the product ions formed by loss of $N(CH_3)_3$ and $HPO_4(CH_2)_2N(CH_3)_3$, loss of LeuEnk and loss of R_1COOH from the precursor ion, as well as the product ions that can be assigned to lyso-GPC (*m/z* 478.4 and 496.4). However, the elimination of LeuEnk from the precursor ion for the Michael adduct cannot occur by a mechanism similar to the one proposed for the Schiff adduct, but can be rationalized through a direct 1,2 elimination mechanism (Supplementary Scheme **2b**). The product ions formed through combined loss of LeuEnk with $N(CH_3)_3$ and $HPO_4(CH_2)_2N(CH_3)_3$ were observed for both peptide-GPC adducts, while b-type peptide cleavages were observed with low relative abundance.

Conclusions

Structural characterization of peptide-GPC alka(e)nal Schiff and Michael adducts by MS/MS showed product ions that resulted from characteristic fragmentations of GPC and of peptides. These differ greatly from the ones described for peptide-lipid adducts, where only peptide cleavages are described. These findings reveal another aspect of cross-linking reactions that may take place in membrane proteins during free radical oxidative damage.

Acknowledgments

The authors acknowledge the PhD grant to AR (SFRH/BD/10358/2002) provided by Fundação para a Ciência e Tecnologia (FCT, Portugal) and Fundo Social Europeu (FSE).

References

1. Berlett, B. S.; Stadtman, E. R. Protein Oxidation in Aging, Disease, and Oxidative Stress. *J. Biol. Chem.* **1997,** *272,* 20313–20316.
2. Carini, M.; Aldini, G.; Facino, R. M. Mass Spectrometry for Detection of 4-Hydroxy-Trans-2-Nonenal (HNE) Adducts with Peptides and Proteins. *Mass Spectrom. Rev.* **2004,** *23,* 281–305.
3. Spiteller G. Linoleic Acid Peroxidation—The Dominant Lipid Peroxidation Process in Low Density Lipoprotein and Its Relationship to Chronic Diseases. *Chem. Phys. Lipids* **1998,** *95,* 105–162.
4. Ishii, T.; Emi, T.; Shigenori, K.; Nakayama, T.; Uchida, K. Molecular Basis of Enzyme Inactivation by an Endogenous Electrophile 4-Hydroxy-2-Nonenal: Identification of Modification Sites in Glyceraldehyde-3-Phosphate Dehydrogenase. *Biochem.* **2003,** *42,* 3474–3480.
5. Reis, A.; Domingues, P.; Ferrer-Correia, A. J. V.; Domingues, M. R. M. Fragmentation Study of Short-Chain Products Derived from Oxidation of Diacyl-Phosphatidylcholines by Electrospray Tandem Mass Spectrometry: Identification of Novel Short-Chain Products. *Rapid Commun. Mass Spectrom.* **2004,** *18,* 2849–2858.
6. Itabe, H.; Yamamoto, H.; Suzuki, M.; Kawai, Y.; Nakagwa, Y.; Suzuki, A.; Imanaka, T.; Takano, T. Oxidized Phosphatidylcholines that Modify Proteins: Analysis by Monoclonal Antibody Against Oxidized Low Density Lipoprotein. *J. Biol. Chem.* **1996,** *271,* 33208–33217.
7. Reis, A.; Domingues, M. R. M.; Amado, F. M. L.; Ferrer-Correia, A. J. V.; Domingues, P. Separation of Peroxidation Products of Diacyl-Phosphatidylcholines by Reverse-Phase Liquid Chromatography-Mass Spectrometry. *Biomed. Chromatogr.* **2005,** *19,* 129–137.
8. Hsu, F.-F.; Turk, J. Electrospray Ionization/Tandem Quadrupole Mass Spectrometric Studies on Phosphatidylcholines: The Fragmentation Process. *J. Am. Soc. Mass Spectrom.* **2003,** *14,* 352–363.
9. Reis, A.; Domingues, P.; Ferrer-Correia, A. J. V.; Domingues, M. R. M. Tandem Mass Spectrometry of Intact Oxidation Products of Diacyl-Phosphatidylcholines: Evidence for the Occurrence of the Oxidation of the Phosphocholine Head and Differentiation of Isomers. *J. Mass Spectrom.* **2004,** *39,* 1513–1522.
10. Qin, X.-Z.; Yuan, Y. Electrospray Ionization/Collision-Induced Dissociation of Protonated Substance P Ions—Effect of Charge on the Fragmentation Pattern. *Int. J. Mass Spectrom.* **2004,** *237,* 123–133.
11. Paizs, B.; Suhai, S. Fragmentation Pathways of Protonated Peptides. *Mass Spectrom. Rev.* **2005,** *24,* 508–548.
12. Cheng, C.; Gross, M. L. Fragmentation Mechanisms of Oxo-Fatty Acids via High-Energy Collisional Activation. *J. Am. Soc. Mass Spectrom.* **1998,** *9,* 620–627.

6. Discussion

Experimental conditions used for fatty acid radical oxidation

Metal-catalysed reaction radical oxidation of fatty acids under the Fenton conditions are influenced by several factors, such as concentration of H_2O_2, concentration of transition metals and its oxidation state, the time of incubation, and concentration of polyunsaturated fatty acid (PUFA). In view of this, the radical oxidation of free and esterified fatty acids were performed at pH 7.4 and in a bath at 37ºC, in order to mimic the physiological conditions, using [Fe^{2+}] in 5mM and a large excess of H_2O_2 (50mM), in order to induce the maximum oxidative damage. The oxidative radical reactions were carried out in freshly prepared diacyl-phosphatidylcholines liposomes, in the dark to prevent the contribution of autoxidation reaction. The initiation of the radical reactions was triggered by the addition of H_2O_2 to the solution containing the fatty acids and the ferrous ions, and not by the addition of ferrous ions which in the presence of pre-existing fatty acid hydroperoxides (LOOH) [Qian et al., 2000; Qian et al., 2005] initiate the radical oxidation (reaction 1). The absence of pre-existing fatty acid hydroperoxides was monitored by ESI-MS prior to the incubation reaction.

$$Fe\ (II) + LOOH \longrightarrow Fe\ (III) + LO^{\bullet} + {}^{-}OH \quad \text{(reaction 1)}$$

For the spin trapping experiments, the spin trap was added to the oxidised fatty acid extract ca. 30 min after the radical oxidation had been initiated. This was done in order to ensure that the spin trap was added during the propagation phase of the reaction, where the concentration of radical propagating species is expected to be high enough. According to Spickett and colleagues (1998), this stage took place after approximately 20 min (latent period) after the addition of the ferrous ions [Spickett et al., 1998], where the decomposition reactions described, by reactions 1-3, contribute to the propagation reaction (Tang et al., 2000).

$$LH + {}^{\bullet}OH \longrightarrow L^{\bullet} + H_2O \quad \text{(reaction 2)}$$

$$LOO^{\bullet} + LH \longrightarrow LOOH + L^{\bullet} \quad \text{(reaction 3)}$$

After radical oxidation, the fatty acid spin adducts were isolated by an additional extraction step with chloroform and methanol (Folch method) which stabilizes the fatty acid spin adducts formed in solution by removal of the ROS and of the metal ions (equations 1 and 2), thus preventing further degradation prior to MS analysis.

Identification of Linoleic acid Free Radicals (manuscripts I and II)

Upon radical oxidation of the linoleic acid several radical oxidation products were identified in the ESI mass spectra. These products included linoleic acid free radicals with oxygen atoms inserted into the unsaturated fatty acid chain, and named linoleic acid long-chain radical products, and linoleic acid small alk(en)yl free radicals formed by carbon-carbon bond cleavage occurring in linoleic acid long-chain radical products by a β-scission mechanism, and named linoleic acid short-chain radical products. With the carbon chain breakdown also non-radical fatty acid short-chain products are formed containing terminal aldehyde and carboxylic moieties, that undergo further radical oxidation with formation of linoleic acid short-chain radical products (Scheme 2, cap 1). The linoleic acid long-chain radical products, the linoleic acid small alk(en)yl radicals and the linoleic acid short-chain radical products were identified as linoleic acid DMPO spin adducts by mass spectrometry. The two latter could only be identified through mass spectrometry coupled with liquid chromatography.

The linoleic acid spin adducts observed in the mass spectra corresponded to the hydroxylamine structures of the spin adducts even the oxidised linoleic acid spin adducts exhibiting a 2Da decrease relative to the *m/z* value of oxidised linoleic acid spin adducts, which based on the *m/z* value, could have been attributed to the cyclic hydroxylamine structure or to the oxidised hydroxylamine structure of the oxidised linoleic acid spin adducts (Scheme 3).

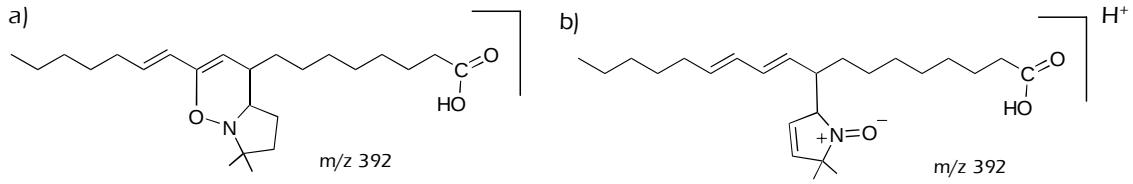

Scheme 3: Proposed structures for the linoleic acid alkyl spin adduct (m/z 392)

However, the product ion spectra obtained for all the linoleic acid spin adducts showed the presence of the product ion at *m/z* 114, assigned to the protonated molecule of the spin trap (5,5-dimethyl-1-pyrroline-N-oxide), $[DMPO+H]^+$. The product ion at *m/z* 114 along with the absence of the product ion at *m/z* 112 (5,5-dimethyl-1-pyrroline-3-ene-N-oxide) suggested that the ions observed in the mass spectrum were cyclic structures of the hydroxylamine spin adducts (Scheme 3).

Common fragmentation features observed in the product ion spectra of the oxidised linoleic acid spin adducts, were loss of water (H_2O), loss of the spin trap (DMPO) and combined losses of both neutral molecules. These fragmentation pathways are in accordance with the fragmentation pattern described for ω-3 and ω-6 polyunsaturated fatty acid spin adducts [Qian et al., 2003a,b], however, these product ions do not provide any structural information regarding the location of the spin trap along the carbon chain. On the other hand, specific product ions attributed to the spin trap (*m/z* 114) and oxidised spin trap (*m/z* 130, $[DMPO\text{-}OH+H]^+$ and 146 $[DMPO\text{-}OOH+H]^+$), together with the odd-numbered product ions containing the spin trap identified to homolytic cleavages in the vicinity of the spin trap, and even-numbered product ions attributed to 1,4 hydrogen elimination mechanism, allylic cleavages involving the substitutents groups (hydroxy and keto), and/or McLafferty-like rearrangements, were the most informative. Considering that the charge was retained at the spin trap, these cleavages were identified as charge-remote fragmentations. Charge-remote fragmentations, which are characteristic of product-ion spectra in high-energy CID conditions, have also been observed under low-energy conditions during fatty acid characterisation [Wheelan et al., 1996; Crow et al., 2002], and have been helpful in the differentiation of lithiated PUFA [Hsu and Turk, 1999], oxo fatty acids [Cheng and Gross, 1998] and poly-hydroxy fatty acids [Wheelan et al., 1996]. In this study, charge-remote fragmentations provided crucial information allowing proposing: i) the presence of carbon and oxygen centred linoleic acid spin adducts; ii) the location of the spin trap along the carbon chain; iii) the location of the hydroxy substitutents; and iv) the contribution of hydroxy derivatives, namely hydroxy-alkyl and hydroxy-alkoxyl to the relative abundance of alkoxyl and peroxyl linoleic acid spin adducts, respectively.

Contribution of fatty acid structural (alkyl and alkoxyl) and positional isomers was thus evidenced by MS/MS data through the identification of the hydroxy substitutents and of the spin trap along the carbon fatty acid chain in long-chain spin adducts. This was corroborated by the identification of the linoleic acid small alky(en)yl spin adducts, namely propyl spin adduct (cleavage from carbon-centred at C-14), heptanoic acid spin adduct (carbon-centred at C-9), hexanoic acid (carbon-centred at C-8), pentyl spin adduct (oxygen-centred at C-13) and octanoic acid spin adduct (oxygen-centred at C-9). The identification of several positional isomers, located between C-8 and C-14 carbon atoms, during non-enzymatic linoleic acid radical peroxidation is not surprising considering that the reaction is initiated by abstraction of the bis-allylic hydrogen atom in the pentadienyl moiety (C-11). After hydrogen abstraction, the linoleic acid radical leads, by isomerisation, to equimolar amounts of two linoleic acid radical isomers placed at C-9 and C-13 [Spiteller,

1998]. These alkyl radical species, in turn, contain allylic hydrogen atoms at C-14 and C-8, respectively, that after hydrogen abstraction may generate radical species at these carbon atoms, or may undergo double bond rearrangement with the formation of radical species at C-10 and C-12, respectively.

The higher S/N ratio observed in the LC-MS spectrum for the octanoic spin adduct (alkoxyl spin adduct in C-9) compared to the RIC counts of the pentyl spin adduct (alkoxyl spin adduct in C-13), although no quantification studies were performed throughout this study, suggested the predominance of the structural isomers located at C-9 carbon atom. Considering that upon non-enzymatic metal radical oxidation of linoleic acid, both C-9 and C-13 carbon atoms are equally likely to be present, and that the trapping rate constants of alkyl radicals are influenced by the chain-length [Taniguchi and Madden, 1999] and steric hindrance effects [Rosen et al., 1999], the predominant occurrence of carbon- and oxygen–centred linoleic acid radicals at C-9 suggests the preferential isomerisation towards the C-9 position over C-13 position. Ultimately, the identification of linoleic acid oxidation products resulting form the preferential oxidation at C-9 position is an oxidation behaviour that may be comparable to the radical oxidation reported during enzymatic oxidation (lipoxygenases) of ω-6 PUFA. During enzymatic radical oxidation of ω-6 fatty acids it was noticed that the oxidation of the ω-6 position was favoured [Qian et al., 2000; Qian et al., 2003b] most probably by blocking the C-9 position of the linoleic acid [Kitaguchi et al., 2005]. Noteworthy, the various positional isomers identified for the linoleic acid spin adducts and the linoleic acid small alky(en)yl spin adducts that derive from them, suggested that cleavage of the unsaturated carbon chain by the β-scission mechanism occurs towards the formation of lower carbon chain length free radicals (manuscript II). This suggests selectivity in the β-scission cleavage of oxidised fatty acids.

The fatty acid short-chain products (aldehydes and dienes) here identified as linoleic acid short-chain radical products have been reported in the human urine [Kim et al., 1999], and are described to be highly cytotoxic [O´Brien-Coker et al., 2001; Niknahad et al., 2003; Deng and Zhang, 2004] particularly the oxo-acids (manuscript II) to endothelial cells in concentrations as low as 1μM [Jian et al., 2005]. Their toxicity is thought to be related to higher chemical stability, when compared to fatty acid free radicals, to the reaction with amino groups of peptides and proteins [De Zwart et al., 1999; Petersen and Doorn, 2004] and to the ability to cross the lipid barrier [De Zwart et al., 1999].

The identification of linoleic acid long-chain radical products, linoleic acid small alk(en)yl radicals and linoleic acid short-chain radical products by mass spectrometry with

spin trapping provided valuable structural information about the lipid intermediate radical species formed and also their breakdown products. Considering that free PUFA in *in vivo* conditions undergo enzymatic and/or non-enzymatic radical oxidation, the knowledge about the lipid peroxidation products (intact or breakdown free radicals products) formed *in vivo* may be improved by the use of mass spectrometry without the limitations of EPR analysis [Dikalov and Mason, 2001; Qian et al., 2000; Anzai et al., 2003; Qian et al., 2005].

Free Radical oxidation of diacyl-glycerophosphatidylcholines (manuscript III-VIII)

Phospholipids of the choline class, namely glycerophosphatidylcholines (GPC) and sphingomyelins (SM), are the most abundant phospholipids in cell membranes of mammals, comprising between 40-80% (dry weight) of the membrane, which in the case of erythrocytes reach to 54% of the lipid content being predominantly located in the outer leaflet [Yorek, 1995]. Considering that 18:1, 18:2, 18:3 and 20:4 fatty acids account for more than 90% of the unsaturated fatty acid content in phospholipids of most membranes [Yorek, 1995], the three diacyl-glycerophosphatidylcholines selected, contained unsaturated fatty acids at the *sn*-2 residue, with increasing number of double bonds (oleoyl-, lineloyl- and arachidonoyl-), and saturated fatty acid at the *sn*-1 residue. The sn-1 acyl residue is resistant towards radical oxidation due to the lack of methylene groups and hence metal catalysed radical oxidation is restricted to the *sn*-2 residue of the phosphatidylcholines, which narrows the presence of the structural modifications to only one of the acyl chains.

Radical oxidation of diacyl-glycerophosphatidylcholines (GPC) results in the formation of oxidation products that include, i) intact GPC free radicals and oxidised unsaturated acid free radicals (manuscript III and IV), ii) intact oxidised GPC products with oxygen atoms inserted in the unsaturated fatty acid chain, named as long-chain products (manuscript V and VI), and oxidised GPC products with the unsaturated fatty acid chain shortened, named short-chain products with terminal aldehyde and dicarboxylic moieties (manuscript VII and VIII), and iii) lyso-phosphatidylcholines, released by ester hydrolysis of the *sn*-1 or *sn*-2 positions. The free fatty acids released by a saponification mechanism may undergo further radical oxidation with formation of short- and long-chain products (discussed in manuscript I and II). In a thorough study aiming the identification of GPC oxidation products formed by metal radical oxidation each of the products identified will be discussed separately in the following sections, with the exception of the lyso-phosphatidylcholines.

Identification of diacyl-glycerophosphatidylcholine free radicals (manuscripts III and IV)

The diacyl-glycerophosphatidylcholines radical products identified by mass spectrometry comprised oxidised intact GPC free radicals and oxidised unsaturated fatty acids free radicals (*sn*-2 residue) containing up to three oxygen atoms.

The identification of oxidised intact GPC spin adducts containing a restricted number of oxygen atoms (up to three) for all the GPC studied, namely (1-palmitoyl-2-oleoyl-glycerophosphatidylcholine - POPC, 1-palmitoyl-2-lineloyl-glycerophosphatidylcholine - PLPC and 1-palmitoyl-2-arachydonoyl-glycerophosphatidylcholine - PAPC), shows that both, the monounsaturated phospholipid (POPC) and the polyunsaturated phospholipids (PLPC and PAPC) were modified to the same extent. This oxidation behaviour was unexpected, since the extent of fatty acid oxidation is reported to be related to the degree of unsaturation (number of allyic hydrogen atoms) [Li et al., 2000]. Considering that the POPC, PLPC and PAPC were prepared in same experimental conditions, namely phospholipid concentration, buffer solution, method of liposome formation, oxidation in freshly prepared liposomes and temperature of incubation, the main differences reside on the *sn*-2 acyl chain and on the size of the liposome. Other factors, such as acyl chain packing [Araseki et al., 2002] and the surface area of the liposome [Li et al., 2000; Borst et al. 2000; Araseki et al., 2002; Vitrac et al., 2004] may also influence the extent of phospholipid radical oxidation. In fact, according to the literature, a larger curvature characteristic of smaller vesicles [Li et al., 2000], might facilitate ROS penetration into the liposome [Borst et al., 2000]. Although, the radical oxidation of GPC liposomes was not performed in liposomes with normalised size diameters, the similarities observed for the oxidised GPC spin adducts identified after radical oxidation of POPC, PLPC and PAPC cannot be rationalised based solely on the *sn*-2 unsaturated fatty acids chains. As noticed elsewhere, the *sn*-2 acyl chains showed minor influence on the size (surface area) of liposomes prepared by sonication [Araseki et al., 2002], and the curvature of the vesicles could not be accounted for the higher oxidative stability observed for 1-palmitoyl-2-docosahexanoyl-glycerophosphatidylcholine (PDPC) and PLPC liposomes when compared to PAPC liposomes [Araseki et al., 2002], through measurement of the unoxidised PUFA by GC.

On the other hand, the identification of POPC, PLPC and PAPC radical spin adducts containing a restricted number of oxygen atoms may be rationalised considering that the addition of DMPO acted as a $HO^{\bullet}$ "scavenger". This prevented the $HO^{\bullet}$ radical to be

available for the bis-allylic hydrogen abstraction in the unsaturated acyl chains, which can be sustained by the DMPO trapping rate constants towards $HO^{\bullet}$ radical ($k \sim 10^9$ $M^{-1}s^{-1}$, [Rosen et al, 1999]) compared to the rate constants exhibited by DMPO towards alkyl radicals ($k \sim 10^6$-10^7 $M^{-1}s^{-1}$) that have a chain-length dependent effect [Taniguchi and Madden, 1999]. Similar conclusions were drawn by Deterding et al. (2004), during the identification of radicals of hemoglobin, where in control experiments performed in the absence of the spin trap (DMPO), several oxidised forms of hemoglobin were identified in the mass spectrum but none of these were observed in the presence of the spin trap [Deterding et al., 2004]. Hence, the addition of the spin trap to the fatty acid radicals extract shows a "retarder" effect on the radical oxidation of fatty acids in liposomes by reaction of the spin trap with radical propagating species, such as $HO^{\bullet}$ and $O_2^{\bullet}$, affecting the formation of fatty acid propagating species, namely $LO^{\bullet}$ and $OLOO^{\bullet}$ [Barclay and Vinqvist, 2000], in spite of the low concentration of the spin trap used, which was approximately 20mM, a relatively low concentration value when compared to other experiments (50-100mM) [Qian et al., 2003a,b; Deterding et al., 2004; Kumamoto et al., 2005]. According to Barclay and colleagues (2000), the effect of the spin trap in retarding the fatty acid radical oxidation is expected to be more pronounced in the presence of low O_2 concentration where, due to the absence of radical propagating species, lower amounts of spin trap are required for retarding the reaction [Barclay and Vinqvist, 2000]. The results obtained in the absence of the spin trap phospholipid peroxidation, showing increasing number of oxygen insertion with increasing number of allylic hydrogen atoms (discussed below), provides further evidence that the radical oxidation of phosphatidylcholines was restricted by the addition of the spin trap, and thus the identification of phosphatidylcholine DMPO spin adducts containing one, two and three oxygen atoms.

The oxidised GPC radical spin adducts identified in the mass spectra contained up to three oxygen atoms corresponding to the hydroxy-alkyl, alkoxyl, hydroperoxide-alkyl and hydroxy-alkoxyl derivatives. Their structural features were obtained by tandem mass spectrometry (MS/MS) through the identification of product ions formed by i) loss of neutral molecules relative to the glycerophosphatidylcholine moiety, ii) loss of saturated (*sn*-1) and unsaturated fatty acid chains (*sn*-2), and iii) charge-remote cleavages. The charge-remote fragmentations resulted in even-numbered product ions that could be assigned to cleavages involving the hydroxy group with hydrogen rearrangement, and odd-numbered product ions assigned to homolytic cleavages. These cleavages, similar to the ones described for the linoleic acid spin adducts (manuscript I and II), allowed proposing the nature of the GPC spin adducts namely the presence of carbon-centred spin

adducts such as alkyl-, hydroxy-alkyl and hydroperoxide-alkyl, and also oxygen centred spin adducts such as alkoxyl-, hydroxy-alkoxyl and hydroperoxide-alkoxyl spin adducts, as well as their position within the carbon chain. The spin adducts were, depending on the GPC, proposed to be placed at different locations of the acyl chain and in spite of the apparent randomness described for the location of carbon and oxygen centred GPC spin adducts, it could be proposed the preferential location of spin adducts at the carbon atoms near the polar head. This is particularly visible by the results achieved for the PAPC spin adducts, where three bis-allylic hydrogen atoms are equally likely to be abstracted (C-7, C-10 and C-13) but the preferential location of the PAPC spin adducts around C-5, C-7, C-8 and C-10, suggested that the hydrogen atom closer to the polar head was easier accessible for abstraction.

To our knowledge, the identification of phospholipid free radicals, initially attempted by Yoshida and colleagues (1996) using spin trapping with ESR detection, is scarce and only carbon-centred phosphatidylcholine DMPO spin adducts were reported. However, the authors make no mention as to whether the carbon centred spin adduct described was a small alkyl fatty acid spin adduct or if it corresponded to the intact GPC alkyl spin adduct. More recently, Kumamoto and colleagues (2005) proposed, by LC-EPR data, the presence of the 13-alkoxyl/POBN di-lineloyl-glycerophosphatidylcholine (DLPC) spin adduct in autoxidised DLPC in the presence of Fe^{2+} ions based on the identification of the breakdown product (pentyl spin adduct). Although, during non-enzymatic radical oxidation both isomers (C-9 and C-13) are equally likely to be present, no mention was made regarding the presence or absence of the 9-alkoxyl/POBN DLPC spin adduct [Kumamoto et al., 2005]. Furthermore, in the case of DLPC containing two unsaturated fatty acid chains it would be expected that intramolecular radical-radical reactions would occur to some extent as terminating steps of the oxidation.

Radical-radical products resulting from terminating steps of radical reactions, such as the ones described by reactions 5-8 were not surveyed in this study, but their formation could also have taken place. In spite of the probable formation of endoperoxides (reaction 5), dialkyltrioxides (reaction 6) and tetraoxides (reaction 7) these species are not stable and decompose with formation of carbonyl compounds, alcohols and in some cases formation of singlet oxygen [Adam et al., 2005].

$$LO^{\bullet} + L^{\bullet} \longrightarrow LOL \qquad \text{(reaction 4)}$$

$$LO^{\bullet} + LO^{\bullet} \longrightarrow LOOL \qquad \text{(reaction 5)}$$

$LOO^{\bullet} + LO^{\bullet} \longrightarrow LOOOL$ (reaction 6)

$LOO^{\bullet} + LOO^{\bullet} \longrightarrow LOOOOL$ (reaction 7)

Characterisation of non-radical peroxidation products of diacyl-glycerophosphatidylcholines (manuscripts V-VIII)

A myriad of non-radical GPC peroxidation products were formed as products of the non-enzymatic radical oxidation of phosphatidylcholines in the absence of the spin trap and identified through mass spectrometry. This was achieved without additional derivatisation or saponification steps, which is an advantage to the approaches reported in the literature for the identification and characterisation of oxidised phospholipids [Kayganich and Murphy, 1994; Iwase et al., 1999; Murphy et al., 2001].

The non-enzymatic metal-catalysed radical oxidation of just 3 GPC phospholipids resulted in the total of more than 50 non-radical peroxidation products identified by mass spectrometry. This myriad of peroxidation products does not consider the isobaric structures or the structural and positional isomers later identified by HPLC coupled with tandem mass spectrometry. From the peroxidation products identified for each GPC it was noticed that the number of peroxidation products, formed by insertion of oxygen atoms (*m/z* values higher than the native GPC and named long-chain GPC products) and formed by cleavage of the *sn*-2 acyl chain (*m/z* values lower than the native GPC named short–chain GPC products) increased as the number of allylic hydrogen atoms (double bonds) in the *sn*-2 acyl chain (POPC, PLPC and PAPC), also increased. These results are in agreement with the published literature where it is stated that the extent of fatty acid modifications during radical oxidation is related to the degree of unsaturation (number of allyic hydrogen atoms) [Li et al., 2000; Niki et al., 2005]. This contrasted with the literature available on the identification of non-radical phospholipid peroxidation products, where, in spite of the work performed on both long-chain and short-chain products was until recently, mainly focused on only 4 structures [Watson et al., 1997; Watson et al., 1999; Subbanagounder et al., 2002; Jerlich et al., 2003; Subbanagounder et al., 2003]. Only recently a more complete identification of long-chain products [Vitrac et al. 2004; Adachi et al., 2005] and of short-chain products [Podrez et al., 2002] was attempted by mass spectrometry data analysis.

The vast number of peroxidation products formed by radical oxidation of GPC obtained in a simple model (monophasic), emphasizes the complexity of radical

peroxidation that may take place in a multicomponent structure such as the biological membrane, in which several classes of phospholipids are present with various acyl chains, as well as proteins. The presence of non-radical GPC peroxidation products which are not propagators of lipid peroxidation have been implicated in: i) the increase of membrane polarity, and through the strengthening of intermolecular forces with changes in the hydrophobic environment in which membrane proteins are partially or fully embedded, affect membrane exchanges, and ii) the increase in membrane disorder, that was described in *in vitro* studies using synthetic and liver phospholipids by EPR [Megli and Sabatini, 2003; 2004; 2005], affecting acyl packing with the decrease of lateral pressure [Borst et al., 2000]. The lateral pressure exerted by the acyl chains has impact on the structural integrity of membrane proteins [Palsdottir and Hunte, 2004] and therefore the decrease in lateral pressure observed in oxidised membranes [Borst et al., 2000] may increase the conformational freedom of the protein with loss of the biochemical function [Palsdottir and Hunte, 2004].

The complexity of the non-radical GPC products identified by reverse phase chromatography coupled with mass spectrometry detection allowed the differentiation of isomeric structures in the case of long-chain products (manuscript VI), and the differentiation of isobaric structures in the case of short-chain products (manuscript VIII). Still, the lack of characterisation studies by tandem mass spectrometry for such products [Podrez et al., 2002; Vitrac et al., 2004], together with the non interpretation of product ions observed in the product ion spectra [Adachi et al., 2004; Adachi et al., 2004b], other than the ones attributed to characteristic losses of GPC [Hsu and Turk, 2003], prevented the authors to ascertain the structures of the oxidised GPC that were detected in the mass spectra.

A) Characterisation of oxidised glycerophosphatidylcholines by insertion of oxygen atoms in the sn-2 acyl chain

The long-chain GPC products that were identified in the mass spectrum were structurally characterised based on the fragmentation pattern obtained in different retention times. The structural variability that may take place within a single phosphatidylcholine was observed by LC-MS data based on the elution of broader chromatographic bands as the number of oxygen atoms increased (manuscript VIII) corroborating the increased structural variability. Similar results were described by Vitrac and colleagues (2004), where keto, hydroxy and hydroperoxide derivatives were proposed to be formed during PLPC oxidation [Vitrac et al., 2004].

The fragmentation pattern of long-chain GPC products showed, apart from characteristic neutral losses of GPC $[MH]^+$ and $[MNa]^+$ ions, the loss of neutral fragments from the precursor ion (nH_2O, H_2O_2 and O_2, n=0,1,2,3), and charge-remote fragmentations involving the substitutent groups and the double bonds (manuscript V). The fragmentations here described together with the *m/z* value allowed proposing structural and positional isomers of hydroxy, keto, epoxy, and hydroperoxide derivatives, although the high incidence of hydroxy derivatives identified as GPC peroxidation products suggested that, under *in vitro* conditions, the hydroxy derivatives are more stable or their formation more favourable. Remarkably, in *in vivo* conditions the hydroperoxide fatty acid derivatives are catalysed to hydroxy derivatives by glutathione peroxidase (GPx), and phospholipid glutathione peroxidase (PhGPx) or selenoproteins catalyses the phospholipid hydroperoxides to hydroxy derivatives [Sergent et al., 1999; Niki et al., 2005]. Surprisingly, the keto derivatives were absent in the mass spectra of phosphatidylcholine spin adducts (manuscript III and IV), which suggests that the formation of the keto derivatives takes place in a later oxidation stage prevented by the addition of the spin trap.

Nonetheless, during the interpretation of GPC peroxidation products tandem mass spectra some limitations were considered, as described in the following:

a) tandem mass spectra of positional isomers of epoxy and hydroxy derivatives show similar product ions due to cleavage of the α bond vicinal to the group with slight differences in the relative abundance, already described for eicosatetraenoic acid compounds [Nakamura et al., 1997]. However, though the formation of epoxy derivatives may be favoured by intramolecular cyclisation of alkoxyl intermediate species ($k \sim 2x10^7\ s^{-1}$) over other pathways (β-scission or H abstraction) in *in vitro* conditions, Fitzpatrick and colleagues (1982) determined that, at pH 7.4 and 25ºC, the half-life of the epoxy derivatives of AA was only 3s [Fitzpatrick et al., 1982]. Nonetheless, epoxy fatty acid derivatives have been identified in human red blood cells [Nakamura et al., 1997; Jiang et al., 2004], together with hydroxy derivatives of ω-3 and ω-6 fatty acids in red blood cells [Nakamura et al., 1997; Inouye et al., 1999; Jiang et al., 2004], with predominance of some positional hydroxy derivatives over others under physiological conditions [Nakamura et al., 1997].

b) tandem mass spectra of hydroperoxide and of vicinal di-hydroxy fatty acid derivatives show loss of 34Da (H_2O_2) from the precursor ion. This is in accordance with previous published works [Spickett et al., 2001; Adachi et al., 2004; Giuffrida et al., 2004b] although other authors based their identification of hydroperoxide derivatives on the

presence of product ions formed by loss of two water molecules from the precursor ion [Giuffrida et al., 2004a].

In view of this, detailed structural information was only achieved for the peroxidation products containing a limited number of oxygen atoms in the *sn*-2 unsaturated fatty chain, namely 8 different structures were proposed to occur by the insertion of one, two and three oxygen atoms during radical oxidation of POPC (manuscript V), and at least 11 different structures were proposed as *sn*-2 acyl derivatives of the PLPC as the result of one and two oxygen atoms and that contributed to the relative abundance of 4 ions (manuscript VI). For the long-chain products containing three and four oxygen atoms in POPC and PLPC, the number of hypothetic structures (structural and positional isomers) restricted the certainty to propose structures due to increase structural variability. In the case of arachidonoyl containing phosphatidylcholines the insertion of two oxygen atoms during non-enzymatic radical oxidation may be attributed to 7 different structural isomers (di-hydroxy, hydroperoxide, hydroxy-epoxy, endoperoxide, isoprostanes, isoketal [Roberts II and Fessel, 2004] and prostaglandins [Gao et al., 2003]). On the other hand, the lack of published literature referring to the identification of oxidised phospholipids with high number of oxygen atoms in biological samples, may result from the absence of such products in *in vivo* conditions caused to their chemical instability or to the low relative abundance of these products in biological matrices. Also, the increasing published work concerning the identification of hydroxy, epoxy and hydroperoxide derivatives of free and esterified fatty acids [Nakamura et al., 1997; Inouye et al., 1999; Adachi et al., 2004b] and of carbonyl derivatives of fatty acids [Schlame et al., 1996; Kim et al., 1999; Frey et al., 2000; Inouye et al., 2000; Hoff et al., 2003; O'Brien-Coker et al., 2003] in biological samples, may reflect that under *in vivo* conditions oxidised fatty acid products containing high number of oxygen atoms are degraded to less complex products, namely to fatty acids with a low number of oxygen atoms, or further degraded to fatty acid short-chain products.

The occurrence of radical oxidation in other points of the GPC molecule had never been described, which was accessed by tandem mass spectrometry through the identification of, product ions at *m/z* 163 suggesting the location of hydroxy group at the phosphocholine polar head in non-radical GPC oxidation products (manuscript V) and of product ions at *m/z* 408, 424, 426 and 442 (manuscript IV) suggesting the presence of the spin trap at the glycerol moiety in radical GPC spin adducts, and that were not observed in the native phosphatidylcholine product ion spectra. The fact that oxidation of the polar head had never been described can be rationalised considering that most of the non-radical phospholipid oxidation products and phospholipid fatty acid spin adducts were

identified in saponified phospholipid extracts. In the event of radical oxidation occurring at the polar head *in vivo* conditions, the hydroxy group at the polar head may, due to hydrogen bonding, lead to a reorientation of the water molecules at the surface of the membrane, and also due to redistribution of counterions of opposite charges at the cytosolic medium, lead to changes of the cell membrane potential. Changes in the membrane potential are involved in membrane transport mechanisms [Cevc, 1995].

Some of the oxidised GPC products here identified were reported in increased levels in the plasma of diabetic patients [Inouye et al., 1999; Inouye et al., 2000], in hypertensive subjects [Ward et al., 2005], and in oxLDL particles [Yoshida et al., 2003; Milne et al., 2005], and even proposed as potential biomarkers of stress related pathologies [Montine et al., 2004]. Recently, phosphatidylcholine hydroperoxide (PCOOH) was found in elevated amounts in plasma, and correlated with high levels of γ-glutamyl transpeptidase (γ-GTP), high density lipoproteins (HDL), triglycerides (TG), and blood alcohol concentration, suggesting the involvement of lipid peroxidation in alcohol induced liver damage, and proposed by the authors as a biomarker of oxidative stress in alcoholic patients [Adachi et al., 2004b].

B) Characterisation of oxidised glycerophosphatidylcholines with the sn-2 acyl chain shortened

As mentioned earlier, the fatty acid intermediate (radical species) and primary (long-chain) oxidation products undergo a number of rearrangements and reactions (Scheme 2) resulting in the formation of carbonyl short-chain products.

In the course of this study aiming the identification and characterisation of GPC radical oxidation, several GPC short-chain products were identified in the mass spectra as $[MH]^+$ and $[MNa]^+$ ions, amongst saturated and unsaturated aldehydes, keto- and hydroxy-unsaturated aldehydes, dicarboxylic acids and also keto- and hydroxy-dicarboxylic acids with various chain lengths. The identification was proposed based on the *m/z* value, which provides a good indication of the oxidation product that is present in an oxidised GPC standard. Furthermore, with the developed HPLC conditions it was observed that dicarboxylic acids, lyso-phosphatidylcholines and aldehydes, eluted in restricted elution zones of the chromatogram (manuscript VIII). It was also noted that in the case of short-chain products with terminal aldehyde group, elution was influenced by the *sn*-2 chain length and by the presence of substitutents. Thus, information about the molecular weight and the retention time allows differentiation of short-chain product with the same

m/z value but arising from the oxidation of different diacyl-phosphatidylcholines (isobaric structures). As an example, differentiation of isomeric structures (saturated aldehydes, unsaturated dicarboxylic acids and unsaturated hydroxy-aldehydes) occurring in different phosphatidylcholines was described. However, with the purpose of carrying out analysis of biological samples, the identification of GPC short-chain products based on the *m/z* value and retention time may be complemented with tandem mass spectrometry. In this case, tandem mass spectrometry data obtained for $[MH]^+$ and $[MNa]^+$ ions identified in the mass spectra (manuscript VII and VIII) showed differences in the fragmentation pattern of compounds with different structural features, which prevent misinterpretations that can arise when the identification is based solely on the *m/z* values [Itabe et al., 1996; Frey et al., 2000] or by multiple reaction monitoring (MRM) [Podrez et al., 2002]. The differences observed in the fragmentation pattern of GPC short-chain products consisted in the presence of product ions that were tentatively assigned to cleavages involving the terminal group at the *sn*-2 residue, namely homolytic cleavage of the β-bond in aldehydes and heterolytic cleavage of the γ-bond in dicarboxylic acids, and also cleavages involving the substitutents groups (1,4 hydrogen elimination mechanism). These cleavages observed with low relative abundance were attributed to charge-remote fragmentations, although abundant product ions resulting from characteristic losses of GPC were also observed, in similarity to the fragmentation described for the glycerophosphatidylcholine $[MH]^+$ and $[MNa]^+$ ions [Hsu and Turk, 2003] and of long-chain products (manuscript V and VI).

In view of the LC-MS data obtained, the elution of GPC short-chain products with the same structural features in restricted elution zones, suggests that LC-MS data may be used as a pre-fractionation method of GPC short-chain products in biological samples, where a myriad of unsaturated fatty acids, that may undergo oxidative damage, exist.

Interestingly, the presence of 2-(9-oxo-nonanoyl)-1-palmitoyl glycerophosphatidylcholine (*m/z* 650.5, $[MH]^+$) and 2-(9-carboxy-nonanoyl)-1-palmitoyl glycerophosphatidylcholine (*m/z* 666.5, $[MH]^+$) observed for PLPC, and the presence of 2-(5-oxo-pentanoyl)-1-palmitoyl glycerophosphatidylcholine (*m/z* 594.4, $[MH]^+$) and 2-(5-carboxy-pentanoyl)-1-palmitoyl glycerophosphatidylcholine (*m/z* 610.4, $[MH]^+$) observed for PAPC (manuscript VII and VIII) with high relative abundance throughout this study, suggested that, during non-enzymatic radical oxidation, the C-9 position in lineloyl moiety and the C-5 in the arachidonoyl moiety, was favoured over other positions, after bis-allylic hydrogen abstraction and double bond rearrangement, or their presence more stable. The predominance of C_9 products in lineloyl and C_5 products in arachidonoyl moieties are

consistent with the abstraction of bis-allylic hydrogen atoms closer to the polar head. This behaviour may reflect the influence of surface area on radical oxidation of phosphatidylcholine liposomes [Li et al., 2000; Araseki et al., 2002] where bis-allylic hydrogen atoms closer to the polar head are more prone (accessible) to radical abstraction. Corroboration may be given by similar observations that were reported during cis-trans isomerisation studies of stearoyl-oleoyl-phosphatidylcholine (SOPC), stearoyl-lineloyl-phosphatidylcholine (SLPC) and stearoyl-arachidonoyl-phosphatidylcholine (SAPC) liposomes by the attack of thyil radical [Chatgilialoglu and Ferreri, 2005], where the selective abstraction of the bis-allylic hydrogen atoms C-11 (linoleoyl) and C-7 (arachidonoyl) was observed, and with the preferential isomerisation to the carbon atoms C-5 in arachidonoyl) and C-9 (lineloyl). On the other hand, recently, it was proposed that the predominance of C_9 products in lineloyl and C_5 products in arachidonoyl was due to oxidative fragmentation of γ-hydroxy-α,β-unsaturated aldehydes, via a Michael addition of a peracyl radical with formation of a β-hydroxyperester, to saturated aldehydes with concomitant loss of a 3 carbons chain [Balamraju et al., 2004]. In other words, this mechanism implies that the formation of C_9 short-chain products in linoleic acid derives from C_{12} products and the C_5 short-chain products in arachidonic acid from C_8 products [Balamraju et al., 2004], and not of preferential attack on the bis-allylic hydrogen atoms closer to the polar head. Remarkably, acyl radical intermediates were identified in the course of this work, namely acyl DMPO spin adduct (*m/z* 256 in manuscript IV) and an hydroperoxide-alkanal derivative (*m/z* 648 in manuscript VII), and may evidence the occurrence of the fragmentation mechanism proposed previously for free γ-hydroxy-α,β-unsaturated aldehydes [Balamraju et al., 2004] may also be proposed to occur in metal-catalysed oxidised γ-hydroxy-α,β-unsaturated alkenal glycerophosphatidylcholines. In summary, the higher relative abundance of the C_9 products in PLPC (*m/z* 650 and 666) and C_5 products in PAPC (*m/z* 594 and 610), that result from the C_{12} in PLPC (*m/z* 704, 720 and 722) and C_8 in PAPC (*m/z* 650, 664 and 666) observed throughout this work (manuscript VIII), may be the result of cumulative effects of positions in the unsaturated fatty cid chain more prone to radical oxidation or of the oxidative fragmentation of secondary fatty acid products. Consequently, the higher relative abundance of C_9 products in lineloyl and C_5 products in arachidonoyl suggests that non-enzymatic metal-catalysed fatty acid radical oxidation generates specific short-chain oxidation products, in resemblance to what is described for enzymatic fatty acid oxidation [Kitaguchi et al., 2005]. This hypothesis needs to be further supported by radical oxidation reactions in other PUFA.

Cross-linking reactions between phospholipid radical oxidation products and peptides: Characterisation of diacyl glycerophosphatidylcholine-peptides covalent adducts (manuscript IX)

The oxidation products of PLPC and PAPC with terminal aldehyde moieties identified throughout this study, and structurally characterised (manuscript V) and surveyed with reverse phase LC-MS (manuscript VII), exhibited high relative abundance and were chemical stable as observed by their maintenance for several days in the oxidised GPC extract. Their reported presence in *in vivo* [Itabe et al., 1996; Frey et al., 2000; Harrison et al., 2000; Khaselev et al., 2000; Podrez et al., 2002; Subbanagounder et al., 2002; Hoff et al., 2003] suggests that other type of reactions, involving the GPC alka(e)nals, may have considerable importance in biological systems.

Phospholipid-peptide adducts were identified by mass spectrometry after incubation of GPC alkenal with leucine-enkephalin (YGGFL). These adducts were formed by reaction between carbonyl groups present in GPC alka(e)nals and nucleophilic groups present in peptides with formation of phospholipid-peptide adducts, similarly to the ones described for HNE and peptides and proteins [Carini et al., 2004; Petersen and Doorn, 2004]. These phospholipid-peptide adducts involve the formation of a covalent bond (imine) which is different from the phospholipid-peptide interactions (electrostatic) observed in many membrane proteins [Hunte, 2004]. The formation of peptide-lipid adducts is described to be time dependent [Fenaille et al., 2003; Ishii et al., 2003; Völkel et al., 2005; Choudhary et al., 2005], although protein-HNE adducts, namely glyceraldehyde-3-phosphate dehydrogenase-HNE adducts, were identified in the MALDI-TOF mass spectrum, with only 5 minutes of incubation [Ishii et al., 2003] evidencing the reactivity of the amino groups towards the carbonyl groups.

Tandem mass spectrometry performed on the new ions observed in the mass spectrum and identified as GPC alkanal-peptide Schiff adducts and GPC alkenal-peptide Schiff and Michael adducts showed substantial differences in the fragmentation pattern consisting of, i) losses characteristic of glycerophosphatidylcholines (loss of 59 Da and 183 Da), ii) loss of the peptide chain, iii) cleavages of the peptide chain, and iv) particularly cleavages characteristic of free fatty acids, and provided information regarding the lipid and the peptide moieties of the adduct. The fragmentation pattern of alkenal GPC-peptide Schiff and Michael adducts shows significant differences relative to the fragmentation pattern described for lipid-peptide adducts, where only peptide cleavages are reported

[Fenaille et al., 2003; Ishii et al., 2003; Isom et al., 2004], which can be attributed to charge retention in the phosphocholine polar head. Interestingly, peptide-phosphatidylcholine adducts were previously identified by immunodetection in oxLDL particles [Bird et al., 1999; Subbanagounder et al., 2000; Friedman et al., 2002] and in liver rats treated with CCl_4 [Brame et al., 2004]. Accumulation of oxLDL is thought to induce monocyte adhesion [Boullier et al., 1997] with formation of foam cells, which is described as an early event in atherosclerosis, and to bound to the surface of apoptotic cells inhibiting the phagocytosis by macrophages [Bird et al., 1999]. This is an increasing topic of research with the purpose to ascertain whether inhibition by the macrophage is caused by recognition of phospholipid or the peptide moieties [Bird et al., 1999; Friedman et al., 2002]. Furthermore, the formation of the imine bond results in the exposure of the phosphocholine polar head, which is a structural feature required for antigenicity recognition [Friedman et al., 2002]. The exposure of the charged polar head may alters protein conformation and depending on the chemical and physical properties of the protein, alteration of phospholipid-protein charge distribution may occur with changes in the isoelectric point (pI) [Bo and Pawliszyn, 2006].

Furthermore, information about the Mw of the peptide chain attached to the phosphatidylcholine moiety, that is inferred by the product ions due to the loss of the peptide moiety, can be extended to the analysis of tryptic digests of larger proteins by MALDI-MS. The information, obtained from tryptic digests, together with three-dimension molecular modelling of protein sequence of X-ray data [Hunte, 2004] may provide information about the location of the modified amino acid residue(s) and relate chemical modifications with conformational changes that may take place during oxidative stress conditions and relate them with loss of enzyme activity.

Bibliography

Adachi J, Yoshioka N, Funae R, Nushida H, Asano M, Ueno Y. Determination of phosphatidylcholine monohydroperoxides using quadrupole time-of-flight mass spectrometry. *J. Chromatogr. B.* 2004, **806**, 41-46.

Adachi J, Matsushita S, Yoshioka N, Funae R, Fujita T, Higuchi S, Ueno Y. Plasma phosphatidylcholine hydroperoxide as a new marker of oxidative stress in alcoholic patients. J. Lipid Res. 2004, 45, 967-971.

Adachi J, Yoshioka N, Sato M, Nakagawa K, Yamamoto Y and Ueno Y. Detection of phosphatidylcholine oxidation products in rat heart using quadrupole time-of-flight mass spectrometry. *J. Chromatogr. B.* 2005, **823**, 37-43.

Adam W, Kazakov DV, Kazakov VP. Singlet-oxygen chemiluminescece in peroxide reactions. Chem. Rev. 2005, 105, 3371-3387.

Anzai K, Aikawa T, Furukawa Y, Matsushima Y, Urano S, Ozawa T. ESR measurement of rapid penetration of DMPO and DEPMPO spin traps through lipid bilayer membranes. *Arch. Biochem. Biophys.* 2003, **415**, 251-256.

Araseki M, Yamamoto K, Miyashita K. Oxidative stability of polyunsaturated fatty acid in phosphatidylcholine liposomes. *Biosci. Biotechnol. Biochem*. 2002, **66**, 2573-2577.

Balamraju YN, Sun M, Salomon RG. γ-Hydroxyalkenals are oxidatively cleaved through Michael addition of acylperoxy radicals and fragmentation of intermediated β-hydroxyperesters. *J. Am. Chem. Soc.* 2004, **126**, 11522-11528.

Barclay LRC and Vinqvist MR. Do spin traps also act as classical chain-breaking antioxidants? A quantitative kinetic study of phenyl tert-butyl nitrone (PBN) in solution and in liposome. *Free Rad. Biol. & Med.* 2000, **28**, 1079-1090.

Bird DA, Gillote KL, Hörkkö S, Friedman P, Dennis EA, Witztum JL, Steinberg D. Receptors for oxidized low-density lipoprotein on elicited mouse peritoneal macrophages can recognize both the modified lipid moieties and the modified protein moieties: implications with respect to macrophage recognition of apoptotic cells. *Proc. Natl. Acad. Sci. USA.* 1999, **96**, 6347-6352.

Bo T and Pawliszyn J. Characterization of phospholipid-protein interactions by capillary isoelectric focusing with whole imaging detection. *Anal. Biochem*. 2006, **350**, 91-98.

Borst JW, Visser NV, Kouptsova O, Visser AJWG. Oxidation of unsaturated phospholipids in membrane bilayer mixtures is accompanied by membrane fluidity changes. *Biochim. Biophys. Acta*. 2000, **1487**, 61-73.

Brame CJ, Boutaud O, Davies SS, Yang T, Oates JA, Roden D, Roberts II LJ. Modification of proteins by isoketals containing oxidised phospholipids. *J. Biol. Chem*. 2004, **279**, 13447-13451.

Carini M, Aldini G, Facino RM. Mass spectrometry for detection of 4-hydroxy-trans-2-nonenal (HNE) adducts with peptides and proteins. *Mass Spectrom. Rev*. 2004, **23**, 281-305.

Cevc G. "solute transport across bilayers" In *Phospholipids Handbook*; Gregor Cevc, Ed.; Marcel Dekker: New York, 1993; p 639-661.

Chatgilialoglu C and Ferreri C. Trans lipids: the free radical path. *Acc. Chem. Res*. 2005, **38**, 441-448.

Cheng C and Gross ML. Fragmentation mechanisms of oxofatty acids via high-energy collisional activation. *J. Am. Soc. Mass Spectrom*. 1998; **9**: 620-627.

Choudhary S, Xiao T, Srivastava S, Zhang W, Chan LL, Vergara LA, van Kuijk FJGM, Ansari NH. Toxicity and detoxification of lipid-derived aldehydes in cultured retinal pigmented epithelial cells. *Toxicol. Applied Pharmacol*. 2005, **204**, 122-134.

Crow FW, Cragun JD, Johnson KL, Ruiz MV, de la Paz MP, Naylor S. On-Line HPLC-UV-mass spectrometry and tandem mass spectrometry for the rapid delineation and characterization of differences in complex mixtures: a case study using toxic oil variants *Biomed. Chromatogr.* 2002, **16**, 311-318.

De Zwart LL, Meerman JHN, Commandeur JNM and Vermeulen NPE. Biomarkers of free radical damage applications in experimental animals and in humans. *Free Rad. Biol. & Med.* 1999, **26**, 202-226.

Deng C and Zhang X. A simple, rapid and sensitive method for determination of aldehydes in human blood by gas chromatography/mass spectrometry and solid-phase microextraction with on-fiber derivatization. *Rapid Commun. Mass Spectrom*. 2004, **18**, 1715-1720.

Deterding LJ, Ramirez DC, Dubin JR, Mason RP, Tomer KB. Identification of free radicals on hemoglobin from its self-peroxidation using mass spectrometry and immuno-spin trapping. *J. Biol. Chem*. 2004, **279**, 11600-11607.

Dikalov SI and Mason RP. Spin trapping of polyunsaturated fatty acid-derived alkyl peroxyl radicals: reassignment to alkoxyl radical adducts. *Free Rad. Biol. & Med*. 2001, **30**, 187-197.

Fenaille F, Guy PA, Tabet J-C. Study of protein modification by 4-hydroxy-2-nonenal and other short chain aldehydes analysed by electrospray tandem mass spectrometry. *J. Am. Soc. Mass Spectrom*. 2003, **14**, 215-226.

Fitzpatrick FA, Morton DR, Wynalda MA. Albumin stabilizes leukotriene A4. *J. Biol. Chem*. 1982, **257**, 4680-4683.

Folch J, Lees M, Stanley GHS. A simple method for the isolation and purification of total lipids from animal tissues. *J. Biol. Chem*. 1957; **226**: 497.

Frey B. Haupt R. Alms S, Holzmann G, König T, Kern H, Kox W, Rüstow B, Schlame M. Increase in fragmented phosphatidylcholine in blood plasma by oxidative stress. *J. Lipid Res*. 2000, **41**, 1145.

Friedman P, Hörkkö S, Steinberg D, Witztum JL, Dennis EA. Correlation of antiphospholipid antibody recognition with the structure of synthetic oxidized phospholipids. *J. Biol. Chem*. 2002, **277**, 7010-7020.

Gao L, Zackert WE, Hasford JJ, Danekis ME, Milne GL, Remmert C, Reese J, Yin H, Tai H-H, Dey SK, Porter NA, Morrow JD. Formation of prostaglandins E2 and D2 via the isoprostane pathway. *J. Biol. Chem*. 2003, **278**, 28479-28489.

Giuffrida F, Destaillats F, Robert F, Skibsted LH, Dionisi F. Formation and hydrolysis of triacylglycerol and sterol epoxides: role of unsaturated triacylglycerol peroxyl radicals. *Free Rad. Biol. Med.* 2004a, **37**, 104-114.

Giuffrida F, Destaillats F, Skibsted LH, Dionisi F. Structural analysis of hydroperoxy- and epoxy-triacylglycerols by liquid chromatography mass spectrometry. *Chem. Phys. Lipids*. 2004b, **131**, 41.

Harrison KA, Davies SS, Marathe GK, McIntyre T, Prescott S, Reddy KM, Falck JR, Murphy RC. Analysis of oxidised glycerophosphocholine lipids using electrospray ionisation mass spectrometry and microderivatization techniques. *J. Mass Spectrom*. 2000, **35**, 224-236.

Hoff HF, O'Neill J, Wu S, Hoppe G, Salomon R. Phospholipid hydroxyalkenals. Biological and chemical properties of specific oxidized lipids present in atherosclerotic lesions. *Arterioscler. Thromb. Vasc. Biol*. 2003, **23**, 275-282.

Hsu F and Turk J. Distinction among isomeric unsaturated fatty acids as lithiated adducts by electrospray ionisation mass spectrometry using low energy collisionally activated dissociation on a triple stage quadrupole instrument. *J. Am. Soc. Mass Spectrom*. 1999, **10**, 600-612.

Hsu F and Turk J. Electrospray ionisation/tandem quadrupole mass spectrometric studies on phosphatidylcholines: the fragmentation processes. *J. Am. Soc. Mass Spectrom*. 2003, **14**, 352-363.

Hunte C. Specific protein-lipid interactions in membrane proteins. *Biochem. Soc. Trans*. 2005, **33**, 938-942.

Inouye M, Mio T, Sumino K. Dicarboxylic acids as markers of fatty acid peroxidation in diabetes. *Atheroscler*. 2000, **148**, 197-202.

Inouye M, Mio T, Sumino K. Formation of 9-hydroxy linoleic acid as a product of phospholipid peroxidation in diabetic erythrocyte membranes. *Biochim. Biophys. Acta*. 1999, **1438**, 204-212.

Ishii T, Tatsuda E, Kumazawa S, Nakayama T, Uchida K. Molecular basis of enzyme inactivation by an endogenous electrophile 4-hydroxy-2-nonenal: identification of modification sites in glyceraldehyde-3-phosphate dehydrogenase. *Biochem*. 2003, **42**, 3474-3480.

Itabe H, Yamamoto H, Suzuki M, Kawai Y, Nakagwa Y, Suzuki A, Imanaka T, Takano T. Oxidized phosphatidylcholines that modify proteins: analysis by monoclonal antibody against oxidized low density lipoprotein. *J. Biol. Chem*. 1996, **271**, 33208-33217.

Iwase H, Takatori T, Nagao M, Nijima H, Iwadate K, Matsuda Y, Kobayashi M. Formation of keto and hydroxy compounds of linoleic acid in submitochondrial particles of bovine heart. *Free Rad. Biol. & Med.* 1998, **24**, 1492-1503.

Jerlich A, Schaur RJ, Pitt AR, Spickett CM. The formation of phosphatidylcholine oxidation products by stimulated phagocytes. *Free Rad. Res*. 2003, **37**, 645-653.

Jian W, Arora JS, Oe T, Shuvaev VV, Blair IA. Induction of endothelial cell apoptosis by lipid hydroperoxide-derived bifunctional electrophiles. *Free Rad. Biol. & Med*. 2005, **39**, 1162-1176.

Jiang H, McGiff JC, Quilley J, Sacerdoti D, Reddy LM, Falck JR, Zhang F, Lerea KM, Wong PY. Identification of 5,6-trans-epoxyeicosatrienoic acid in the phospholipids of red blood cells. *J. Biol. Chem*. 2004, **279**, 36412-36418.

Kayganich-Harrison KA and Murphy RC. Characterization of chain-shortened oxidized glycerophosphocholines lipids using fast atom bombardment and tandem mass spectrometry. *Anal. Biochem*. 1994; **221**, 16.

Kern H, Volk T, Knauer-Schiefer S, Mieth T, Rüstow B, Kox WJ, Schlame M. Stimulation of monocytes and platelets by short-chain phosphatidylcholines with and without terminal carboxyl group. *Biochim. Biophys. Acta*. 1998, **1394**, 33-42.

Khaselev N and Murphy RC. Peroxidation of arachidonate containing plasmenyl glycerophosphocholines: facile oxidation of esterified arachidonate at carbon-5. *Free Rad. Biol. & Med*. 2000, **29**, 620-632.

Kim SS, Gallaher DD, Csallany AS. Lipophilic aldehydes and related carbonyl compounds in rat and human urine. *Lipids*. 1999, **34**, 489-496.

Kitaguchi H, Ohkubo K, Ogo S, Fukuzumi S. Direct ESR detection of pentadienyl radicals and peroxyl radicals in lipid peroxidation: mechanistic insight into regioselective oxygenation in lipoxygenases. *J. Am. Chem. Soc.* 2005, **127**, 6605-6609.

Kumamoto K, Hirai T, Kishioka S, Iwahashi H. Identification of a radical formed in the reaction mixtures of oxidised phosphatidylcholines with ferrous ions using HPLC-ESR and HPLC-ESR-MS. *Free Rad. Res.* 2005, **39**, 987-993.

Li Q-T, Yeo MH, Tan BK. Lipid peroxidation in small and large phospholipid unilamelar vesicles induced by water-soluble free radical sources. *Biochem. Biophys. Res. Commun*. 2000, **273**, 72-76.

Megli FM and Sabatini K. EPR studies of phospholipid bilayers after lipoperoxidation. 1. Inner molecular order and fluidity gradient. *Chem. Phys. Lipids*. 2003, **125**, 161-172.

Megli FM and Sabatini K. Mitochondrial phospholipid bilayer structure is ruined after liver oxidative injury in vivo. *FEBS Lett*. 2004, **573**, 68-72.

Megli FM and Sabatini K. Oxidized phospholipids induce phase separation in lipid vesicles. *FEBS Lett*. 2005, **579**, 4577-4584.

Milne GL, Seal JR, Havrilla CM, Wijtmans M, Porter NA. Identification and analysis of products formed from phospholipids in the free radical oxidation of human low density lipoproteins. *J. Lipid Res*. 2005, **46**, 307-319.

Murphy RC, Fiedler J, Hevko J. Analysis of non-volatile lipids by Mass Spectrometry. *Chem. Rev.* 2001, **101**, 479-526.

Nakamura T, Bratton DL, Murphy RC. Analysis of epoxyeicosatetraenoic and monohydroxyeicosatetraenoic acids esterified to phospholipids in human red blood cells by electrospray tandem mass spectrometry. *J. Mass Spectrom*. 1997, **32**, 888-896.

Niki E, Yoshida Y, Saito Y, Nguchi N. Lipid peroxidation: mechanisms, inhibition, and biological effects. *Biochem. Biophys. Res. Commun*. 2005, **338**, 668-676.

Niknahad H, Siraki AG, Shuhendler A, Khan S, Teng S, Galati G, Easson E, Poon R, O'Brien PJ. Modulating carbonyl cytotoxicity in intact rat hepatocytes by inhibiting carbonyl-metabolizing enzymes. I. Aliphatic alkenals. *Chem. Biol. Interact*. 2003, **143-144**, 107-117.

O'Brien-Coker IC, Perkins G, Mallet AI. Aldehyde analysis by high performance liquid chromatography/tandem mass spectrometry. *Rapid Commun. Mass Spectrom*. 2001, **15**, 920-928.

Palsdottir H and Hunte C. Lipids in membrane protein structures. *Biochim. Biophys. Acta*. 2004, 1666, 2-18.

Petersen DR and Doorn JA. Reactions of 4-hydroxynonenal with proteins and cellular targets. *Free Rad. Biol. & Med*. 2004, **37**, 937-945.

Podrez EA, Poliakov E, Shen Z, Zhang R, Deng Y, Sun M, Finton PJ, Shan L, Gugiu B, Fox PL, Hoff HF, Salomon RG, Hazen SL. Identification of a novel family of oxidised phospholipids that serve as ligands for the macrophage scavenger receptor CD36. *J. Biol. Chem*. 2002, **277**, 38503-38516.

Qian SY, Wang HP, Schafer FQ and Buettner GR. EPR detection of lipid-derived free radicals from PUFA, LDL, and cell oxidations. *Free Rad. Biol. & Med*. 2000, **29**, 568-579.

Qian SY, Guo Q, Mason RP. Identification of spin trapped carbon-centered radicals in soybean lipoxygenase-dependent peroxidations of ω-3 polyunsaturated fatty acids by LC/ESR, LC/MS and tandem MS. *Free Rad. Biol. & Med*. 2003a, **35**, 33-44.

Qian SY, Yue G-H, Tomer KB, Mason RP. Identification of all classes of spin-trapped carbon-centred radicals in soybean lipoxygenase-dependent lipid peroxidation of ω-6 polyunsaturated fatty acids via LC/ESR, LC/MS and tandem MS. *Free Rad. Biol. & Med*. 2003b, **34**, 1017-1028.

Qian SY, Kadiisha MB, Guo Q, Mason RP. A novel protocol to identify and quantify all spin trapped free radicals from in vitro/in vivo interaction of HO and DMSO: LC/ESR, LC/MS, and dual spin trapping combinations. *Free Rad. Biol. & Med*. 2005, **38**, 125-135.

Roberts II LJ and Fessel JP. The biochemistry of the isoprostane, neuroprostane, and isofuran pathways of lipid peroxidation. *Chem. Phys. Lipids*. 2004, **18**, 173-186.

Rosen, G.M.; Britigam, B.E.; Halpern, H.J.; Pou, S., Eds. Kinetics of spin trapping free radicals. In *Free Radicals, Biology and Detection by Spin Trapping*; Oxford University Press: N.Y. 1999, pp 321-353.

Salomon RG, Kaur K, Podrez E, Hoff HF, Krushinsky AV, Sayre LM. HNE-derived 2-pentylpyrroles are generated during oxidation of LDL, are more prevalent in blood plasma from patients with renal disease or atherosclerosis and are present in atherosclerotic plaques. *Chem. Res. Toxicol*. 2000, **13**, 557-564.

Schlame M, Haupt R, Wiswedel I, Kox WJ, Rüstow B. Identification of short-chain oxidized phosphatidylcholine in human plasma. *J. Lipid Res*. 1996, **37**, 2608-2615.

Sergent O, Morel I, Cillard J. "Involvement of metal ions in lipid peroxidation: biological implications" *In* Metal Ions in Biological Systems, ed. Sigel, A. and Sigel H, Vol 36, Marcel Dekker, INC. New York, 1999, pp 251-262.

Spickett CM, Pitt AR, Brown AJ. Direct observation of lipid hydroperoxides in phospholipid vesicles by electrospray mass spectrometry. *Free Rad. Biol. & Med*. 1998, **25**, 613-620.

Spickett CM, Rennie N, Winter H, Zambonin L, Landi L, Jerlich A, Schaur RJ, Pitt AR. Detection of phospholipid oxidation in oxidatively stressed cells by reverse-phase HPLC coupled with positive-ionization electroscopy MS. *Biochem. J*. 2001, **355**, 449-457.

Spiteller G. Linoleic acid peroxidation- the dominant lipid peroxidation process in low density lipoprotein and its relationship to chronic diseases. *Chem. Phys. Lipids* 1998, **95**, 105-162.

Subbanagounder G, Leitinger N, Schwenke DC, Wong JW, Lee H, Rizza C, Watson AD, Faull KF, Fogelman AM, Berliner JA. Determinants of bioactivity of oxidized phospholipids. Specific oxidized fatty acyl groups at the *sn*-2 position. *Arterioscler. Tromb. Vasc. Biol.* 2000, **20**, 2248-2254.

Subbanagounder G, Deng Y, Borromeo C, Dooley AN, Berliner JA, Salomon RG. Hydroxy alkenal phospholipids regulate inflammatory functions of endothelial cells. *Vasc. Pharmacol.* 2002, **38**, 201-209.

Tang L, Zhang Y, Qian Z, Shen X. The mechanism of Fe2+-initiated lipid peroxidation in liposomes: the dual function of ferrous ions, the roles of the pre-existing lipid peroxides and the lipid peroxyl radical. *Biochem. J.* 2000, **352**, 27-36.

Taniguchi H and Madden KP. An *in situ* time-resolved ESR study of the kinetics of spin trapping by 5,5-dimethyl-1-pyrroline-N-oxide. *J. Am. Chem. Soc.* 1999, **121**, 11875-11879.

Velasco J, Andersen ML, Skibsted LH. Electron spin resonance spin trapping form analysis of lipid oxidation in oils: inhibiting effect of the spin trap α-phenyl-N-tert-butylnitrone on lipid oxidation. *J. Agric. Food Chem.* 2005, **53**, 1328-1336.

Vitrac H, Courrègelongue M, Couturier M, Collin F, Thérond P, Rémita S, Peretti P, Dore D, Gardès-Albert M. Radiation-induced peroxidation of small unilamellar vesicles of phosphatidylcholine generated by sonication. *Can. J. Physiol. Pharmacol.* 2004, **82**, 153-160.

Völkel W, Alvarez-Sanchez R, Weick I, Mally A, Dekant W, Pähler A. Glutathione conjugates of 4-hydroxy-2(E)-nonenal as biomarkers of hepatic oxidative stress-induced lipid peroxidation in rats. *Free Rad. Biol. & Med.* 2005, **38**, 1526-1536.

Ward NC, Ouddey IB, Hodgson JM, Beilin LJ, Croft KD. Urinary 20-hydroxyeicosatetraenic acid excretion is associated with oxidative stress in hypertensive subjects. *Free Rad. Biol. & Med.* 2005, **38**, 1032-1036.

Watson AD, Leitinger N, Navab M, Faull KF, Hörkkö S, WitztumJL, Palinski W, Schwenke D, Salomon RG, Sha W, Subbanagounder G, Fogelman AM, Berliner JA. Structural identification by mass spectrometry of oxidized phospholipids in minimally oxidized low density lipoprotein that induce monocyte/endothelial interactions and evidence for their presence in vivo. *J. Biol. Chem.* 1997, **272**, 13597-13607.

Watson AD, Subbanagounder G, Welsbie DS, Faull KF, Navab M, Jung ME, Fogelman AM, Berliner JA. Structural identification by mass spectrometry of oxidized phospholipids in minimally oxidized low density lipoprotein that induce monocyte/endothelial interactions and evidence for their presence in vivo. *J. Biol. Chem.* 1999, **274**, 24787-24798.

Wheelan P, Zirrolli JA, Murphy RC. Electrospray ionisation and low energy tandem mass spectrometry of polyhydroxy unsaturated fatty acids. *J. Am. Soc. Mass Spectrom.* 1996, **7**, 140-149.

Yorek MA. "Biological Distribution" *In* Phospholipids Handbook; Gregor, Cevc, Ed.; Marcel Dekker: New York, 1993; p 745-775.

Yoshida T, Otake H, Aramaki Y, Hara T, Tsuchiya S, Hamada A, Utsumi H. Free radicals from 1-palmitoyl-2-arachidonoyl-phosphatidylcholine liposomes in Fe^{2+}/ascorbic acid solution. *Biol. Pharm. Bull.* 1996, **19**, 779-782.

Yoshida Y, Ito N, Shimakawa S, Niki E. Susceptibility of plasma lipids to peroxidation. *Biochem. Biophys. Res. Commun.* 2003, **305**, 747-753.

7. Conclusions

In order to access the applicability of mass spectrometry in the detection and structural characterisation of fatty acid and other biomolecule radical products, using methodology developed for the detection of free radicals, where some aspects may be highlighted, namely:

Mass spectrometry applied in the study of oxidative modifications induced by free radicals to free and esterified fatty acids (GPC) resulted in the identification of a wide variety of fatty acid radical products, which in the case of GPC were identified for the first time. Tandem mass spectrometry data provided confirmation of proposed structures and particularly of structures with ambiguous assignments through the interpretation of product ions, observed with low relative abundance in the product ion spectra, that resulted from charge remote fragmentation pathways. These product ions were the most informative allowing establishing the nature of the fatty acid radical enabling to propose the presence of carbon and oxygen centred radicals. Also, they provided information about location of the free radical and the functional group along the unsaturated fatty acid chain (for radical products), which until this date had not been described. Furthermore, product ions with low relative abundance also provided structural information about the non-radical GPC products regarding the functional group and its location along the unsaturated fatty acid chain.

Based on the MS and MS/MS data, structural differentiation was achieved for linoleic acid and GPC radical products, many of which were identified and characterised in this study for the first time, and also differentiation of non-radical GPC products by association of mass spectrometry with liquid chromatography, namely of isobaric and isomeric structures, which to date had not yet been discussed.

Furthermore, the identification of cross-linking products by MS was extended to the identification of cross-linking products between oxidised phosphatidylcholines and peptides, which until now was focused solely on the identification of cross-linking reactions of oxidised fatty acids and peptides/proteins. Upon collision-induced dissociation these cross-linking products revealed unique fragmentation patterns resulting from the cumulative fragmentations characteristic of GPC and of peptides.

In view of the results described, some considerations can be proposed:

a) Mass spectrometry reveals to be a more suitable technique for the identification of products formed during radical reactions of free and esterified fatty acids due to the possibility in identifying both radical and non-radical products, in opposition to other techniques.

b) In spite of the structural heterogeneity of the radical and non-radical linoleic acid and GPC oxidation products formed during non-enzymatic radical reaction, it appears that a trend in the formation of oxidation products exists towards the formation of structurally simple products, namely the occurrence of fatty acid alkyl radicals of smaller carbon chain (by β-scission mechanism), the predominance of short-chain GPC products of lower carbon chain lengths and the predominance of hydroxy long-chain GPC derivatives.

c) The trend in the product identified allows proposing that, during non-enzymatic radical oxidation of phospholipids, a preferential attack by free radicals of bis-allylic hydrogen atoms positioned closer to the polar head takes place.

d) The predominance of specific products formed upon non-enzymatic radical lipid peroxidation, may facilitate the profiling of phospholipids oxidation products in biological samples, where both enzymatic and non-enzymatic radical reactions occur, by LC-MS and LC-MS/MS.